EXPLORING MECHANISMS OF DRUG RESISTANCE IN MULTIPLE MYELOMA: THE ROLES OF THE PROGENITOR COMPARTMENT, APRIL AND NOTCH SIGNALING

Laura Ann Percy

A thesis submitted for the degree of Doctor of Philosophy

University College London

DECLARATION

I, Laura Ann Percy, declare that the work presented within this thesis is solely my own work and where information from other sources is included, I have indicated this in the text and have provided the appropriate reference.

Signed:

Date:

ABSTRACT

Multiple myeloma (MM) is characterised by the proliferation of clonal plasma cells and a number of novel, highly effective anti-MM agents have improved long-term survival. However, eventually all patients become resistant and the disease remains incurable. The occurrence of disease relapse after the apparent eradication of the clonal population indicates the persistent survival of a drug resistant, 'progenitor' subpopulation. Understanding the mechanisms that underlie these patterns of resistance, including the characterisation of MM progenitors, is therefore critical to improving clinical outcomes. A cancer stem cell model has been proposed in the context of MM, based on the lack of syndecan-1 (CD138) in clonal, light chain-restricted cells. This work did not substantiate this claim, and data from a series of primary samples suggest that lack of CD138 is not a robust marker for a progenitor population of MM cells. The bone marrow (BM) microenvironment is known to play a critical part in MM cell survival and resistance, mediated by cytokines present within MM cell niches, and by cell-contact dependent pathways activated in MM cells and within adjacent supportive BM cells. This work examines the role of A Proliferation-Inducing Ligand (APRIL), and of the Notch signalling pathway. The data suggest that soluble APRIL confers protection against Dexamethasone-induced apoptosis, whilst the Notch ligand Delta-like ligand-1, expressed on the stromal cell line, HS-5, enhances stroma-mediated protection against bortezomib.

ACKNOWLEDGEMENTS

I would like to thank my supervisor, Professor Yong, for her untiring support and guidance during my time working with her and completing this thesis. It would also have been quite impossible without the encouragement and patience of my husband Daniel and son Thomas. I would also like to thank those who have provided funding to support my work, including the Wellcome Trust, and finally I am hugely grateful to the myeloma patients who provided the bone marrow samples that made this work possible and the inspiration to pursue it.

COMMONLY USED ABBREVIATIONS

APRIL	A proliferation inducing ligand
ASCT	Autologous stem cell transplant
BCMA	B cell maturation antigen
BM	Bone marrow
BZM	Bortezomib
CM	Culture medium
CSC	Cancer stem cell
Dex	Dexamethasone
DL1/4	Delta-like ligand 1/4
FACS	Fluorescent activated cell sorting
FBS	Foetal bovine serum
HMCL	Human myeloma cell line
HSPG	Heparan sulfate proteoglycan
IGF-I	Insulin-like growth factor-I
IgH	Immunoglobulin heavy chain
IL	Interleukin
MM	Multiple myeloma
MNC	Mononuclear cell
MGUS	Monoclonal gammopathy of undetermined significance
PCR	Polymerase chain reaction
SCID	Severe combined immunodeficiency
SP	Side population
TACI	Transmembrane activator and calcium-modulator and cyclophilin ligand interactor

TABLE OF CONTENTS

TABLE OF FIGURES

CHAPTER 1

CHAPTER 2

CHAPTER 3

CHAPTER 4

CHAPTER 5

TABLE OF TABLES

CHAPTER 1

CHAPTER 2

CHAPTER 3

CHAPTER 4

CHAPTER 5

CHAPTER 1. INTRODUCTION

1.1 Multiple myeloma - the clinical problem

Multiple myeloma (MM) is a haematological malignancy characterised by the proliferation of clonal, terminally differentiated plasma cells. It is typified by infiltration of the bone marrow (BM) compartment by malignant plasma cells, associated with the presence of a detectable paraprotein, and causes symptoms due to a variety of end-organ injuries: anaemia, bone pain and pathological fractures, renal failure, hypercalcaemia and recurrent infection.

1.1.1 Epidemiology

MM accounts for 1-2% of all newly diagnosed cancers and around 10-15% of newly diagnosed haematological malignancies. In the UK there are around 4,000 new cases per year and this incidence has been stable over the last two decades. It is predominantly a disease of older people, with a median age at presentation of 73 years. It is 40-50% more common in men than women, and shows varying ethnic distribution, with twice as many patients of Afro-Caribbean origin, compared to European, and a lower incidence in those of Asian descent.

The prevalence of the condition in affluent countries is increasing steadily as survival rates improve following the introduction of a number of novel therapies [1,2]. Most recently, five-year survival estimates of 41% in all ages have been reported [1,3]. However, importantly, despite the notable advances over the last few decades, MM remains incurable.

The aetiology of the disease is unclear, with increasing age, male sex, preceding monoclonal gammopathy of undetermined significance and African ethnicity, as noted above, being the clearest epidemiological risk factors. It is almost certainly not a single disease entity [4] and a variety of genetic and environmental factors have been implicated in its pathogenesis.

1.1.2 Presentation and diagnosis

Most cases of MM present *de novo* with a combination of the symptoms outlined above but a proportion are preceded by the pre-malignant condition, monoclonal gammopathy of undetermined significance (MGUS). It is now felt that all MM cases are preceded by MGUS [5-7], which in the majority goes undetected.

1.1.2.1 MGUS

This is usually picked up with the incidental finding of a blood serum or urinary paraprotein. By definition it is asymptomatic, with evidence of a small population of clonal plasma cells (<10% on BM trephine immunohistochemistry) but with no evidence of end-organ damage attributable to this clone. This may be harder to determine in individuals with other comorbidities which cause similar clinical problems to myeloma, e.g. anaemia and renal impairment. It has the same epidemiological risk factors as myeloma, increasing in incidence with age particularly - 5% of those over 70 years [8]. There is an overall annual progression rate of 1%, but a number of factors are linked to higher progression rates, including a paraprotein concentration >15g/l, IgA or IgM paraproteins and/or an abnormal free light chain ratio [9].

1.1.2.2 Smouldering or asymptomatic myeloma

This term describes a condition in which there is evidence of a larger plasma cell clone than can be attributed to MGUS alone (clonal BM plasma cells >10%, paraprotein >30g/l) but with no evidence of end-organ impairment. The annual progression rate falls with time from diagnosis, with 10% progressing annually in the first five years, 3% per year in the subsequent five years and then 1% per year for the final ten years [10]. The current consensus is that treatment of these patients prior to the development of symptomatic myeloma is not beneficial, but this may change with studies of pre-emptive chemotherapy in high risk smouldering MM [11].

1.1.2.3 Symptomatic myeloma

Symptomatic myeloma is defined by the presence of a substantial clone of BM plasma cells (>10%, i.e. equivalent to that present in smouldering MM), a detectable

monoclonal protein in blood serum or urine and symptoms indicative of myeloma-related organ or tissue injury (so-called 'CRAB criteria'): hypercalcaemia, renal dysfunction, anaemia and bone disease (osteopaenia, lytic lesions, pathological fractures) [12]. Other features may be present including fatigue, weight loss, recurrent, severe or atypical bacterial infections, symptomatic hyperviscosity or amyloidosis. The diagnosis is made by demonstrating these features on blood and urine tests, bone marrow biopsy (aspirate and trephine) and imaging (plain radiographs, computed tomography scans, magnetic resonance imaging). The International Staging System [13] uses albumin and beta-2-microglobulin levels to stratify disease severity at diagnosis and has prognostic value (Table 1-1).

Table 1-1 International Staging System for Multiple Myeloma.

Stage	Criteria	Median survival (months)
I	Serum β_2-microglobulin <3.5mg/L Serum albumin ≥3.5g/dL	62
II	Not stage I or III*	44
III	Serum β_2-microglobulin ≥5.5mg/L	29

**There are two categories for stage II: serum β_2-microglobulin <3.5mg/L and serum albumin <3.5g/dL; or serum β_2-microglobulin 3.5 to <5.5mg/L, irrespective of the serum albumin level [13].*

Additionally, characterising any genetic abnormalities present in the clonal plasma cell, by G-banding or fluorescence-in-situ-hybridisation (FISH), can also aid prognostication (see section 1.1.3).

At this stage the malignant plasma cells are confined to the BM, and the disease is therefore termed 'medullary'.

1.1.2.4 Extramedullary myeloma and plasma cell leukaemia

A small proportion of patients present with highly aggressive disease characterised by extensive extramedullary involvement. This may be in the form of soft tissue masses, i.e. extramedullary plasmacytomas, or of circulating malignant plasma cells, so-called plasma cell leukaemia. These two disease manifestations may also arise in

later stage disease. Plasma cell leukaemia is associated with a number of distinctive features that distinguish it from MM, but it is highly likely that it reflects evolution of the BM disease rather than being a truly separate disease entity. The clonal plasma cells are usually CD138+ but typically CD56−.

1.1.3 Multiple myeloma - the genetic context of pathogenesis

The clonal population in MGUS is believed to originate from post-germinal-centre B cells. A number of sequential genetic, epigenetic and BM microenvironmental changes then govern the evolution of MGUS to symptomatic MM, with additional step-wise changes underpinning the progression of MM to terminal end-stage disease, with extramedullary involvement. These changes are summarised in Figure 1-1.

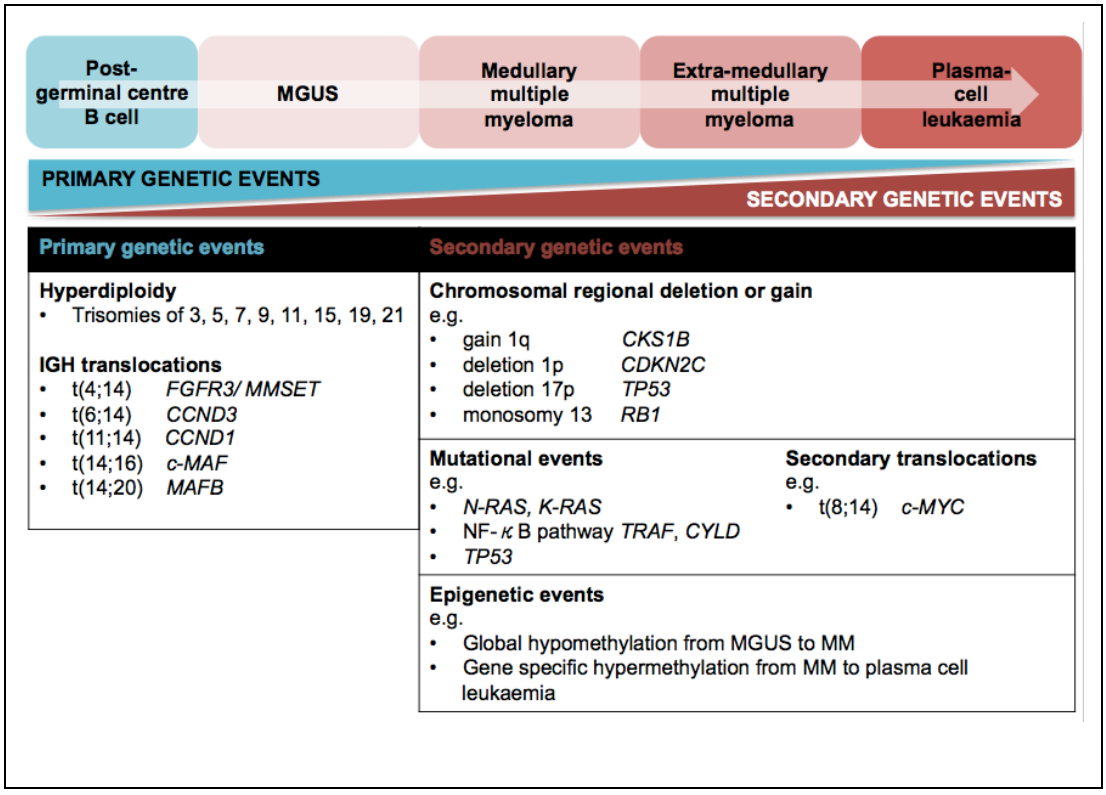

Figure 1-1 Multistep pathogenesis of multiple myeloma.

Primary genetic events, namely hyperdiploidy or IgH translocations, constitute the initiation events that trigger evolution from MGUS to MM. These various events result in aberrant expression of D-type cyclins (D1, D2 and D3). Secondary genetic events occur during the progression of MM and include chromosomal regional deletions or gains, additional translocations and discrete mutations affecting known oncogenes or cell survival pathways. Adapted from Kaiser et al, Chapter 5: The genetic and epigenetic mechanisms underlying the behaviour of myeloma. Myeloma. Cambridge University Press, 2014.

Primary genetic events (so-called 'initiation events') are present at the MGUS stage and fall into two broad categories. Around half of patients develop hyperdiploidy, in the form of trisomies of chromosomes 3, 5, 7, 9, 11, 15, 19 and 21, either singly or in combination. The other 50% ('non-hyperdiploid') have immunoglobulin heavy chain (IgH) translocations, in which the strong IgH transcriptional promoters are juxtaposed with known oncogenes, such as critical cell cycle proteins. These lesions appear more common in female patients (50% versus 38% of male patients). There are five commonly observed translocations.

1. t(4;14) is present in 10% of MM patients, has a positive association with IgA MM and independently predicts for poorer outcome. It results in increased expression of two genes, *fibroblast growth factor receptor 3* (*FGFR3*) and *multiple myeloma SET-domain containing protein* (*MMSET)* on chromosome 4p16 [14]. *FGFR3* overexpression seems to drive MM cell proliferation but *MMSET* may be more critical to disease pathogenesis and has global epigenetic effects.
2. t(6;14) is rare and only present in 0.8% of MM patients. It results in overexpression of *cyclin D3* (*CCND3*) on chromosome 6p21, a cell cycle regulator that promotes proliferation.
3. t(11;14) affects 15% of MM patients, approximating the IgH promoter with another cell cycle regulator, *cyclin D1* (*CCND1*) on chromosome 11q13. It is associated with lambda light chain expression and slowly progressive disease.
4. t(14;16) is present in 3% of MM patients and results in overexpression of the transcription factor *c-MAF* on chromosome 16q23, with upregulation of its downstream target, *cyclin D2* (*CCND2*).
5. t(14;20) is another rare event (in 1%), which results in overexpression of the transcription factor *MAFB* on chromosome 20q21, which has overlapping downstream targets to *c-MAF* and therefore also upregulates *CCND2.*

Table 1-2 Translocation and Cyclin D groups.

Group	Primary translocation	Gene at Breakpoint	D-Cyclin	Ploidy	Proliferation Index	Bone disease (% MRI Pos)	Frequency (%)	Prognosis
6p21	*6p21*	*CCND3*	D3	NH	Average	100	3	? Good
11q13	*11q13*	*CCND1*	D1	D, NH	Average	94	16	Good
D1	None	None	D1	H	Low	86	34	Good
D1 + D2	None	None	D1 and D2	H	High	100	6	? Poor
D2	None	None	D2	H, NH	Average	67	17	?
None	None	None	None	NH	Average	100	2	? Good
4p16	*4p16*	*FGFR3/MMSET*	D2	NH > H	Average	57	15	Poor
maf	*16q23* *20q11*	*c-maf* *mafB*	D2	NH	High	55	5 2	Poor

Abbreviations: D1, cyclin-D1; D2, cyclin-D2; D3, cyclin-D3; MRI, magnetic resonance imaging; pos, positive; D, diploid; H, hyperdiploid; NH, non-hyperdiploid; adapted from [15].

One consistent finding in the majority of MM patients is increased aberrant expression of one of the D-type cyclins [16]. This was initially shown by gene expression profiling, but has since been confirmed on western blotting and immunohistochemistry [17,18]. This group of proteins is involved in the tight regulation of mammalian cell proliferation, acting to control entry to the cell cycle at the G1/S border. Primary genetic events in MM lead directly and indirectly to upregulation of CCND-1, -2 or -3, which therefore constitutes a major oncogenic phenomenon in MM. MM patients may be classified by their translocation and cyclin D-type status [15] (see Table 1-2) and this has been shown to have biological correlates and prognostic relevance [19].

Secondary genetic events occur during the progression to symptomatic MM. These include copy number changes, mutations, e.g. in the RAS oncogenes, and epigenetic changes, that are likely to influence prognosis. At disease relapse, progression events (e.g. translocations involving the *c-MYC* gene - t(8;14) - and mutations or deletions causing loss of *TP53* function) and the emergence of dominant and/or drug resistant clones [20] makes the disease more difficult to treat. The acquisition of TP53 loss often heralds end-stage disease.

1.1.4 Current treatment approaches and disease course.

Management of MM should be directed towards both disease modification and symptom control. Despite significant improvements in clinical outcomes and overall survival associated with a broader array of more effective novel therapies, the condition remains incurable. Consequently all treatment decisions need to weigh up the short and medium term disease reduction benefits with the not-insignificant treatment-associated toxicities that may persist and accumulate over the course of the disease.

Management strategies will be principally determined by the age and comorbidities of a patient (Figure 1-2); those patients that are medically 'fit' (usually <65 years old, without major renal, cardiac, liver or lung dysfunction) are candidates for intensive chemotherapy ('induction therapy'), consolidated with high-dose melphalan and autologous stem cell transplant (ASCT) [21]. The aim of this is to achieve as deep a

remission as possible, as this is believed to correlate with longer-term disease control. Of note, agents used at induction need to have minimal stem cell toxicity in order to allow sufficient numbers of patient stem cells to be harvested prior to treatment with high dose melphalan.

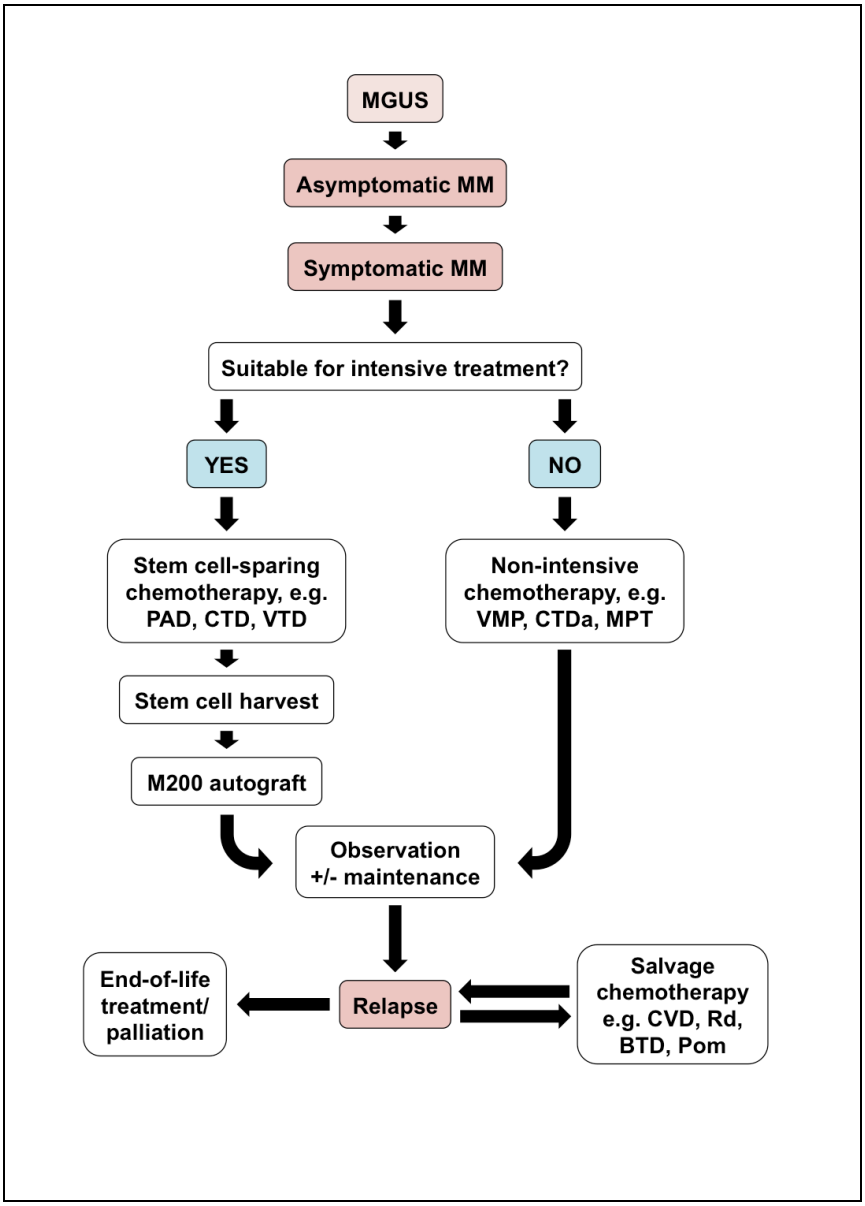

Figure 1-2 Natural history and treatment overview in multiple myeloma.

Abbreviations: PAD, bortezomib, adriamycin, dexamethasone; CTD(a), cyclophosphamide, thalidomide, dexamethasone (attenuated); VTD, bortezomib, thalidomide, dexamethasone; VMP, bortezomib, melphalan, prednisolone; MPT, melphalan, prednisolone, thalidomide; M200, melphalan 200mg/m^2; CVD, cyclophosphamide, bortezomib, dexamethasone; Rd, lenalidomide, dexamethasone; BTD, bendamustine, thalidomide, dexamethasone; Pom, pomalidomide (adapted from Myeloma and MGUS, M J Streetly, Medicine 41:5).

The standard of care for ASCT-eligible patients is generally a triple regimen incorporating bortezomib (e.g. PAD, VTD; Figure 1-2), as this has been shown to achieve deeper responses more quickly [22], before consolidation with high-dose melphalan. Patients who are not fit for intensive chemotherapy are treated on chemotherapy regimens that are often dose- and schedule-adjusted to reduce toxicities and improve tolerability.

Anti-myeloma agents are combined in a number of different regimens and at different doses depending on disease stage and treatment goal. Melphalan, for example is used at 200mg/m^2 in the context of high dose therapy with ASCT (also known as M200 autograft). It is also prescribed in elderly patients unfit for intensive treatment, at 0.25mg/kg orally, in combination with prednisolone and thalidomide. The characteristics of the commonly used and more novel anti-myeloma agents are summarised in Table 1-3**.**

Response to treatment is assessed by a number of parameters in combination: serum or urine paraprotein quantification by protein electrophoresis, serum free light chain quantification and BM plasma cell infiltration on trephine biopsy. Clinical parameters, such as reduction in bone pain, and radiological assessments are also valuable.

In addition to disease-modifying approaches, supportive care is critical in MM. Bone disease is tackled specifically using bisphosphonates, and pain is managed pro-actively with analgesia (non-opiate and opiate), titrated carefully to minimise toxicity. Blood product support, in the form of red cell or platelet transfusions, are useful at all stages of disease for symptom-relief and to allow effective delivery of chemotherapy. Surgical interventions, such as vertebroplasty or kyphoplasty, and radiotherapy may also be useful in the context of troublesome or isolated bone or soft tissue disease.

Table 1-3 Key anti-myeloma agents.

Compound	Context of use	Mechanism of action
Steroids, e.g. dexamethasone, prednisolone	Component of majority of chemotherapy combinations. Presentation & relapse.	Immunomodulatory and directly toxic to lymphocytes.
Cyclophosphamide	CVD, CTD(a). Presentation & relapse.	Alkylating agent.
Adriamycin	PAD. Presentation.	Cytotoxic anthracycline.
Melphalan	M200 autograft, MPT, MPR, VMP. Presentation & relapse.	Alkylating agent.
Bortezomib	PAD, CVD, VTD. Presentation & relapse.	Reversible proteasome inhibitor.
Thalidomide	CTD, MPT, VTD, BTD. Presentation & relapse.	Anti-angiogenic.
Lenalidomide	Rd. Relapse.	Immunomodulatory, anti-angiogenic, apoptotic.
Pomalidomide	Pom/D. Relapse.	Immunomodulatory, anti-angiogenic.
Bendamustine	BD, BTD. Relapse.	Alkylating agent.

Abbreviations: CVD, cyclophosphamide, bortezomib, dexamethasone; CTD(a), cyclophosphamide, thalidomide, dexamethasone (attenuated); PAD, bortezomib, adriamycin, dexamethasone; M200, melphalan 200mg/m^2; MPT, melphalan, prednisolone, thalidomide; MPR, melphalan, prednisolone, lenalidomide; VMP, bortezomib, melphalan, prednisolone; VTD, bortezomib, thalidomide, dexamethasone; BTD, bendamustine, thalidomide, dexamethasone; Rd, lenalidomide, dexamethasone; Pom/D, pomalidomide, dexamethasone; BD, bendamustine, dexamethasone.

1.1.5 Clinical drug resistance

Eventually patients will become resistant to currently available anti-myeloma agents and/or are unable to receive chemotherapy because of co-morbidities including

treatment-related toxicities. The occurrence of disease relapse after the apparent eradication of all evidence of the clonal population (i.e. after so-called stringent complete response, defined by no evidence of clonal BM plasma cells, no detectable serum or urine monoclonal proteins, and normal serum free light chain quantification and ratio) indicates the persistent survival of a small population of clonal cells resistant to the original treatment. More frank drug resistance is seen when, clinically, there is the loss of disease response to an agent being currently used, and/or failure to respond to an agent that was previously effective.

1.2 Multiple myeloma - current biological models of drug resistance

1.2.1 The progenitor compartment

The cancer stem cell (CSC) is hypothesised to be responsible for tumorigenesis, disease relapse and metastases in malignant disease and putative CSCs have been identified in diverse malignancies including acute myeloid leukaemia [23], breast cancer [24], and brain tumours [25]. In these examples, fractions with distinctive phenotypes (e.g. CD34++CD48− in AML) have been identified which show consistently greater capacity to engraft in xenograft models, compared to the bulk tumour. These sub-populations have also been found to possess various 'stem cell' attributes: formation of spheroids *in vitro* [25]; expression of stem cell markers such as Oct-4 [24] and dysregulation of important self-renewal pathways such as Wnt, Hedgehog [26] and Notch.

The existence of a CSC in multiple myeloma was first proposed in 1977 when Hamburger and Salmon [27] established a soft agar-based assay to grow colonies of malignant plasma cells from the bone marrow aspirates of patients with MM. The authors demonstrated a plating efficiency of 0.001-0.1% with a linear relationship between the concentration of cells plated and the number of colonies generated; this supported the theory that each colony was derived from a single (stem) cell. The cells comprising each colony had plasmablast or plasma cell morphology, intra-cytoplasmic immunoglobulin and a high proportion of actively cycling cells.

It was not until 2004 that a specific phenotype was proposed for the putative MM-CSC. Syndecan-1 (CD138) is a transmembrane heparan sulfate proteoglycan and is a highly specific marker for terminally differentiated plasma cells, being absent from all other B-lineage and haematopoietic cells. Matsui et al. [28] postulated that the precursor population in MM might be clonally related to the bulk malignant cell population but lack the maturity marker and therefore be CD138-negative (CD138−). The heparan sulfate proteoglycans (HSPGs) are an important group of transmembrane macromolecules, comprising a core protein to which un-branched, polysaccharide heparan sulfate (HS) chains are covalently attached. Their pattern of expression is tightly regulated and cell type- and lineage-specific. They are thought to be involved in cell-cell and cell-matrix adhesion and also in cell proliferation (review [29]). HSPGs function both through their core protein and their attached HS chains. The core protein of syndecan-1 is known to bind integrin molecules [30] and signaling is believed to occur via the cytoplasmic domain, which contains peptide sequences that may interact with cytoskeletal proteins and serve as substrates for cellular kinases. Additionally the HS chains of HSPGs may bind and present a variety of proteins including cytokines. CXCL12 is an important chemokine within the BM plasma cell niche and the splice variant CXCL12γ has been demonstrated to bind HS chains with particular avidity [31].

Syndecan-1 is the principal HSPG expressed on malignant plasma cells and suppressing its expression results in the absence of HS chains on MM cells, coupled with reduced cell proliferation and survival [32,33]. It has been shown to bind a number of chemokines, cytokines, growth factors and ECM proteins in MM: it acts as a co-receptor for hepatocyte growth factor (HGF) and other members of the epidermal growth factor (EGF) family [34], promoting signaling via the phosphatidylinositol 3-kinase (PI3K)/AKT and RAS/mitogen-activated protein kinase (MAPK) pro-survival pathways. Two other important growth factors for MM cells within the BM niche are A PRoliferation-Inducing Ligand (APRIL) and B-cell activating factor (BAFF) which both act through the nuclear factor-κB (NF-κB) as well as the PI3/AKT and MAPK pathways. Both factors bind to B-cell maturation antigen (BCMA) and transmembrane-activator and calcium-modulator and cyclophilin ligand-interactor (TACI) receptors, which are widely expressed on MM cells, but it is known that the activation of TACI by APRIL usually requires interaction with syndecan-1 [35,36].

Matsui's hypothesis that the CD138− sub-population of the MM clone was clonogenic was supported by the finding of clonotypic (clonally-related) circulating B-cells in the peripheral blood of some MM patients [37-39]. Matsui's group evaluated CD138+ and CD138− sub-populations within two human myeloma cell lines (HMCL), RPMI-8226 and NCI-H929. It was shown that the CD138− cells had greater colony-forming ('clonogenic') potential than the CD138+ cells within an *in vitro* colony-forming assay; they expressed typical B-cell antigens such as CD19 and CD20 and they appeared more proliferative (higher Ki67 expression). This pattern was also seen in primary tumour cells isolated from MM patient BM aspirates (21 out of 24 aspirates) and a smaller number of patient PB samples (two out of four); CD138+CD34− MNCs were compared to CD138−CD34− MNCs, both presumed to be clonal. Primary CD138−CD34− BM MNCs successfully engrafted into NOD/SCID mice, with subsequent infiltration of the murine BM by human CD138+ cells and detectable human immunoglobulin (matching the original patient isotype) in the peripheral blood of the mice. In contrast, primary CD138+CD34− BM MNCs did not engraft or recapitulate disease in the NOD/SCID system. Colony formation (assessed by the *in vitro* colony-forming assay) was reduced by depleting the CD138−CD34− BM MNCs of CD45+CD19+CD22+ cells or by treating with a monoclonal anti-CD20 antibody (Rituximab).

Following this landmark work, Matsui et al. [40] extended their characterisation of the MM CSC by demonstrating persisting clonogenicity of HMCL-derived CD138− cells after treatment with commonly used anti-MM agents, specifically dexamethasone, lenalidomide, bortezomib and cyclophosphamide. This was also seen in primary MM cells and supported the concept of a drug resistant stem cell compartment. Additional stem cell characteristics were reported in the HMCL CD138− sub-population: enhanced ABCG2/BCRP transporter activity (Hoescht side population assay), high aldehyde dehydrogenase activity (Aldefluor assay) and quiescence. Further evidence for the CD20+CD27+ phenotype was provided by demonstrating reduced colony formation following (i) depletion of CD138− cells bearing these antigens using Microbeads; (ii) treatment of CD138− cells with Rituximab (anti-CD20) or (iii) treatment of CD138− cells with Alemtuzumab (anti-CD52). Finally CD138−CD19+CD27+ B cells were isolated from the peripheral blood of four patients with MM and all were successfully engrafted into NOD/SCID

mice, with resultant human CD138+ marrow infiltration. The clonality of the cells was demonstrated by PCR of patient-specific sequences in the immunoglobulin heavy chain gene.

In a parallel study by the same group, Peacock et al. [41] reported on the role of Hedgehog (Hh) signaling in MM cancer stem cells. The greatest Hh activity was concentrated in the CD138−CD19+ subset of HMCL and primary MM cells. Administration of an Hh ligand promoted expansion of this compartment, without differentiation, and blockade of the Hh pathway inhibited colony formation by CD138− cells and led to terminal differentiation into CD138+ cells. More recently this group [42] examined baseline telomerase activity (TA) in HMCL and primary MM cells and used imetelstat to block TA. Prolonged TA blockade in CD138− cells resulted in reduced telomere length and reduced clonogenicity. Seventy-two hour treatment of CD138− cells also reduced clonogenicity and led to downregulation of key stem cell genes such as *OCT3/4*, *NANOG*, *SOX2*, *GAS1* and *HES1*. Treatment of NOD/SCID mice with imetelstat after infusing HMCL reduced MM cell engraftment and prolonged survival, as did infusing HMCL pre-treated with imetelstat. Most recently the Matsui group used the 5T33 MM mouse model [43] to evaluate the CD138+ and CD138− fractions. Interestingly, in this setting the CD138+ fraction had greater clonogenic and tumour-initiating capacity, coupled with an increased proportion of side population cells and enhanced aldehyde dehydrogenase activity, when compared to the CD138− fraction.

MM CSCs were studied indirectly by Kirshner et al. [44]; they reported a novel system in which whole BM MNCs were cultured in a three-dimensional, semisolid media - Matrigel. When BM MNCs from normal donors were set up, the system recapitulated normal BM micro-architecture. This was lost when MM BM MNCs were cultured; they developed a more disordered three-dimensional structure. However, non-proliferating, clonogenic, CD20+ cells localised to the ‘endosteum’ (fibronectin/collagen coating wells), mimicking normal haematopoietic stem cells, and were resistant to melphalan.

Reports from other groups have challenged the postulated CD138− MM stem cell phenotype. In 1998 Yaccoby et al. devised a novel xenograft model for MM [45].

Primary MM cells were injected into fragments of human foetal bone implanted into SCID mice (so-called SCID-Hu model). Engraftment was confirmed by the finding of detectable human immunoglobulin in murine peripheral blood and the disease was recapitulated with high blood calcium levels and enhanced osteoclast activity in the human bone fragments, coupled with abnormally high bone resorption. This was the first model in which primary MM cells (as opposed to HMCL) were successfully engrafted into a xenograft host and the presence of the human BM microenvironment provided by a foetal bone fragment was clearly critical. Using this system, the group then went on to explore requirements for successful primary MM cell engraftment [46]. Purified CD38++CD45− primary BM plasma cells from MM patients consistently engrafted and proliferated in SCID-hu mouse models and sequential transfer of tumour cells into fresh murine hosts was possible. Unselected BM and peripheral blood MNCs from MM patients also engrafted. However, plasma cell-depleted (i.e. CD138−) BM and peripheral blood cells were not capable of engraftment.

A number of groups have demonstrated that CD138 (syndecan-1) plays a critical role in the growth, dissemination and survival of both HMCL and primary MM cells. In 2002 the Sanderson group [47] reported that overexpression of soluble syndecan-1 by the B cell line ARH-77 made it hyperinvasive in a collagen-gel model relative to controls. Reducing syndecan-1 expression [48] by three different methods inhibited the growth of both primary MM tumours in a SCID-Hu model and CAG myeloma cell line tumours in SCID mice. Impaired growth of MM cells was also seen when syndecan-1 was knocked down using small hairpin RNA (shRNA) in a different xenograft model [33]. More recently Reijmers et al. [32] evaluated the importance of syndecan-1 HS core proteins and HS side chains in HMCL. They demonstrated that knockdown of HS on HMCL reduced growth rates and increased baseline apoptosis *in vitro*. A similar effect was seen after knockdown of EXT1, a co-polymerase essential for HS side chain synthesis. *In vivo*, the same pattern was seen, with a striking suppression of tumour growth in the xenograft model when EXT1 was knocked down. They postulated that syndecan-1 and its side chains are crucial for growth and survival of MM cells due to their interactions with ligands in the BM microenvironment such as integrins and cytokines.

Following on from the observations of Matsui, a number of other groups sought to examine the CD138+ and CD138− subpopulations from the specific perspective of clonogenicity and so-called stem cell characteristics. Like Matsui's group, the Anderson group [49] utilised Hoescht 33342 staining to identify and characterise the so-called 'side population' (SP) in a number of HMCL and in primary MM BM samples. This technique has been used in a number of malignancies to identify cells that may have stem cell-like properties, with distinctive flow cytometric characteristics owing to enhanced efflux of the DNA-binding dye Hoescht 33342. The group observed that the SP cells expressed CD138 (in contrast to Matsui's findings) had enhanced ABCG2 transporter expression and activity and higher proliferation compared to non-SP cells. SP cells possessed both clonogenic potential and the capacity to regenerate the original population containing both SP and non-SP fractions. *In vivo*, the SP population had higher tumorigenicity compared to non-SP cells. Interestingly, adherence to BM stroma increased the size and activity of the SP fraction. Thus this work seemed to suggest that clonogenic function was independent of CD138 expression levels. The side population was also evaluated by Nara et al. [50]. SP and non-SP cells were isolated from a number of HMCL (including RPMI-8226) and CD138− populations were found in both. Serial transplantation of both SP and non-SP cells into NOD/Shi-SCID IL-2γnul mice revealed that SP cells had a much greater capacity for self-renewal. In keeping with this, HMCL SP cells upregulated a number of oncogenes involved in cell cycle and mitosis, such as *CCNB1*, when compared to non-SP cells, and some of the same genes were upregulated in primary MM SPs.

These findings were supported by those of Chiron et al., who examined the clonogenicity of the CD138+ and CD138− fractions of two primary plasma cell leukaemia samples [51]. In both patients, the number of colonies generated correlated directly to the percentage of CD138+ cells in the starting cell fraction, with no colonies generated by the CD138− fractions. A novel cell line was generated from the CD138+ fraction of one primary sample.

The impact of CD138 expression on clinical outcome has only been reported by one group: Kawano et al. [52] analysed a large series of primary MM BM samples (90 new diagnosis, 15 relapse), specifically evaluating the phenotype of CD38++ clonal

tumour cells, and dividing them into patients with 'high' CD138 (>20% CD38++CD138−) and 'low' CD138 (<20% CD38++CD138−). A correlation between relapsed/progressive disease and low CD138 expression was found, and in patients with newly diagnosed MM or in those receiving high-dose melphalan with autologous stem cell rescue, a poorer outcome and reduced overall survival was seen in those with low CD138. Two cell lines were established from a single MM patient with low CD138 expression, derived from the CD138− (KYMM-1) and CD138+ (KYMM-2) MM cells. When expression of key B lineage genes was examined, KYMM-1 had a more immature phenotype with upregulation of *BCL6* and *PAX5*, and downregulation of *IRF4*, *PRDM1* and *XPB1*, when compared to KYMM-2. In killing assays, KYMM-1 cells were less sensitive to lenalidomide. It was hypothesised that these features were associated with lower CD138 expression.

Hosen et al. [53] sought to clarify whether Matsui's subpopulation of CD138−CD19+ clonogenic cells was the same as the clonotypic CD19+ B cells previously identified by groups such as Pilarski et al. Their *in vitro* MM colony-forming cells were enriched for CD138−CD19−CD38++ plasma cells, while in contrast CD19+ B cells failed to generate MM colonies. *In vivo*, in a SCID-rab model, CD138−CD19−CD38++ plasma cells and CD138+ plasma cells engrafted (three out of nine and four out of nine respectively) while CD19+ B cells did not. This suggested that CD19+ clonal MM cells lacked the capacity to engraft, in contrast to Matsui's reports.

The ability of different primary MM BM cell fractions to engraft different xenograft models (NOD/SCID, NSG or RAG2−/γc− mice) was evaluated by Kim et al [54]. A clonogenic CD38++CD138+ fraction was identified prospectively, which was capable of repopulating a human foetal bone graft with clonotypic CD19+CD38low and CD38+CD138+. Sub-fractionating CD38++CD138+ cells showed that specifically CD45low/− or CD19− cells were capable of engraftment, while those that were CD45+ or CD19+ were not. Some of the inconsistencies between their findings and those of Matsui et al. were attributed to differences in the xenograft model, emphasising the critical role of the BM microenvironment in allowing engraftment of tumour-initiating MM stem cells.

Christensen et al. [55] examined 31 primary MM patient BM MNCs and two HMCL using the same flow cytometry-based strategies and antibodies as Matsui and found a number of important discrepancies. When MM BM MNCs were analysed immediately after sampling, a single CD138+ population was seen with no evidence of a second CD138− clonal population. However, if there was a time lag between sampling and analysis, a CD138− population was apparent. In all cases the CD138− cells were AnnexinV-positive (AV+), indicative of apoptosis. In optimally growing HMCL, the CD138− population was very small and also AV+. Dexamethasone (Dex) treatment and starvation were both able to generate increased percentages of CD138−AV+ cells. Finally, qPCR was employed to look for evidence of differential translation of CD138 in the two cell sub-populations but none was found. The group concluded that the CD138− subpopulation was an apoptotic artefact resulting from sampling and handling differences. This supports the observation that apoptotic MM cells shed syndecan-1, made in 1998 [56].

1.2.2 The bone marrow microenvironment

It is now well-accepted that the BM microenvironment is critical for maintaining the malignant clone *in vivo*, through the interactions of multiple pathways (for example, the PI3K/AKT-pathway, the JAK/Stat3-pathway and the NF-κB-pathway) in ways which are not fully understood. The critical players in the BM microenvironment are manifold and varied - the current list is tabulated in Table 1-4 - and these influence homing, migration and adhesion, and with that survival and potentially drug resistance.

These interactions also mediate the secondary effects of the malignant MM cells, for example bone disease. The hallmark uncoupling of the balanced functioning of bone-producing osteoblasts and bone-resorbing osteoclasts in MM is mediated through soluble factors. Receptor activator of NF-κB (RANK)/ RANK-ligand (RANKL) interactions, reduced osteoprotegrin (OPG) and increased MIP-1α all increase osteoclast activity, while MM cell-derived DKK1 and T cell-derived IL-3 inhibit osteoblast function. Osteoclasts are in turn potent producers of IL-6, APRIL and BAFF, further stimulating MM cell growth and survival.

Table 1-4 Factors mediating interactions between MM cells and the BM microenvironment.

Soluble factors	Cell types	Cell surface receptors	Extracellular matrix
IL-6 **IGF-1** **IL-3** **VEGF** **HGF** **MIP-1α** **DKK1** **TNF-α** **SDF-1** **APRIL** **BAFF** **MMP2, 7, 9**	Osteoblasts Osteoclasts Endothelial cells Bone marrow stromal cells Mesenchymal stromal cells T cells Dendritic cells Monocytes/ macrophages	Integrins • VLA-4 • LFA-1 • Integrin β7 CD44 CXCR4 CCR2, 7 N- and E-Cadherin	Collagen Laminin Fibronectin

Abbreviations: IL-3/6, interleukin-3/6; IGF-1, insulin-like growth factor I; VEGF, vascular endothelial growth factor; HGF, hepatocyte growth factor; MIP-1α, macrophage inflammatory protein-1α; DKK1, Dickkopf-related protein 1; TNF-α, tumour necrosis factor-α; SDF-1, stromal-derived factor-1; APRIL, a proliferation inducing ligand; BAFF, B cell activating factor; MMP, matrix metalloproteinases; LFA-1, lymphocyte function-associated antigen-1; VLA-4, very late antigen-4. Adapted from Khwaja et al, Chapter 6: The myeloma bone marrow microenvironment and survival signaling. Myeloma. Cambridge University Press, 2014.

Initially it was believed that soluble factors within the BM liquid milieu were most important for the maintenance and expansion of MM cells *in vivo*. IL-6, VEGF, IGF-I, TNF-α, SDF-1α and CD40 are just some of the cytokines and growth factors which have been implicated in promoting MM cell survival (see reviews [57,58], Figure 1-3).

In 1994, Kim et al. [59] demonstrated that the adhesion of HMCL to vascular cellular adhesion molecule 1 (VCAM-1) on BMSCs upregulated IL-6 secretion by BMSC, which in turn induced proliferation and blocked apoptosis in HMCL. Paraformaldehyde fixation of BMSCs prior to co-culture with HMCL abrogated IL-6 secretion without impairing adherence [60], confirming the BMSCs as the source of the

soluble factor. IL-6 upregulation is triggered at least in part through the NF-κB-binding motif in the IL-6 gene promoter. IL-6 may act both as a proliferative factor and also to directly inhibit Dex-induced apoptosis [61].

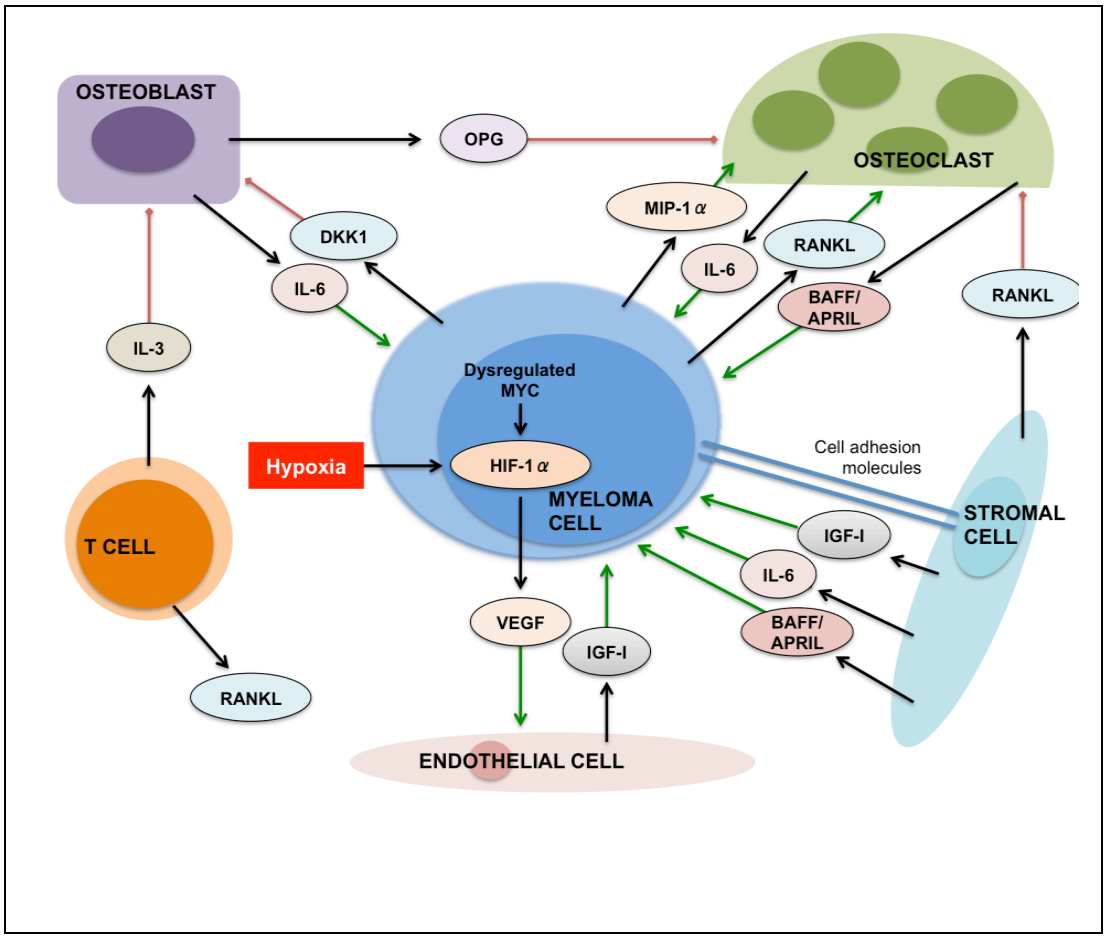

Figure 1-3 Interactions between myeloma cells and the bone marrow microenvironment.

This depicts five key cellular players within the BM microenvironment which interact with MM cells via soluble factors or direct cell-cell contact. Adapted from [58].

It has subsequently become apparent that cell-cell interactions are also critical, between myeloma cells and their multiple cell neighbours, including other haematopoietic cell types (B- and T-lymphocytes, NK cells, dendritic cells and macrophages, megakaryocytes and platelets) and non-haematopoietic BM stromal cells (fibroblasts, chondrocytes, osteoblasts and osteoclasts). The contributions of these two broad categories were examined by Dalton's group [62], in the context of drug resistance. They had previously demonstrated that HMCL and leukaemia cells adhering to the extracellular matrix (ECM) component fibronectin had increased

resistance to a number of cytotoxic drugs [63]. They went on to examine the influence of intact live BMSCs on HMCL sensitivity to the topoisomerase II inhibitor mitoxantrone. This was chosen as a surrogate for doxorubicin, the topoisomerase inhibitor used most commonly clinically against myeloma, because doxorubicin fluoresces and can therefore interfere with flow cytometry-based assays. They compared four culture conditions: (1) HMCL co-cultured (both adherent and non-adherent) with BMSCs; (2) HMCL adhered to BMSCs; (3) HMCL in Transwell-culture with BMSCs (i.e. without direct cell-cell contact); and (4) HMCL cultured in media conditioned by the prior presence of BMSCs. BMSCs were derived from normal healthy donors after long term culture of BM MNCs, and comprised predominantly fibroblasts. When NCI-H929 or RPMI-8226 cells were treated with mitoxantrone, those cultured alone in suspension had almost twice as much apoptosis compared to those co-cultured with BMSCs. When HMCL were co-cultured with BMSC for varying durations, then separated into stably adherent and suspension fractions, and then treated with mitoxantrone, the same trend was seen with significantly reduced killing in the BMSC-adherent HMCL. When HMCL cultured in Transwell inserts above BMSC were treated alongside HMCL cultured in BMSC-conditioned media, there was much greater killing seen in conditioned media. This implied that while soluble factors secreted by BMSC were important, a dynamic interplay was required between HMCL and BMSCs to stimulate production of the most protective factors by BMSCs. Interestingly the addition of anti-VEGF, anti-IL-6 or anti-bFGF blocking antibodies individually to the co-cultures did not ablate the protection, implying that a combination of factors was involved rather than a single dominant one. It was striking that when HMCL were co-cultured with BMSCs there was time-dependent inhibition of DNA synthesis (as assessed by [^{3}H]thymidine incorporation) in MM cells, indicative of cell cycle arrest. A BrdU uptake-based assay confirmed that this occurred in G1 phase. If a Transwell insert was used, such that MM cells were only exposed to soluble factors, the opposite finding was seen, with proliferation of HMCL. This highlights the importance of the cellular context - the additional cell-cell interactions present with direct co-culture clearly had a dramatic effect on the influence of secreted soluble factors on HMCL.

1.2.2.1 APRIL

A PRoliferation-Inducing Ligand (APRIL) is a member of the tumour necrosis factor (TNF) superfamily, with both structural and functional homology to other family members. It was first implicated in cancer in 1998, when it was found to be abundantly expressed in a number of different transformed cells lines and several cancer types [64]; recombinant APRIL was able to stimulate cell growth in various malignant cell lines.

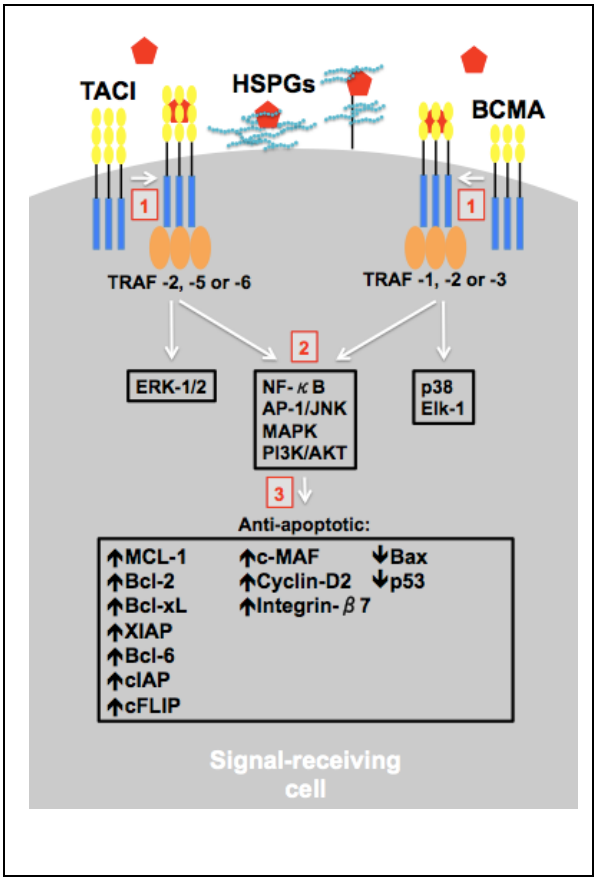

Figure 1-4 APRIL-driven signaling pathways.

APRIL (red hexagon) interacts with HSPGs, TACI and BCMA on the cell surface (1). This interaction with the latter two receptors triggers the recruitment of TRAF molecules, with resultant activation of a number of transcription factors (2). This leads to upregulation and downregulation of various proteins involved in apoptosis and cell survival (3). Abbreviations: HSPGs, heparin sulphate proteoglycans; TRAF, TNF-receptor associated factor. Adapted from [65].

APRIL acts via two receptors: B-cell maturation antigen (BCMA) and transmembrane-activator and calcium-modulator and cyclophilin ligand-interactor (TACI). These are both shared with another member of the TNF superfamily, B-cell

activation factor (BAFF, also known as BLyS), and binding of these receptors by APRIL or BAFF activates classical survival pathways including NF-κB [66] (see Figure 1-4).

There is now much greater understanding of APRIL's physiological importance. Initially Varfolomeev et al. [67] observed that an APRIL knockout mouse appeared to be entirely normal, in viability, fertility and in immune cell compartment number and function. It was therefore assumed that APRIL was dispensable and that BLyS/ BAFF was the dominant plasma cell survival factor in mice. Subsequently it was noted that these mice had decreased secreted IgA, secondary to defects in class-switch recombination [68]. This effect appeared to be mediated through the TACI receptor, with co-ligation of HSPGs playing an essential role within this pathway [69]. APRIL has also been shown to be a critical survival factor for activated B cells and plasmablasts in adult bone marrow, and once again co-binding to HSPGs appeared important [70]. This population of transitory plasmablasts required APRIL in order to differentiate into long-lived plasma cells, enhancing immunoglobulin responses. Plasma cells outside the BM have also been shown to require APRIL for their survival. Huard's group demonstrated that in human mucosal tissue, APRIL was secreted by neutrophils and retained by HSPGs in APRIL-rich 'plasma cell niches' containing increased numbers of IgG-producing plasma cells [71]. The same group went on to explore the source of APRIL within the BM [72], and demonstrated that APRIL production was triggered during haematopoiesis by stem cell factor, thrombopoietin, IL-3 and FMS-like tyrosine kinase 3 ligand. Thus secretion peaked in myeloid precursors, ensuring that haematopoiesis and long-term plasma cell survival were linked within the BM. The role of HSPGs in APRIL-plasma cell interactions was evaluated by Reijmers et al [73]. They knocked-down a key enzyme controlling HSPG chain flexibility, and thereby ligand binding, and demonstrated that this resulted in decreased plasma cells numbers and immunoglobulin levels. There appeared to be a particular failure to respond to APRIL-mediated survival signals, implying that normally conformed and functioning HSPGs are essential for the recruitment and retention of factors needed to support plasma cell survival. Syndecan-1 has been specifically shown to act as a co-receptor for APRIL and TACI on the MM cell surface [74].

It has been shown that the majority of HMCL and primary MM cells express either BCMA, TACI or BAFF-R [75], while APRIL and BLyS/BAFF are also consistently present in the BM of MM patients. Moreaux et al. were the first group to propose that APRIL and BAFF were directly implicated in drug resistance in MM cells [76]. They first confirmed the over-expression of BCMA, TACI and BAFF-R by HMCL and primary MM cells. APRIL and BAFF were also expressed by the majority of HMCL and primary MM cells, detectable as RNA and, in the case of APRIL, in the culture supernatant. IL-6-dependent HMCL (XG-13, -14 and -20) were able to proliferate in the absence of IL-6 if APRIL or BAFF were present, and were also protected from IL-6 deprivation-induced apoptosis. Cytokine-independent HMCLs proliferate autonomously, but growth of RPMI-8226 and L363 was blocked by the addition of the receptor antagonist TACI-Fc, and this effect could be reversed by the addition of excess recombinant APRIL and BAFF. These two lines were sensitive to Dex-induced apoptosis, but significant protection was seen in the presence of both APRIL and BAFF. Enhanced survival after Dex treatment was also seen in primary MM cells in the presence of APRIL or BAFF. These effects were mediated by NF-κB and PI3K/AKT pathway activation, and could be inhibited by small molecule inhibitors of these pathways.

Subsequently the same group demonstrated that differences in *TACI* gene expression and that of 658 other genes in primary MM tumours at diagnosis allowed two groups to be distinguished [77], with a BM microenvironment-dependent ($TACI^{high}$) and a plasmablastic signature ($TACI^{low}$). Importantly, $TACI^{low}$ patients had clinical parameters associated with a poorer clinical prognosis. Moreaux et al. also confirmed that monocytes, neutrophils and osteoclasts are the main source of BAFF and APRIL. The implication of this segregation was that $TACI^{high}$ patients might specifically benefit from treatment by BAFF/APRIL inhibitors. This was evaluated by Yaccoby et al. [78] when they tested two compounds: Atacicept (TACI-Ig) which blocks both APRIL and BAFF binding, and BAFFR-Ig, which only blocks BAFF. Using their SCID-hu model, they confirmed Moreaux's proposal, showing that the growth of MM cells derived from $TACI^{high}$ patients were inhibited by Atacicept to a much greater degree than those derived from $TACI^{low}$ patients. BAFFR-Ig treatment produced similar but weaker inhibition.

Our own group has recently demonstrated abundant expression of APRIL in MM patient BM trephines, synthesized by myeloid cells and taken up by MM cells [18]. It was also seen that APRIL stimulated cell cycle progression in primary CD138+ MM cells, but only in genetic sub-types of MM carrying two recurrent translocations into the IgH gene locus and expressing cyclin D2.

1.2.3 Survival pathways underlying drug resistance

A wide array of interacting factors have been implicated in MM cell survival and drug resistance, and these feed into a number of key cellular pathways known to be relevant in cell survival more broadly.

1.2.3.1 NF-κB

Dysregulated NF-κB signaling has been implicated in a number of cancer types, which reflects its central physiological role in immunity and inflammation. NF-κB itself is a key regulator of cell survival and proliferation, and may be activated by one of two routes: the canonical classical pathway, activated by ligands such as TNF, or the non-canonical alternative pathway, activated by APRIL/ BAFF. Within MM, a number of genetic abnormalities in NF-κB pathway components have been identified, for example TRAF3 deletion or inactivation of the negative regulator CYLD [79]. There are also a number of BM microenvironmental stimuli that seem to act through this pathway, including BAFF and APRIL [80] and adhesion to extracellular matrix components such as fibronectin [81]. Importantly, it is thought that the proteosome inhibitors, of which bortezomib (BZM) is the most widely used example, are potential antagonists to this pathway, although some groups have demonstrated resistant NF-κB activation in the presence of BZM [82].

1.2.3.2 PI3K/AKT/mTOR

PI3K proteins are a group of enzymes that activate downstream targets through a series of phosphorylation steps, leading to the activation of AKT and the formation of mTOR signaling complexes. Ultimately this pathway has a profound influence on cellular proliferation and survival through a host of complex positive and negative downstream regulators, and is commonly dysregulated in malignancy. This may occur through mutational events that either increase activation of the component

parts or through loss of function mutations that impair the natural inhibitors of the pathway, such as PTEN. In MM a number of the BM microenvironment factors, both soluble and contact-based, activate the PI3K pathway, including IL-6, IGF-I, BAFF and APRIL [18,76,83,84]. A number of preclinical studies have suggested that inhibitors of this pathway may be toxic to MM cells, particularly those with t(4;14) or t(14;16) [85], and the alkylphospholipid perifosine which impairs AKT activation has entered early phase clinical trials. It appears that combination treatments are most likely to be effective [86].

1.2.3.3 RAS/RAF/MEK

A large proportion of MM patients are found to have activating mutations in *NRAS* or *KRAS* genes [87]. RAS activation has numerous complex downstream targets, but a key effector is the RAF/MEK/MAPK protein complex. As with PI3K/AKT, a number of the known MM survival factors act through this pathway, including IL-6, IGF-I, MIP-1α and SDF-1.

1.2.3.4 JAK/STAT

IL-6 and SDF-1 are both considered to act via activation of JAK signaling in MM. Activated Janus tyrosine kinases then activate a number of downstream signaling pathways, including STAT, PI3K/AKT and RAS/RAF/MEK. Mutations in these factors are rare in MM but they are likely to be involved intermediates for a number of survival factors within the BM.

1.2.3.5 Notch signaling

In addition to soluble factors, the resistance offered by BMS in MM also results from interactions requiring direct cell-cell contact [62]. The Notch pathway is a highly conserved pathway with critical embryological roles in cell proliferation, survival, apoptosis and differentiation in a number of tissues. Increasingly it is a pathway of interest in the context of malignancy as it appears to be dysregulated or abnormally activated in a number of malignancies (reviewed in [88]), both solid, e.g. breast, lung, colon, and haematological, e.g. T-ALL [89]. There is growing evidence that the Notch pathway may be involved in both inherent and acquired drug resistance and has been

associated with cancer stem cells in a number of solid organ malignancies (breast cancer, glioma).

Mammalian cells may express any one or all of four cell-associated Notch receptors (Notch1, Notch2, Notch3 and Notch4), which may be activated by any one of five Notch ligands from either the Jagged- (Jagged1 (Jag1), Jag2) or Delta-like families (Delta-like Ligand1 (DL1), DL3, DL4) (see Figure 1-5).

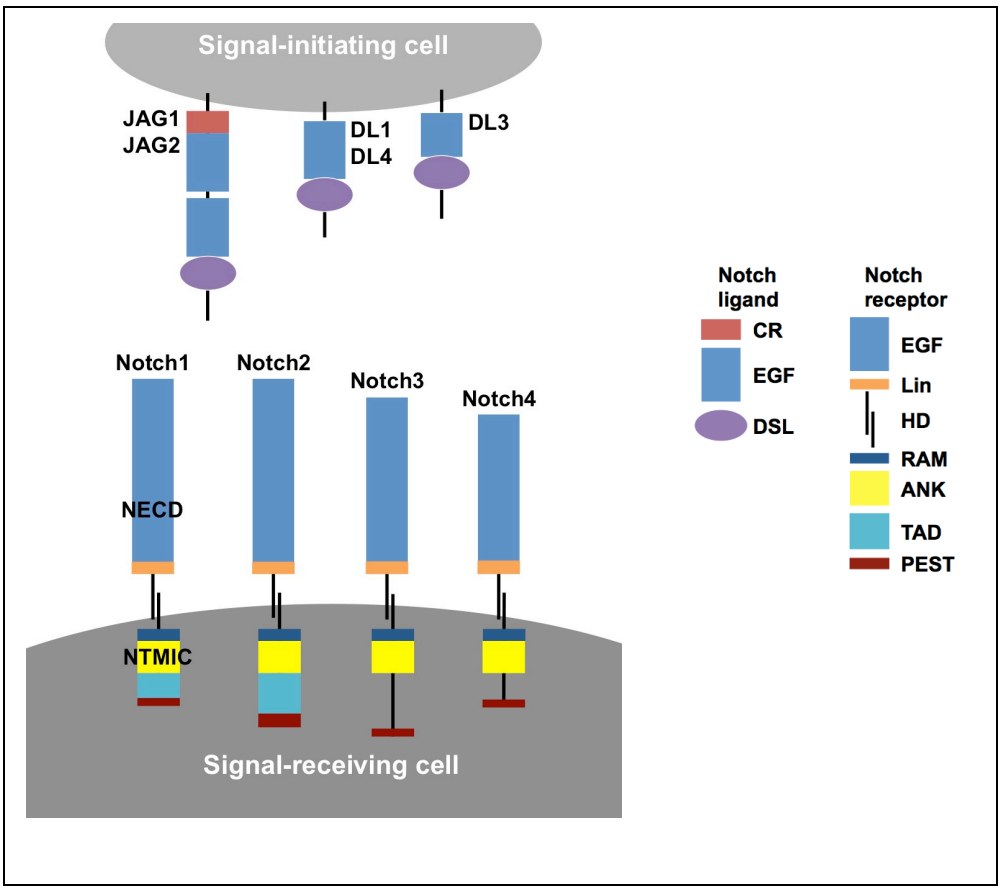

Figure 1-5 Mammalian Notch receptors and ligands

Signal-initiating cells express Notch ligands of the Jagged families (JAG1, JAG2) or Delta-like (DL1, DL3, DL4). There are four mammalian heterodimeric Notch receptors (Notch1, Notch2, Notch3 and Notch4) are expressed by signal-receiving cells. Abbreviations: NECD, Notch extracellular domain; NTMIC, Notch transmembrane and intracellular domain; CR, cysteine rich; EGF, epithelial-like growth factor; DSL, Delta, Serrate and Lag-2; Lin, LIN-12 repeats; HD, heterodimerisation domain; RAM, RBP-J-associated molecule; ANK, ankyrin repeats; TAD, transactivation domain; PEST, proline, glutamic acid, serine, threonine sequence; (adapted from [90]).

There is significant structural homology between both the ligands and the receptors. Epithelial growth factor-like (EGF) repeats and the distal amino-terminal domain called DSL (Delta, Serrate, and Lag-2) are present in all the ligands. DSL is involved in receptor binding. Jag1 and Jag2 contain an additional proximal cysteine-rich (CR) domain between the EGF-like repeats and the plasma membrane. The Notch receptors are heterodimeric - following translation, the Notch receptor polypeptide is glycosylated and then cleaved to form two subunits (see review [91]). These are the Notch extracellular domain (NECD) and the Notch transmembrane and intracellular domain (NTMIC) and they are transported to the cell membrane as a complex held together by non-covalent bonds between the N- and C- terminal halves of the heterodimerization domain. The NECD contains EGF-like repeats, a cysteine-rich LIN-12 repeats (LIN domain), which prevents ligand-independent activation, and the proximal HD domain. The NTMIC contains an RBP-J-associated molecule (RAM) domain (closest to the cell membrane), followed by ankyrin repeats (ANK) that bind to the CSL (CBF1/RBP-J/Suppressor of Hairless/LAG-1) transcription factor, a transactivation domain (TAD; only Notch1 and Notch2), and a PEST (proline, glutamic acid, serine, threonine) sequence that regulates the stability of NICD.

The mechanism of signal transduction is a hallmark of the Notch pathway - activation relies on the ligand causing proteolysis of the receptor, with the release of an active fragment capable of forming a transcription complex. Signaling is initiated when DSL and areas of the EGF-repeat domain of the ligand bind to particular EGF-repeats within NECD (Figure 1-6 (1)). This causes a conformational change in the Notch receptor, exposing a cleavage site in the NTMIC. Cleavage at this point by ADAM (A Disintergrin And Metalloprotease) proteases creates a membrane-tethered intermediate (Figure 1-6 (2)) called Notch extracellular truncation (NEXT), which is a substrate for gamma secretase.

The action of gamma secretase on NEXT releases the intracellular portion of the receptor (NICD; Figure 1-6 (3)) into the cytoplasm, from where it can translocate into the nucleus (Figure 1-6 (4)). Here NICD heterodimerizes with DNA-binding transcription factor CSL (Figure 1-6 (5)). CSL (CBF1/ RBP-J) is a transcriptional repressor but interaction with NICD converts it into a transcriptional activator. A complex is formed with additional transcriptional regulators such as MAML1. Thus

activation of Notch receptors leads directly to transcriptional de-repression of genes, including the HES and HEY families of transcription factors [92]. Recent work in T-ALL suggests that Notch signaling also activates the NF-κB pathway, mediated by Hes-1-induced suppression of CYLD [93], a negative regulator of NF-κB.

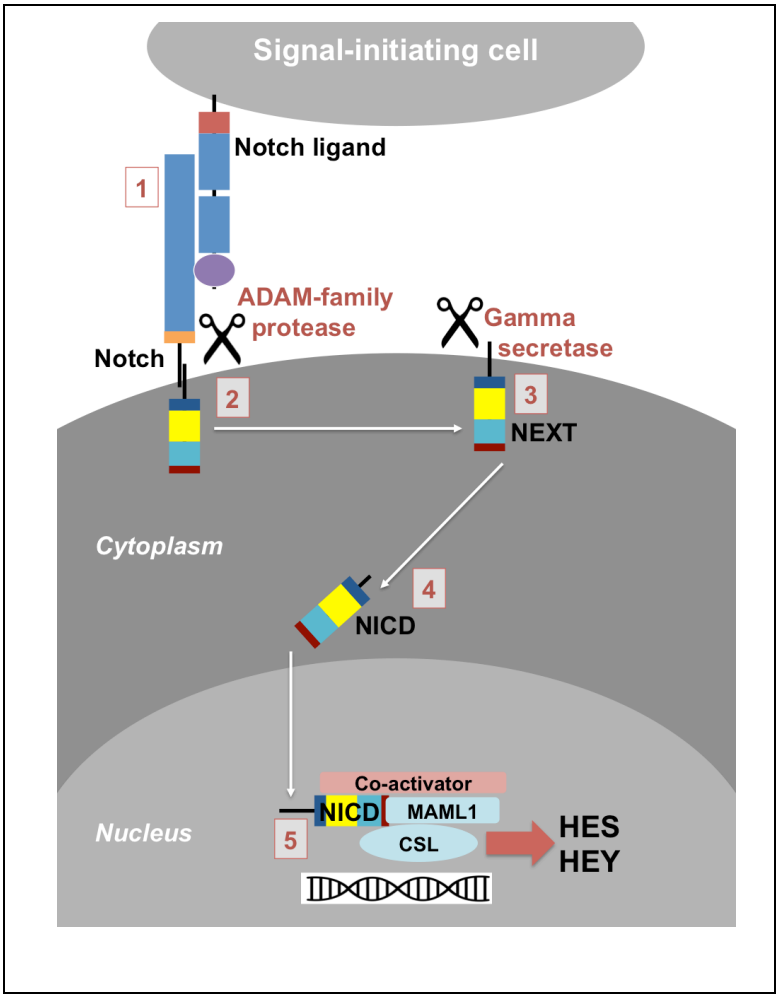

Figure 1-6 Activating the Notch signaling pathway.

Signaling is initiated by ligand binding to Notch receptor (1). This initiates two subsequent proteolytic cleavages of the Notch receptor by the ADAM-family protease (2) and then γ-secretase (3). The NICD is thus released into the cytoplasm (4) and translocates to the nucleus where NICD heterodimerises with the DNA-binding transcription factor CSL (5). Additional co-activators are also recruited, including mastermind-like proteins (MAML1-3) ultimately leading to transcription of downstream target genes, such as those belonging to the HES and HEY families. Abbreviations: ADAM, a disintergrin and metalloprotease; NEXT, Notch extracellular truncation; NICD, Notch intracellular domain; CSL, CBF1/RBP-J/Suppressor of Hairless/LAG-1; adapted from [90] and [91].

Activation of Notch signaling therefore requires interaction between cell surface receptors and membrane-associated ligands on adjacent cells. There is cross-talk with bi-directional signaling (both heterotropic and homotropic) activated by receptor-ligand interactions, allowing downstream modulations in both cell populations. The second cleavage step in Notch activation (Figure 1-6 (3)), in which gamma secretase acts on NEXT to release NICD into the cytoplasm, has become an attractive target for pharmacological intervention. Gamma secretase inhibitors (GSI) [94] are under investigation in a number of haematological malignancies but Notch proteins are not their only substrate - they may also cleave β-amyloid precursor protein (hence their use in Alzheimer's disease), syndecan and CD44. There are therefore potential off-target effects, which may be erroneously attributed to Notch pathway inhibition.

Notch ligands (Jag1/2, DL1/3/4) are expressed by BM stromal cells [95,96] and several genes involved in Notch signaling are aberrantly expressed in mouse plasmacytoma [97]. Notch receptors and ligands have been described in HMCL [96,98,99] and in primary tumours by immunohistochemistry (IHC) on BM sections. Skrtic et al. [100] evaluated Notch1 and Jag1 expression by IHC on 80 newly diagnosed MM BM trephines and 20 MGUS patients. Notch1 and Jag1 were both positive in 92% of MM but 0% of MGUS cases. Notch1 was strongly expressed in the majority whereas Jag1 expression was relatively weak. Progression from MGUS to MM was associated with upregulation of both proteins. There was no association between expression of either Notch1 or Jag1 and IgH translocation status or clinical outcome. However, strong Notch1 signaling was associated with a diffuse infiltrative pattern of BM involvement.

There do not appear to be fixed relationships between specific Notch receptors and their various ligands, with different ligands implicated in different disease settings or by different research groups. Cheng et al. [101] looked at the regulation of dendritic cell (DC) differentiation and demonstrated that while DL1 promoted DC maturation, Jag1 stimulated the accumulation of DC precursors and prevented their subsequent transition to a more mature phenotype. Expression of the two ligands by stromal cells differed by location, such that BM stroma was strongly Jag2+ whereas splenic stroma expressed more DL1, and Notch activation by the two ligands produced

different patterns of downstream HES1 expression. This suggests the presence of ligand-specific effects in which Notch signaling results in differing outcomes. Choi et al. [102] lent further support to this concept in their work looking at expression of Notch ligands by non-small cell lung cancer cell lines. Jag1, Jag2, DL1, and DL3 were all present, but Jag1 and Jag2 were differently regulated - in certain EGFR-dependent lines Jag1 expression was also dependent upon EGFR activation whereas Jag2 expression was not. Jag1 appeared critical for cell survival, whereas Jag2 functioned as a chemoattractant for human monocytes. Jag2 depletion led to enhanced expression of IL-1 and other related pro-inflammatory cytokines. In these lines at least distinct biological roles for Jag1 and Jag2 were present.

In 2004, Nefedova et al. [96] demonstrated Notch1 activation in HMCL (NCI-H929, RPMI-8226 & U266) after co-culture with primary BM stromal cells, fibroblast cell lines (3T3) expressing Jag1 and in the presence of soluble recombinant Jag1. This activation was evidenced by upregulation of the downstream target HES1 in HMCL expressing Notch1 and Notch2. Jag1-mediated Notch activation was associated with HMCL cell cycle arrest. When treating HMCL with melphalan and mitoxantrone, apoptosis could be attenuated by prior Notch1 activation, and it was therefore proposed that Notch-1 signaling might be a mechanism mediating BM stromal influence over MM cells, including drug resistance. Of note, they demonstrated that U266 cells lacked Notch1 and that they did not have any reduction in chemotherapy-associated killing in the presence of Jag1+ fibroblasts. After overexpressing either intact Notch1 or intracellular Notch1 in U266 cells, there was a significant increase in resistance to drug-induced apoptosis, suggesting that Notch1 was a critical requirement for drug resistance in this system.

In the same edition of Blood, Jundt et al. [98] described high Notch1, Notch2 and Jag1 expression on primary MM cells (detected by IHC) and HMCL (by Western blotting), in contrast to low or absent expression by non-maligant plasma cells. They also demonstrated baseline constitutive Notch activation in RPMI-8226, OPM-2, NCI-H929, LP-1 and U266 cells by RT-PCR of HES1. Upregulation of HES1 was seen in all but NCI-H929 and U266 cells after co-culture with Jag1+ HtTA-jag10 cells (a modified HeLa-derived cell line). Interestingly and in direct contrast to the findings of Nefedova et al., Jag1 exposure was associated with increased proliferation in all

HMCL with the exception of NCI-H929 and U266 cells (measured by thymidine incorporation). This effect could be inhibited by the addition of a gamma secretase inhibitor (GSI) - DAPT.

More recently the ability of GSI (unspecified, Enzo Life Sciences) to inhibit MM cell growth has also been demonstrated by Hu et al [103]. They treated RPMI-8226 cells with escalating doses of GSI and showed that proliferation (quantified by MTT assay) was inhibited in a dose- and time-dependent manner, with higher proportions of cells in G0/G1 after treatment. Notch1, Jag1 and Jag2 were downregulated in GSI-treated cells, in a similar dose- and time-dependent fashion. This appeared to confirm that Notch activation in MM cells causes proliferation.

Houde et al. [99] postulated a link between IL-6 and Notch activation; they proposed that when NICD binds CBF1/RBP-Jk, it is transformed into a transcription factor for, amongst other things, NF-κB2 and IL-6. Thus when the Notch pathway is activated in BM stromal cells (as opposed to in MM cells), IL-6 production and secretion might be induced, acting as a growth factor to adjacent MM cells. They demonstrated overexpression of Jag2 in a panel of HMCL (by RT-PCR, IHC, flow cytometry and Western blotting), when compared to non-MM cell lines and normal peripheral blood plasmablasts. The relevance of this finding was confirmed by demonstrating similar Jag2 overexpression in a series of MM and MGUS patient samples. Notch1/2/3/4 and Jag1 were variably present in the HMCL. Interestingly, in the U266 cells evaluated Notch1 was present (albeit at much lower levels than those seen in other lines) and Notch2 was absent; this contradicts the findings of Nefedova and Jundt et al. and does suggest that expression of Notch receptor subtypes is not fixed. Jag2 overexpression was attributed to hypomethylation of the Jag2 promoter sequence. Co-culture of MRC5 immortalised fibroblasts with RPMI-8226 cells was associated with induction of HES1 expression by the fibroblasts, at a level proportional to the number of MM cells in the co-culture. This was accompanied by an increase in IL-6 detected in the culture supernatant, which was not seen when a Transwell insert was used to separate the two cell types. VEGF, IGF-I and IGF-II were also increased in the co-culture. Incubation of the MRC5 cells with a Jag2-binding peptide (which activates Notch signaling) had a similar effect on IL-6, VEGF and IGF-I secretion, while use of an anti-Notch1 monoclonal antibody (shown

to block Notch signaling) reversed the effect of co-culture with MM cells. Thus it appeared in this system that Jag2++ MM cells were inducing IL-6 production by stromal cells via activation of the Notch pathway, and this may be an important mechanism by which Notch signaling promotes MM cell survival and proliferation.

Chiron et al. [104] also argued for a critical role of Jag2 in MM self-renewal. In 2012 they demonstrated that only HMCL expressing high levels of Jag2 were capable of spontaneous colony formation in additive-free collagen. Jag1 and Notch1/2 receptors were widely expressed in HMCL but did not correlate with colony formation. The addition of Notch1/2-Fc to previously clonogenic HMCL (KMM1 & JJN3) inhibited colony formation by 90%, as did stable silencing of Jag2 expression using shRNA.

In 2005 Zweidler-McKay et al. [105] explored the issue of whether Notch activation caused proliferation or cell cycle arrest in a number of haematological malignancies by transducing various malignant B- (including RPMI-8226, NCI-H929 and U266) and T-cell lines with constitutively active Notch1-4 receptors. All four activated receptor subtypes were capable of inducing cell cycle arrest in B-cell malignancies but had the opposite effect on T-cell malignancies. This effect was also achieved by transducing the cells with HES1, suggesting that it was a key regulator of this phenomenon.

Nefedova et al. [106] reported on the effects of Notch signaling on the sensitivity of MM cells to anti-myeloma drugs in 2008. They inhibited Notch signaling pharmacologically using a GSI (GSI-XII, Z-IL-CHO, Calbiochem) and demonstrated a reduction in MM cell Notch activity using both a luciferase reporter assay and RT-PCR to confirm HES1 downregulation. MTT assays confirmed that GSI treatment led to a reduction in the viability of HMCL and primary MM cells but not of normal BM stromal cells. AV/PI staining confirmed that this was secondary to apoptosis, and time course measurements of HES1 expression and apoptosis confirmed that HES1 downregulation preceded any evidence of apoptosis in MM cells. When HES1 was overexpressed in HMCL, the apoptotic effects of the GSI were reduced. When HMCL were co-cultured on a BMS monolayer, the stroma-associated protection seen against doxorubicin-mediated or mitoxantrone-mediated killing was reduced in the presence of GSI. *In vivo*, in a SCID/NOD xenograft MM tumour model, tumour

growth was significantly reduced when mice were co-treated with GSI and doxorubicin, while modest results were seen after the same doses of single agents. The same result was seen when the SCID/hu model was employed and serum human immunoglobulin levels were assayed. They concluded that pharmacological inhibition of Notch signaling in MM cells abrogates BM-mediated drug resistance and sensitises MM cells to chemotherapy, implying that a major route of BM-mediated protection is the activation of Notch signaling in MM cells by Notch ligands present on stroma cells.

This group subsequently evaluated the effect of combination treatment with GSI-XII and the proteosome inhibitor bortezomib (BZM) [107]. HMCL (NCI-H929, RPMI-8226, U266) and primary CD138+ MM cells were treated with low doses of GSI-XII (3-5μM, Calbiochem, as before) and BZM (2-3 nM) singly and together. This confirmed potent synergistic cytotoxicity from the combination. Interestingly, when active Notch1 ICD was overexpressed in HMCL, GSI-XII+BZM-associated apoptosis was reduced but not completely prevented. This suggested that other Notch-independent mechanisms might be involved. For comparison, an alternative GSI - DAPT (GSI-IX, Calbiochem) - was combined with BZM. This combination did not result in synergistic cytotoxicity, and Notch inhibition was confirmed by a dose-dependent reduction in HES1 expression in HMCL treated with DAPT alone. Thus it appeared that GSI-XII specifically synergised with BZM via a Notch-independent route. Further investigations revealed that GSI-XII had an additional ability to inhibit trypsin-like activity within the proteosome. This study highlights the dangers of attributing all GSI-associated effects to Notch pathway inhibition.

An independent study reported by Xu et al. [108] also examined potential interactions between the Notch pathway and BZM effects in MM. This group had previously reported that a modified MS5 stromal line expressing the Notch ligand DL1 was able to activate Notch signaling in murine (5T33MMvt) and human MM cells in co-cultures [109], with upregulation of a number of downstream Notch targets including HES1. This activation could be blocked with the GSI DAPT. Interestingly the group also demonstrated that Notch activation was associated with enhanced colony-forming capabilities, which was similarly inhibited by DAPT. This enhanced clonogenicity had *in vivo* implications as murine 5T33MMvt cells with prior Notch

activation engrafted more rapidly into naive animals with more rapid disease development. Cell cycle analysis of the murine MM cells revealed an association between Notch activation and a higher percentage of cells in S phase.

Their subsequent work with BZM [108] used the same method of Notch activation (MS5.Dll1 stromal cells). In MM cells, Notch2 appeared to mediate Notch signaling - after co-culture, Notch2 was decreased and NICD2 was upregulated. Both murine and human MM cell lines were less sensitive to BZM after prior Notch stimulation but became more sensitive after co-treatment with DAPT. A drug resistance and metabolism gene array was used to investigate molecular mechanisms for this effect, and the cytochrome P450 enzyme CYP1A1 and its transcription factor AhR were identified as potential players. DL1 stimulation led to downregulation of AhR expression but upregulation of CYP1A1, implying that the latter's upregulation after DL1/Notch interaction was independent of its usual transcription factor. When CYP1A1 activity was inhibited either pharmacologically or using siRNA, BZM sensitivity was restored in DL1-stimulated MM cells. *In vivo*, in the 5T33MMvv model, co-treatment of mice with BZM and DAPT enhanced their survival compared to those treated with BZM or DAPT alone, and DAPT treatment was associated with downregulation of Notch targets. It is interesting that the synergistic killing of MM cells by DAPT and BZM seen in this model is in contrast to the absence of synergism seen by Nefedova's group when a different panel of HMCL and primary CD138+ MM cells were evaluated (see above [107]).

The effects of a novel Notch pathway inhibitor, arsenic trioxide (ATO), were reported by Hu et al [110]. ATO treatment caused dose-dependent growth inhibition of RPMI-8226 cells (MTT assay), associated with both cell cycle arrest in G0/G1 and apoptosis. There was a dose-dependent reduction in the expression of Notch1 and Jag2 in ATO-treated cells, coupled with a reduction in HES1 transcripts. The PI3P/AKT pathway inhibitor PTEN was upregulated after ATO treatment. This suggests potential cross-talk between the Notch signaling pathway and the pro-survival PI3P/AKT pathway, and may be another mechanism by which Notch activation promotes MM cell survival.

Schwarzer et al. [111] also examined the effect of GSI treatment on MM cells, but looked specifically at the impact on MM cell-osteoclast (OCL) interactions. They treated HMCL classed as Notch1+ (OPM-2, LP-1, NCI-H929) and Notch1− (U266) with GSI 15 (RH02015SC, Maybridge, Acros Organics). In OPM-2 cells, which had high baseline HES1 expression, a dose-dependent reduction in HES1 and a concomitant reduction in cell proliferation was seen. No effect on proliferation was seen in U266 cells, implying that the effect was specific to Notch1. The anti-proliferative effect was secondary to apoptosis, as evidenced by AVPI staining and cleaved PARP levels. When OPM-2 cells were co-cultured with human OCL, upregulation of HES1 was seen in the OCL but not in OPM-2. When co-cultured OPM-2 and OCL were treated with GSI15, apoptosis was seen in both cell types, coupled with downregulation of HES1 and markers of OCL activity. Osteoblasts and mesenchymal stem cells co-cultured with OPM-2 did not appear sensitive to GSI15, with no sign of apoptosis or changes in proliferation in these cell types. Schwarzer's group proposed that Notch signaling is a critical part of the specific interaction between MM cells and osteoclasts, and may play a key role in the evolution of bone disease in MM.

Stromal cell-derived factor-1 (SDF-1) and its receptor CXCR4 mediate MM cell localisation within the BM and some interactions with osteoblasts and osteoclasts. Elevated serum SDF-1 levels are associated with MM bone disease and CXCR4 expression correlates with poorer clinical outcomes. Mirandola et al. [112] reported an interaction between Notch receptors and the SDF-1/CXCR4 axis. GSI (GSI-XII) treatment reduced the viability of KMS-12, OPM-2 and RPMI-8226 cells, although interestingly this was associated with an increase in the G2/M phase (and a comparable reduction in G0/G1 and S phases). This contrasts to the findings of Hu et al [103,110]. Notch pathway inhibition by GSI-XII was confirmed by the observation of HES1 downregulation after treatment. This was coupled with a reduction in SDF-1 and CXCR4 expression (seen both by RT-PCR and flow cytometry (for surface CXCR4) and ELISA (for secreted SDF-1 in conditioned culture medium)). These findings were also seen after treatment with a highly specific Notch pathway inhibitor - SAHM1 (an antagonist for the Notch co-activator MAML1). The functional consequence of Notch-blockade (by GSI-XII) was a reduction in CXCR4-driven migration of MM cells along a SDF-1 gradient. Forced Notch1 activation (by

transfection with extracellular domain-deleted, constitutively active Notch1) led to upregulation of SDF-1 and CXCR4, and this was shown to result from an interaction between ICN1 and the CXCR4 promoter. Having confirmed CXCR4/SDF-1 axis activity in the studied HMCL, the group then demonstrated that hyper-stimulation of this pathway was able to overcome GSI-XII-associated decrease in viability and cell cycle arrest.

- **Cellular effects of Notch receptor-mediated signaling in MM cells**

Diverse mechanisms have been proposed to explain the protective effect of Notch activation in MM cells and it is highly likely that there are complex interactions with other more classic pro-survival pathways. The binding of APRIL to its receptors, TACI and BCMA, activates NF-κB and PI3K pathways [76,113,114] and thus Notch activation by BM-derived ligands, such as Jag1, may boost pathway activation triggered by APRIL. HES1 also acts to downregulate PTEN, a negative regulator of PI3K activity [115], hence activated Notch receptors may co-operate with APRIL to potentiate PI3K pathway activation. These interactions provide a rationale for investigating potential synergy between these two pathways in promoting tumour cell survival. They may also explain the proliferative effect associated with Notch activation that has been reported in some systems.

1.2.4 The HS-5 stromal cell line

The HS-5 cell line was derived from human BM stromal cells, by immortalisation using replication-defective recombinant retrovirus containing the human papilloma virus E6/E7 genes (LXSN-16 E6E7) [116]. The HS-5 cells were described as fibroblastoid and shown to secrete significant levels of granulocyte colony-stimulating factor (G-CSF), granulocyte-macrophage-CSF (GM-CSF), macrophage-CSF (M-CSF), Kit ligand (KL), macrophage-inhibitory protein-1 alpha, interleukin-6 (IL-6), IL-8, and IL-11. Additionally, of all the derived human stromal lines, only HS-5 cells support the proliferation of hematopoietic progenitor cells when co-cultured in serum-deprived media with no exogenous factors. Conditioned media from HS-5 promotes growth of myeloid colonies to significantly greater extent than a cocktail of recombinant factors containing 10ng/mL of IL-1, IL-3, IL-6, G-CSF, GM-CSF, and KL and 3 U of erythropoietin (Epo).

Unmodified HS5 cells have been used to evaluate the contribution of the BM microenvironment in enhancing MM cell drug resistance - Perez et al. demonstrated that haemopoietic stroma induced resistance to Apo2L/TRAIL apoptosis in HMCL [117] and subsequently that this resistance could be partially reversed by BZM [118]. Co-culture of certain HMCL with HS5 induced or upregulated expression of tumour-associated B7-H1 molecules and this was attributed to IL-6 production by HS-5 cells.[119] B7-H1+ HMCL were more proliferative and less chemosensitive than their BY-H1- counterparts.

A direct comparison between primary long-term BM stromal cell cultures and HS5 cells in evaluating cell-cell contact mediated signals in myeloma was carried out by Schmidmaier et al. [120]; they concluded that HS5 cells were superior in this setting in terms of feasibility and reproducibility.

1.3 Hypotheses

This work aims to evaluate the following hypotheses:

- CD138− tumour cells derived from myeloma patient bone marrow aspirates displayed stem cell-like features including drug resistance, quiescence and enhanced clonogenicity, when compared to their CD138+ counterparts.
- APRIL offers protection to myeloma cells exposed to anti-myeloma agents and is therefore a potential effector of bone marrow microenvironmental drug resistance. The effects of APRIL vary between different genetic subtypes of MM.
- Notch pathway activation in MM cells renders them less sensitive to anti-myeloma agents. This mechanism contributes to the protection offered to MM cells by their BM microenvironment.

CHAPTER 2. MATERIALS AND METHODS

2.1 Cell culture

2.1.1 Human myeloma cell lines

The following autonomously growing human myeloma cell lines (HMCL) were routinely cultured in RPMI-1640 supplemented with 10% foetal bovine serum (FBS) and 1% penicillin/streptomycin (hereafter referred to as RPMI/10%FBS). Cells were usually grown in tissue-culture (TC)-treated 75cm^2 (TC75) flasks and passaged every 48-72 hours. The IgH/TCs found within each of these HMCLs are detailed Table 2-1 . HMCL were independently authenticated by LGC Standards.

Table 2-1 Human myeloma cell lines and D-type cyclin and genetic lesions.

Predominant D-type cyclin expressed and IgH/TC	**HMCL**
Cyclin D1 and t(11;14)	U266, KMS-12PE, KMS-21BM
Cyclin D2 and t(4;14)	NCI-H929, JIM3, OPM2, KMS-11, JJN3, JIM1
Cyclin D2 and t(14;16)	MM1S, KMS-11
Cyclin D2 and t(16;22)	RPMI-8226
Uncharacterised	KMS-27, KMS-28PE

2.1.2 Adherent cell lines

The following adherent cell lines (Table 2-2) were grown in Dulbecco modified Eagle Medium (DMEM, with glucose 4.5g/l and L-glutamine) supplemented with 10% foetal bovine serum (FBS) and 1% penicillin/streptomycin (hereafter referred to as DMEM/10%FBS). The cells were grown in TC75 flasks (lying flat) and passaged every 48-72 hours. The old media was aspirated and discarded and the cells washed gently with warmed Hank's balanced salt solution, which was then discarded. Warmed trypsin (0.25%)/EDTA was then added to the cells (2ml for a TC75 flask) and the cells were incubated at 37°C until the cells were fully dissociated from the flask and in a single cell suspension (five minutes). The trypsin was then neutralised by the addition of warmed DMEM/10% (twice the volume of the trypsin) and the

cells pipetted well to mix and further dissociate. The cells were split according to the growing speed and confluence of the starting population (usually 1:2-4) and the media topped up to a final volume of 8-10ml/TC75 flask.

Table 2-2 Characteristics of commonly used adherent cell lines.

Cell line	Abbreviation	Comments
Human Embryonic Kidney 293T cells	(HEK) 293T cells	Highly transfectable derivative of HEK-293T cells; used in transfection and transduction protocols.
Human Stromal-5 cells	HS5 cells	Human bone marrow stromal line derived from long-term bone marrow cells, transformed with the amphotropic retrovirus vector LXSN16E6E7. One of 27 different clones generated.

2.1.3 Reagents

Table 2-3 Commonly used reagents.

Reagent	Abbreviation	Product number	Manufacturer
Cell culture reagents			
Hank's balanced salt solution	HBSS	14175-053	Lonza
Foetal bovine serum (heat inactivated)	FBS	10500-064	Gibco
Bovine serum albumin	BSA	A2058	Sigma Aldrich
Phosphate buffered saline	PBS	17-516	Lonza
RPMI1640 (with L-glutamine)	R or RPMI	BE12-702F	Lonza
Dulbecco modified Eagle medium (with L-glutamine and 4.5g/l glucose)	DMEM	BE12-604F	Lonza
Trypsin (0.25%)/ EDTA		T4049-100ml	Sigma Aldrich
Ficoll-Paque PLUS		17-1440-02	GE Healthcare

Penicillin/Streptomycin	P/S	15140-122	Gibco
0.4% Trypan blue		T8154	Sigma Aldrich
autoMACS running buffer	ARB	130-091-221	Miltenyi Biotech
CD138 microbeads		130-051-301	Miltenyi Biotech
Matrigel basement membrane matrix	Matrigel	356234	BD
Human plasma fibronectin purified protein		FC010	Millipore
Human collagen type I		234138	Millipore
Recombinant growth factors			
A PRoliferation-Inducing Ligand (TNFSF13)	APRIL	884-AP	R&D Systems
Insulin-like growth factor-I	IGF-I	100-11	Peprotech
Interleukin-6	IL-6	200-06	Peprotech
Chemotherapeutic agents			
Dexamethasone (water soluble)	Dex	D2915	Sigma Aldrich
Bortezomib	BZM	Clinical excess	Janssen-Cilag Ltd
Lenalidomide	Len	sc-218656	Santa-Cruz Biotechnology
Melphalan		M2011	Sigma Aldrich

2.1.4 Plastic-ware and equipment

- 5ml, 10ml and 25ml sterile pipettes
- Tissue culture (TC)-treated 25 cm^2, 75cm^2 flasks and 175cm^2 flasks
- TC-treated 6-, 12-, 24-, 48- and 96-well plates
- TC-treated 10cm plates
- 10cm petri dishes

- 5ml polypropylene and polystyrene FACS tubes
- 15ml, 25ml and 50ml universal containers
- 0.5ml and 1.5ml sterile and RNase-free microtubes
- 20-40μm cell strainers

2.1.5 Trypan blue exclusion

This allowed determination of the number of viable cells in a cell suspension. Cell suspensions were diluted with 0.4% Trypan Blue (1:10-1:40) and applied to a haemocytometer. The viable cells were counted in all four quadrants of the chamber by light microscopy. The total number was divided by four and adjusted for the dilution factor, giving a viable cell concentration ($x10^4$/ml).

2.1.6 Preparation and handling of primary MM bone marrow mononuclear cells

2.1.6.1 Isolation of primary mononuclear cells from bone marrow aspirates by density centrifugation

Mononuclear cells (MNCs) and CD138-positive (CD138+) MM cells were isolated from fresh bone marrow (BM) aspirates from patients with MM (after informed consent and with full approval of local ethics committee). BM aspirate samples were collected into EDTA Vacutainer (BD) blood collection tubes at the bedside. The whole BM sample was then washed through a 40μm cell strainer with HBSS and made up to a total volume of 25ml with HBSS. This solution was layered carefully over 25ml of Ficoll-Paque media in a 50ml universal tube and centrifuged at 1,900rpm for 30 minutes with no acceleration or breaking. The mononuclear layer was carefully aspirated and re-suspended in 20ml of HBSS/5%FBS to wash the cells. The cell suspension was then centrifuged at 1,700rpm for ten minutes, the supernatant discarded and the pellet resuspended in media or buffer depending on the final destination of cells. The number of viable MNCs was ascertained by manual counting with a haemocytometer and using Trypan Blue dye exclusion.

2.1.6.2 Selection of primary CD138+ MM cells

Freshly isolated MNCs were resuspended in autoMACS running buffer (ARB) and CD138 Microbeads were added. The required volume of both was determined by cell number: 20µl of CD138 Microbeads and 80µl of ARB per $10x10^6$ viable cells. After thorough mixing, the cells were incubated for 20 minutes at 4°C. The cells were then washed with 10mls ARB and after centrifugation (1,600rpm, ten minutes) the pellet was resuspended in 1-3ml ARB (depending on total cell number) before being passed through a primed LS column set in a magnetic holder. The first run-through fraction of CD138-negative cells were set aside for further use as necessary. Having removed the column from the magnetic field, the CD138+ cells were flushed out of the column with further ARB and counted by Trypan Blue dye exclusion. Plasma cell purity was assessed by MGG-stained cytospins and flow cytometry.

2.1.6.3 Preparation of culture media for primary MM cell culture

Primary MM BM MNCs or CD138+ cells were cultured in RPMI containing 20% plasma pooled from MM patients (hereafter termed culture media; CM). Previous work in our group [18] had demonstrated superior survival of primary MM cells in this CM over RPMI/10%FBS (R10). Plasma samples were collected from MM patients (who were not on any active anti-myeloma treatment) into lithium-heparinised Vacutainers. These were centrifuged at 3,000rpm for 15 minutes and the plasma aspirated and pooled before freezing at −80°C. When required, the pooled plasma was thawed at 37°C and added to RPMI-1640 at a concentration of 20%. Prior to use, CM was passed through a 20µm filter. All CM was freshly prepared for each culture set up.

2.1.6.4 Cryopreservation of primary MM cells

A small number of experiments were performed on thawed CD138+ cells. These were frozen immediately after purification. The cells were pelleted at 1,500rpm for ten minutes and then resuspended in 100%FBS at 10^6/ml and placed on ice. An equal volume of freezing medium (80%FBS/20%DMSO) was added drop-wise over five minutes to the cell suspension with continual gentle agitation on ice and then the cell suspension was aliquoted into pre-chilled cryovials and frozen at −80°C using a freezing chamber (Mr Frosty) to ensure 1°C/min cooling.

2.1.6.5 Preparation of cytospins for staining and for cytogenetic analysis

Each slide required ~20,000 cells. The appropriate volume of cells in solution (at ~10^6/ml) was pipetted into a 1,500µl Eppendorf tube. The final volume was topped up to 100µl/slide with PBS. A glass slide was assembled with a piece of filter paper and the cytofunnel in a metal cage and the complex was placed into the cytospin centrifuge (Cytospin 3, Thermo Shandon). 95µl of the prepared cell suspension was pipetted into the cytofunnel and spun at 400rpm for two minutes. The slides were then removed and allowed to air-dry overnight before staining or sending for FISH analysis.

2.1.7 Culture of unselected BM MNCs

A variety of different approaches were used to culture MM BM MNCs (unselected or CD138-depeleted) with the goal of optimising *in vitro* MNC and LC-restricted subset survival over time periods of one to three weeks. The three-dimensional culture methodology employed by Kirshner's group [44] was trialled in various formats.

Certain materials were used specifically in the culture of primary MM BM MNCs and CD138+ cells:

- BD Matrigel basement membrane matrix (354234; BD)
- Human plasma fibronectin purified protein (FC010; Millipore)
- Human collagen type I (CC050; Millipore)

Prior to plating cells, tissue culture (TC)-treated wells were coated with collagen and fibronectin, as per Kirshner et al, to recapitulate the BM endosteum. Cells were cultured in RPMI/20% pooled MM patient plasma (thereafter referred to as culture media, CM). Previous work in our group [18] had demonstrated superior survival of primary MM cells in this culture media over RPMI/10% FBS (R10). Additionally a number of MM BM MNCs were cultured suspended in a semi-solid culture media (Matrigel), sandwiched by the collagen/fibronectin well coating and a layer of CM [44].

MNCs were harvested at various time points up to three weeks and evaluated by flow cytometry to elucidate survival of sub-populations of LC-restricted cells. The

addition of cytokines (IL-3, IL-6 and IGF-I) was evaluated in terms of effect on the viability and cell cycle characteristics of the LC-restricted subpopulations. Additionally these parameters were assessed after the addition of anti-MM agents to the culture system (dexamethasone (Dex) and bortezomib (BZM)). Unfortunately, owing to limited numbers of primary BM MNCs, a dose response was not possible for each drug and patient; dosages were therefore chosen based on literature and experience within the group.

2.1.8 Clonogenic assays

In order to evaluate the clonogenicity of BM MNCs, a colony assay was set up in which CD34-depleted MNCs were suspended in methyl-cellulose supplemented with cytokines to stimulate MM colony growth. A number of different supplements were compared, including lymphocyte-conditioned media; pooled patient plasma (as per CM); IL-3/IL-4/IL-6; IL-2/IL-6/IL-10/IL-15; and SCF/GM-CSF/GCSF/IL-3/Epo. The latter cocktail was chosen as it supported the most numerous and clearly demarcated colonies. Assays were set up with either freshly isolated MNCs or with cells harvested after a period of time in culture, from control and drug-treated cultures. Colonies were counted from two weeks, and thereby the clonogenicity of the starting cells was enumerated.

2.1.9 Culture of CD138-selected BM MNCs

CD138+ cells were cultured in suspension in CM. Cultures were set up in 96-well plates using 100,000 cells/well in 200µl CM. Cytokines were added at set up depending on the assay: APRIL (200ng/ml), IL-6 (100ng/ml) or IGF-I (500ng/ml).

Anti-myeloma treatments were also added at set up. Based on previous work, Dex was used at a final concentration of 1µM, with additional conditions wells treated with 100nM if sufficient cells were available from a given primary sample. Bortezomib (BZM) was used at a final concentration of 20nM and Lenalidomide (Len) at 100µM for the same reasons. PI103 (1µM; sc-203193; Santa Cruz Biotech) was used to block PI3K/AKT signaling.

Surviving cells were harvested after 48 to 72 hours in culture. A fixed volume from each well (e.g. 150µl) was aspirated and pipetted into a pre-labelled FACS tube. The contents were stained by the direct addition of 300µl of AV/PI master mix (see 2.4.2.1) and the percentage and absolute number of viable cells was analysed by AV/PI staining and Fluorosphere bead counts.

2.1.10 HMCL cell culture

HMCL were cultured in suspension in RPMI/10%FBS (R10) or serum-free RPMI (R). For the purposes of evaluating the effect of cytokines or drug treatments, cultures were set up in 96-well plates using 30,000 CD138+ cells/well in 100µl media. Cytokines were added at set-up while drugs were added in 50µl fresh media 24 hours later. Surviving cells were harvested after 48-72 hours after exposure to drug.

2.1.11 Co-culture of MM cells with modified stromal cell lines

HS5 cells were modified to express either APRIL or Notch ligands (see Chapters 4 and 5 respectively). Co-cultures were usually set up in TC-treated 48-well plates in DMEM/10%FBS, using FACS-based analysis as the final readout. Where alternative readouts were being utilised, for example protein expression by Western blotting or gene expression using qPCR, the co-cultures were scaled up to a 24- or 12-well format. The relative proportions of seeded cell numbers and media volumes were carefully preserved.

For 48-well plates, HS5 cells were seeded on day one at 15,000 cells/well in 300µl DMEM/10%FBS. Where cell number allowed, conditions were always set up in triplicate. Control wells of HS5 cells alone were routinely seeded. By day four, the HS5 cells had formed a confluent layer over the base of the well. MM cells were then seeded into the wells in additional DMEM/10%FBS. The original media was not removed to avoid depleting the co-cultures of important secreted soluble factors. HMCL were seeded at 75,000 cells/well in 200µl. At this time HMCL were also seeded into a fresh TC-treated 48-well plate at the same concentration and in the same volume so that viability of the MM cells alone could be compared to that of the MM cells cultured with stroma. Drug treatments were undertaken on day five, with

drugs added in 50µl/well with a final volume of 550µl in the co-culture wells and 250µl in the HMCL-alone wells. Bortezomib (BZM) was used at 0, 4 and 8nM. These doses were selected after a BZM dose-response killing assay was performed on HMCL cultured alone (see 4.2.5.1).

Cells were harvested 24-48 hours after drug treatment (days seven to eight). Cells in suspension were harvested separately to those adhering to the well. The former fraction contained predominantly MM cells while the latter fraction contained a mixture of adherent MM cells and HS5 cells. The media in each well was pipetted up and down gently and then aspirated fully and reserved for analysis (suspension fraction) in a 5ml FACS tube. The well was rinsed once with 600µl warmed HBSS, and this was pooled with the reserved suspension fraction. 100µl of warmed Trypsin/EDTA was added to each well and the plate then incubated at 37°C for five minutes. Once the adherent cells were fully dissociated, the trypsin was neutralised by the addition of 100µl warmed DMEM/10%FBS and the resultant mixture pipetted well to disperse any cell aggregates. The well was fully aspirated and the contents set aside for analysis (adherent fraction) in a second 5ml FACS tube. The well was washed once with an additional 600µl DMEM/10%FBS, which was then aspirated and pooled with the reserved adherent fraction. Both fractions were then pelleted at 1,500rpm for five minutes and then stained with antibodies as per the planned FACS analysis.

The above method was employed when harvesting cells for FACS-based analysis. If cell lysis to extract protein or RNA was required, then different sample collection tubes were used and the adherent fraction was washed with HBSS and then lysed *in situ* (using RIPA lysis buffer or Trizol Reagent as appropriate) without prior trypsinisation.

2.2 Flow cytometric analysis

2.2.1 Materials for flow cytometric analysis

- FACS (fluorescence-activated cell sorting) buffer - PBS with 0.1% BSA
- Cytofix/Cytoperm buffer (554714; BD)

- Permwash buffer (PW; 10x; 554723; BD)
- Cytoperm Plus buffer (559619 (kit); BD)
- DNase (559619 (kit); BD)
- Bromodeoxyuridine (BrdU; 559619 (kit); BD)
- 7-Aminoactinomycin (7-AAD; 559619 (kit); BD)
- Antibodies used in FACS analysis - Table 2-4

Table 2-4 Antibodies used for flow cytometry.

Target antigen	Fluorophore	Product number	Manufacturer
CD138	APC	130-091-250	Miltenyi Biotech
CD138	PE	120-000-431	Miltenyi Biotech
CD19	PB	MCA1940	AbD Serotec
CD27	PE	MHCD2704	Invitrogen
CD38	PE-Cy5	555461	BD
BrdU	FITC	347583	BD
IgG kappa light chain	APC	130-093-043	Miltenyi Biotech
IgG lambda light chain	APC	130-093-038	Miltenyi Biotech
Annexin V-FLUOS	FLUOS	11828681001	Roche
Annexin V	APC	550474	BD
Human DLL4	PE	346505	Biolegend
Human Jagged 2	PE	346904	Biolegend
Human DLL1	PE	346403	Biolegend

Abbreviations: APC Allophycocyanin, PE Phycoerythrin, PB Pacific Blue, FITC Fluorescein isothiocyanate.

2.2.2 Detection of surface and intracellular targets by flow cytometry

Cells (0.5-5x10^5 per tube in 50µl FACS buffer) were placed in 5ml polyethylene FACS tubes. An appropriate volume (1-10µl) of conjugated antibody directed against surface antigens was added to the cell suspension and after mixing this was incubated on ice for 30 minutes. The cells were washed with 1ml of FACS buffer, and then centrifuged at 1,500rpm for five minutes and the supernatant discarded. Where an intracellular target was to be assessed, the cells were then permeabilised with 100µl Cytofix/Cytoperm solution for 15 minutes on ice, and then washed with PW (1x). After pelleting the cells again (1,500rpm, five minutes), conjugated antibody directed against intracellular targets was added and mixed thoroughly and the solution incubated for a further 30 minutes on ice. After a final wash in PW, the cells were resuspended in FACS buffer for flow cytometric analysis. Analysis was performed using the Beckman Coulter CyAn ADP Analyzer or the BD FACSVerse Flowcytometer.

2.2.3 Flow cytometric analysis of cell cycle in primary MM cells

In order to assess cell cycle status of freshly isolated MM cells, MNCs were incubated in RPMI/10%FBS with BrdU for three hours (10µl of 1mM stock per ml culture media - i.e. final concentration 10µM) at a cell density not greater than 2x10^6/ml. The cells were then harvested, distributed between individual FACS tubes and washed once in FACS buffer. They were stained for extracellular antigens (CD138) in the usual fashion.

After incubation with this first antibody, the cells underwent a three-phase permeabilisation. They were first incubated in 100µl BD Cytofix/Cytoperm Buffer (1x) for 15 minutes on ice. After washing in BD Perm/Wash Buffer (PW; 1x) and re-pelleting, the cells were then incubated in 100µl BD Cytoperm Plus Buffer (1x) for ten minutes on ice. After washing in PW and re-pelleting, the cells were incubated again in 100µl BD Cytofix/Cytoperm Buffer (1x) for five minutes on ice. They were washed once again in PW and pelleted.

In order to expose incorporated BrdU, the cells were then treated with DNase (30µl DNase (1mg/ml stock) and 70µl PBS per tube) for one hour at 37°C and washed with

PW. The cells were then stained for intracellular antigens, specifically BrdU (using FITC-conjugated anti-BrdU antibodies) and light chains kappa and lambda. Prior to analysis, the cells were washed once more and then resuspended in 500µl FACS buffer with 20µl 7-AAD added.

Samples were analysed by flow cytometry to measure BrdU incorporation as a marker of cell cycle progression and 7-AAD staining as an indicator of total cellular DNA content. This allowed estimation of the proportion of cells in sub-G0/G1, G0/G1, S and G2+M, both within the MNCs and within the LC-restricted CD138+ and CD138− sub-populations (Figure 2-1).

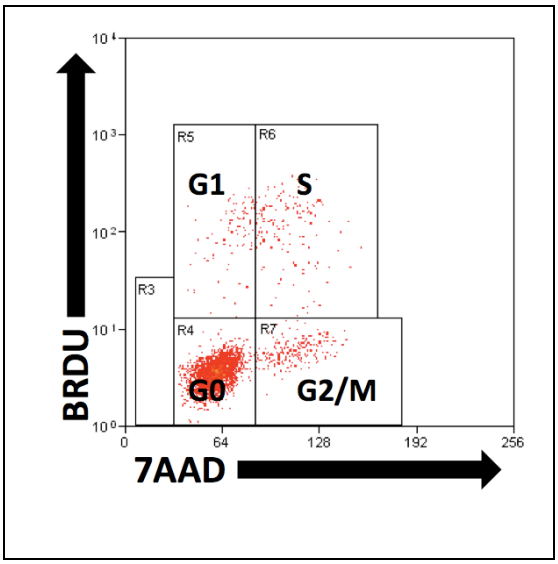

Figure 2-1 Representative FACs plot of BrdU uptake and 7AAD staining in primary MM cells.

Freshly isolated whole BM MNCs were pulsed with BrdU for three hours and then processed as detailed above. Cell cycle characteristics of clonotypic subsets were assessed. A representative plot for LC+CD138+ cells is shown.

The gating strategy to allow analysis of these sub-populations separately is detailed in Figure 2-2.

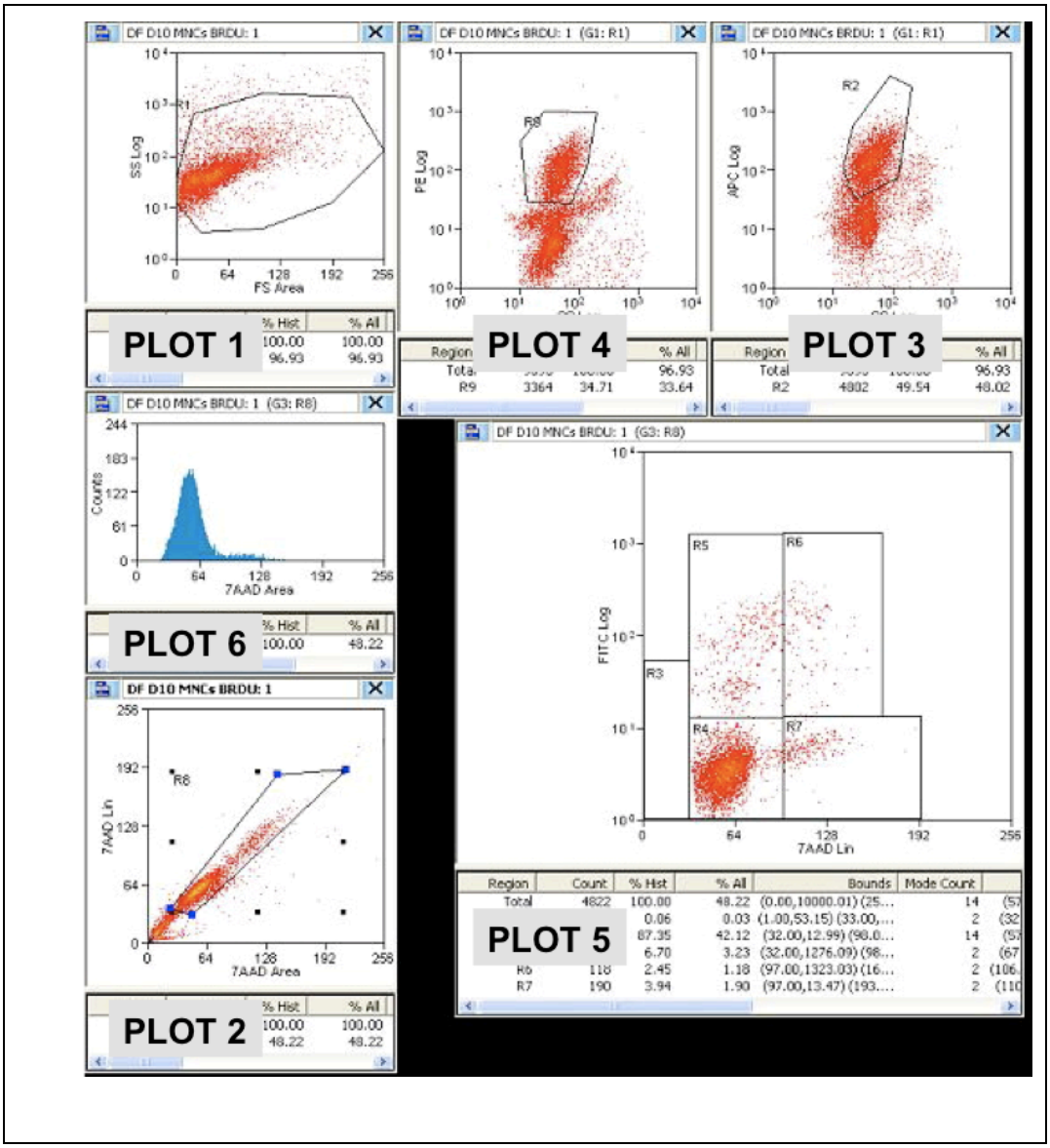

Figure 2-2 Flow cytometric analysis of BrdU uptake and 7AAD staining in primary MM cells.

The gating strategy for a representative primary BM MNC sample is shown. ***Plot 1*** *shows all events by forward scatter (FS) area/side scatter (SS) log (x/y respectively and hereafter) with a gate around intact cells. These are gated on to* ***Plot 2*** *(7AAD area/7AAD linear) to allow exclusion of cell doublets. A gate around single cells is gated onto* ***Plot 3*** *(SS log/anti-kappa or -lambda-conjugated APC) where a gate delineates the LC-restricted (LC+) population. The LC+ population is then gated onto* ***Plot 4*** *(SS log/anti-CD138-conjugated PE) to allow LC+ CD138+ and CD138− fractions to be discriminated. The subset is finally gated onto* ***Plot 5*** *and* ***Plot 6****.* ***Plot 5*** *(7AAD linear/anti-BrdU-conjugated FITC) is used to distinguish subG0/G1, G0/G1, S, G2/M cells, as shown in Figure 2-1.* ***Plot 6*** *(7AAD histogram) allows a simpler quantification of cellular DNA content.*

2.3 Additional methods used to characterise primary cells

2.3.1 Fluorescent *in situ* hybridisation

Fluorescent *in situ* hybridisation (FISH) was also used in patients with known translocations to track clonotypic MM cells through the whole BM MNC culture system. This analysis was kindly performed by Dr Fiona Ross, Wessex Regional Cytogenetics Laboratory, Salisbury District Hospital, on cytospins prepared from cells of interest (see section 2.1.6.5).

2.3.2 Immunocytochemistry and immunohistochemistry

Cells extracted from the colony assay were evaluated by immunocytochemistry (performed by Dr Naina Chavda, University College London Hospital) and immunohistochemistry (performed by Dr Teresa Marafioti, University College London Hospital). This was undertaken on cytospins prepared from harvested cells.

2.3.3 May-Grünwald Geimsa (MGG) staining

Cytospins were prepared for the cells of interest. After drying completely, the slides were first immersed in May-Grünwald stain (MG1L; Sigma Aldrich) for five minutes. They were then washed in distilled water. The slides were immersed in a 1X solution of Geimsa stain (GS1L; Sigma Aldrich; diluted 1:20 in deionized water) for 20 minutes. They were washed once more in distilled water, air dried and then evaluated by light microscopy.

2.4 Apoptosis and survival assays

2.4.1 Materials

- AnnexinV buffer (150mM NaCl, 10mM $CaCl_2$, 10mM Hepes (pH 7.4) made up with ddH_2O)
- Propidium iodide (PI; 81845; Sigma Aldrich)
- FlowCheck Fluorospheres (6605359; Beckman Coulter)

2.4.2 AnnexinV/Propidium Iodide staining

This assay allows viable, apoptotic and necrotic cells within a suspension to be distinguished. Cells undergoing apoptosis undergo changes in the extracellular membrane, leading to externalisation of the membrane phospholipid, phosphatidylserine. AnnexinV (AV) is a calcium-dependent phospholipid binding-protein which binds to cells with exposed phosphatidylserine. Propidium iodide (PI) is a DNA dye, taken up by non-viable cells which have lost their membrane integrity, while live cells exclude the dye. Using both agents together, the percentage of viable (AV−/PI−), apoptotic (AV+/PI−) and dead (AV+/PI+) cells can be evaluated. The addition of a fixed volume of FlowCheck Fluorospheres to the cell suspension allows absolute numbers of intact cells to be calculated.

Two protocols were devised and used depending on the choice of AnnexinV antibody. FLUOS-conjugated AnnexinV (Roche) emits at 488nm and was used for viability assays on CD138-selected MM cells and HMCLs. When assessing HMCL cell viability in co-culture with modified HS5 cells, APC-conjugated AnnexinV was used as the transduced HS5 cells co-expressed GFP which also emits at 488nm.

2.4.2.1 AnnexinV-FLUOS protocol used for cells cultured in suspension

A fixed volume (e.g. 150µl) of cell suspension, from either flasks or plates, was harvested and placed into a 5ml FACS tube on ice. To this was added 0.2µl FLUOS-conjugated AV, 1.4µl PI (2.5mg/ml), 17.6µl Fluorospheres ($1x10^6$/ml in PBS/1%BSA), 175.5µl AV buffer and 105.3µl PBS. This was added from a master mix made up for all the tubes to be analysed. The cells were vortexed briefly to mix and, after incubation for a maximum of five minutes on ice, analysed by flow cytometry. Samples were run until 1,000 Fluorosphere beads had been counted. This enabled the absolute number of intact cells to be calculated.

A representative result is shown in Figure 2-3.

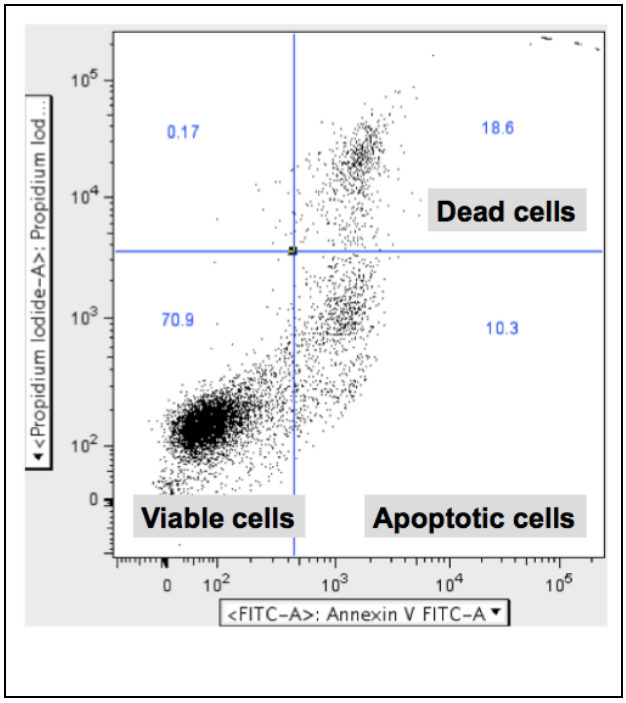

Figure 2-3 Representative Annexin V/PI flow cytometry plot.

Untreated NCI-H929 cells were harvested from culture and stained with AV-FLUOS and PI according to the protocol above. The plot is gated on intact cells, with the bottom left quadrant representing AV−/PI− viable cells (70.9%), the bottom right quadrant representing AV+/PI− apoptotic cells (10.3%) and the top right quadrant representing AV+/PI+ dead cells (18.6%).

2.4.2.2 AnnexinV-APC protocol used for cells co-cultured with GFP-expressing cells

This protocol was employed when analysing cells mixed with or expressing GFP. Cells growing in suspension were pipetted gently up and down and then fully aspirated from each well and reserved in a 5ml FACS tube on ice. The well was then washed with HBSS and this added to the reserved suspension fraction. Where adherent cells were also being evaluated these were harvested after trypsinisation and neutralisation and pipetted into a fresh 5ml FACS tube. Both fractions were then pelleted at 1,500rpm for five minutes and the supernatant discarded. To each tube was added 1µl APC-conjugated AV, 2µl PI (2.5mg/ml), 17µl Fluorospheres ($1x10^6$/ml in PBS/1%BSA), and 450µl AV buffer. This was added from a master mix made up for all the tubes to be analysed. The cells were vortexed briefly to mix and, after incubation in the dark for 15 minutes at room temperature (RT), analysed by flow cytometry. Samples were run until 1,000 Fluorosphere beads had been counted.

This enabled the absolute number of intact cells to be calculated. Each 500µl sample was run until 1,000 Fluorospheres had been counted. As each sample contained 17µl of Fluorospheres at a concentration of $1x10^6$/ml, i.e. 17,000 Fluorospheres, the absolute number of viable cells was calculated as (number of AV−PI− events) x 17.

A typical result looked identical to that seen with AV-FLUOS staining (shown in Figure 2-3).

2.4.3 MTS assay

This assay utilises a colorimetric method for determining the number of viable cells in a cell suspension. 3-(4,5-dimethylthiazol-2-yl)-5-(3-carboxymethoxyphenyl)-2-(4-sulphophenyl)-2H-tetrazolium (MTS) is an insoluble tetrazolium compound, which is reduced by viable cells to a soluble formazan product. This reaction is dependent on dehydrogenase enzymes found in cells which are metabolically active. The quantity of formazan product may be measured by absorbance of the cell suspension at 490nm and is proportional to the number of viable cells.

Cells were cultured in a 96-well tissue culture plate with conditions in triplicate. At the time point of interest, 20µl MTS solution was added to each well and incubated for one to four hours. Absorbance at 490nm was measured using a Varioskan platereader.

2.5 APRIL Enzyme-linked immunosorbant assay (ELISA)

Soluble APRIL was quantified in the culture supernatant of modified HS5 using commercially available APRIL ELISA kits from Invitrogen (KHC3051) and Biolegend (439307).

Culture supernatant was harvested into 15ml Falcon tubes, centrifuged at 3,000rpm for ten minutes at room temperature and stored in 500µl aliquots at −80°C

The samples were thawed on ice and thereafter the ELISA was performed as per the manufacturer's instructions.

2.6 Western blotting analysis

2.6.1 Materials, buffers and reagents

- RIPA lysis buffer (10x; 20-188; Millipore)
- Phosphatase inhibitor cocktails II and IV (539132 & 539136; Calbiochem)
- Complete protease inhibitor cocktail (04693116001; Roche)
- Pierce BCA Protein assay (PI-23227; Pierce)
- Methylene Bis-acrylamide (Acrylamide; 146072 Sigma Aldrich)
- Tris (Hydroxymethyl) methylamine (Tris)
- Sodium dodecyl sulphate (SDS; L3771; Sigma Aldrich)
- Ammonium persulphate (APS; A3678; Sigma Aldrich)
- Double-distilled H_2O (dd H_2O)
- *N*, *N*, *N*′, *N*′-Tetramethylethylenediamine (TEMED; T9281; Sigma Aldrich)
- Bromophenol blue (114391; Sigma Aldrich)
- NuPAGE® SDS-PAGE 4–12% Bis-Tris Gel (Life Tech)
- NuPAGE® LDS Sample Buffer (4X; NP0007; Life Tech)
- NuPAGE® Sample Reducing Agent (10X; NP0009; Life Tech)
- NuPAGE® MOPS SDS Running Buffer (20X; NP0001-02; Life Tech)
- NuPAGE® Antioxidant (NP0005; Life Tech)
- Amersham Hybond-C-Extra nitrocellulose membrane (10339574; GE Healthcare)
- Tween-20 (P9416; Sigma Aldrich)
- Dried skimmed milk powder (Marvel)
- Amersham ECL Prime Western blotting detection reagent (ECL Prime; RPN2232; GE Healthcare)
- High performance chemiluminescence film (28-9068; GE Healthcare)

Buffers:

- RIPA lysis buffer: 0.5M Tris-HCl (pH 7.4), 1.5M NaCl, 2.5% deoxycholic acid, 10% NP-40, 10mM EDTA, 0.1%SDS.
- Loading buffer (LB; 2x): 4% SDS, 10% 2-mercaptoethanol, 20% glycerol, 0.004% bromophenol blue, 0.125M Tris HCl.
- Running buffer (RB): 0.025M Tris (pH 8.5), 0.192M Glycine, 0.1% SDS, made up with ddH_2O.
- NuPAGE® MOPS SDS Running Buffer (20x): 50mM MOPS, 50mM Tris Base, 0.1% SDS, 1mM EDTA, pH 7.7
- Transfer buffer (TB): 0.025M Tris, 0.192M Glycine, 10% methanol, made up with ddH_2O.
- Tris-buffered saline with Tween: (TBS-Tw; 0.05M Tris (pH 7.5), 0.15M NaCl, made up with ddH_2O, with 0.05% Tween-20)

Gels:

- Resolving gel: volumes dependent on % acrylamide gel required (Table 2-5); dd. H_2O, acrylamide, IM Tris (pH 8.8), 10% SDS, 25% APS, TEMED

Table 2-5 Volumes of reagents required to make resolving gels of different acrylamide percentages (10ml, volumes in ml).

Acrylamide %	**5%**	**7.5%**	**12.5%**
dd.H_2O	4.1	3.66	2
Acrylamide	2.1	2.54	4.2
IM Tris (pH 8.8)	3.74	3.74	3.74
10% SDS	0.1	0.1	0.1
25% APS	0.075	0.075	0.075
TEMED	0.009	0.009	0.009

- Stacking gel: 3.5ml dd. H_2O, 835µl acrylamide, 625µl IM Tris (pH 6.8), 50µl 10% SDS, 12.5µl 25% APS, 10µl TEMED.

Resolving gels were prepared in gel casters (BioRad), covered in isopropanol and allowed to set for 30-40 minutes. Once set the isopropanol was removed and the stacking gel was layered over the resolving gel and a 10- or 15-well comb inserted.

Alternatively NuPAGE pre-cast SDS-PAGE gradient (4–12%) gels were used.

Antibodies

Table 2-6 lists antibodies used for Western blotting.

All primary antibodies were at a 1/1,000 dilution in 5%BSA/TBS-Tw unless indicated. Secondary antibodies were at 1/2,000 dilution in 5% milk for targets of interest and 1/10,000 for loading controls.

Table 2-6 Antibodies used in Western blotting.

Target protein	Product number	Manufacturer	Special instructions
Primary antibodies			
Notch1 (D6F11) XP® Rabbit mAb	#4380	Cell Signalling Technology	1/1,000 in 3% milk for one hour at room temperature
Notch2 (D76A6) XP® Rabbit mAb	#5732	Cell Signalling Technology	
Notch3 (D11B8) Rabbit mAb	#5276	Cell Signalling Technology	
Cleaved Notch1 (Val1744) (D3B8) Rabbit mAb	#4147	Cell Signalling Technology	
DLL1 Antibody	#2588	Cell Signalling Technology	
DLL4 Antibody	#2589	Cell Signalling Technology	
Jagged2 (C23D2) Rabbit mAb	#2210	Cell Signalling Technology	
Jagged 1 (C-20)	sc-6011	Santa Cruz	

		Biotechonology	
Secondary antibodies		*Both from GE Healthcare*	
Amersham ECL anti-rabbit IgG horseradish peroxidase-linked antibody	NA934		
Amersham ECL anti-mouse IgG horseradish peroxidase-linked antibody	NXA931		

2.6.2 Protein lysate preparation

Protein lysates were prepared from freshly isolated or cultured cells. Cells were washed once in ice cold PBS and then resuspended in RIPA lysis buffer, supplemented with complete protease inhibitor and phosphatase inhibitor cocktails. They were incubated on ice for 15-30 minutes and then centrifuged for 15 minutes at 14,000rpm at 4°C. The lysate was aspirated and aliquoted into pre-chilled 1.5ml Eppendorf tubes.

The protein concentration in lysates was quantified using the Pierce Protein quantification assay. In a 96-well plate, a BSA standard was prepared using dd. H_2O as a diluent, in duplicate. Blanks were also prepared containing dd. H_2O alone. Samples were diluted 1:12.5 in dd. H_2O. The quantification reagent was prepared by combining 4µl Reagent B with 196µl Reagent A per well and adding this to each well containing lysate, standards or blanks. The plate was incubated for 30 minutes at 37°C in the dark and then protein levels were quantified colorimetrically looking at absorption at 562nm on the Varioskan platereader.

Lysates were then used immediately or stored at −80°C until required.

2.6.3 Western blot method

Gels were placed within the gel tank (BioRad or Invitrogen) and running or MOPPs buffer added (depending on gel used).

20-40μg protein was aliquoted into a 1.5ml Eppendorf tube on ice. To this was added sample loading buffer, sample reducing agent and dd. H_2O if required to achieve necessary dilutions of the latter two reagents. The mixture was then boiled at 100°C for five to ten minutes, spun briefly at 5,000rpm and replaced on ice prior to loading into the gel wells. A molecular weight marker was loaded into one well. The gel was run at 50V until the proteins passed the interface between stacking and resolving gels, and then the voltage was increased in stages to a maximum of 150V until the proteins had separated.

Proteins were transferred from the gel to the nitrocellulose membrane by 'wet transfer' over two to three hours at 30V using transfer buffer and the XCell II Blot Module in the XCell SureLock Tank (both Novex). Successful transfer of proteins was visualised using Ponceau S staining.

The membrane was blocked for one hour with 5% dried skimmed milk/TBS-Tw at RT and, after washing three times for ten minutes in TBS-Tw, the membrane was incubated in the primary antibody under conditions optimized for each antibody. Most were incubated in a 1/1,000 solution in 5%BSA/TBS-Tw overnight at 4°C. Following incubation with the primary antibody, the membrane was washed three times as before and then incubated with the appropriate secondary antibody conjugated to horseradish peroxidase-linked antibody for two hours at RT. The membrane was then washed three times as before and then incubated with ECL Prime for one minute, before being washed very briefly in PBS and drained. The membrane was then exposed to X-ray film for between five seconds and five minutes depending on the signal strength.

2.7 Cloning

2.7.1 Materials

- Tris EDTA buffer (TE; 10mM Tris 1mM EDTA, pH 8.0)
- Chemically-competent E.coli bacteria (subcloning or high-efficiency; New England Biolabs)
- SOC outgrowth media (B9020S; New England Biolabs)

- Lysogeny broth (LB) medium (capsules; 113002041; MP)
- Agar powder (05040; Sigma Aldrich)
- Glycerol (>99%; G5516; Sigma Aldrich)
- NucleoBond Xtra Midi kit (740410.50; Macharey-Nagel)
- Genejuice (70967; Merck Millipore)
- Polybrene (10mg/ml; TR-1003; Merck Millipore)
- DH5α Subcloning Efficiency Competent E.Coli (18265-017; Invitrogen)

2.7.2 Equipment

- Waterbath
- Heated mixing block (Eppendorf Thermomixer Comfort)
- Sterile bacterial cell spreaders
- Sterile bacterial inoculation loops
- Incubator with shaker

2.7.3 Preparation of LB media & LB agar plates

LB medium was prepared by adding 25 capsules of powdered LB medium per litre of purified water and autoclaving at 121°C for 15 minutes. Ampicillin or other antibiotics required for selection were added at the time of media usage to avoid deterioration of antibacterial activity.

LB-Agar plates were prepared by adding 25 capsules of LB medium and 15g Agar per litre of purified water and autoclaving at 121°C for 15 minutes. Once the autoclaved LB/Agar had cooled to hand warmth (<60°C), ampicillin (or other selection antibiotic) was added for a final concentration of 50µg/ml. After flaming the neck of the flask/bottle of warm LB/Agar, it was poured into sterile 10cm Petri dishes immediately next to a lit Bunsen burner. The lid of each Petri dish was replaced immediately after pouring. Once the whole flask of LB/Agar had been poured, the top surface of the poured plates was briefly ‘flamed’ to pop any bubbles in the cooling solution and sterilise the surface. Plates were left to set overnight at

RT and, once set, the base of each plate was labelled with the antibiotic used for selection.

2.7.4 Amplification of DNA by bacterial transformation

DNA was amplified in chemically-competent E.coli bacteria by transformation. DNA was first quantified by spectrophotometer (Nanodrop) and then diluted to 20ng/µl. For each transformation one vial (50µl) of competent E.coli was thawed on ice. 2µl of DNA solution (40ng) was added to each vial as soon as the bacteria were fully thawed and the vial flicked gently to mix the DNA into bacterial suspension. The DNA-bacterial mixture was incubated on ice for 15-30 minutes, depending on the type of competent bacteria used and the manufacturer's recommendations. The bacteria were then heat-shocked in a water bath at 42°C for 30 seconds (or as per manufacturer's recommendations) and then replaced on ice for five minutes. 250µl SOC outgrowth medium at RT was added to each vial of bacteria, which were then placed on a heated mixing block (250rpm) at 37°C for one hour.

Agar plates containing the appropriate selection antibiotic for the bacteria used (normally ampicillin) were warmed to 37°C and then a range of volumes (e.g. 20µl and 200µl) of bacterial solution were pipetted onto each plate and spread evenly using a bacterial cell spreader. Plates were left agar-down for one to two minutes to allow the bacteria/SOC solution to be absorbed and then inverted and incubated overnight at 37°C.

The following day starter cultures were prepared from colonies which had grown on the agar plate. Single colonies were plucked with a sterile inoculating loop and used to inoculate a starter culture of 2ml of LB media (with freshly added ampicillin; final concentration 50µg/ml; fresh LB/amp media). Further steps depended on the final quantity of DNA required and in most instances a 'maxi-prep' was undertaken.

- For **'mini-preps'** (up to 20µg DNA from 1-5ml bacterial culture suspension) the starter culture was incubated overnight at 37°C on a shaker at 250rpm.
- For **'midi-preps'** (100-350µg DNA from 15-25ml bacterial culture suspension) the starter culture was incubated for ~eight hours at 37°C on a shaker at 250rpm

and then ~200µl was used to inoculate 10-25ml fresh LB/amp media. This was incubated overnight at 37°C on a shaker at 250rpm.

- For **'maxi-preps'** (500-850µg DNA from 100-200ml bacterial culture suspension) the starter culture was incubated for ~eight hours at 37°C on a shaker at 250rpm and then ~2ml was used to inoculate 100-200ml fresh LB/amp media. This was incubated overnight at 37°C on a shaker at 250rpm.

In all cases amplified plasmid DNA was harvested the following morning. Bacterial cells were lysed under alkaline conditions, denaturing genomic DNA and protein while the more stable plasmid DNA remains intact. The NucleoBond Xtra Midi kit (Macharey-Nagel) was used for maxi-preps, according to the manufacturer's instructions. Following elution and washing plasmid DNA was resuspended in sterile RNase-free H_20 and quantified by spectrophotometer (Nanodrop).

A small volume of bacterial culture (850µl) was set aside prior to DNA harvesting. After mixing well with 150µl glycerol (>99%), this was stored at −80°C as a long-term glycerol stock.

2.7.5 Using viral vectors to modify protein expression

Viral vectors were used to deliver genetic material into cell lines in order to produce lines with stable long-term expression of a particular protein. Both retroviral and lentiviral vectors were utilised, and their differing biology had implications for their downstream use. Lentiviruses are capable of infecting both dividing and non-dividing cells. In contrast, retroviruses are only able to infect dividing cells, because the breakdown of the nuclear envelope which occurs during mitosis is required for the pre-integration complex (viral DNA, RNA and proteins) to gain access to the cell nucleus.

2.7.5.1 Retroviruses

2.7.5.1.1 Triple transfection of adherent cells to generate intact retrovirus

Retroviral vector was produced by transiently transfecting 293T cells with expression plasmids supplying *gagpol, env* (RD114) and the gene of interest. Supernatant was then harvested and frozen on two subsequent occasions.

The day prior to transfection, $1x10^6$ rapidly growing 293T cells were seeded into a 100mm TC-treated plate in 10ml of DMEM/10%FBS. This was repeated for sufficient plates, allowing one per transfection. The following day, the degree of confluence was assessed and only if cells were 50-60% confluent did the transfection protocol continue. For each plate, 470µl of serum-free DMEM was pipetted into a sterile 1.5ml Eppendorf tube. 30µl of Genejuice was added to this and mixed by gentle pipetting. The mixture was incubated for five minutes in a tissue-culture (TC) hood. The three plasmids were then added: a total cargo of 12.5µg DNA/plate, comprising 3.13µg env (RD114), 4.69µg gagpol and 4.69µg construct gene of interest. This was mixed by gentle pipetting and then incubated once again for 15 minutes in a TC hood. Following incubation, the Genejuice-DNA mixture was added drop-wise to each plate and swirled gently to distribute.

Forty-eight hours following transfection (when the 293T cells were 80-90% confluent), the supernatant was harvested and stored at 4°C overnight. Each plate received 10ml of fresh DMEM/10% FBS. Twenty-four hours later, the second aliquot of supernatant was harvested and added to the first, which was then frozen at −80°C.

2.7.5.1.2 Transduction of adherent cells with retrovirus containing gene of interest

The relevant human adherent cell line, e.g. HS-5, was washed, trypsinised, neutralised, harvested and counted. The cells were resuspended at $1x10^5$ cells/ml in DMEM/10% FBS and 2ml was plated into each well of a TC-treated 6-well plate. The following day the appropriate retroviral supernatant was thawed on ice (one vial/well). Once fully thawed, the old media from each well was aspirated and replaced with the entire vial of retroviral supernatant. 1µl of polybrene (10mg/ml) was added to each transduced well, and swirled gently to mix.

Forty-eight hours after the first transduction, a second transduction was attempted with a freshly thawed vial of supernatant and another 1µl of polybrene, if the adherent cells were not confluent. The transduced cells were then harvested and the efficiency of the transduction assessed.

Where a pure population was required, transduced cells were sorted using the Beckmann Coulter MoFlo High Speed Cell Sorter, gating on cells expressing either the protein of interest of a co-transduced fluorescent marker (e.g. GFP).

2.7.5.2 Lentiviruses

2.7.5.2.1 Triple transfection of adherent cells to generate intact lentivirus

293T cells were transfected with the plasmid encoding the gene of interest in combination with the p8.91 plasmid encoding *gag*, *pol* and *rev* genes and the VSV.G-expressing envelope plasmid. This so-called triple transfection allowed the production of lentiviral supernatant capable of transiently infecting a second population of mammalian cells.

The day prior to the transfection 293T cells growing well were trypsinised, harvested, washed, resuspended and counted. The cells were seeded at $1x10^6$ per 10cm TC-treated plate in their usual media (DMEM/10%FBS). The following day the plates were inspected under low-power microscopy to ensure that they were at 40-60% confluence.

The transfection mixture was then prepared. 30µl Genejuice was added to 470µl serum-free DMEM in a sterile 1.5ml Eppendorf, pipetting up and down to mix. After incubating at RT for five minutes the DNA was added - 4µg target gene, 3µg p8.91 and 3µg VSV-G (total 10µg; 1µg per 3µl Genejuice) - and mixed by pipetting up and down. The resultant DMEM-Genejuice-DNA mixture was incubated at RT for 15 minutes to allow the formation of liposomes.

Meanwhile the 293T cells were washed twice gently with HBSS and then given fresh serum-free DMEM (7ml/10cm plate). All of the DMEM-Genejuice-DNA mixture was then added drop-wise to the plate, with gentle agitation to distribute the mixture as evenly as possible. The 293T cells were then returned to the incubator.

The media was replaced after 24 hours with DMEM/10%FBS. Supernatant containing lentiviral particles was then harvested at 48 hours following transfection and the media replaced with fresh DMDM/10%FBS. The supernatant was kept at

4°C overnight and then pooled with a second batch of supernatant harvested at 72 hours following transfection. The pooled lentiviral particles were then concentrated by ultracentrifugation (23,000rpm at 4°C for two hours) and, after discarding the supernatant, were resuspended in 500µl DMEM/10%FBS and then stored in 100µl aliquots at −80°C.

2.7.5.2.2 Titration of lentivirus

This was done to compare the transduction efficiency of different preparations and dilutions of lentiviral supernatant.

Optimally growing 293T cells were trypsinised, harvested, washed, resuspended and counted. They were seeded at $0.05x10^6$/well in 400µl DMEM/10%FBS in a TC-treated 24-well plate. The following day the media was aspirated and replaced with fresh DMEM/10%FBS containing Polybrene (10µg/ml). Dilutions of freshly thawed concentrated lentiviral supernatant were prepared (e.g. 1x, 0.1x and 0.01x) and added in a total volume of 60µl/well. Dilutions were tested in triplicate.

The cells were harvested 48 hours later and the transduction efficiency assessed either by qPCR of the target gene (undertaken on total cellular DNA) or by flow cytometry to quantify protein expression (e.g. GFP expression). The former allows more accurate assessment of the lentiviral copy number/cell, while the latter may be a more functionally relevant readout.

2.7.5.2.3 Transduction of adherent cells with lentivirus containing gene of interest

The adherent cells to be transduced were trypsinised, harvested, washed, resuspended in their usual media and counted. Cells were seeded in TC-treated 24-well plates at $0.05x10^6$/well. The following day their confluence was assessed under low-power microscopy. Transduction was attempted if their confluence was 40-60%. The media was aspirated from the wells and replaced with fresh media to which Polybrene had been added (10µg/ml). Lentiviral supernatant was then added to each well at a volume previously determined by titration, ensuring that the final volume of media/Polybrene/viral supernatant is identical in each well transduced.

Twenty-four hours after transduction the media was either replaced or the transduction repeated to increase transduction efficiency. The transduced cells were then harvested and the efficiency of the transduction assessed. As for retrovirally-transduced cells, if a pure population was required, transduced cells were sorted.

2.7.6 Specific methodology for the production of modified HS5 cell lines

2.7.6.1 Producing APRIL+HS5 cells

2.7.6.1.1 The APRIL construct

The APRIL construct was kindly donated by Dr Martin Pule. It contained the unmodified sequence for APRIL, preceded by eGFP, cloned into the retroviral SFG vector (Figure 2-4).

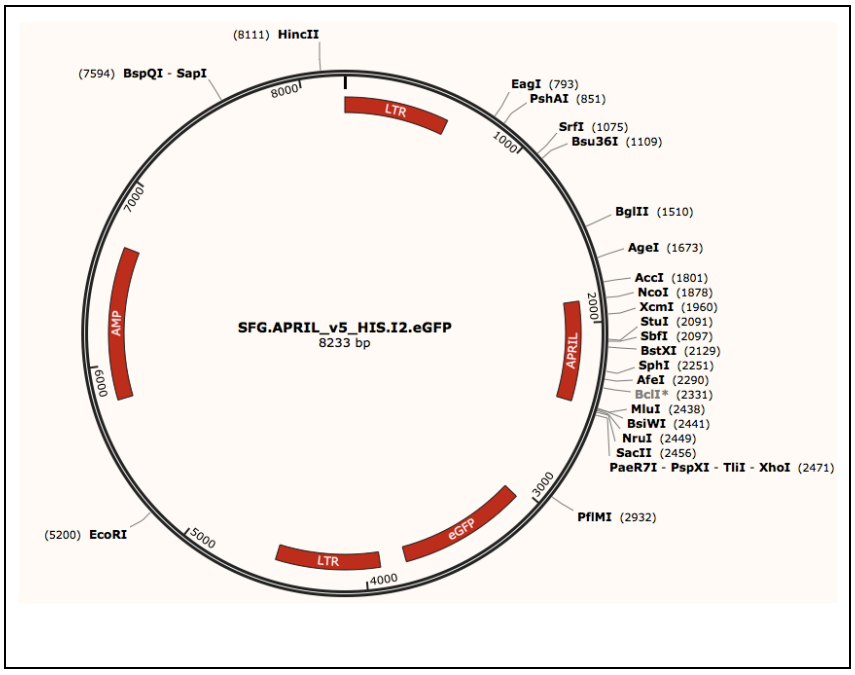

Figure 2-4 APRIL construct.

The SFG vector [121] is based on the Moloney murine leukaemia virus, with the transgene start codon located at the start site of the deleted viral envelope gene. Bicistronic transgene expression was achieved by inclusion of the encephalomyocarditis internal ribosomal entry site (IRES) allowing expression of the downstream reporter gene enhanced green fluorescent protein (eGFP). The retroviral long terminal repeat (LTR) acted as the promoter driving expression of both transgenes, although expression following an IRES tends to be considerably reduced

compared to that of the primary transgene. The APRIL protein was double tagged containing an amino terminal v5 tag and a carboxy terminal HIS tag. The plasmid backbone also contained the pBR322 origin of replication for amplification in bacterial culture and an ampicillin resistance cassette for selection.

2.7.6.1.2 Making APRIL retrovirus

293T cells were transiently transfected with expression plasmids, supplying *gagpol, env* (RD114) and either the APRIL construct (SFG.APRIL_v5-HIS.12.eGFP) or the empty vector negative control (SFG.eGFP). Supernatant was then harvested and frozen on two subsequent occasions.

The supernatant produced using the SFG.APRIL_v5-HIS.12.eGFP construct will hereafter be referred to as APRIL.eGFP retrovirus, and the supernatant produced using the SFG.eGFP construct will hereafter be referred to as eGFP negative control retrovirus

2.7.6.1.3 Producing an APRIL-positive HS5 line and its negative control

HS5 cells were transduced as detailed in section 2.7.5.1.2 with the APRIL.eGFP and the eGFP negative control retroviral supernatants. The APRIL.eGFP-transduced HS5 (Ap+HS5) were 14% GFP-positive (GFP+) while the eGFP negative control-transduced HS5 (NC(Ap)HS5) were 3% GFP+. The transduced cells were then FACS-sorted by eGFP expression to obtain a ≥95% pure population in both the Ap+HS5 and NC(Ap)HS5 (Figure 2-5).

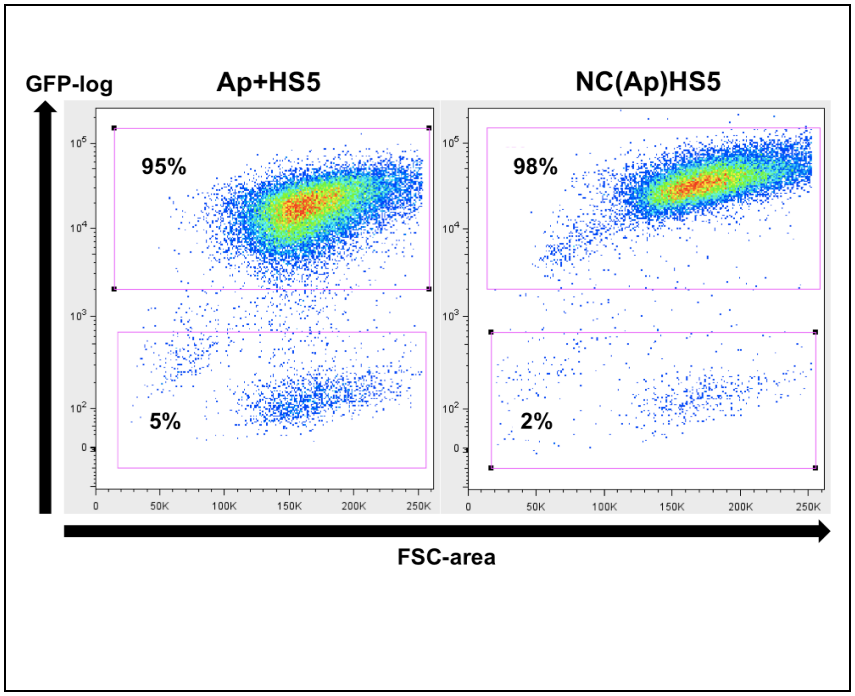

Figure 2-5 Purity of modified HS5 cells as assessed by eGFP expression.

Two representative FACS plots are shown for Ap+HS5 (left) and NC(Ap)HS5 (right); intact adherent cells are shown. Abbreviations: FSC, forward scatter.

2.7.6.2 Producing a Delta ligand-1 (DL1)-expressing stromal cell line

2.7.6.2.1 The DL1 construct

The bicistronic lentiviral plasmid pTRIPΔU3-EF1α-DL1-IRES-GFP, together with the empty vector negative control (NC; pTRIPΔU3-EF1α-GFP) was kindly donated by Dr Francoise Pflumio (Université Paris Descartes, Paris). Her group modified the mouse stromal cell line MS5 in order to investigate the role of Notch in human T-ALL[122], and Xu et al[108,109] went on to use the DLl+ MS5 line in MM. Figure 2-6 shows the plasmid map and structure of the vectors. Both plasmids contained GFP under the EF1α promoter so expression of GFP would be predicted to correlate with expression of DL1.

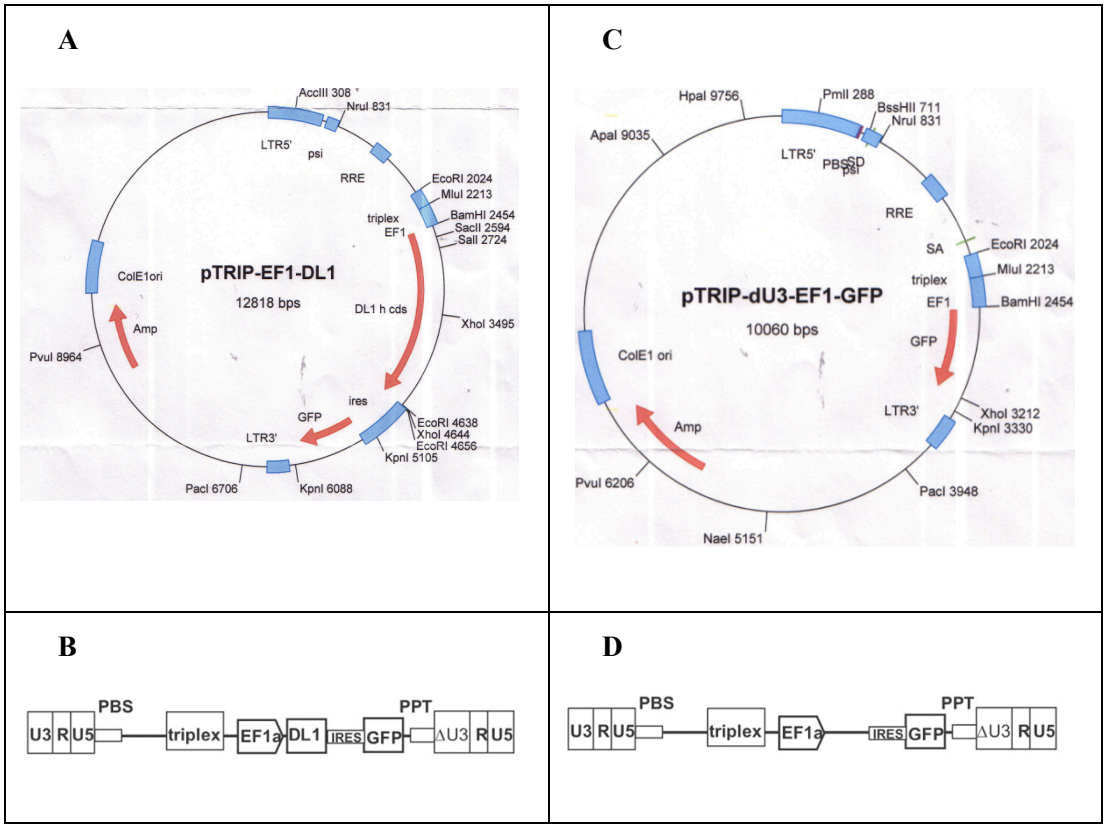

Figure 2-6 Plasmid maps and structures for pTRIPΔU3-EF1α-DL1-IRES-GFP lentiviral plasmid (A, B) and empty vector negative control (C, D).

2.7.6.2.2 Reconstitution of DL1-expressing lentiviral plasmids

Lentiviral plasmids were donated on filter paper (1µg). The annotated paper was trimmed and placed in a 1.5ml Eppendorf tube with 100µl TE buffer. After incubation at RT for four hours, to allow plasmid DNA to enter solution, the resultant DNA solution was stored at −20°C until required.

2.7.6.2.3 Amplification of pTRIPΔU3-EF1α-DL1-IRES-GFP and pTRIPΔU3-EF1α-GFP

2.5µl of thawed plasmid DNA solution for each plasmid was used to transform a vial of DH5α (subcloning efficiency) competent E. coli (18265-017; New England Biolabs). Starter cultures were prepared from single colonies generated and subsequently a maxi-prep was used to amplify the plasmid for further work. Glycerol stocks were made for each plasmid at this point.

2.7.6.2.4 Production of pTRIPΔU3-EF1α-DL1-IRES-GFP and pTRIPΔU3-EF1α-GFP lentivirus

293T cells were triple transfected (using Genejuice) with (i) p8.91; (ii) VSV-G and (iii) the DL1-expressing pTRIP vector or the empty vector negative control. Lentiviral supernatant was harvested at 24 and 48 hours following transfection and concentrated by ultracentrifugation. The transfection efficiency was assessed at this time by evaluating GFP expression by the 293T cells; the EF1α-DL1-IRES-GFP-transfected 293T cells were 66% GFP-positive (GFP+) and the EF1α-GFP-transfected 293T cells were 96% GFP+.

2.7.6.2.5 Titration of EF1α-DL1-IRES-GFP and EF1α-GFP lentiviral supernatants

The titration was undertaken in 293T cells to determine the optimum volume of concentrated EF1α-DL1-IRES-GFP and EF1α-GFP (NC) lentiviral supernatant required to transduce sufficient target cells to allow sorting for a pure population.

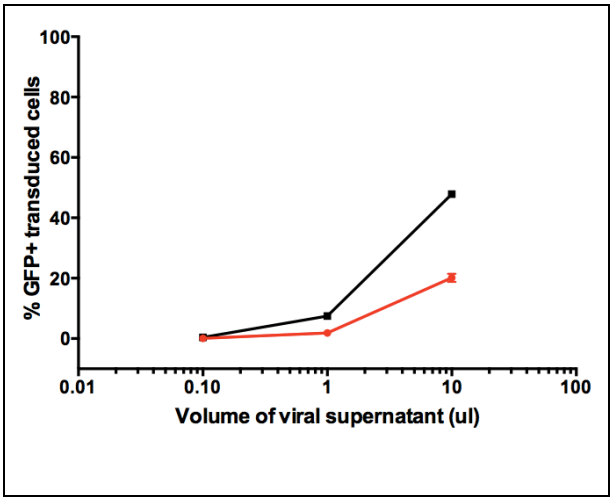

Figure 2-7 Titration of EF1α-DL1-IRES-GFP and EF1α-GFP lentiviral supernatants.

293T cells were transduced with increasing volumes of lentiviral supernatant (in 500µl total volume) as indicated on the x-axis, and analysed for GFP expression by FACS. One representative experiment.

Figure 2-7 shows percentage transduction of 293T cells using a range (0.1-10µl) of volumes of viral supernatant. As the transduction efficiency was relatively low even at the highest supernatant doses (10µl), a volume of 50µl was selected to transduce the target cell (HS5 cell).

2.7.6.2.6 Transduction of HS5 cells with EF1α-DL1-IRES-GFP and EF1α-GFP lentiviral supernatants

Optimally growing HS5 cells were transduced with 50µl of lentiviral supernatant. The resultant EF1α-DL1-IRES-GFP and EF1α-GFP-transduced cells were 87% and 96% GFP+ respectively. Hereafter they will be referred to as DL1+HS5 and NC(DL1)HS5. The transduced cells were then FACS-sorted by eGFP expression to obtain a >95% pure population in both the DL1+HS5 and NC(DL1)HS5.

2.7.6.3 Production of Jagged-2 and Delta ligand-4 (DL4)-expressing stromal cell line

Retroviral supernatants for bicistronic retroviral vectors encoding Jagged-2 (Jag2) or Delta-like ligand-4 (DL4) in combination with eGFP were kindly provided by Dr Tom Taghon (Ghent University, Belgium). The Jag2 construct was generated in-house by Dr Taghon's group and cloned into a bicistronic LZRS-IRES-EGFP vector [123]. The DL4 construct was donated to this group by Professor Adrian Harris [124] and cloned into the same vector backbone. The negative control for both ligands was therefore the empty vector expressing eGFP alone.

2.7.6.3.1 Transduction of HS5 cells with LZRS-Jag2-IRES-EGFP, LZRS-DL4-IRES-EGFP and LZRS-EGFP

Optimally growing HS5 cells were transduced on two consecutive days. The transduction efficiency was relatively poor, with only 13% GFP+ LZRS-Jag2-IRES-EGFP-transduced HS5 cells, 46% GFP+ LZRS-DL4-IRES-EGFP-transduced HS5 cells and 12% GFP+ LZRS-EGFP-transduced HS5 cells. These are hereafter referred to as Jag2+HS5, DL4+HS5 and NC(DL4)HS5 respectively.The transduced cells were then FACS-sorted by eGFP expression to obtain a >95% pure population in all three cell subtypes.

2.8 Quantitative polymerase chain reaction

This is a method of quantifying expression of a specific gene by amplifying and simultaneously quantifying the transcript numbers from a cDNA template derived from RNA from the cell of interest.

2.8.1 Materials

- TRIzol reagent (15596-026; Ambion, Life Tech)
- Chloroform (288306; Sigma-Aldrich)
- PureLink RNA Micro kit (12183016; Ambion, Life Tech)
- Absolute ethanol (459844; Sigma-Aldrich)
- RNase-free H2O (AM9914G; Life Tech)
- Oligo(dT)18 primers (BIO-38029; Bioline)
- dATP, dCTP, dGTP, dTTP (BIO-39036; BIO-39038; BIO-39037; BIO-39039; Bioline)
- SuperScript III Reverse Transcriptase (200U/µl; kit - 18080-044; Invitrogen)
- 5X First-Strand Buffer (kit - 18080-044; Invitrogen)
- 0.1M DTT (kit - 18080-044; Invitrogen)
- RNaseOUT Recombinant RNase Inhibitor (10777-019; Invitrogen)
- QuantiFast SYBR Green PCR Master Mix (204054; Qiagen)
- Hs_HES1_1_SG QuantiTect primer assay (QT00039648, Qiagen)
- Hs_DTX1_1_SG QuantiTect primer assay (QT00058744, Qiagen)
- Beta-2 microglobulin (B2M) primers - forward: 5' TCT CTC TTT CTG GCC TGG AG 3'; reverse: 5' AAT GTC GGA TGG ATG AAA CC 3' (Integrated DNA Technologies)

2.8.2 RNA extraction using Trizol

RNA was extracted from HMCL co-cultured with NL-expressing HS5 using TRIzol reagent and the PureLink RNA Micro kit. Usual measures to minimise RNase contamination and RNA degradation were undertaken. The suspension fraction of the co-cultures was aspirated into an RNase-free container, pelleted at 1,500rpm for ten minutes and the media was discarded. The pellet was then re-suspended in 500µl TRIzol and vortexed to mix well and allow complete lysis of the cells. The solution was then frozen at −80°C until RNA extraction could be resumed (within one week).

Following aspiration of the media and suspension cell fraction, the adherent cell fraction was lysed *in situ*: 400µl TRIzol was added directly to each well (12-well plate) and pipetted up and down to mix thoroughly and lyse all adherent cells. The solution was then frozen at −80°C as for the suspension fraction.

RNA extraction was performed using the PureLink kit as per the manufacturer's instruction for TRIzol Plus Total Transcriptome Isolation. The thawed cell lysate with TRIzol was incubated at RT for five minutes. Where necessary, lysates were transferred into RNase-free 1.5ml Eppendorf tubes. Chloroform was added (0.2ml per 1ml TRIzol) and the capped sample was shaken vigorously by hand for 15 seconds and then incubated at RT for two minutes. The samples were then centrifuged at >12,000 x g for 15 minutes at 4°C. The colourless aqueous upper phase was aspirated and transferred into a clean RNase-free tube. An equal volume of 100% ethanol was added to each sample (to obtain a final concentration of 50% ethanol) and the sample was vortexed to mix well. After inverting the sample twice, it was transferred into a PureLink Micro Kit Column and centrifuged at >12,000 x g for one minute at RT in order to bind the RNA to the silica-based membrane of the column. The bound RNA was then washed twice with 500µl Wash Buffer II with ethanol. Finally the RNA was eluted into a fresh tube with RNase-free water. It was then quantified by spectrophotometer (Nanodrop ND-1000). RNA samples were stored at −80°C for up to one month prior to cDNA synthesis.

2.8.3 First-Strand cDNA Synthesis

RNA samples were diluted to 50ng/µl. The following components were mixed in an RNase-free microcentrifuge tube:

- 1.25µl oligo(dT)18 primers
- 1.25µl each of dATP, dCTP, dGTP, dTTP (10mM)
- 5µl RNase-free water
- 5µl RNA at 50ng/µl

This mixture was heated to 65°C for five minutes and then incubated on ice for two minutes. The following components were then added and mixed by gentle pipetting:

- 5µl 5x First-Strand Buffer
- 1.25µl 0.1M DTT
- 1.25µl RNaseOUT
- 1.25µl SuperScript III RT

This generated a total volume of 25µl, sufficient for 12 qPCR reactions. Where more RNA template was required, the reaction was scaled up, up to a maximum volume of 50µl per microcentrifuge tube. This mixture was then incubated in a PCR thermocycler at 25°C for five minutes, 50°C for 40 minutes, 55°C for ten minutes and finally 70°C for 15 minutes to inactivate the reaction. cDNA samples were stored at −80°C for up to one month prior to amplification in PCR.

2.8.4 Quantitative reverse transcriptase PCR

Quantitative reverse transcriptase PCR (qPCR) using the QuantiFast SYBR Green PCR system was used to quantify the transcript levels of genes of interest in parallel with the transcript levels of a reference gene such as B2M.

Each 25µl amplification reaction contained:

- 12.5µl QuantiFast SYBR Green PCR Master Mix (2x)
- 2.5µl Primer (10x)
- 2µl cDNA template
- RNase-free water to make up volume

All cDNA samples were amplified in triplicate for each target gene and the reference gene. RNase-free water samples were run for each primer master mix as a negative control to exclude DNA contamination of the primers or SYBR Green Master Mix. Reactions were undertaken in MicroAmp Optical 96-Well Reaction Plates (Applied Biosystems) with MicroAmp 12-cap strips. qPCR reactions were run on the Mastercycler ep realplex real-time PCR machine (Eppendorf).

Gene expression was quantified by subtracting the mean threshold cycle (C_T) for the reference gene, B2M, from that of the target gene, either HES1 or DTX1 and this

value was termed ΔC_T. Where the C_T deviation value was >0.5 for a triplicate group, outlying samples were excluded and a more representative mean C_T was calculated. Data was then presented as $2^{-\Delta CT}$ values for each sample.

2.8.4.1 Quantitative reverse transcriptase PCR for HES1 and DTX1

This was undertaken to verify Notch activation in HMCL co-cultured with NL-expressing HS5 cells. On day one modified HS5 cells were seeded in 12-well plates at 86,000 cells/well in 1,700µl DMEM/10%FBS. On day four, when the HS5 cells were confluent, HMCL or DND41 cells were added to the wells at 430,000 cells/well in 1,100µl DMEM/10%FBS. Additional wells were seeded for U266, MM1S and DND41 cells, cultured alone at this stage. All cultures were also treated at this stage with the GSI L685 (final concentration 1µM). Cells were harvested 48 hours later on day six in two fractions: suspension and adherent and RNA was extracted according to the method detailed in section 2.8.2.

cDNA synthesis was carried out as detailed in section 2.8.3. qPCR using the QuantiFast SYBR Green PCR system was used to quantify the transcript levels of Notch downstream targets HES1 and DTX1 in parallel with the transcript levels of the reference gene beta-2-microglobulin (B2M). This was chosen as a reference gene as expression varies minimally with experimental conditions [125,126].

The multiple conditions mandated the use of 11 PCR plates, and so to allow comparisons between PCR plates, two standard cDNA samples were amplified in triplicate for each target gene and B2M on every plate. The cDNA was derived from DND41 cells cultured alone and treated with vehicle or L685 1µM (termed positive control (PC) and negative control (NC) respectively). These were generated from a different experiment. The conditions included in each qPCR plate are detailed in Table 2-7.

Table 2-7 Details of conditions and cDNA evaluated in each qPCR plate.

qPCR plate number	cDNA evaluated
1	U266, MM1S & DND41 cultured alone +/- GSI DND41 cultured alone +/- GSI (PC & NC)
2	U266, MM1S & DND41 co-cultured with Jag2+HS5 +/- GSI SUSPENSION FRACTION DND41 cultured alone +/- GSI (PC & NC)
3	U266, MM1S & DND41 co-cultured with Jag2+HS5 +/- GSI ADHERENT FRACTION DND41 cultured alone +/- GSI (PC & NC)
4	U266, MM1S & DND41 co-cultured with DL4+HS5 +/- GSI SUSPENSION FRACTION DND41 cultured alone +/- GSI (PC & NC)
5	U266, MM1S & DND41 co-cultured with DL4+HS5 +/- GSI ADHERENT FRACTION DND41 cultured alone +/- GSI (PC & NC)
6	U266, MM1S & DND41 co-cultured with NC(DL4)HS5 +/- GSI SUSPENSION FRACTION DND41 cultured alone +/- GSI (PC & NC)
7	U266, MM1S & DND41 co-cultured with NC(DL4)HS5 +/- GSI ADHERENT FRACTION DND41 cultured alone +/- GSI (PC & NC)
8	U266, MM1S & DND41 co-cultured with DL1+HS5 +/- GSI SUSPENSION FRACTION DND41 cultured alone +/- GSI (PC & NC)
9	U266, MM1S & DND41 co-cultured with DL1+HS5 +/- GSI ADHERENT FRACTION DND41 cultured alone +/- GSI (PC & NC)
10	U266, MM1S & DND41 co-cultured with NC(DL1)HS5 +/- GSI SUSPENSION FRACTION DND41 cultured alone +/- GSI (PC & NC)
11	U266, MM1S & DND41 co-cultured with NC(DL1)HS5 +/- GSI ADHERENT FRACTION DND41 cultured alone +/- GSI (PC & NC)

The layout for Plates 1 and 3 are shown in Figure 2-8 below, as representative examples of the arrangement of samples and primers.

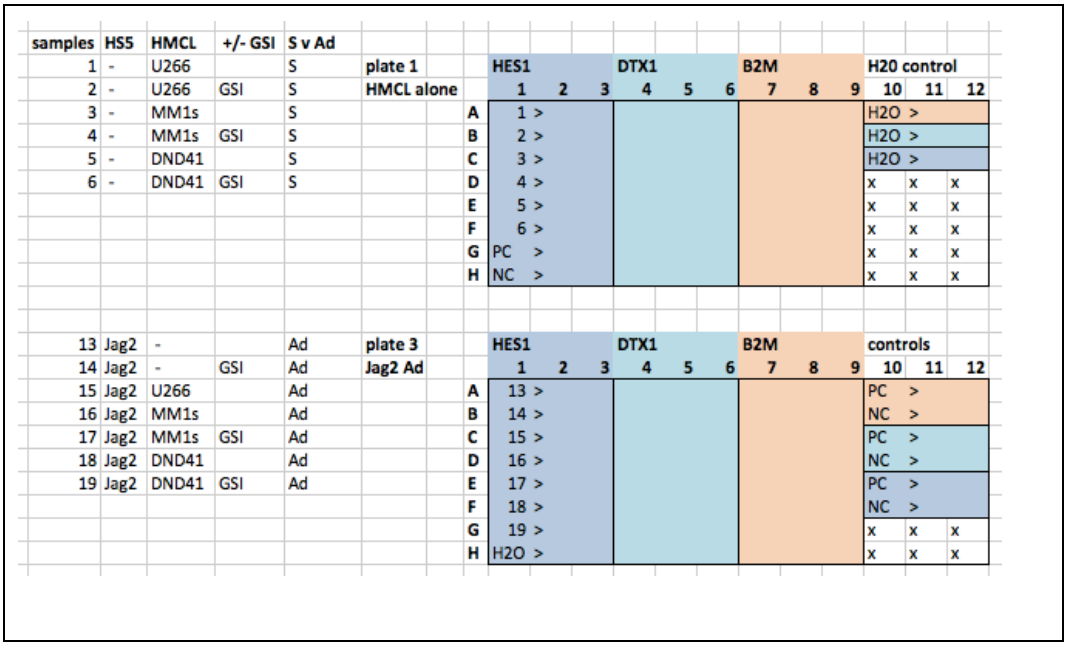

samples	HS5	HMCL	+/- GSI	S v Ad												
1	-	U266		S	plate 1		HES1			DTX1			B2M			H20 control		
2	-	U266	GSI	S	HMCL alone		1	2	3	4	5	6	7	8	9	10	11	12
3	-	MM1s		S		A	1 >									H2O >		
4	-	MM1s	GSI	S		B	2 >									H2O >		
5	-	DND41		S		C	3 >									H2O >		
6	-	DND41	GSI	S		D	4 >									x	x	x
						E	5 >									x	x	x
						F	6 >									x	x	x
						G	PC >									x	x	x
						H	NC >									x	x	x
13	Jag2	-		Ad	plate 3		HES1			DTX1			B2M			controls		
14	Jag2	-	GSI	Ad	Jag2 Ad		1	2	3	4	5	6	7	8	9	10	11	12
15	Jag2	U266		Ad		A	13 >									PC >		
16	Jag2	MM1s		Ad		B	14 >									NC >		
17	Jag2	MM1s	GSI	Ad		C	15 >									PC >		
18	Jag2	DND41		Ad		D	16 >									NC >		
19	Jag2	DND41	GSI	Ad		E	17 >									PC >		
						F	18 >									NC >		
						G	19 >									x	x	x
						H	H2O >									x	x	x

Figure 2-8 Representative qPCR plate layouts.

Abbreviations: S, suspension; Ad, adherent; H2O, water; x, empty well.

2.8.5 Patient-specific VDJ PCR

To allow tracking of clonotypic primary MM cells through the whole BM MNC culture system, a method of isolating and amplifying the patient-specific IgH heavy chain VDJ region was optimised.

RNA was extracted from patient tumour samples (~ $5x10^6$ freshly isolated CD138-selected primary BM MNCs) using the RNeasy Mini Kit (Qiagen) as per the manufacturer's protocol. First strand cDNA synthesis was then performed using Superscript III Reverse Transcriptase (Invitrogen) according to the manufacturer's protocol (see section 2.8.3 for more detail), using 500ng RNA.

RT-PCR was performed using 12 primer pairs. All sets used a common reverse primer taken from the constant region of the IgH heavy chain locus (selected according to patient monoclonal protein isotype), with 12 different forward primers.

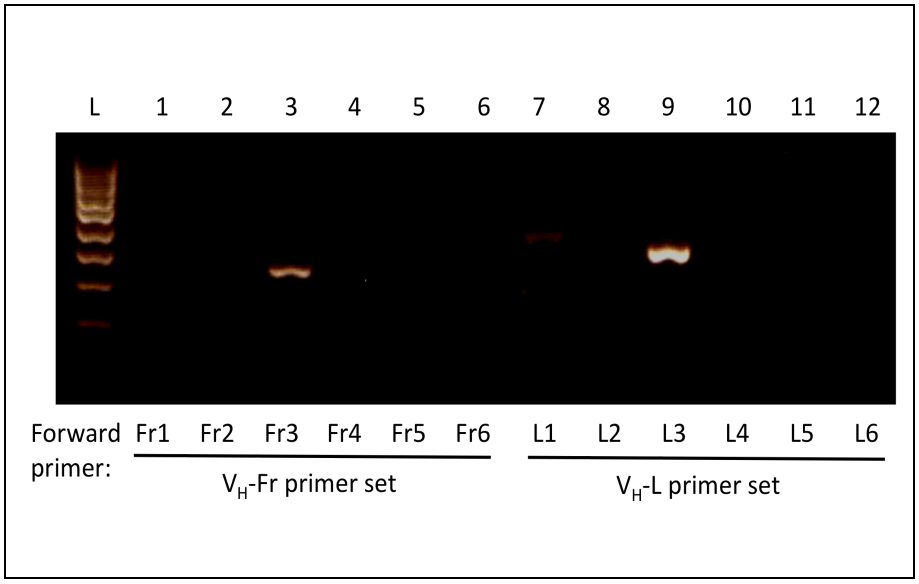

Figure 2-9 PCR amplification of patient-specific VDJ region using cDNA from freshly purified bone marrow CD138+ cells.

RT-PCR performed on cDNA extracted from MM patient purified BM CD138+ cells using 12 primer pairs. The patient-unique VDJ product was successfully amplified using the primers complementary to V_H3 family (lanes 3 and 9). Abbreviations: L, ladder.

Primers 1 to 6 were from the V_H framework (V_H-Fr) region and primers 7 to 12 were from the V_H leader (V_H-L) region. Primers Fr1 and L1 were from V_H family 1, Fr2 and L2 from family 2, and so on for six V_H families (Figure 2-9).

CHAPTER 3. EVALUATING THE CD138-NEGATIVE POPULATION IN MULTIPLE MYELOMA

3.1 Introduction

3.1.1 Background

The stem cell progenitor compartment in myeloma was championed for many years after it was initially proposed by Hamburger and Salmon in 1977 [27]. However, it was only in 2004 that a specific phenotype was proposed by Matsui et al [28]. Building on the finding of clonotypic circulating B cells in the peripheral blood of myeloma patients [37-39], Matsui's group suggested that as CD138 expression signalled terminal differentiation of both normal and malignant plasma cells, the pre-CD138 state might represent a myeloma progenitor. They demonstrated that within two CD138+ human myeloma cell lines (HMCL), there was small subset of CD138-negative (CD138−) cells. It was reported that this subset were more 'clonogenic', as evidenced by the formation of greater numbers of colonies in a methylcellulose-based colony formation assay (an *in vitro* technique designed to quantify clonogenicity and thereby 'stemness'). This subset also expressed B cell markers (CD19 and CD20) as well as higher levels of the proliferation marker Ki67. When primary myeloma cells from both bone marrow aspirates and peripheral blood were evaluated, a similar pattern was found. Colony formation by CD138+CD34− MNCs was less than that of CD138−CD34− MNCs, although only with serial re-plating. CD138−CD34− BM MNCs successfully engrafted into NOD/SCID mice, with subsequent infiltration of the murine BM by human CD138+ cells and detectable human immunoglobulin. In contrast, primary CD138+CD34− BM MNCs did not engraft or recapitulate disease. The importance of B-cell markers on this CD138− fraction was also reiterated by the observation that pre-treatment of the subset with the monoclonal anti-CD20 antibody Rituximab reduced colony formation.

The Matsui group's second paper supporting the CD138− phenotype of myeloma stem cells was published in 2008 [40], and it was this that triggered the experiments that form the bulk of this results chapter. They reported a number of additional stem cell-like features found within the CD138− subset of both HMCL and primary tumour cells. Firstly, they appeared to be relatively resistant to the cytotoxic effects

of commonly used anti-myeloma agents (dexamethasone, cyclophosphamide, bortezomib and lenalidomide), with preserved colony formation after treatment. Secondly, they segregated to the so-called 'side population' when stained with the DNA dye Hoescht 33342 (a feature reported for many different physiological and malignant stem cells). Thirdly, they had enhanced aldehyde dehydrogenase activity and finally, they displayed quiescence (in apparent contradiction to their previous finding of higher Ki67 staining).

At around the same time, Julia Kirshner's group published details of their novel culture system model for BM MNCs [44], which recapitulated elements of the normal BM architecture by culturing unselected cells within a layer of semisolid media (Matrigel). They used their system to culture myeloma patient BM MNCs and demonstrated prolonged survival of the tumour cells and specifically of apparent MM stem cells, which were CD20+ and localised in a quiescent state to the model's 'endosteum'.

Reviewing the literature (see Chapter 1. Introduction - section 1.2.1), it is apparent that Matsui's proposed CD138− MM stem cell phenotype has by no means been widely accepted and the phenotype of the MM stem cell remains unknown. At the time that the work in this chapter was initiated many of the more recent reports examining the CD138+ and CD138− sub-populations had not yet been published and the phenotype hypothesised by the Matsui group was the most up-to-date and apparently robust. It was therefore taken as a starting point for the work presented here.

3.1.2 Hypothesis and aims

Hypothesis: CD138− tumour cells derived from myeloma patient bone marrow aspirates displayed stem cell-like features including drug resistance, quiescence and enhanced clonogenicity, when compared to their CD138+ counterparts.

Aim 1: to phenotype primary myeloma tumour cells in terms of their expression of CD138, CD19, CD20 and CD27 in order to explore the proposal of Matsui et al that the CD138− compartment expressed B cell markers.

Aim 2: to set up and optimise an *in vitro* culture system that supported CD138− tumour cells from MM patient BM samples.

Aim 3: to use the culture system to characterise this population in terms of drug resistance, cell cycle profile and colony-forming potential.

3.2 Results

3.2.1 Phenotyping fresh MM BM MNCs

In order to achieve the first aim, the phenotype of freshly extracted BM MNCs was evaluated by flow cytometric analysis (method detailed in Chapter 2 – section 2.2) using antibodies for extracellular antigens including CD138, CD20, CD19, CD27 and CD38. Additionally, cells were permeabilised in order to detect expression of intracellular antigens such as kappa and lambda light chains (LC). This allowed an assessment of the tumour burden within the sample as well as co-expression of other antigens by LC-restricted CD138+ ('mature') and CD138− ('immature') cells. Matsui proposed that in addition to lacking CD138, the progenitor compartment in MM expresses B-cell markers, such as CD19, CD20 and CD27 (specifically found on memory B-cells) [28,40].

Two panels of antibodies were used to evaluate these cell populations. The first group of freshly isolated primary MM BM MNCs were phenotyped to quantify the proportions of the malignant clone (LC-restricted, LC+) expressing B-cell (CD20) and memory B-cell (CD27) markers, in combination with CD138. Analysis was confined to those with a LC+ clone greater than 10% and the percentages of the three subpopulations were expressed as a percentage of the malignant clone to allow comparison between patient samples. In all figures the samples were ranked by the percentage of CD138+ cells. Figure 3-1A shows the percentages of LC+ CD138+ vs. LC+ CD138−CD20+ vs. LC+ CD138−CD20− cells in 16 primary samples, while Figure 3-1B shows the percentages of LC+ CD138+ vs. LC+ CD138−CD27+ vs. LC+ CD138−CD27− cells in nine primary samples. In the second group of samples, using a second panel of markers, combined CD38 and LC positivity were used as an alternative, more stringent, method of quantifying the malignant clone, with CD19 used as a B cell marker, alongside CD138 as before. Figure 3-1C shows the

percentages of LC+CD38+ **CD138+** vs. LC+CD38+ **CD138−CD19+** vs. LC+CD38+ **CD138−CD19−** cells in 18 primary samples.

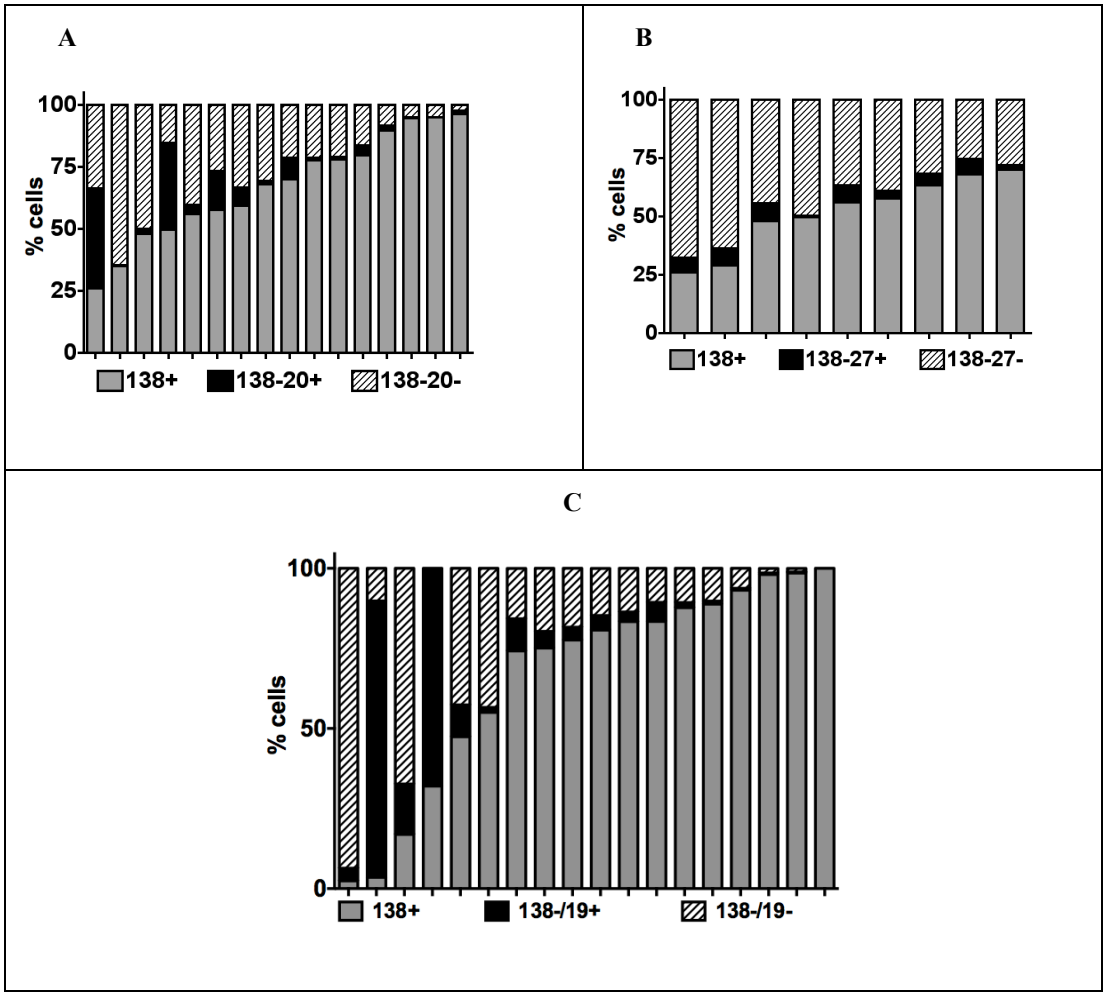

Figure 3-1 Phenotyping primary MM BM MNCs.

A. *The proportions of LC+* ***CD138+*** *(grey), LC+* ***CD138−CD20+*** *(black) and LC+* ***CD138−CD20−*** *(hatched) cells are shown, as a % of the LC+ cells (n=16; three new diagnoses, 13 relapses).* ***B.*** *The proportions of LC+* ***CD138+*** *(grey), LC+* ***CD138−CD27+*** *(black) and LC+* ***CD138−CD27−*** *(hatched) cells are shown, as a % of the LC+ cells (n=9; three new diagnoses, six relapses).* ***C.*** *The proportions of LC+CD38+* ***CD138+*** *(grey), LC+CD38+* ***CD138−CD19+*** *(black) and LC+CD38+* ***CD138−CD19−*** *(hatched) are shown, as a % of the LC+CD38+ clonal cells (n=18; seven new diagnoses, 11 relapses). All primary samples have LC+ cells populations >10% and are ranked in order of % of LC+CD38+ cells.*

Subgroup analysis looking at disease state or cytogenetic abnormalities did not reveal any association between B-cell marker expression and CD138 expression. It is

therefore apparent that the LC+CD138− sub-population is heterogeneous and does not reliably express B-cell markers.

3.2.2 The whole BM culture system maintains LC-restricted MM cells *in vitro* for up to three weeks

Previous work by John Quinn in the group had established the superiority of pooled MM patient plasma when compared with foetal bovine serum (FBS) for *in vitro* culture of primary MM cells. In addition, Kirshner et al [44] described how Matrigel-based whole BM culture was able to maintain the MM clone in culture for several weeks. Thus initial experiments were set up to compare suspension and Matrigel-based culture systems (see Chapter 2 – section 2.1.7 for methodology). Both the suspension and Matrigel-based systems were able to maintain viable LC+ tumour cells for up to three weeks. Figure 3-2 shows LC+ cells at baseline (D0) and after one week (D7) in culture.

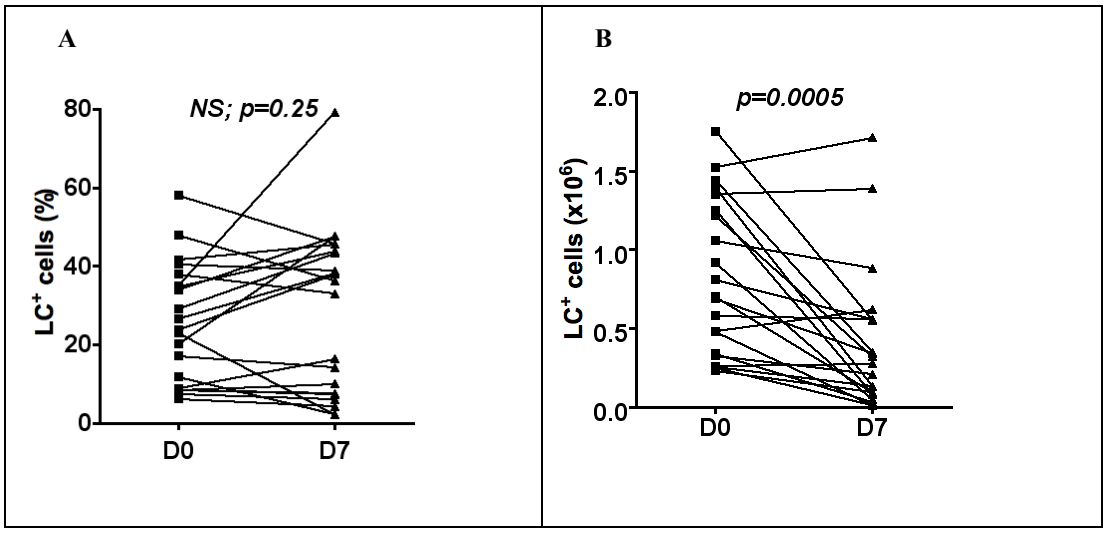

Figure 3-2 Survival of LC-restricted MM cells *in vitro*.

Freshly isolated unselected MNCs from MM patient BM aspirates were cultured for up to three weeks in a system utilising CM (14 suspension culture, seven Matrigel culture). FACs analysis was used to quantify the LC+ population at baseline, day 0 (D0), and when harvested at D9 (n=21; two new diagnoses, 19 relapses). ***A.*** *Survival of LC+ cells as a % of whole MNC population on D0 vs. D7.* ***B.*** *Absolute numbers of LC+ cells on D0 vs. D7. Significance values refer to the results of paired t-tests.*

Absolute numbers of total MNCs declined over the duration of the culture period to 43.65±5.91% of starting values. However, the MM clone, identified by those cells

which were LC+, was well maintained as a proportion of the whole and even increased in some cultures; at D7 absolute numbers of LC+ cells were 49.24±9.11% of starting values (Figure 3-2B; *p=0.0005*).

For some patient samples, the presence of a known translocation in the starting tumour cell population made FISH analysis a useful method of confirming clonality of the harvested D9 cells. The example in Figure 3-3 below shows a CD138+ cell harvested after nine days in culture, stained with May-Grunwald Geimsa (MGG; see Chapter 2 – section 2.3.3 for methodology) to confirm plasma cell morphology and probed for translocations using FISH (see Chapter 2 – section 2.3.1 for methodology). It demonstrates a fusion signal consistent with t(11;14), which was known to be present in the patient's MM cells.

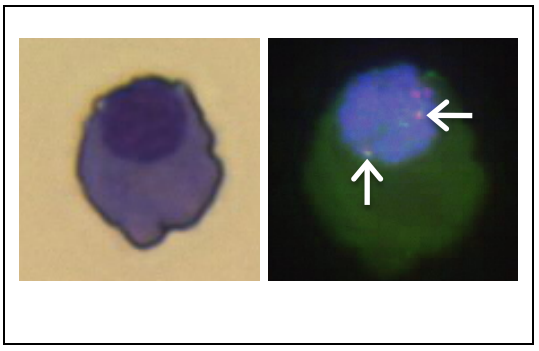

Figure 3-3 Paired MGG staining and FISH analysis of cells harvested from whole BM culture on D9.

MGG staining (left) of plasma cell harvested after nine days in culture, accompanied by FISH (right) showing fusion signal of t(11;14), arrowed.

3.2.3 Comparison of suspension and Matrigel whole MNC culture systems

Subsequently the survival of the CD138+ and CD138− subpopulations was compared between suspension and Matrigel-based cultures. Both systems included fibronectin and collagen and some cultures incorporated pro-survival cytokines (e.g. IL-6, IGF-I). The Matrigel system proved to be superior in terms of preservation of CD138− cells harvested following culture (Figure 3-4).

By D7 there had been a reduction in LC+CD138− cells grown in suspension culture (49.4±18.97% compared to D0), whereas in Matrigel culture there had been an

increase (155.7±54.85%; Figure 3-4B). As this was the main sub-population of interest, the Matrigel method was selected for further work.

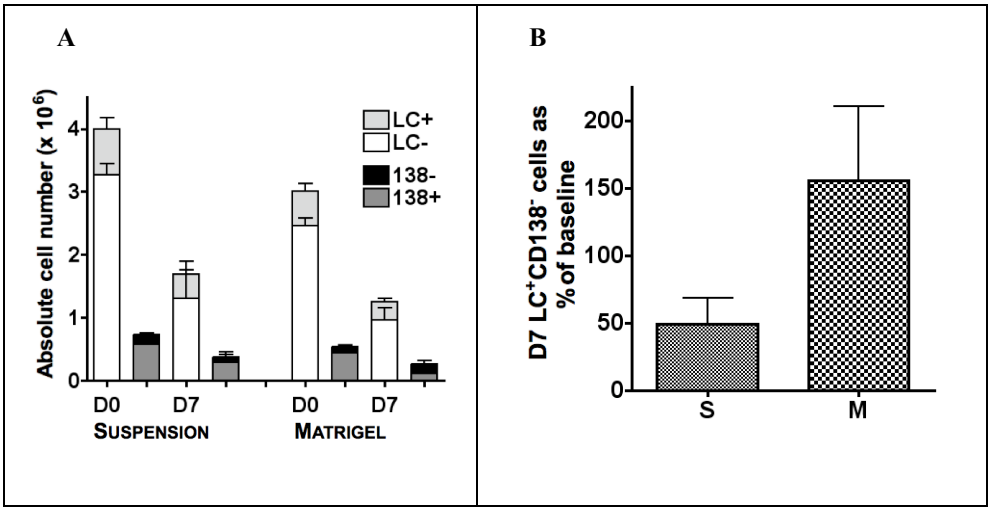

Figure 3-4 A. Survival of primary BM MNCs in suspension vs. Matrigel cultures. B. Survival of primary LC-restricted CD138− cells in suspension vs. Matrigel cultures.

Primary whole BM MNCs were cultured in parallel for seven days in two different culture systems using CM: suspension- and Matrigel-based (n=9; all relapses). Viable cells were quantified by trypan blue exclusion. ***A.*** *FACs analysis quantified LC+ (light grey) vs. LC− (white) MNCs, and, within the LC+ population, CD138+ (dark grey) and CD138− (black) cells. Absolute numbers of cells within each subpopulation on D0 and D7 are shown (mean & SEM).* ***B.*** *Viable LC+CD138− cells on D7 (as a % of baseline) are shown for both suspension (S) and Matrigel (M) culture systems (mean ±SEM; paired t-test NS).*

The system preserved MNCs, CD138+ and CD138− cells for up to three weeks, allowing assessment of the effect of cytokines and anti-myeloma drugs on the different sub-populations. The addition of pro-survival CKs had no impact on sub-population survival in either system.

Importantly, cultures set up from CD138-depleted MNCs were not able to repopulate a CD138+ clone, despite the hypothesised CD138− precursor phenotype (Figure 3-5). At seven and 14 days from set-up there were extremely low numbers of CD138+ cells present in the CD138-depleted condition, with no evidence of expansion of this compartment.

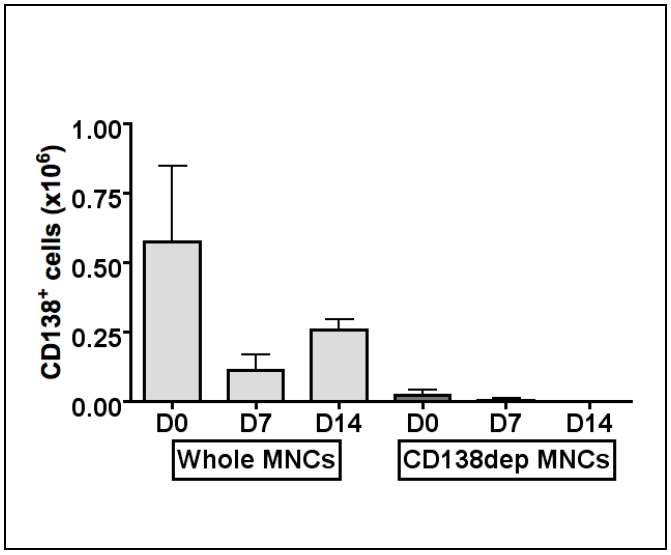

Figure 3-5 Enumeration of LC-restricted CD138+ cells cultured from whole BM MNCs compared to CD138-depleted BM MNCs.

Primary BM MNCs were cultured in two parallel systems for seven days, either whole or following CD138-depletion at set up (to <1.5%; n=3; all relapses). Viable cells were quantified by trypan blue exclusion and FACs analysis was used to quantify LC+CD138+ cells. Absolute numbers of CD138+ cells present are shown (mean ±SEM).

3.2.4 Effect of anti-MM agents in the whole BM culture system

Using the Matrigel culture system, whole BM MNCs were grown *in vitro* for seven days and then treated with dexamethasone (Dex) or with the proteosome inhibitor bortezomib (BZM) for 48 hours prior to harvest on day nine.

In this system Dex did not reliably cause a reduction of either LC+ or LC− cells (Figure 3-6A & B). Absolute numbers of CD138+ cells at D9 were 23.5±7.5% of baseline in the control condition compared to 22.0±9.7% in Dex-treated condition (paired t-test NS). In the LC+CD138− compartment, there was an increase in absolute terms at D9, to 132.1±46.5% in the control condition and 107.4±29.0% in the Dex-treated arm (paired t-test NS).

In contrast, BZM treatment (Figure 3-6C & D) was associated with a reduction in CD138+ cells at D9: 23.1±6.4% in the control arm compared to 7.7±4.8% in the BZM-treated arm (paired t-test *p=0.0239*). At D9 there was enrichment of LC+CD138− cells, 138.9±43.58% in the control arm and 201.6±64.9% after BZM treatment (paired t-test NS).

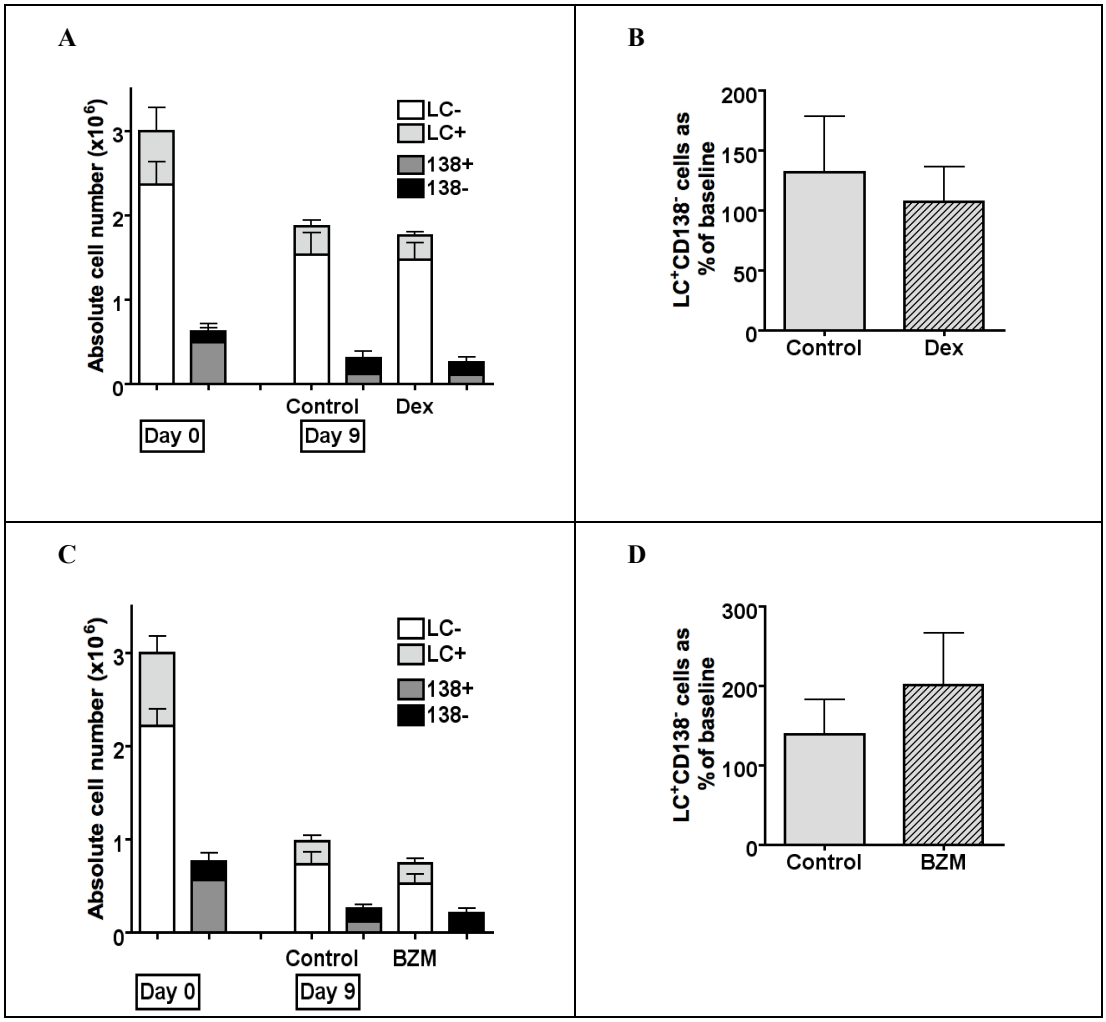

Figure 3-6 Drug treatment of primary BM MNCs in Matrigel culture: A. dexamethasone and B. bortezomib.

*Primary whole BM MNCs were cultured in Matrigel & CM for seven days and then treated with Dex 1μM (**A & B**; n=3; all relapsed MM) or BZM 20nM (**C & D**; n=11; one new diagnosis, ten relapsed MM) for a further two days prior to harvest (D9). **A & C.** FACs analysis as per Figure 3-4, with pooled data for all sub-populations shown at baseline (D0) and D9 (A: Dex, C: BZM; mean ±SEM). **B & D.** Viable LC+CD138− cells on D9 as a % of baseline as shown for control (light grey) and treatment (hatched) arms (B: Dex, D: BZM; mean ±SEM).*

3.2.5 Cell cycle properties of CD138+ and CD138− cells

The cell cycle characteristics of the LC+ sub-populations after a week in culture were assessed using a BrdU uptake-based flow cytometric analysis (see Chapter 2 – section 2.2.3 for methodology). This assay allowed evaluation of the cell cycle characteristics of the whole BM MNC population and comparison between them and those of LC+CD138+ and LC+CD138− cells (Figure 3-7A).

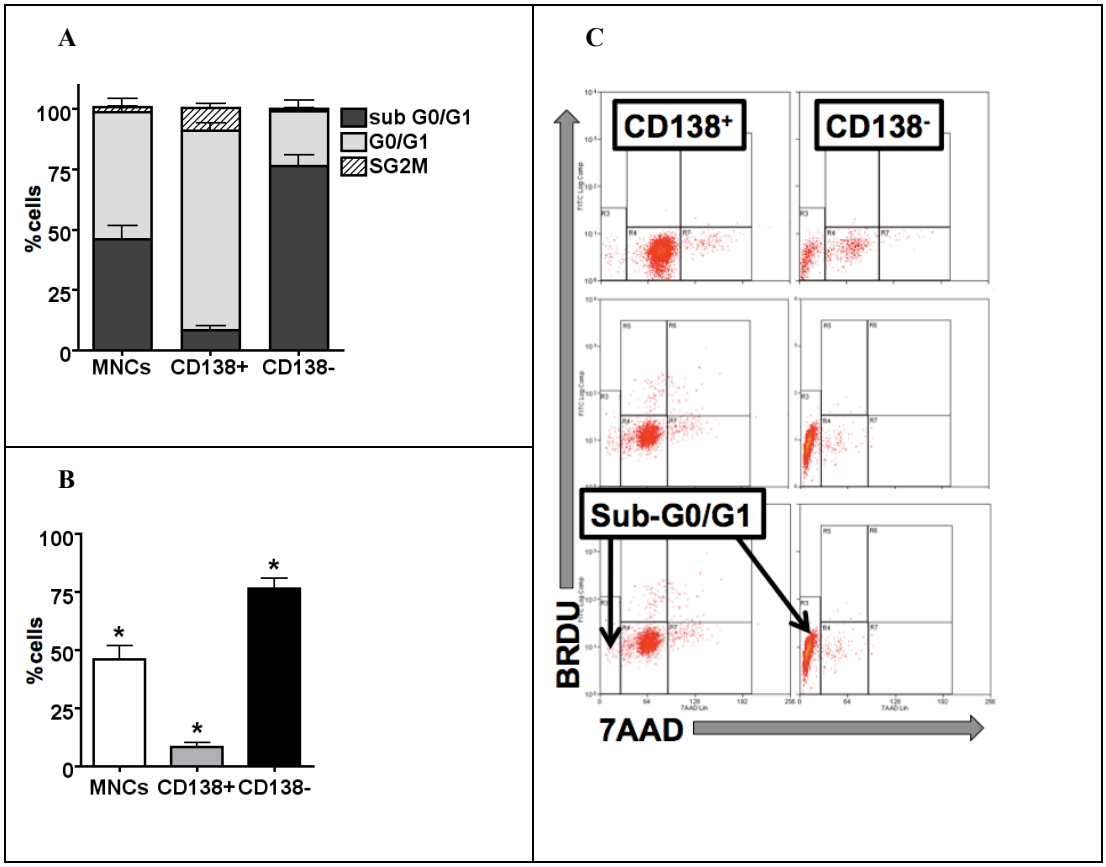

Figure 3-7 A&B. Cell cycle status of whole MNCs, CD138+ and CD138− cells, based on BrdU uptake and 7AAD staining. C. Representative cell cycle plots of CD138+ vs. CD138− cells, highlighting sub-G0/G1.

A. *Whole BM MNCs were cultured in Matrigel-CM. At nine days, cultures were pulsed with BrdU for three hours prior to harvest. Cell cycle characteristics at day nine were assessed using BrdU uptake and 7AAD staining. LC+CD138+, LC+CD138− and whole MNCs were analysed separately and the proportion of cells in sub-G0/G1 (black), G0/G1 (light grey) and S/G2M (hashed) are shown (n=9; one new diagnosis, eight relapsed MM; mean & SEM).* ***B.*** *Sub-G0/G1% for each subpopulation shown. *p<0.001.* ***C.*** *Representative FACs plots of CD138+ and CD138− cells (D9) from three primary samples are shown, highlighting proportion in sub-G0/G1.*

When the whole population of BM MNCs was examined, 2.19±0.3% was in S/G2M, while within LC+CD138+ cells the proportion was higher at 9.60±1.8% and in LC+CD138− cells the proportion was 1.00±0.2%. These differences were significant (MNCs vs. CD138+ *p=0.001*; MNCs vs. CD138− *p=0.004*; CD138+ vs. CD138− *p=0.0003*).

The proportion of unselected MNCs in sub-G0/G1, indicative of dying cells, was 45.95±5.7%, while in the LC+CD138+ subpopulation the proportion was much less

at 8.18±1.8%. LC+CD138− cells had the greatest proportion with 76.44±4.5% cells in sub-G0/G1. These differences were significant ($p<0.001$) in all combinations (Figure 3-7 B&C).

Thus while the culture system had seemed on FACs analysis to demonstrate an enrichment of the LC+CD138− cell population, cell cycle analysis revealed that the majority (76%) of this sub-population were apoptotic (sub-G0/G1), although trypan blue-excluding, at day nine.

3.2.6 Enumeration of clonogenic cells and evaluation of colony assays

The colony assay was developed in order to quantify the colony-forming potential of primary MM cells *in vitro*, as a surrogate for self-renewal and proliferative capacity and a measure of 'stemness'. The assay was modified from a methodology reported by Matsui et al [28]. Here whole primary BM MNCs were depleted of normal CD34+ haematopoietic progenitors and plated at 1-5x10^5 in methylcellulose supplemented with 30% bovine serum albumin, 2-mercaptoethanol, glutamine and 10% lymphocyte conditioned media (LCM). Colonies were counted from 14 days post-set up.

The method is detailed in Chapter 2 – section 2.1.8. Due to difficulties sourcing commercial LCM a number of supplementary cytokine combinations and lab-produced LCM were tested in order to optimise the colony assay. Table 3-1 charts the different conditions trialled and resultant colony characteristics.

Table 3-1 Methylcellulose additives trialled and resultant colony features

	Methylcellulose additives	**Colony features**
1	GMCSF 25ng/ml, Epo 2u/ml, IL-3 30ng/ml, GCSF 25ng/ml, SCF 10ng/ml	Consistent colony formation although highly variable morphology and colony density. Occasional erythroid colonies (BFU).
2	GMCSF 25ng/ml, Epo 2u/ml, IL-3 30ng/ml, GCSF 25ng/ml, SCF 10ng/ml + 5% pooled MM patient plasma	Some colony formation. Acellular precipitate throughout methylcellulose.
3	IL-3 30ng/ml, IL-4 10ng/ml, IL-6 20ng/ml	No colonies.
4	LCM	No colonies.
5	LCM (made without adherent monocytes)	No colonies.
6	No additives (methylcellulose alone)	No colonies.
7	10% pooled MM patient plasma	No colonies. Extensive acellular precipitate.
8	IL-2 20u/ml, IL-6 50ng/ml, IL-10 50ng/ml, IL-15 10ng/ml	No colonies.
9	IL-2 20u/ml, IL-6 50ng/ml, IL-10 50ng/ml, IL-15 10ng/ml + 10% pooled MM patient plasma	No colonies. Extensive acellular precipitate.

Following this comparison, it was decided that methylcellulose supplemented with GMCSF, Epo, IL-3, GCSF and SCF produced the greatest number and best demarcated colonies, allowing greater ease of counting. The addition of pooled MM patient plasma was associated with acellular precipitate, which made colony identification very difficult.

A typical colony is shown in Figure 3-8.

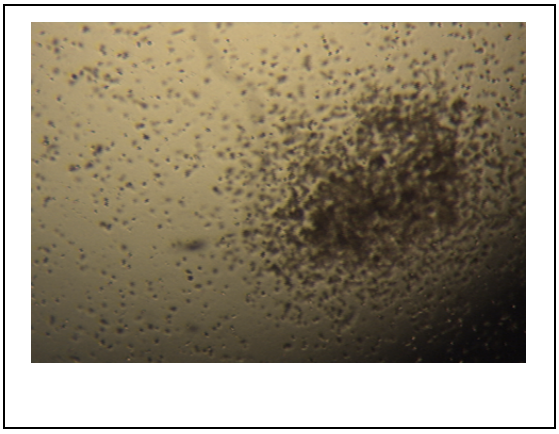

Figure 3-8 A representative colony grown from CD34-depleted MM BM MNCS.

Photomicrograph of a single colony growing in methylcellulose, four weeks from set up, photographed in situ at 10X magnification.

Additionally the concentration at which cells were seeded in methylcellulose was optimised. Colony assays were set up from freshly isolated MNCs (day 0) and after time in culture (Figure 3-9). Freshly isolated MNCs consistently generated higher numbers of colonies and therefore were seeded at $0.25x10^5$cells/ml and $0.12x10^5$cells/ml, while colony assays set up on day seven to nine were seeded at $1x10^5$cells/ml and $0.25x10^5$cells/ml.

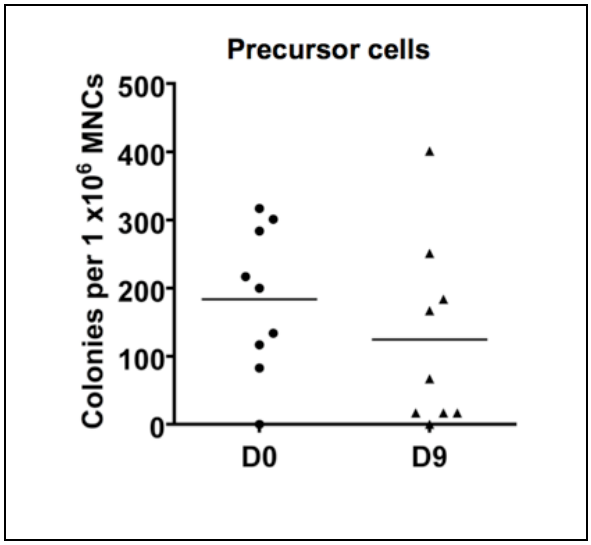

Figure 3-9 Colony formation at day zero versus day nine.

Clonogenic assays were set up at baseline (day zero, D0) and D9 to enumerate precursor cells. Colonies were counted at 14 days. Data from individual samples, with medians indicated; n=8.

Colony formation by different subpopulations of BM MNCs was then compared. All colony assays were set-up using MNCs which had been depleted of CD34+ cells (using Miltenyi Biotec CD34-MicroBeads and leucodepletion columns), to prevent the outgrowth of normal haematopoietic progenitor cells. Clonogenic potential was then examined in CD34− MNCs, CD34−CD138− MNCs and CD34−CD138+ MNCs. Absolute numbers of colonies varied widely between primary samples, but there was not a significant difference in colony number between these three groups.

Despite extensive efforts at optimisation, the colony assay had clear limitations. There was extremely variable colony formation between primary samples, even those taken at similar disease stages. Despite rigorous CD34+ cell depletion, erythroid burst-forming units (BFU) were sometimes seen, implying that there was CD34+ haematopoietic stem cell contamination or erythroid lineage cells were potentially arising from mesenchymal stem cells. Macroscopically, colonies grown were morphologically variable within a single assay and between D0 and D9. The cells within a single colony were also morphologically variable, as seen by MGG staining of cytospins from individual colonies (Figure 3-10). The majority of cells were plasmacytoid, while some had a monocytoid or macrophage-like appearance.

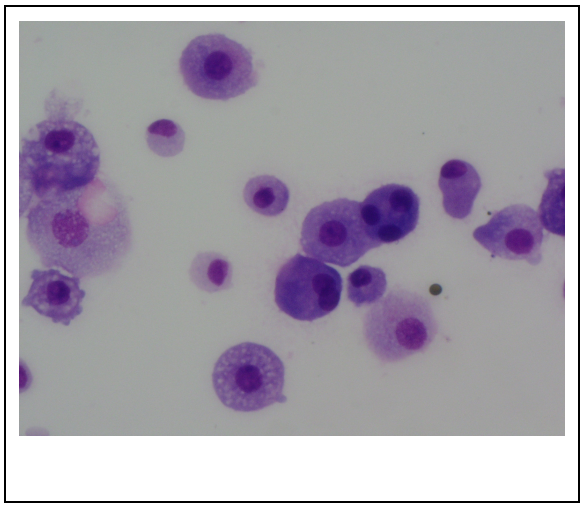

Figure 3-10 Morphology of cells derived from colony assay.

Single colonies were aspirated from methylcellulose and washed, and cytospins were made. Morphology was evaluated following MGG staining.

A number of approaches were used to identify the cells making up the colonies. FACs analysis of single colonies was not possible owing to low cell number,

exacerbated by the necessity for multiple washes to remove sufficient methylcellulose to allow antibody binding. FACs analysis of pooled colonies from single primary samples did not show a CD138+ population (Figure 3-11A). It was postulated that syndecan-1 (CD138) might be disrupted or even removed by methylcellulose, but colonies generated from unselected HMCL were consistently CD138+ (Figure 3-11B).

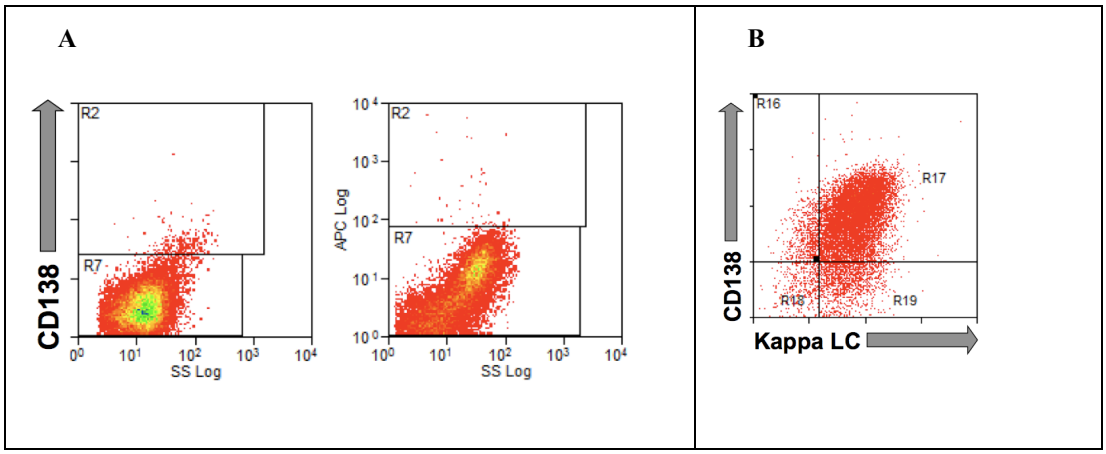

Figure 3-11 Flow cytometric analysis of cells from colony assays.

A. *Freshly isolated MM BM CD34−CD138− MNCs were seeded in methylcellulose. After four weeks colonies were plucked and pooled. After washing in warmed PBS, cells were stained for CD138-expression and examined by flow cytometry. Two examples are shown from two individual patients.* ***B.*** *KMS11 colonies were grown in methylcellulose. After 14 days colonies were plucked and pooled. After washing in warmed PBS, they were stained for CD138 and kappa LC expression and examined by flow cytometry.*

Immunohistochemistry confirmed that cells within plucked colonies were CD138−, MUM1− but occasionally BLIMP-1+ (Figure 3-12).

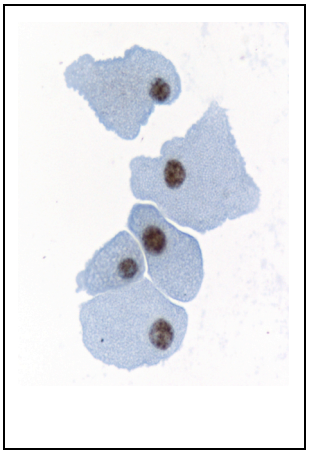

Figure 3-12 BLIMP-1 staining of cells isolated from colony assay.

Single colonies were aspirated from methylcellulose and washed, and cytospins were made. These were stained for CD138, MUM-1 and BLIMP-1. Representative cells positive for BLIMP-1 are shown; courtesy of Dr Teresa Marafioti.

Immunocytochemistry using dual esterase staining (method detailed in Chapter 2 – section 2.3.2) demonstrated that in excess of 90% of cells from the plucked colonies were positive for alpha naphthyl butyrate (Figure 3-13), a stain for monocytes and macrophages.

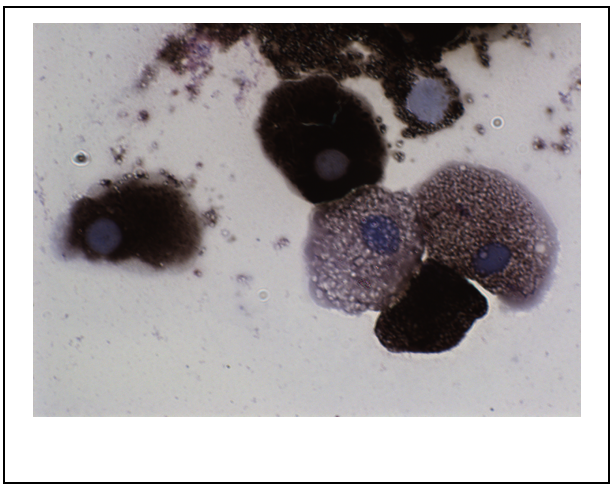

Figure 3-13 Dual esterase staining of cells isolated from colony assay.

Single colonies were aspirated from methylcellulose and washed, and cytospins were made, as per Figure 3-10. These were stained for alpha naphthyl butyrate and chloroacetate. Representative cells positive for alpha naphthyl butyrate are shown.

FISH analysis could not identify specific translocations in colony-cells grown from primary samples known to possess those translocations. It was not possible to analyse patient-specific VDJ sequences from colonies (see section 0 for method);

RNA extraction and RT-PCR of housekeeping genes was successfully performed from single colonies but the IgH VDJ sequence was not expressed at sufficiently high levels to be detectable by RT-PCR.

3.3 Summary and discussion

Phenotyping the MNCs in a large number (43) of MM patient BM aspirates demonstrated variable proportions of LC+CD138+ and LC+CD138− sub-populations. LC+CD138− cells did not consistently express B cell antigens, in fact the majority had extremely low expression of CD19, CD20 and CD27. This contradicted the findings of Matsui et al.

The modified three-dimensional culture system using fibronectin/collagen well-coating, RPMI/20% pooled patient plasma and Matrigel was able to maintain LC+ MM cells over a period of up to two weeks and this allowed analysis of the LC+CD138+ and LC+CD138− sub-populations after a number of microenvironmental modifications and drug treatments.

Over time and in the presence of anti-MM agents, there appeared to be an absolute increase in the number of LC+CD138− cells, although this was not accompanied by an increase in colony-forming potential, as might be anticipated. Cultures set up from CD138-depleted BM MNCs were not capable of generating mature CD138+ cells.

When the cell cycle profiles of CD138− and CD138+ cells were examined separately using BrdU uptake and 7AAD staining, more than 70% of CD138− cells were found to be sub-G0/G1 (i.e. apoptotic), compared to <10% of CD138+ cells. This confirmed the findings of Jourdan et al. [56] and Christensen et al. [55]. Hence a reinterpretation of the drug resistance assays was required: it appeared that the increasing number of CD138− cells in the culture system after anti-MM treatment reflected increased apoptosis and not enrichment for drug-resistant CD138− cells.

It was also clear that our main assay for enumerating precursor cells (i.e. the colony assay), derived from the methodology reported by Matsui et al [28,40], was not reproducible and therefore not sufficiently robust to accurately and consistently quantify colony forming potential of tumour cell subsets.

In evaluating our hypothesis we accomplished our first and second aims, but our characterisation of the 'stemness' of the CD138− subpopulation (Aim 3) was limited by the colony assay. As this was not robust, despite extensive attempts at optimisation, clonogenicity of myeloma cell subpopulations could not be accurately evaluated. Nevertheless it was concluded that our hypothesis did not hold true, and CD138 negativity was not a reliable phenotypic marker for a stem-cell sub-population in primary MM cells.

CHAPTER 4. APRIL-MEDIATED DRUG RESISTANCE IN MULTIPLE MYELOMA

4.1 Introduction

4.1.1 Background

In the next phase of exploring the tumorigenic progenitor compartment within multiple myeloma, it seemed sensible to look from a functional angle and explore cellular mechanisms of drug resistance within primary myeloma cells and human myeloma cell lines. Drug resistance is a key feature of cancer stem cells, as it is for physiological stem cells, and appears to be mediated by a number of both intrinsic and microenvironmental mechanisms.

It has been established that the bone marrow microenvironment is critical to MM cell drug sensitivity and that both soluble factors and direct cell-cell contacts are heavily implicated (see Chapter 1 - section 1.2.2). In this results chapter, the specific contribution of the cytokine APRIL will be explored. There is an increasing understanding of the importance of APRIL in the differentiation and long-term survival of memory B cells, plasma cells [68,70,71] and also to the survival of malignant plasma cells [75,76]. APRIL is produced by a number of cell types within the bone marrow including all members of the myeloid lineage, osteoclasts and BM stromal cells[71]. It was recently demonstrated that levels of APRIL within the BM remain constant despite varying levels of MM cell infiltration at different points in the disease [127]. When APRIL-producing cells within the marrow were characterised at different stages in the disease, it was apparent that as MM infiltration increased, the proportion of immature CD16− myeloid cells, which secrete the most APRIL, also increased. The same group have subsequently showed that MM cells were able to influence proportions of haematopoietic precursors. The majority are suppressed, with the exception of CD16− myeloid precursors [128] because this cell sub-group proliferate in response to IL-6 (in a RANKL-dependent fashion). It seems therefore that MM cells are able to modulate their environment to enhance APRIL secretion.

The contribution of cytokines such as IL-6, VEGF and IGF-I to the survival of malignant plasma cells after treatment with anti-myeloma agents is relatively well-

understood but it is only recently that APRIL has also been implicated as a potential effector of drug resistance [76]. Moreaux et al demonstrated high levels of expression of APRIL receptors, BCMA and TACI, on both HMCL and primary MM cells and the secretion of APRIL into the culture media by MM cells. They also reported that APRIL was able to rescue IL-6 dependent HMCL from IL-6 deprivation and blockade of APRIL binding reduced the proliferation of cytokine-independent HMCL. The effects of dexamethasone on sensitive HMCL and primary MM cells were mitigated by the addition of excess APRIL. These findings were attributed to the actions of the NF-κB and PI3K/AKT pathways.

Affymetrix microarrays were used to examine protein expression in purified MM cells from newly diagnosed patients[77]. Two groups were identified with higher versus lower TACI expression, and it was found that higher TACI expression correlated with better clinical outcomes. Analysis of the genes that were differentially expressed by the two groups showed that high TACI expression was associated with a mature plasma cell signature, implying dependence on the BM microenvironment, while low TACI expression was associated with a plasmablast gene signature, implying attenuated dependence on the BM, such as that seen in extramedullary MM cells. This hints towards the potential contribution of APRIL to BM microenvironmental support and protection of MM cells.

Work published by our group showed that APRIL was able to trigger cell-cycle progression in primary MM cells [18], but only in those overexpressing cyclin D2 as a result of translocations involving the IgH gene locus (t(4;14) and t(14;16)). APRIL-mediated drug resistance might similarly segregate to different genetic subtypes. Dependence on APRIL-mediated survival pathways may therefore render particular genetic sub-groups suitable for anti-APRIL strategies, as an alternative approach to those distinguished by *TACI* expression signature.

4.1.2 Hypothesis and aims

Hypothesis: APRIL offers protection to myeloma cells exposed to anti-myeloma agents and is therefore a potential effector of bone marrow microenvironmental drug resistance. The effects of APRIL vary between different genetic subtypes of MM.

Aim 1: to investigate the effect of soluble recombinant APRIL on the sensitivity of primary MM cells of different genetic subtypes to anti-myeloma agents.

Aim 2: to identify cellular mechanisms underlying protection seen.

Aim 3: to investigate the effect of APRIL-secreting HS5 cells on the sensitivity of co-cultured HMCL to anti-myeloma agents.

4.2 Results

4.2.1 Effect of soluble recombinant APRIL on drug resistance in primary MM cells

4.2.1.1 APRIL does not influence survival of primary CD138+ cells

Primary CD138+ MM cells were cultured in the presence of APRIL (see Chapter 2 – section 2.1.9 for detailed methodology). The addition of APRIL to CM at the time of culture set up had no consistent effect on the survival of CD138+ cells. Our group had previously reported that APRIL stimulated cell-cycle progression in CD138+ cells of specific genetic subtypes [18], and therefore the results were re-analysed by cyclin D-type expression into Cyclin D1 (CCND1) and Cyclin D2 (CCND2)-expressing patients (see Figure 4-1) but no difference in survival was seen.

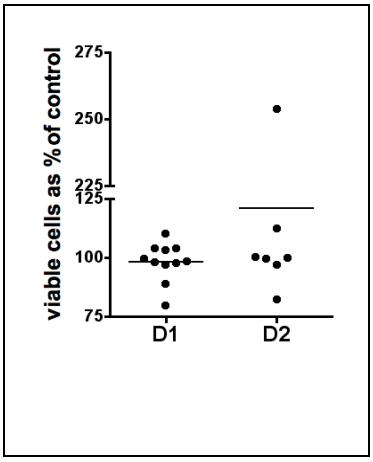

Figure 4-1 Effect of APRIL on CD138+ cell survival.

Primary CD138+ cells were cultured in CM +/- APRIL 200ng/ml. Cell viability was assessed after 48 hours by AV/PI staining. Viable AV−PI− cells in APRIL-treated condition are shown, as % of control (CM alone), sub-divided into CCND1 (D1; n=11) and CCND2 (D2; n=7) MM cells.

4.2.1.2 APRIL attenuates dexamethasone-mediated apoptosis in primary CD138+ cells

CD138+ MM cells were treated with dexamethasone (Dex) in the presence of APRIL as detailed in Chapter 2 – section 2.1.9.

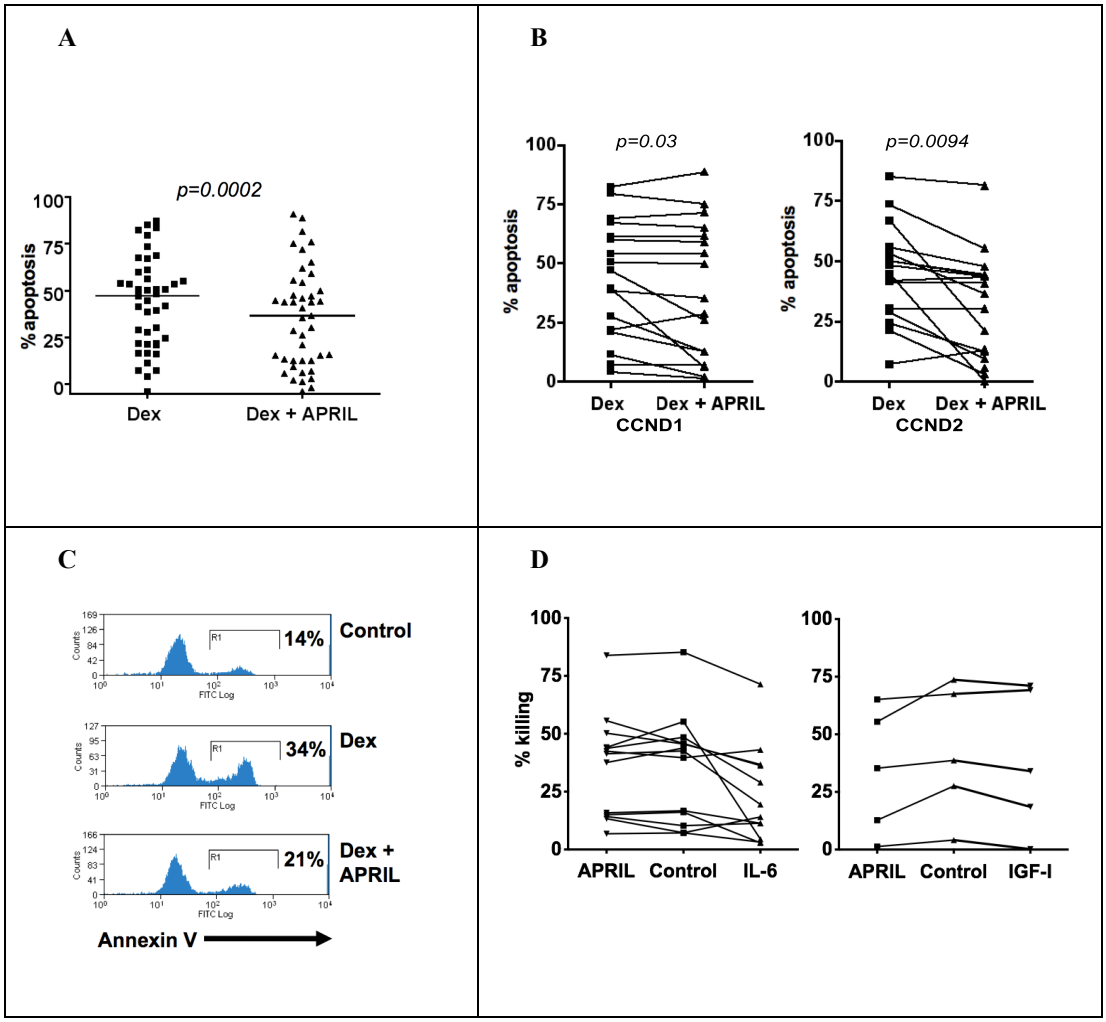

Figure 4-2 Effect of APRIL, IL-6 and IGF-I on dexamethasone-induced apoptosis in CD138+ cells.

Primary CD138+ cells were treated with Dex +/- APRIL, IL-6 or IGF-I for 48 hours. Apoptosis was quantified by AV/PI staining. Results are presented as apoptosis as a % of control. ***A.*** *Pooled results from 43 experiments comparing treatment with Dex alone to Dex + APRIL (individual results and median indicated).* ***B.*** *Results from 35 experiments are analysed by CCND-type expression (CCND2 n=17, CCND1 n=18; paired results shown).* ***C.*** *Representative FACs plots of CCND2 MM cells. The % of apoptotic cells is shown.* ***D.*** *Primary CD138+ cells were treated with Dex (control) +/- APRIL +/- IL-6 (n=13) or IGF-I (n=5).*

APRIL reduced Dex-induced apoptosis at 48 hours. This was seen in the majority of primary MM cells and was highly significant (paired t-test *p=0.0002*; Figure 4-2A). Segregation of primary samples into CCND1-expressing (CCND1+) and CCND2-expressing (CCND2+) subtypes revealed more consistent and greater degrees of protection in CCND2+ CD138+ cells compared to CCND1+ CD138+ cells (paired t-tests *p=0.0094* and *p=0.03* respectively; Figure 4-2B). The degree of Dex-induced apoptosis in the control condition varied between samples but a representative FACs plot from a CCND2+ sample is shown in Figure 4-2C.

APRIL-mediated protection against Dex killing was compared to that associated with IL-6 or IGF-I in a small number of primary samples (Figure 4-2D). The numbers are limited and sub-group analysis by CCND expression was not possible. However, there is broad trend towards protection being greatest in cells treated with IL-6, then APRIL, with the least protection seen in samples treated with IGF-I.

4.2.1.3 APRIL does not influence bortezomib- or lenalidomide-induced apoptosis

CD138+ cells were treated with bortezomib (BZM) (Figure 4-3). BZM induced apoptosis in the majority of samples (median apoptosis 84.7% (range 1-95.2%), mean (±SD) apoptosis 67.9% ±28.6; n=13; see Figure 4-3A).

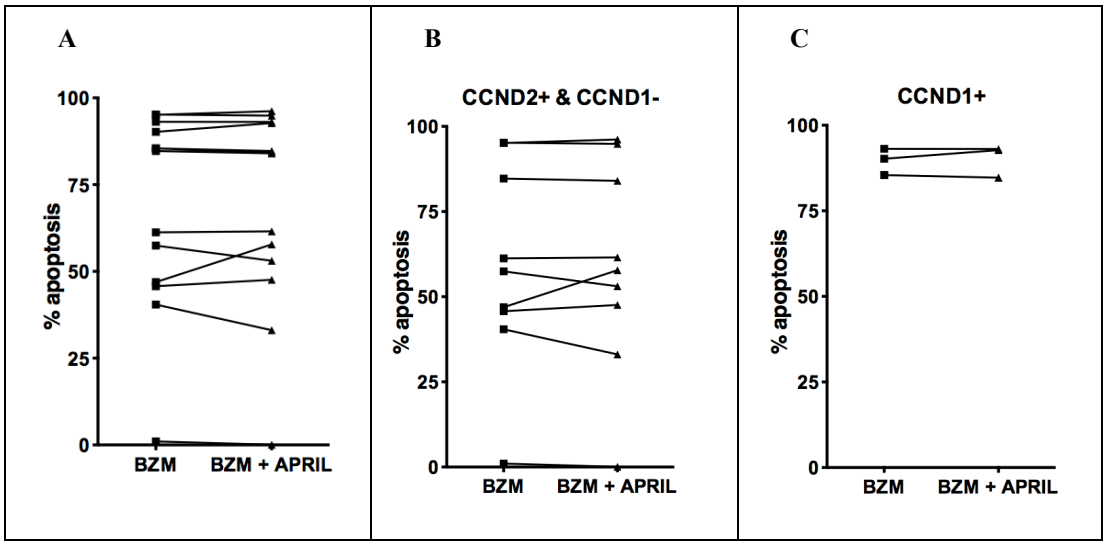

Figure 4-3 Effect of APRIL on bortezomib-induced apoptosis in CD138+ cells.

Primary CD138+ cells were treated with BZM +/- APRIL for 48 hours. Apoptosis was quantified by AV/PI staining. Results are presented as apoptosis as a % of control (paired

results shown). ***A.*** *All patients (n=13).* ***B.*** *CCND2+ and CCND1- patients (n=9).* ***C.*** *CCND1+ patients (n=3).*

However, there was no protection from apoptosis seen with the addition of APRIL (median 84.0% (range 0.1-96.2%), mean (±SD) apoptosis 67.9 ±29.1; paired t-test non-significant). This was true even when samples were analysed according to CCND-type (Figure 4-3B&C), although analysis was limited by the sample number of CCND1+ samples.

MM cells were also treated with lenalidomide (Len) (Figure 4-4). Len induced apoptosis in all samples (median apoptosis 44.6% (range -10.5-89.6%), mean (±SD) 46.9 ±33.6; n=18; see Figure 4-4A) but as with BZM there was no protection seen in cells co-treated with APRIL (median apoptosis 35.4% (range 0.77-88.8%), mean (±SD) 42.5 ±30.12; paired t-test non-significant). Analysis of CCND1+ and CCND2+ samples separately did not reveal any protection (Figure 4-4B&C).

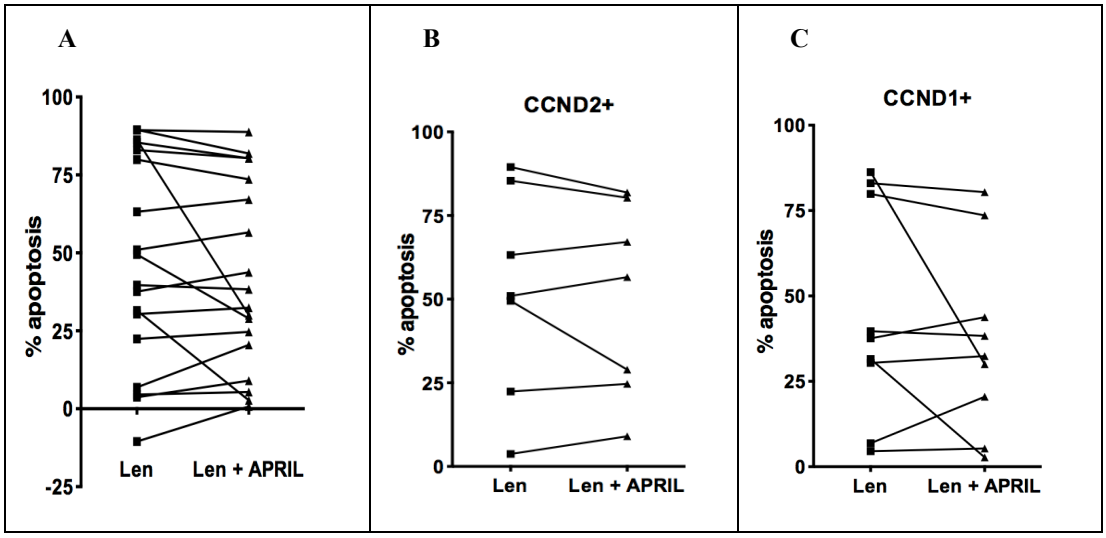

Figure 4-4 Effect of APRIL on lenalidomide-induced apoptosis in CD138+ cells.

Primary CD138+ cells were treated with Len +/- APRIL for 48 hours. Apoptosis was quantified by AV/PI staining. Results are presented as apoptosis as a % of control (paired results shown). ***A.*** *All patients (n=18).* ***B.*** *CCND2+ patients (n=7).* ***C.*** *CCND1+ patients (n=9).*

4.2.1.4 The effect of PI3K/AKT pathway inhibition on APRIL-mediated protection from dexamethasone killing

In order to explore whether the PI3K/AKT pathway was involved in APRIL-mediated protection from Dex killing, the small molecule inhibitor PI103 was added to cells exposed to APRIL and/or Dex. This acts both on PI3K and the mTOR complex to cause complete blockade of the pathway.

PI103 alone has a modest effect on MM cell viability (Figure 4-5A), which appears to be partially reduced in the presence of APRIL. In the five patient samples evaluated in this series of experiments, Dex killing was highly variable (as it was across the larger series in 4.2.1.2), hence the large error bars in Figure 4-5A. Thus drawing conclusions regarding the effects of both APRIL, PI103 and the combination is impossible in this series. Figure 4-5B highlights the differences in levels of apoptosis seen between patient samples and while there is a trend towards confirmation of APRIL-mediated protection against Dex killing, it is not statistically significant.

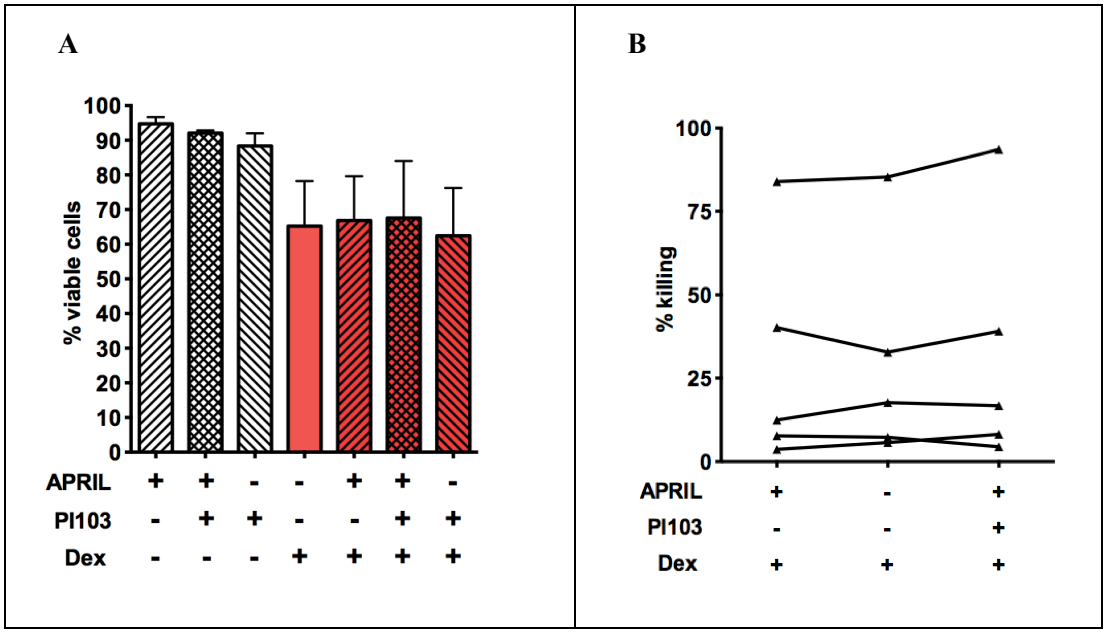

Figure 4-5 Effect of APRIL and PI103 on dexamethasone-induced apoptosis in CD138+ cells.

Primary CD138+ cells were treated with Dex +/- APRIL and/or PI103 1μM for 48 hours. Apoptosis was quantified by AV/PI staining (n=5; all conditions set up in triplicate) ***A.*** *Viable cells are shown as a % of control for all seven conditions (mean ±SEM).* ***B.*** *Apoptotic cells are shown as a % of control for each experiment.*

This experiment highlighted the difficulty of working exclusively with primary MM cells, as the baseline viability and drug sensitivity was extremely variable between different samples. For this reason, it was decided to screen HMCL for sensitivity to Dex, in order to select suitable cell lines for further mechanistic work.

4.2.2 HMCL cultured in the presence of soluble recombinant APRIL

A panel of HMCL were screened to identify first those that were sensitive to Dex and secondly those who also had protection from Dex cytotoxicity in the presence of APRIL.

4.2.2.1 HMCL sensitivity to dexamethasone

The first stage of screening was undertaken using two Dex doses (1μM and 10μM) in RPMI/10%FBS (R10) and in serum-free RPMI (R) (for methodology see Chapter 2 – section 2.1.10). The following HMCL were screened: U266, KMS-12PE, KMS-21BM, NCI-H929, JIM1, JJN3, KMS-11, OPM2, MM1S, RPMI-8226, KMS-27 and KMS-28PE.

The effect on cell growth and viability is displayed below graphically in Figure 4-6. The results are tabulated in Table 4-1 (only figures for Dex 10μM are displayed).

These experiments demonstrated that Dex-sensitivity was highly variable between the different lines, with no obvious pattern seen based on translocation group. The lines could be broadly grouped into moderately, minimally and in-sensitive based on ranking the effect of Dex on cell viability and cell growth (Table 4-2). KMS-11 and KMS-28PE were the most sensitive lines, both in terms of cytotoxicity and inhibition of growth.

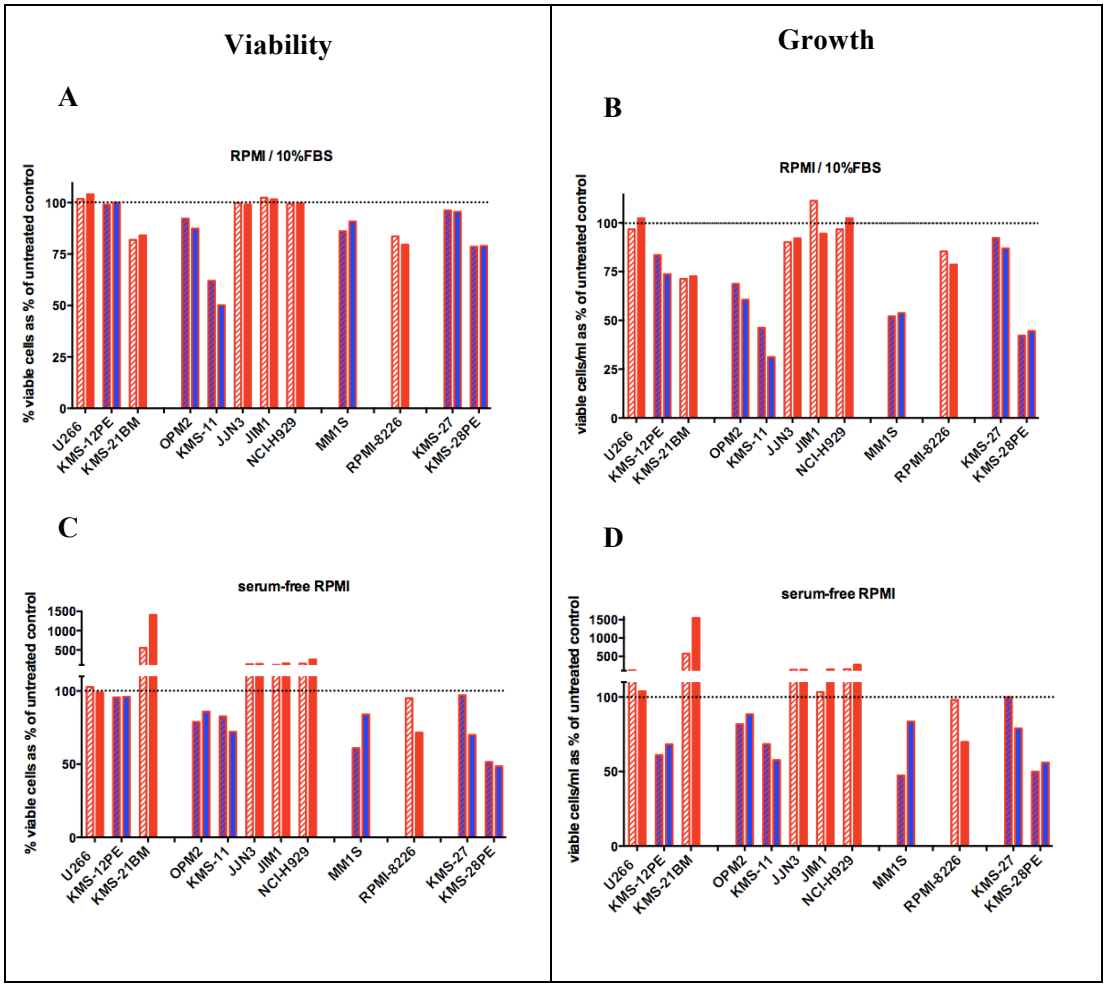

Figure 4-6 Effect of dexamethasone treatment on HMCL cultured in R10 and R alone.

HMCL were cultured in R10 or R alone and treated with Dex (hashed 1uM, block colour 10uM; blue in-filled bars represent HMCL that were subsequently re-evaluated with APRIL) for 48 hours. Cells were harvested and viability and growth were assessed by AV/PI staining. All conditions were in triplicate and values above represent mean viable cell % or cell concentration of Dex-treated cells, as a % of untreated control cells. HMCL are arranged into groups by translocation type.

Table 4-1 Effect of dexamethasone treatment on HMCL cultured in R10 and R alone.

Translocation Status	HMCL	Effect of dexamethasone treatment (10μM)			
		Proliferation (Viable cells/ml as % of untreated control)		Viability (% Viable cells as % of untreated control)	
Culture media		**R10**	**R**	**R10**	**R**
t(11;14)	**U266**	127.84	103.84	104.04	99.02
	KMS-12PE	73.69	68.23	99.95	95.99
	KMS-21BM	72.62	1548.12	84.06	1408.56
t(4;14)	**OPM2**	60.62	88.37	87.32	85.95
	KMS-11*	31.23	57.68	50.12	72.04
	JJN3	92.00	139.83	99.06	138.13
	JIM1	94.39	148.82	101.59	152.03
	NCI-H929	102.35	275.74	99.60	254.07
t(14;16)	**MM1S**	53.75	83.48	90.81	83.95
t(16;22)	**RPMI-8226**	78.60	69.84	79.54	71.51
Uncharacterised	**KMS-27**	86.89	78.98	95.54	69.99
	KMS-28PE	44.53	56.04	78.91	48.55

*HMCL were cultured, Dex treated, harvested and analysed as per Figure 4-6. Values above represent mean viable cell % or cell concentration of Dex-treated cells, as a % of untreated control cells. *Also t(14;16)*

In all but MM1S cells, viability and growth were influenced in the same way by the presence or absence of serum (see Table 4-2, right-hand column); for example, KMS-11 cells were both less sensitive to Dex-associated cytotoxicity and Dex-associated growth inhibition in the absence of serum.

Table 4-2 HMCL sensitivity to dexamethasone.

Sensitivity	HMCL	Effect of Dex in R alone cf. R10
Moderate	KMS-28PE	Viability & growth *decreased*
	KMS-11	Viability & growth *increased*
	RPMI-8226	Viability & growth *decreased*
	MM1S	Viability *decreased* but growth *increased*
Low	KMS-12PE	Viability & growth *decreased*
	KMS-27	Viability & growth *decreased*
	OPM2	Viability & growth *increased*
	KMS-21BM	Viability & growth *increased*
No	U266	Not applicable
	JJN3	
	JIM1	
	NCI-H929	

Based on the findings of these experiments, five HMCL were taken forward for further testing of Dex sensitivity in the presence of APRIL: KMS-28PE, KMS-11, MM1S, KMS-12PE and KMS-27. Although RPMI-8226 were also Dex-sensitive, their growth in culture was erratic and their baseline viability was often poor.

4.2.2.2 HMCL sensitivity to dexamethasone in the presence of APRIL

HMCL were cultured in R10 and APRIL was added 24 hours before Dex treatment. Once again HMCL were treated with 0, 1 or 10μM Dex. Initial results were promising, with APRIL-associated protection seen in KMS-28PE and MM1S (Figure 4-7). However, this protection was only seen in the form of mitigation of Dex-associated growth inhibition.

Similar levels of cytotoxicity were seen at both doses of Dex, compared to the previous screening experiments. No protection from Dex-associated cytotoxicity was seen in the presence of APRIL in any of the HMCL evaluated.

HMCL	Viability	Growth
KMS-28PE	A	B
KMS-11	C	D
MM1S	E	F

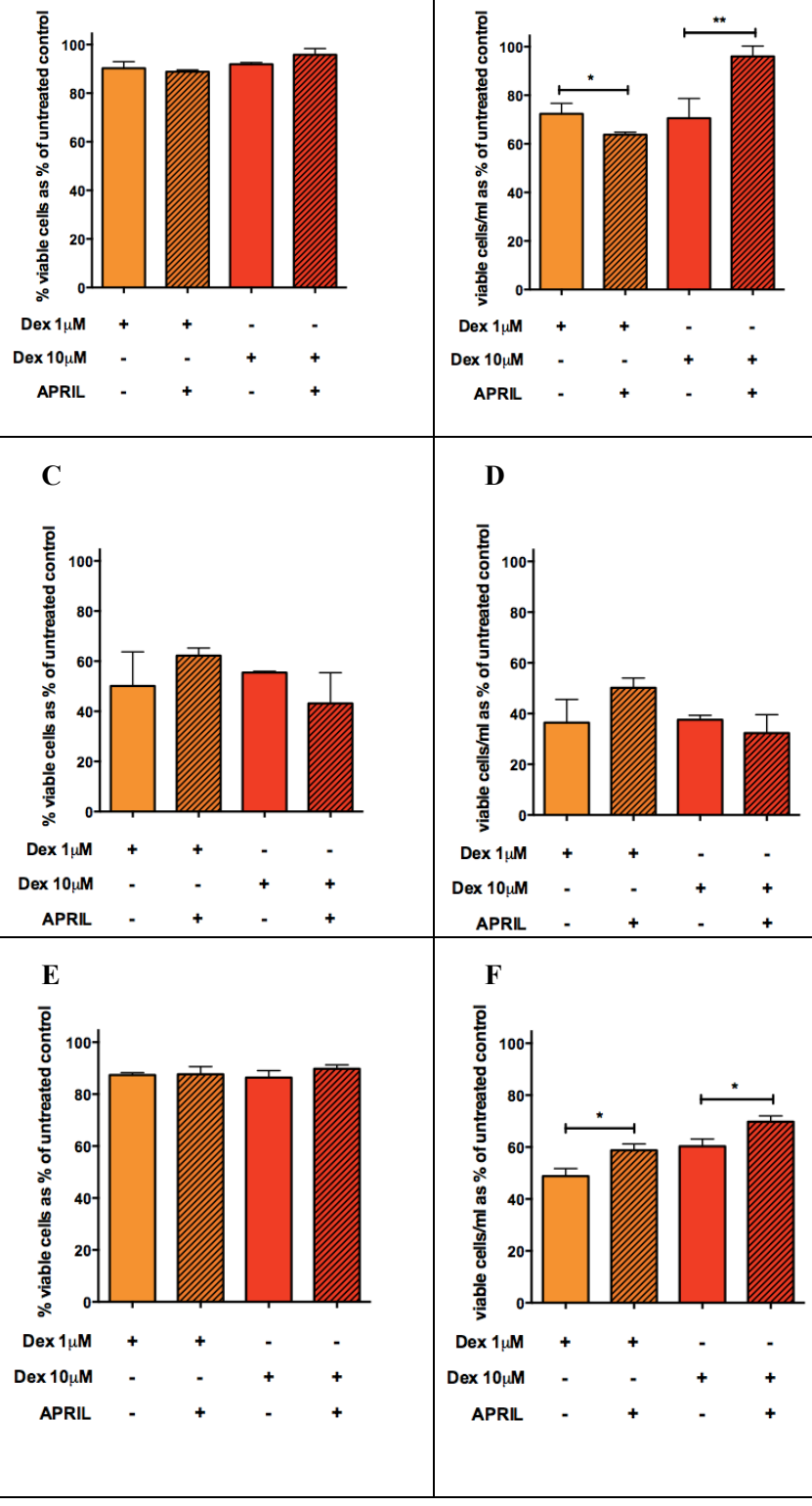

Figure 4-7 Moderately dexamethasone-sensitive HMCL exposed to APRIL.

*Three moderately sensitive HMCL were evaluated: KMS-28PE (**A** & **B**), KMS-11 (**C** & **D**) and MM1S (**E** & **F**). HMCL were cultured in R10 ± APRIL and treated with Dex for 48*

*hours (orange 1μM, red 10μM). Cells were harvested and viability and growth were assessed by AV/PI staining. All conditions were in triplicate and values above represent mean ±SD viable cell % or cell concentration of Dex-treated cells, as a % of untreated control cells. Hashed bars represent HMCL that were exposed to APRIL. The results of statistically significant analyses are shown (unpaired t-test; *p<0.05, **p<0.01).*

The relative resistance of many HMCL to Dex, and the variable sensitivity of the remaining cell lines, with no clear dose dependence of Dex-mediated killing, or of APRIL-mediated protection meant that this was not a suitable model to explore the drug resistance activity of APRIL.

It is possible that the protective effect of APRIL is best explored in a stromal cell co-culture system, utilising stromal cells modified to express APRIL. This was the next system that was evaluated.

4.2.3 Modifying HS5 to express and secrete APRIL

APRIL(Ap)+HS5 and their empty vector negative control NC(Ap)HS5 were produced as detailed in Chapter 2 – section 2.7.6.1.

4.2.3.1 Confirmation of APRIL secretion by Ap+HS5

ELISA was used to quantify APRIL protein in media in which Ap+HS5 or NC(Ap)HS5 had been cultured. The relationship between HS5 cell number and APRIL concentration is charted in Figure 4-8.

Cells were harvested on days four, five and six. These time points were chosen as by day four the HS5 cells were usually >90% confluent and HMCL could be seeded onto them for co-culture experiments. Culture media was harvested at the same time points and APRIL was quantified by ELISA. Figure 4-8 shows that the growth of the two modified HS5 cell lines was not significantly different. It also shows that the modified HS5 cells exerted contact inhibition with minimal additional growth after reaching confluence.

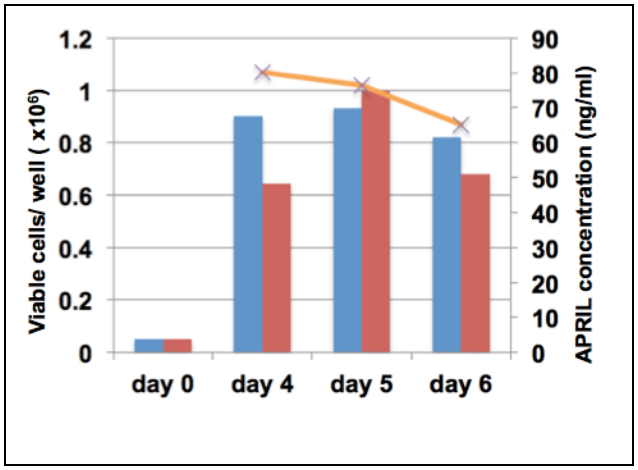

Figure 4-8 Growth of modified HS5 cells in culture and the secretion of APRIL.

NC(Ap)HS5 (blue bars) and Ap+HS5 (red bars) were seeded on day 0 at 50,000 cells/well in a TC-treated 12-well plate. Viable cells (trypan blue-excluding) harvested on days 4, 5 and 6 are charted. APRIL concentration in culture media harvested from Ap+HS5 cultures is shown as an orange line.

APRIL was only detectable in the media harvested from Ap+HS5 cultures, confirming that HS5 cells had no inherent APRIL secretion and that the transduced APRIL construct was functional. Interestingly APRIL did not accumulate significantly over the time frame evaluated. This may reflect negative feedback to secretion or a short half-life to the secreted protein.

4.2.4 HMCL co-culture with Ap+HS5 for growth and cytotoxicity assays

4.2.4.1 Co-culture set-up and interpretation

U266 and MM1S cells were cultured alone or in co-culture with either Ap+HS5 or their empty vector negative control - NC(Ap)HS5. Cultures were set up according to the protocol detailed in Chapter 2 – section 2.1.11.

The purity of the modified HS5 cells was regularly assessed by flow cytometry for GFP expression. Both Ap+HS5 and NC(Ap)HS5 were consistently >90% GFP+. In samples containing both HMCL and modified HS5, GFP− cells were assumed to be HMCL and GFP+ cells were assumed to be modified HS5 cells. Figure 4-9 illustrates the gating strategy with representative plots from both suspension and adherent fractions.

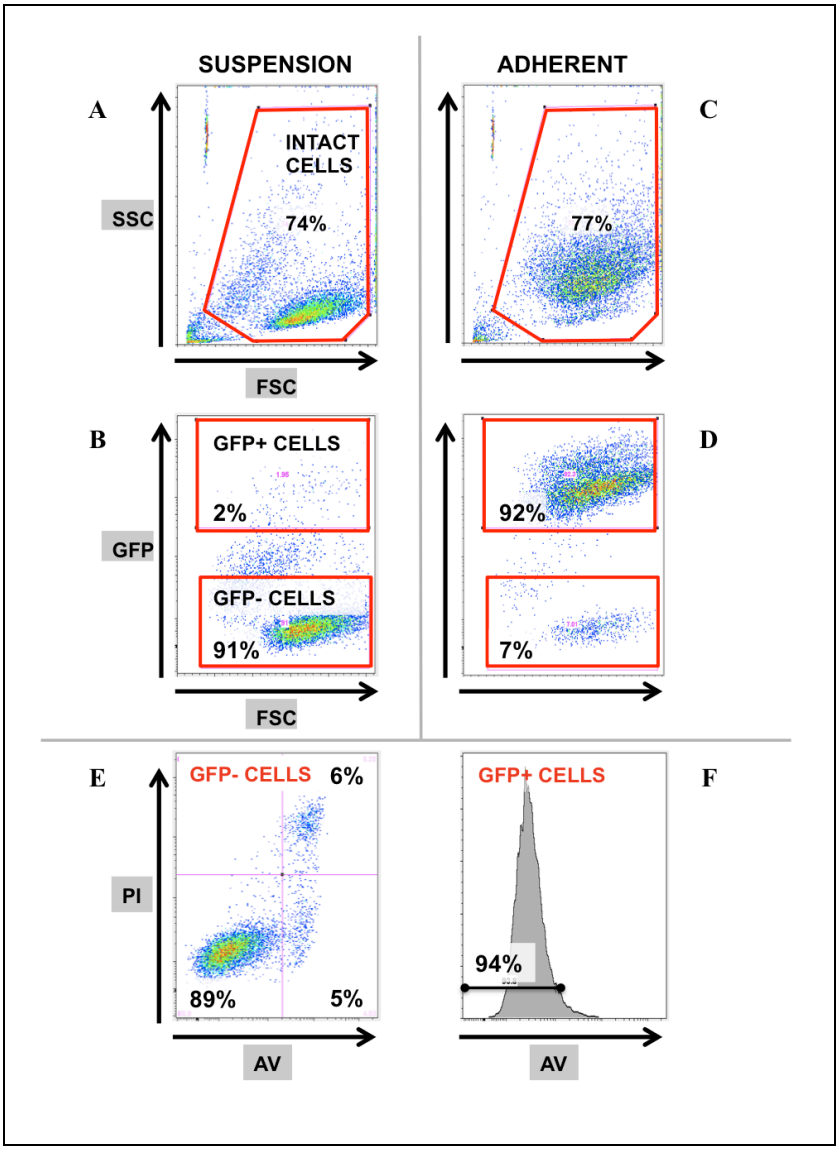

Figure 4-9 Gating strategy with representative FACS plots showing AV/PI staining on HMCL grown in co-culture with modified HS5.

*The gating strategy and representative plots from an assay in which untreated U266 cells were co-cultured with Ap+HS5 are shown. The % of cells in the various gates are shown. The **left**-hand top two plots (**A & B**) are derived from a suspension fraction sample and the **right**-hand two top plots (**C & D**) are derived from an adherent fraction sample. Dot-plots **A** & **C** show all events by forward scatter (FSC) area/ side scatter (SSC) log (x/y respectively and hereafter) with a gate around intact cells. These are gated on to **B** and **D** respectively (FSC area/GFP log) to allow determination of GFP+ and GFP− populations. The viability of GFP− cells is evaluated in dot-plot **E** (AV-APC log/PI log); in this example 89% of cells are viable (AV−PI−), 5% are apoptotic (AV+PI−) and 6% are dead (AV+PI+). The viability of GFP+ cells is evaluated in histogram **F** (AV-APC); in this example 94% of GFP+ cells are viable (AV−).*

Intact cells were identified by their forward and side scatter characteristics (A and C) and then separated into two groups based on GFP expression. As Figure 4-9B and D show, GFP+ and GFP− populations were easily distinguished. The viability of GFP− cells was evaluated by AV and PI staining but PI staining in the GFP+ cells could not be interpreted as both PI and GFP emit at 488nm. For this reason viability of GFP+ cells was derived purely from AV staining (hence the use of the AV histogram).

In order to compare sensitivity to anti-myeloma treatments under different conditions, the absolute number of viable MM (AV−PI−) cells was calculated. To correct for any contamination of the GFP− HMCL by GFP− (un-transduced) HS5, the proportion of viable GFP− HS5 cells was measured in the HS5-only wells (suspension and adherent fractions) and this value was subtracted from the number of viable MM cells. This method of correction made the assumption that HS5 cell growth was the same when cultured alone compared to cultured with HMCL, and that HS5 cell growth was not affected by treatment with anti-MM agents.

In order to verify this assumption, the viability and growth of the adherent GFP+ fraction of the modified HS5 lines was analysed. NC(Ap)HS5 (Figure 4-10) and Ap+HS5 (Figure 4-11) were analysed separately but the same patterns emerged for both modified lines.

There was no difference between the viability or growth of HS5 cultured alone compared to those co-cultured with either HMCL. BZM treatment was associated with a modest reduction in viability (Figure 4-10A and Figure 4-11A), which reached statistical significance in NC(Ap)HS5 when doses 0 and 8nM were compared (*p=0.0331* for co-culture with MM1S, *p=0.0422* for co-culture with U266). BZM treatment was associated with a more striking reduction in HS5 growth (Figure 4-10B and Figure 4-11B) in both modified lines, which reached statistical significance in NC(Ap)HS5 when 0 and 8nM, and 4 and 8nM were compared (*p=0.0042* & *p=0.0029* respectively for HS5 co-cultured with MM1S; *p=0.0486* & *p=0.0307* respectively for HS5 co-cultured with U266).

NC(Ap)HS5

A

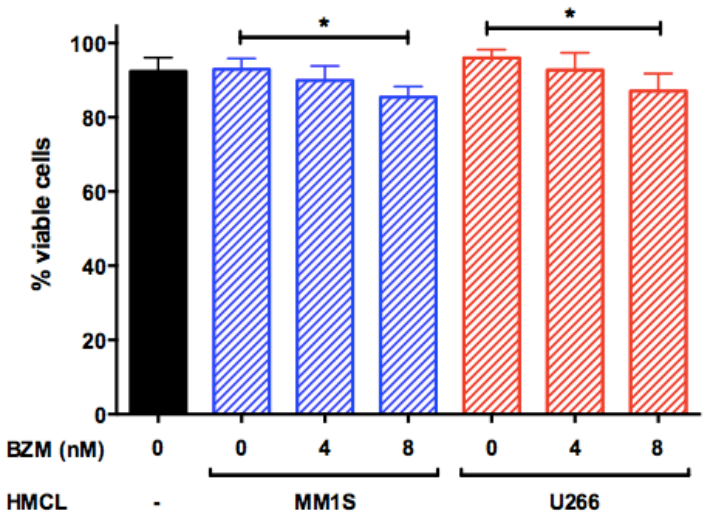

B

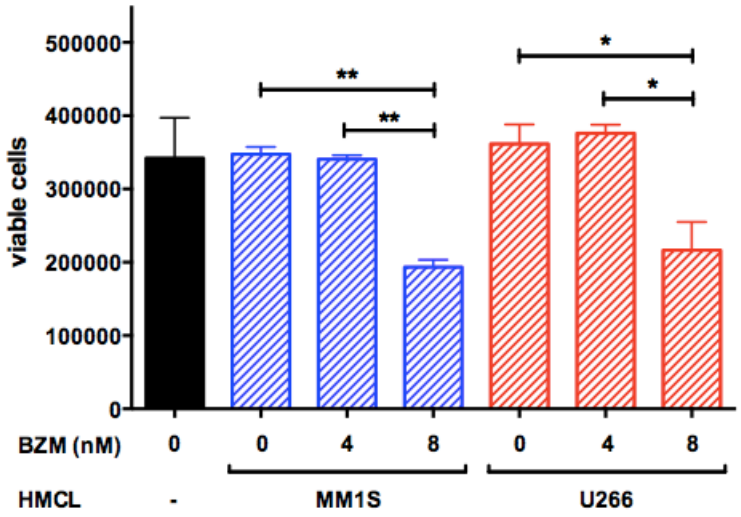

Figure 4-10 Viability and growth of NC(Ap)HS5 cultured alone compared to with HMCL and following treatment with bortezomib.

*NC(Ap)HS5 were cultured in D10 & once confluent either MM1S or U266 cells were added. BZM was added 24 hours later. Cells were harvested after 48 hours exposure to BZM and the viability (**A**) & growth (**B**) of adherent GFP+ HS5 cells was analysed after AV staining. Data from three experiments (conditions in triplicate) is shown; mean ±SEM. Bars signify statistically significant differences (unpaired t-test; * $p<0.05$; ** $p<0.01$).*

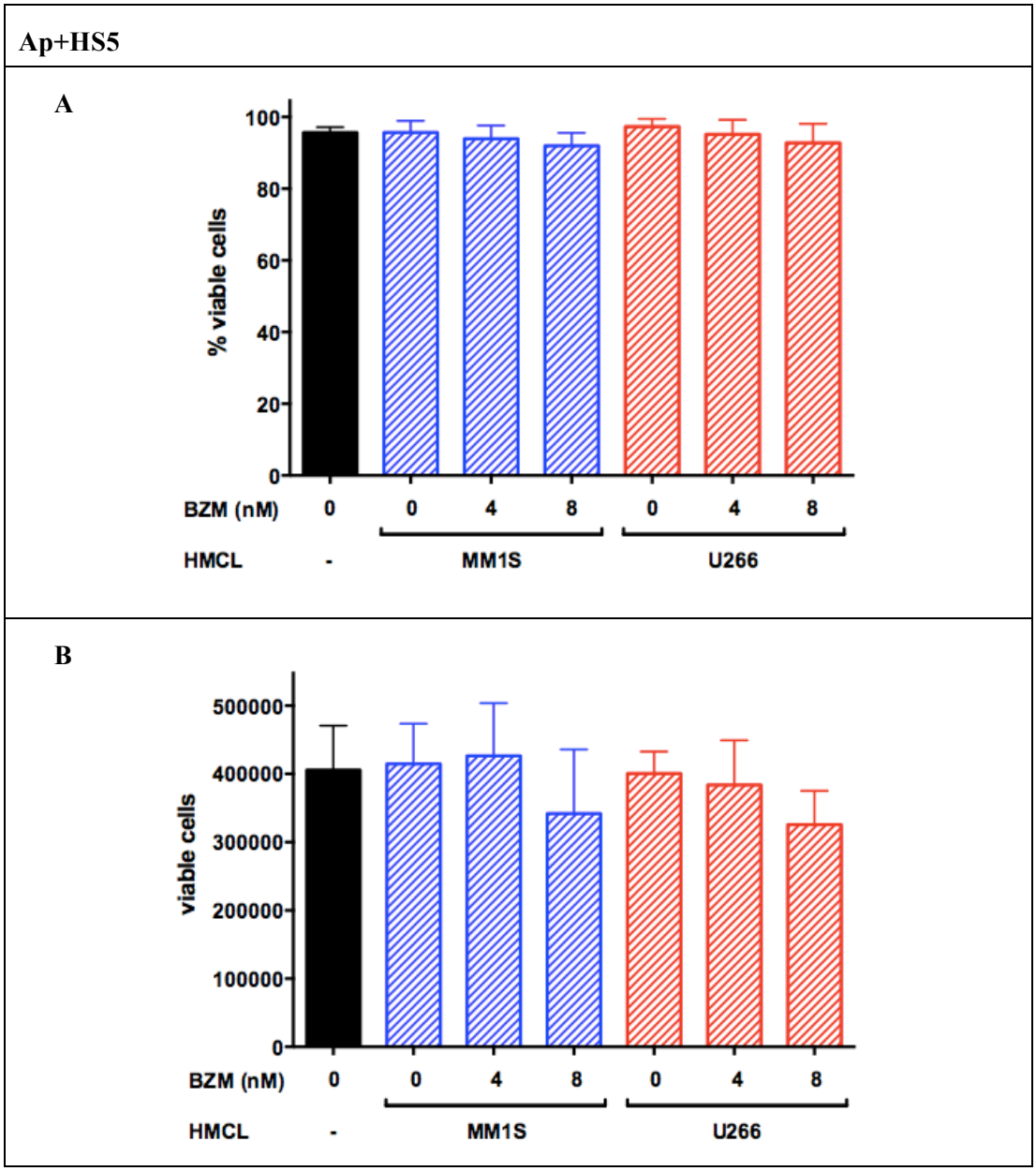

Figure 4-11 Viability and growth of Ap+HS5 cultured alone compared to with HMCL and following treatment with bortezomib.

*Ap+HS5 were cultured, drug treated and harvested as per NC(Ap)HS5 (Figure 4-10). Viability (**A**) & growth (**B**) of adherent GFP+ HS5 cells was analysed after AV staining. Data from three experiments (conditions in triplicate) is shown; mean ±SEM.*

The implication of this analysis was that in order to accurately correct for potential contamination of the GFP− HMCL fraction within harvested cells by GFP− modified HS5 cells, an additional correction for the reduction in HS5 growth associated with BZM treatment at 4 and 8nM would need to be included. This was incorporated. All results displayed subsequently show absolute HMCL corrected in this way for GFP− HS5 contamination.

4.2.5 The effects of co-culture of HMCL with APRIL-expressing HS5 cells: growth and bortezomib cytotoxicity

For this series of experiments, HMCL were co-cultured with HS5 modified to express and secrete APRIL, and exposed to bortezomib (BZM) to investigate APRIL-mediated protection in the context of stroma. BZM was selected to explore whether a novel system might reveal protection which was not seen when recombinant soluble APRIL was used.

4.2.5.1 Bortezomib dose response in HMCL cultured alone

While baseline untreated viability of HMCL varied slightly between replicates, their sensitivity to BZM was very consistent (Figure 4-12A).

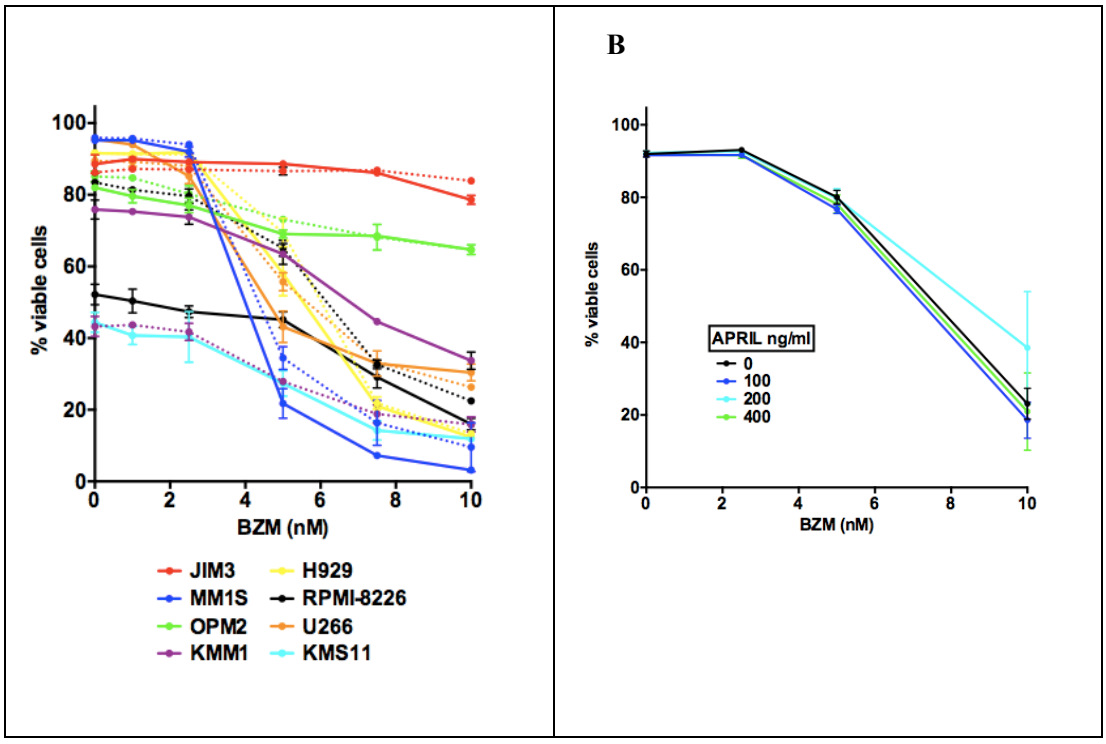

Figure 4-12 HMCL viability twenty-four hours after treatment with bortezomib.

A. *Eight HMCL were cultured in R10 and treated with BZM 24 hours after set-up. Two replicates are shown for each HMCL, except KMS11 (solid line, 1st experiment; dotted line, 2nd experiment).* ***B.*** *MM1S cells were cultured in R10 and four concentrations of APRIL before being treated with BZM. Cells were harvested 24 hours after drug treatment and % viability assessed by AV/PI staining and FACS. All conditions were set up in triplicate. Data is shown as mean ±SD.*

JIM3 and OPM2 were relatively resistant to BZM; KMM1 and RPMI-8226 were moderately sensitive to BZM; and U266, MM1S and NCI-H929 were fully sensitive to BZM at the dose range examined. KMS11 had poor baseline viability and thus, as only one replicate was possible, sensitivity to BZM is hard to comment on.

Based on these experiments, two HMCL were chosen for on-going experiments in co-culture with modified HS5 cells, U266 and MM1S. These two HMCL have different pathogenic (presumed) mechanisms, as a result of different IgH translocations, t(11;14) in the case of U266 and t(14;16) in MM1S. They are sensitive to BZM to a varying degree over doses between 2.5 and 10nM.

In an exploratory assay, MM1S cells were cultured in R10 in the presence of escalating concentrations of recombinant soluble APRIL (0, 100, 200 and 400ng/ml) and treated with BZM 0, 2.5, 5 and 10nM. There was no difference in cytotoxicity seen at each BZM dose between the different concentrations of APRIL (Figure 4-12B).

4.2.5.2 The effect of co-culture with modified HS5 on growth of U266 and MM1S cells

Co-culture of U266 cells with modified HS5 cells resulted in slightly higher numbers of MM cells compared to U266 cells cultured alone (Figure 4-13A), with the highest number of viable cells seen in co-culture with NC(Ap)HS5 (not significant on paired t-test). The same pattern was seen with MM1S cells but again, this did not reach statistical significance. This may be due to baseline variability in HMCL growth between the three experiments (hence the wide SEM).

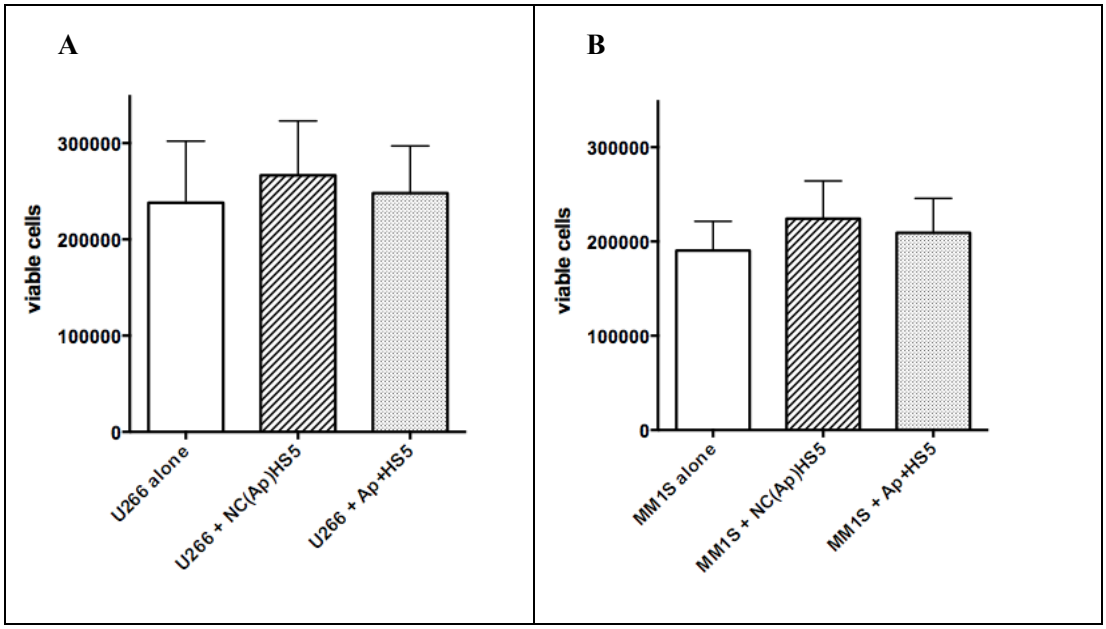

Figure 4-13 Growth of U266 and MM1S cells alone compared to co-cultured with modified HS5.

U266 ***(A)*** *or MM1S* ***(B)*** *cells (GFP−) were seeded onto confluent Ap+HS5 or NC(Ap)HS5 or cultured alone. Cells were harvested 48 hours later and stained with APC-conjugated AV and PI and analysed. Total viable (AV−PI−) GFP− cells are represented as the mean ±SEM of triplicates, corrected for viable GFP− HS5 cells (n=3).*

4.2.5.3 Bortezomib cytotoxicity in HMCL cultured alone compared to those co-cultured with modified HS5 (NC(Ap)HS5)

HMCL were cultured in R10 alone, or co-cultured with modified NC(Ap)HS5, and BZM was added as detailed in section 4.2.4. Three experiments were undertaken for each line and the total number of viable cells as a percentage of the untreated control is shown in Figure 4-14.

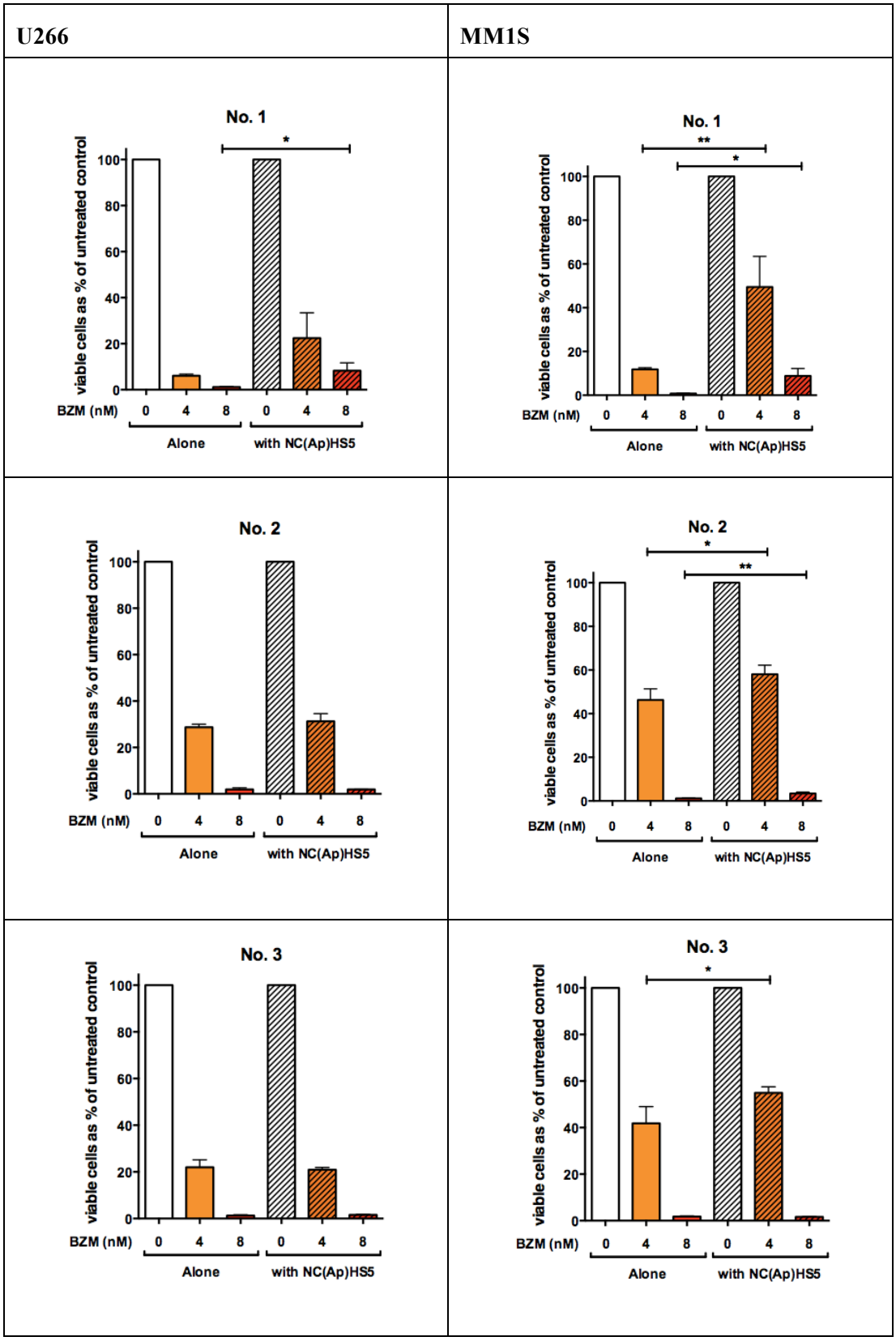

Figure 4-14 Bortezomib cytotoxicity in HMCL cultured alone compared to those co-cultured with NC(Ap)HS5.

U266 and MM1S cells were cultured alone or seeded onto confluent NC(Ap)HS5. After 24 hours, cells were treated with BZM and harvested 48 hours later. Viable (AV−PI−) GFP−

*cells (corrected for viable GFP− HS5 cells) are shown as % of untreated control for each of three assays (cultured alone - empty bars, or co-cultured with NC(Ap)HS5 - hashed bars; mean ±SD of triplicates; paired t-tests: *p<0.05; **p<0.01)*

Co-culture on stroma reduced the sensitivity of both HMCL to BZM, but the effect was less pronounced in U266 cells (left-hand column, Figure 4-14), and only reached statistical significance in one experiment at the 8nM dose (*p=0.0320*). Protection was more striking in MM1S cells (right-hand column, Figure 4-14). Statistically significant increases in viable cell number were seen in all experiments at the 4nM dose, and in two out of the three at 8nM. It can therefore be surmised that the modified HS5 exert a protective effect on the HMCL, which is independent of any growth advantage as the results presented are standardised to the appropriate untreated control.

Results from a representative experiment are displayed as absolute cell numbers in Figure 4-15 (**A** & **B** U266, **C** & **D** MM1S). When the distribution of viable cells between suspension and adherent fractions is considered it is apparent that U266 and MM1S cells display very different growth characteristics in this setting. Within U266 cells a small proportion of the total number of viable cells was adherent, although it increases in the presence of stroma (Figure 4-15B). A much greater proportion of viable MM1S cells was adherent, both when cultured alone or with stroma, and this proportion does not change significantly with different culture conditions (Figure 4-15D).

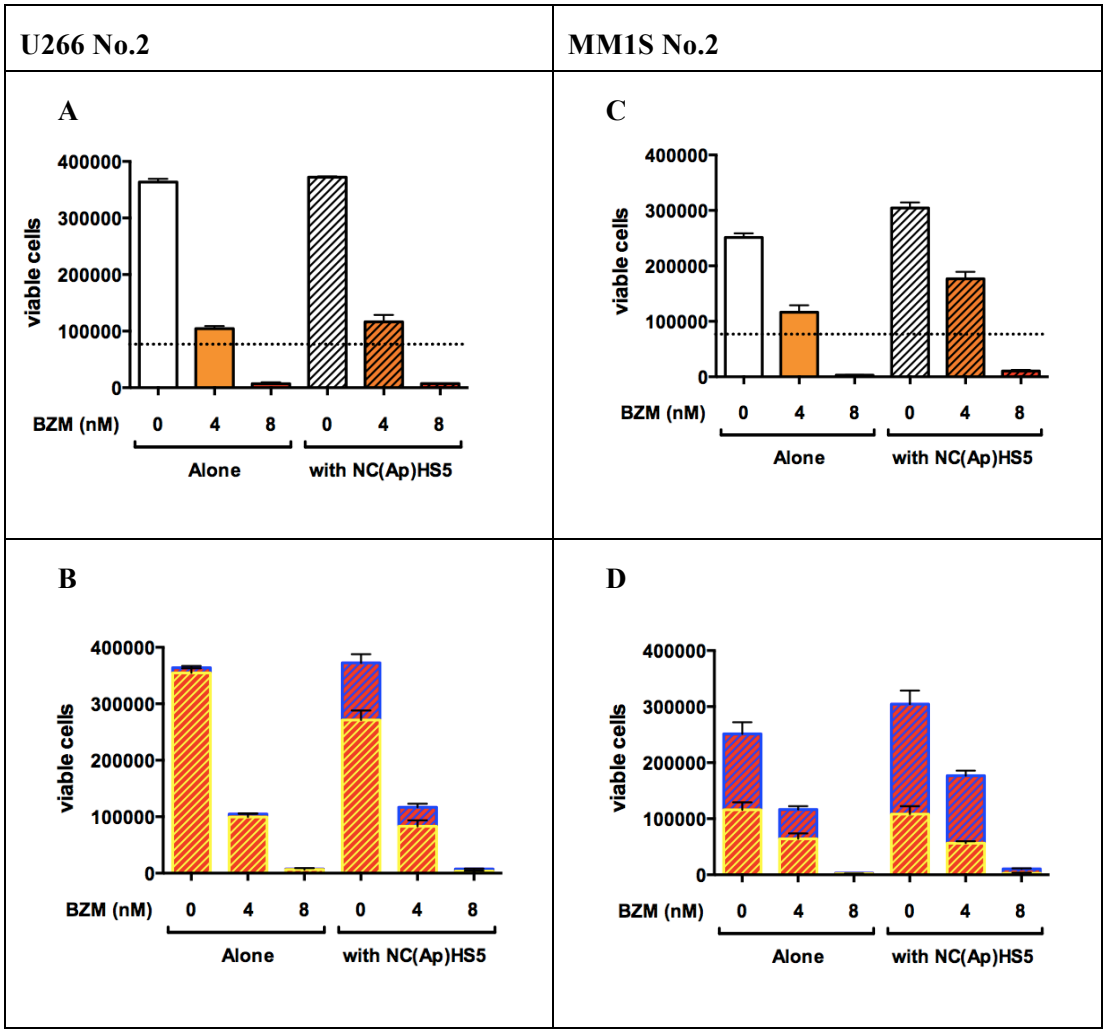

Figure 4-15 Bortezomib cytotoxicity in HMCL cultured alone compared to those co-cultured with NC(Ap)HS5 - two representative experiments.

*Experimental set-up as per Figure 4-14. The results are presented in two different ways. In graphs **A** & **B**, representative plots from the same experiment (No. 2) using U266 cells are shown, while in graphs **C** & **D**, experiment No.2 using MM1S is presented. **A** & **C** show total absolute viable cells, treated with escalating doses of BZM. The dashed line represents the starting number of viable U266 cells seeded into the culture system. **B** & **D** show absolute numbers of suspension (red bars hatched with yellow) and adherent (red bars hatched with blue) viable cells, and the effect of BZM.*

Comparison of the three experiments for each HMCL reveals some variation in the sensitivity of the MM cells (Figure 4-14). For example, treatment of U266 cultured alone with 4nM BZM results in quite different numbers of viable cells: 6.09 ±0.71, 28.72 ±1.28 and 21.96 ±3.22 (expressed as a percentage of the untreated control; mean ±SD). This probably reflects variation in the baseline growth of the HMCL at the time of each experimental set-up.

4.2.5.4 Effect of stromal cell-derived APRIL on bortezomib cytotoxicity in HMCL

In the next series of experiments, HMCL were co-cultured with NC(Ap)HS5 or Ap+HS5, and effect of BZM on cell viability and total number of viable cells was assessed. Three experiments were performed for each HMCL.

In U266 cells (Figure 4-16, left-hand panel), there was a clear trend for APRIL-associated protection at the 4nM dose, across all three experiments. This only reached statistical significance with Experiment No.3 ($p=0.0032$). At 8nM there was no consistent pattern, with protection seen in Experiment No.3 but apparent sensitisation in the other two.

With MM1S cells (Figure 4-16, right-hand panel), there was again a trend towards APRIL-associated protection at 4nM ($p=0.0189$ in Experiment No.2), but the trend was reversed in the third experiment and was similarly variable at 8nM.

These results suggest that HS5 cells modified to express and secrete APRIL may confer additional specific protection against BZM killing and is worthy of further investigation.

U266	MM1S
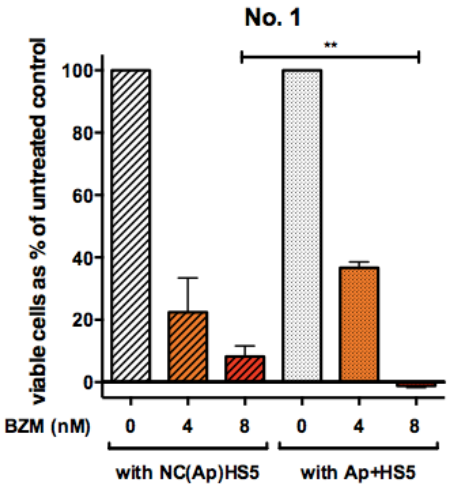 No. 1 ** viable cells as % of untreated control 100 80 60 40 20 0 BZM (nM) 0 4 8 0 4 8 with NC(Ap)HS5 with Ap+HS5	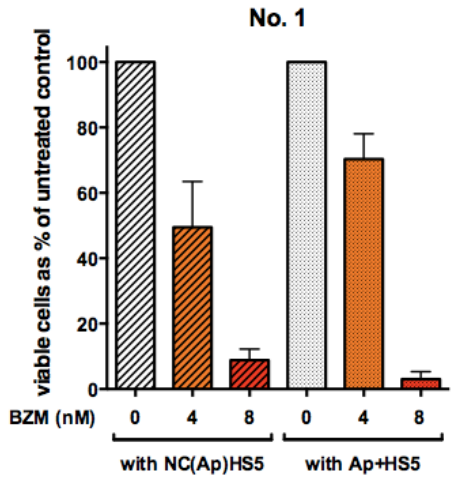 No. 1 viable cells as % of untreated control 100 80 60 40 20 0 BZM (nM) 0 4 8 0 4 8 with NC(Ap)HS5 with Ap+HS5
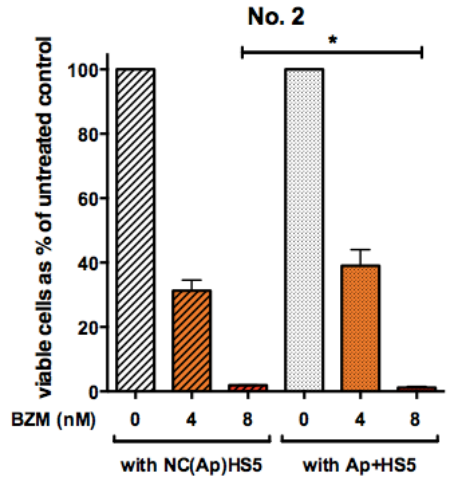 No. 2 * viable cells as % of untreated control 100 80 60 40 20 0 BZM (nM) 0 4 8 0 4 8 with NC(Ap)HS5 with Ap+HS5	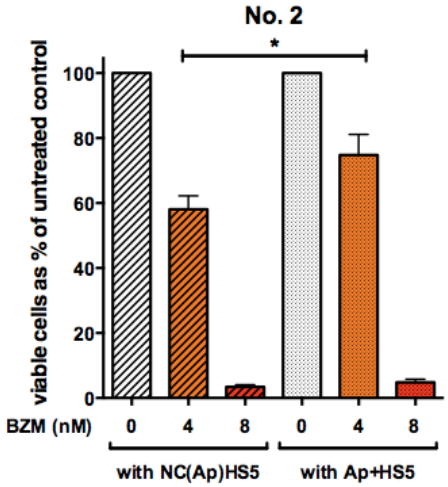 No. 2 * viable cells as % of untreated control 100 80 60 40 20 0 BZM (nM) 0 4 8 0 4 8 with NC(Ap)HS5 with Ap+HS5
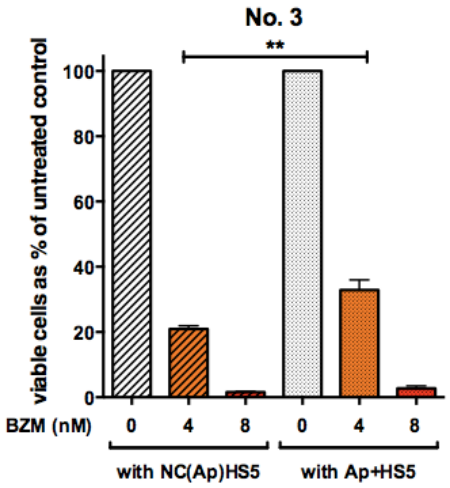 No. 3 ** viable cells as % of untreated control 100 80 60 40 20 0 BZM (nM) 0 4 8 0 4 8 with NC(Ap)HS5 with Ap+HS5	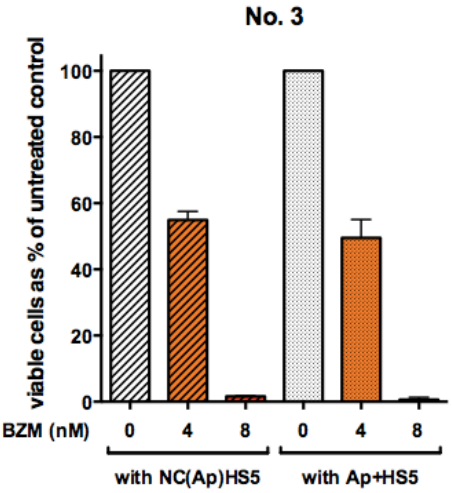 No. 3 viable cells as % of untreated control 100 80 60 40 20 0 BZM (nM) 0 4 8 0 4 8 with NC(Ap)HS5 with Ap+HS5

Figure 4-16 Bortezomib cytotoxicity in HMCL co-cultured with NC(Ap)HS5 compared to those co-cultured with Ap+HS5.

*U266 and MM1S cells were seeded onto confluent NC(Ap)HS5 or Ap+HS5. After 24 hours, cells were treated with BZM and harvested 48 hours later. Viable (AV−PI−) GFP− cells (corrected for viable GFP− HS5 cells) are shown as % of untreated control for each of three experiments (co-cultured with NC(Ap)HS5 - hashed bars, co-cultured with Ap+HS5 - dotted bars; mean ±SD of triplicates; paired t-tests: *p<0.05; **p<0.01)*

4.3 Summary and discussion

Initial experiments to explore Aim 1 were carried out using primary freshly selected CD138+ MM cells as this model was considered to more closely represent the *in vivo* disease, compared with immortalised cell lines. Challenges of this approach include the significant variability of primary MM samples in terms of viability in culture and sensitivity to drug treatment. The absolute numbers of CD138+ cells available for each experiment was often small, thus limiting the number of conditions that could be tested.

Although APRIL alone had no effect on the survival of primary MM cells cultured in suspension, some attenuation of dexamethasone (Dex)-mediated killing was seen in the presence of APRIL, confirming the findings of Moreaux et al [76]. This finding was statistically significant in the whole cohort of samples studied ($p<0.001$), with more consistent protection seen in samples derived from patients whose disease expressed CCND2. In a limited series of experiments, APRIL-mediated protection was more pronounced than that seen with IGF-I but less than that seen with IL-6. This is not surprising as IL-6 is a critical survival factor in MM, important both in the survival of primary MM cells and that of a number of HMCL.

Soluble APRIL did not appear to reduce killing associated with MM cell treatment with bortezomib (BZM) or lenalidomide (Len). This indicates that soluble APRIL-associated protection may act through specific pathways relevant to Dex-killing, which are not involved in the cytotoxicity associated with BZM or Len. This is consistent with the absence of a general pro-survival or pro-growth effect in MM cells treated with APRIL alone.

Exploration of the pathways involved in APRIL-mediated protection, which constituted Aim 2, was undertaken using a small molecule PI3K/AKT pathway inhibitor, PI103. However it proved extremely difficult in primary MM cells, owing to the subtlety of the protective effect and the variability of primary samples, discussed above.

Screening an extended panel of HMCL to identify a Dex-sensitive line that might act as a model for APRIL protection was not fruitful. It is worth noting that the majority of HMCL are derived from primary extramedullary MM samples and have therefore evolved to proliferative autonomously without the network of cytokine and cell-cell interactions that are required for the survival of medullary MM cells. These cells are likely to be biologically quite different from primary CD138+ MM cells, which are critically dependent on the BM microenvironment, and hence more responsive to APRIL protection.

In Aim 3, APRIL was examined within the context of other BM supportive signals, by modifying HS5 cells to express and secrete APRIL. U266 and MM1S cells were co-cultured on a confluent layer of Ap+HS5 or the empty vector negative control, and then treated with BZM. There appeared to be a modest growth advantage to HMCL co-cultured on HS5 cells, more noticeable with the negative control than those expressing APRIL, but this did not reach statistical significance in either HMCL used. Following drug treatment, a degree of protection from BZM killing was seen in HMCL co-cultured on stroma compared to those cultured in suspension. This reached statistical significance in MM1S cells.

The results of drug treatment when HMCL were co-cultured with Ap+HS5 versus NC(Ap)HS5 were less consistent. At BZM 4nM, both U266 and MM1S cells appeared to be less sensitive in the presence of APRIL (seen in five out of six experiments), but this only reached statistical significance in one experiment. At BZM 8nM, the picture was more variable. Clearly this needs to be evaluated in a broader dose range in order to establish whether true protection is present.

There is apparent contradiction in the effects of BZM between the experiments using soluble APRIL and that expressed and secreted in a co-culture system, whereby no

protection was seen in primary MM cells treated with BZM in the presence of recombinant soluble APRIL, while some protection was seen in HMCL treated with BZM in co-culture with Ap+ HS5. This may reflect biological differences between the MM cells evaluated (primary versus HMCL), but may also reflect the context and the effect of additional BM stromal signals. The same phenomenon was observed by Nefedova et al [62], when apparently opposing effects on cell cycle were observed in the same target cell population when cultured in direct contact with BMS compared to those cultured separated by a Transwell device.

Ultimately, the results presented in this chapter support the hypothesis that APRIL contributes to drug resistance provided by the BM microenvironment in MM. However, that effect in the systems used here was modest, and that limited the exploration of underlying pathways involved. Modest differences were seen between the different genetic subtypes but these were not statistically significant.

Further work in this area would usefully include extending the range of BZM doses evaluated, looking at alternative anti-myeloma treatments (including Dex and Len) and using the co-culture system with primary MM cells. It might be anticipated that culturing CD138+ MM cells on HS5 might enhance their baseline survival *in vitro*. This would potentially make the effects of drug treatments easier to evaluate.

CHAPTER 5. THE ROLE OF THE NOTCH PATHWAY IN DRUG RESISTANCE

5.1 Introduction

5.1.1 Background

In additional to soluble factors, the resistance offered by BM stromal cells in MM also results from interactions requiring direct cell-cell contact [62]. In this results chapter, an evaluation of the role played by the Notch pathway is reported. Notch pathway dysregulation has now been observed in a number of malignancies, both solid and haematological. The Notch pathway has also been implicated specifically in the context of cancer stem cells, with suggestions that it may play a role in the stem cell-like characteristics observed in these cell sub-populations [129].

The structure and functioning of Notch receptors (Notch1, 2, 3 and 4) and their ligands (Jag1, Jag2, DL1, DL3 and DL4) is described in some detail in section 1.2.3.5 of Chapter 1. Notch was first implicated in MM in 2004 when three independent groups demonstrated expression of Notch receptors and ligands on both myeloma cells and bone marrow stromal cells [96,98,99]. Nefedova et al. reported that co-culture of HMCL with primary BM stromal cells led to activation of Notch1 [96] (as evidenced by increased expression of intracellular Notch1 (ICN1) and the downstream Notch target, HES1). They were also able to activate Notch1 by co-culture of HMCL with Jag1-expressing (Jag1+) fibroblasts and by adding recombinant soluble Jag1 to the culture media. The result of this activation was cell cycle arrest and activation was associated with a reduction in melphalan- and mitoxantrone-associated apoptosis. The HMCL U266 did not express Notch1 and showed no reduction of apoptosis after co-culture with Jag1+ fibroblasts. However, overexpression of the Notch1 receptor in U266 cells was able to reverse this finding, leading the authors to suggest that Notch1 activation of MM cells by Jag1 presented by adjacent BM stromal cells might be a mechanism of BM microenvironment-associated drug resistance.

Jundt et al. [98] found constitutive activation of Notch in a number of HMCL, as evidenced by HES1 expression. They were able to increase HES1 expression by co-

culture of selected HMCL with Jag1+ adherent cells, but interestingly this triggered proliferation of HMCL rather than the cell cycle arrest observed by Nefedova et al.. Notch-induced proliferation was inhibited by the addition of gamma secretase inhibitors (GSI) and other groups have subsequently reported that treatment of HMCL with GSI reduced their proliferation [103], implying that Notch pathway activation leads to cell cycle progression and growth. This controversy was addressed directly by Zweidler-McKay et al. [105]. This group transduced various B and T cell malignant cell lines with constitutively active Notch receptors and showed that this had a proliferative effect on T cell lines but induced cell cycle arrest in all B cell lines.

The role of Notch activation in drug resistance was examined further by Nefedova's group in 2008 [106]. They showed that GSI was directly cytotoxic to HMCL and primary MM cells in HES1-dependent manner. MM cells grown on a BM stromal monolayer were protected from anti-myeloma drugs (mitoxantrone, doxorubicin) but this protection was reduced by the addition of GSI. In a SCID/NOD mouse model, myeloma tumour growth was inhibited by treatment of the mice with doxorubicin and GSI, in a synergistic fashion. They proposed that pharmacological inhibition of Notch signaling in MM cells abrogates BM-mediated drug resistance and sensitises MM cells to chemotherapy, implying that a major route of BM-mediated protection is the activation of Notch signaling in MM cells by Notch ligands present on stroma cells.

An independent group examined Notch activation in MM cells and bortezomib resistance [108], using DL1-expressing MS5 cells to activate Notch in murine 5T33MMvt cells and in human MM cells. They had previously demonstrated that Notch activation enhanced both colony formation and *in vivo* engraftment by murine MM cells, an effect which could be inhibited by GSI treatment [109]. In their work, Notch2 was the critical receptor with decreased surface Notch2 and upregulated ICN2 in MM cells after co-culture with DL1+MS5. The cytotoxic effect of bortezomib was significantly attenuated by Notch activation, but sensitivity could be restored by treatment with the GSI DAPT.

Notch activation has also been demonstrated in BM stromal cells so it is likely that there is bi-directional signalling. Houde et al. [99] reported high expression of the ligand Jag2 in a panel of HMCL and primary MM samples (not seen in non-MM cell lines or normal plasmablasts). HES1 induction was then demonstrated in fibroblasts co-cultured with Jag2++ HMCL and this was accompanied by an increase in IL-6, VEGF and IGF-I levels in the culture supernatant. Thus MM cell activation of the Notch pathway in adjacent stromal cells might enhance production of pro-MM cytokines by those stromal cells, contributing to the survival and proliferation of the tumour population.

5.1.2 Hypothesis and aims

Hypothesis: Notch pathway activation in MM cells renders them less sensitive to anti-myeloma agents. This mechanism contributes to the protection offered to MM cells by their BM microenvironment.

Aim 1: to confirm and characterise Notch receptor expression by HMCL.

Aim 2: to activate the Notch pathway in HMCL by co-culturing them with Notch ligand-expressing stromal cells.

Aim 3: to demonstrate that Notch activation is associated with a reduction in bortezomib-associated MM cell apoptosis.

Aim 4: to identify key Notch receptors and ligands involved in this process.

5.2 Results

5.2.1 Notch receptor and ligand expression in HMCL

Expression of the four subtypes of the Notch receptor present on mammalian cells (Notch1, Notch2, Notch3 and Notch4) was evaluated by Western blotting in a number of HMCL expressing a range of IgH translocations. MM1S cells have t(14;16), RPMI-8226 have t(16;22), NCI-H929, LP-1 and OPM-2 have t(4;14) and U266 cells have t(11;14).

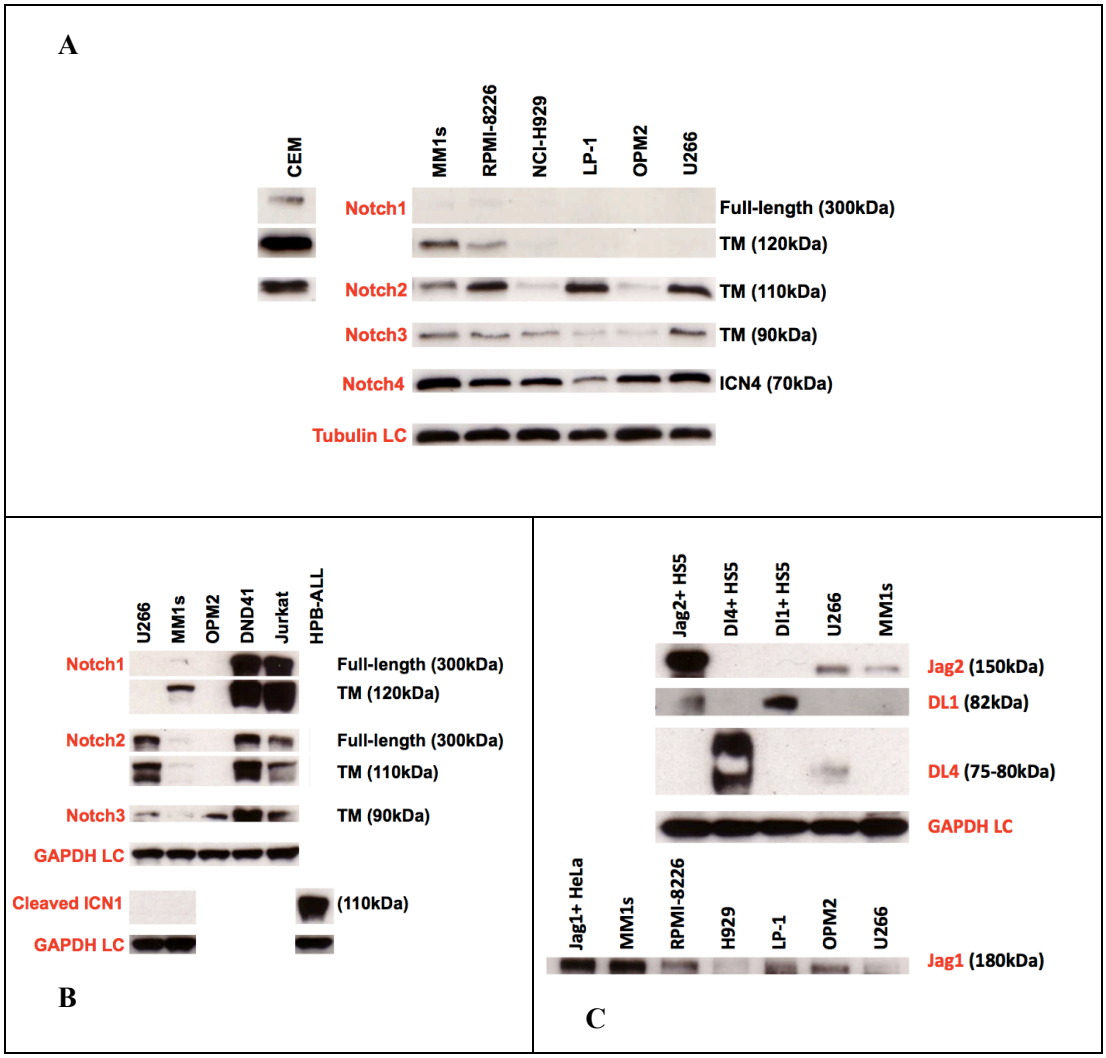

Figure 5-1 Baseline expression of Notch receptors (1, 2, 3 & 4), cleaved intracellular Notch1 (ICN1) and Notch ligands (Jag1, Jag2, DL1 & DL4) by HMCL.

Whole cell lysates were prepared using RIPA lysate buffer from optimally growing but otherwise un-manipulated HMCL. Precast 4-12% gradient gels were used. T-ALL cell lines CEM, DND41, Jurkat and HPB-ALL whole cell lysates were used as positive controls for Notch1, Notch2 and cleaved intracellular Notch1 (ICN1; they all have constitutive Notch1 activation). Housekeeping proteins tubulin and GAPDH were used as LCs. ***A.*** *Expression of Notch1, Notch2, Notch3 and Notch4 was evaluated in a panel of HMCLs. 20µg of protein was loaded per lane.* ***B.*** *Expression of Notch1, Notch2, Notch3 and ICN1 was evaluated in MM1S, U266 & OPM2 lysates (40µg protein).* ***C Upper panel.*** *Expression of Jag2, DL1 and DL4 was evaluated in U266 and MM1S lysates (40µg protein), using HS5 cells transduced to express the ligands as positive controls.* ***C Lower panel****. Expression of Jag1 was evaluated in a panel of HMCL, using Jag1-transfected HeLa cell whole cell lysate as a positive control. Abbreviations: TM, transmembrane; LC, loading control.*

Notch1 expression was only seen in MM1S and RPMI-8226 cells (Figure 5-1A&B); notably there was no expression of Notch1 by U266 cells, in confirmation of the

findings of Nefedova et al [96] and Houde et al [99]. Unexpectedly Notch1 expression was not demonstrated on NCI-H929 cells, in contrast to what is reported [96]. Notch2 was expressed in all HMCL, although expression levels appeared to vary, with the highest expression seen in U266, RPMI-8226 and LP-1. Notch3 and Notch4 (intracellular Notch4; ICN4) were expressed by all HMCL evaluated, with some variation in levels. ICN1 was not seen in either U266 or MM1S cells (Figure 5-1B), suggesting that neither cell line had constitutive Notch1 pathway activation. There are no reports of baseline ICN1 expression by HMCL.

Notch ligand (NL) expression was also evaluated in HMCL by Western blotting (Figure 5-1C). Jag2 was present in U266 cells and to a lesser degree in MM1S cells. DL4 was seen only in U266 cells. Jag1 was expressed in all six of the HMCL examined: levels appeared highest in MM1S, and lowest in NCI-H929 and U266 cells.

5.2.2 Activating the Notch pathway in MM cells using Notch ligand-expressing stromal cell lines

In order to evaluate the contribution of Notch pathway activation to drug resistance in MM cells in a physiological way, the HS-5 stromal cell line was modified to express a panel of Notch ligands (NL) individually (methods are detailed in Chapter 2 – section 2.7.6.2 and 2.7.6.3). Stromal cell-based activation of the Notch pathway within a co-culture system would recapitulate some aspects of the BM microenvironment. HS5 cells were selected for modification as they are known to resemble BM stroma and have been used as a feeder layer for primary haematopoietic progenitor cells. Mouse stromal cells (MS5) modified to express the NL DL1 were an effective means of Notch pathway activation employed by Xu et al [109].

5.2.2.1 Confirming the functional capabilities of DL1+, DL4+ and Jag2+HS5

5.2.2.1.1 Expression of the transduced Notch ligands

NL expression was first confirmed by flow cytometry by GFP expression and labelling with PE-conjugated anti-DL1/4 or Jag2 antibodies (detailed in Chapter 2 -

section 2.2.2). Results are shown in Figure 5-2. All modified HS5 cell subtypes expressed GFP in >99% of cells. 90.99% of DL1+HS5 cells (first row) expressed DL1 and GFP, but not DL4 (<1%). 96.5% of DL4+HS5 cells (third) row expressed DL4 and GFP, but not DL1 (<1%). Only 27% of Jag2+HS5 (fourth) row expressed Jag2 and GFP, although 94% expressed GFP alone. With the exception of low level Jag2 (~2-4%), the NC subtypes transduced with the empty vector alone did not express significant levels of any of the NLs.

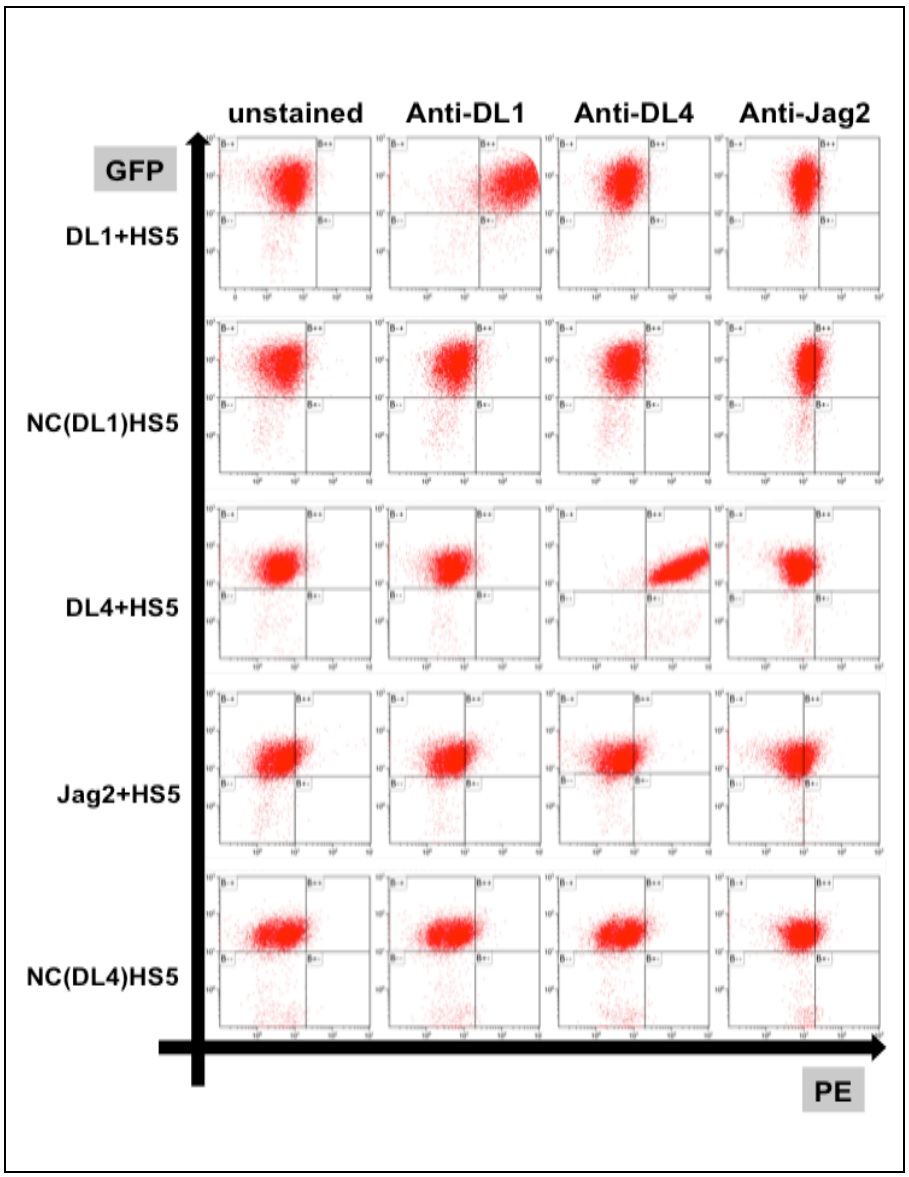

Figure 5-2 Expression of Notch ligands and GFP in modified HS5 cells.

Optimally growing, sorted, modified HS5 cells were trypsinised, harvested, washed and stained with PE-conjugated anti-DL1, anti-DL4 and anti-Jag2 antibodies, as indicated. Intact cells were gated onto dot plots for FITC (GFP) on the y-axis and PE on the x-axis, shown above. Unstained cells are shown in the far left-hand column.

In order to confirm expression of DL1 and DL4 by the DL1+ and DL4+HS5 cells and clarify expression of Jag2 by all sets of HS5 cells, protein expression was then evaluated by Western blotting (Figure 5-3).

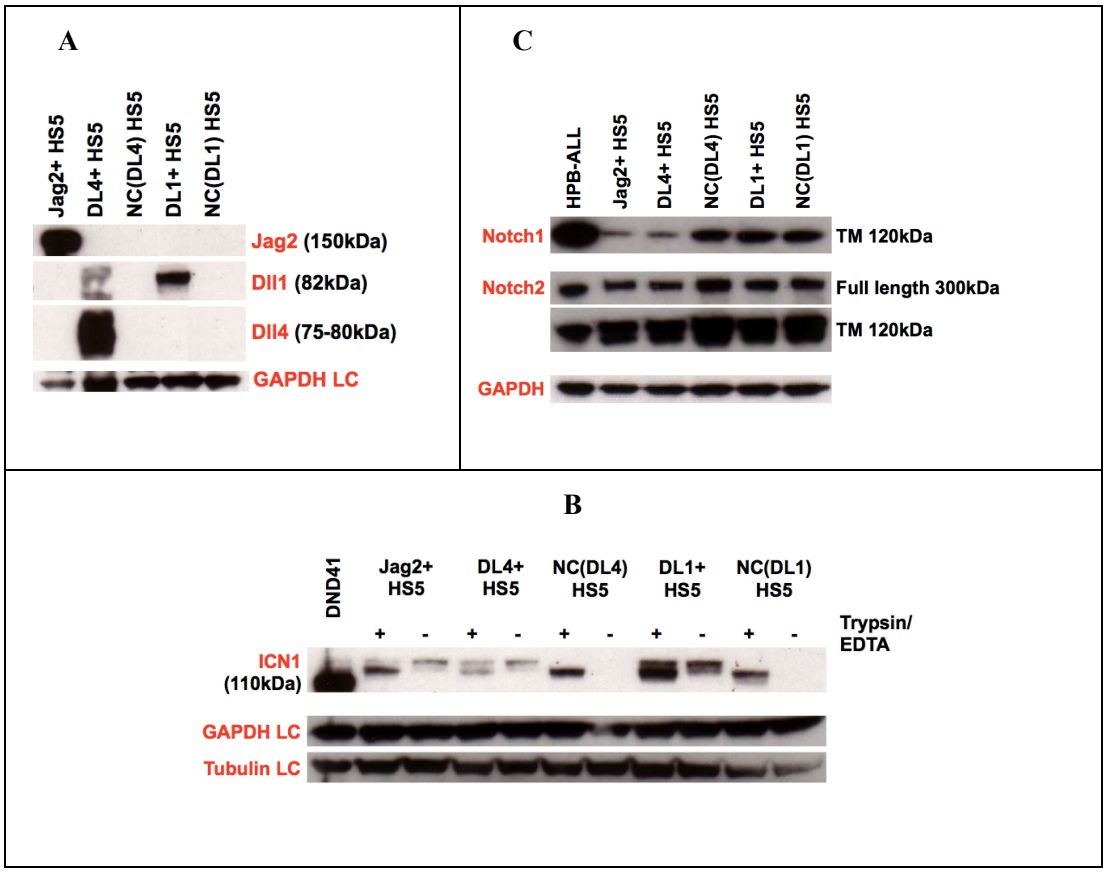

Figure 5-3 Expression of Notch ligands and Notch receptors by modified HS5 and the effect of EDTA on ICN1 expression.

Whole cell lysates were prepared from 5x10^6 optimally growing modified HS5 cells using RIPA lysis buffer. Precast 4-12% gradient gels were used. 40µg protein was loaded per lane. ***A.*** *The membrane was probed for NLs Jag2, DL4 and DL1.* ***B.*** *Modified HS5 cells were washed with warm HBSS and then dissociated from their wells in the usual fashion with trypsin/EDTA. The cells were then harvested, washed in ice-cold PBS, pelleted and then lysed with RIPA lysis buffer for 30 minutes on ice (designated +). Alternatively the HS5 cells were washed in their wells with ice-cold PBS and then RIPA lysis buffer was added to the cells in their wells and after incubating on ice for 30 minutes, the lysate was aspirated from the wells (designated −). The resultant membrane was probed for ICN1. DND41 whole cell lysate was used as a positive control for ICN1.* ***C.*** *Whole cell lysates were prepared from modified HS5 cells without exposure to EDTA and probed for Notch1 and Notch2. HPB-ALL whole cell lysate was used as a positive control for Notch1 and Notch2. The housekeeping genes GAPDH and tubulin were used as loading controls.*

There is clear overexpression of Jag2 by Jag2+HS5, DL4 by DL4+HS5 and DL1 by DL1+HS5 (Figure 5-3A). A weak band is seen for DL1 in the DL4+HS5 lysates but this is a remnant on the membrane, which had been probed first for DL4. Jag2 protein is not seen in the lysates prepared from any cell subtype other than Jag2+HS5. Importantly there is no evidence of NL expression of any type probed in the NC(DL1/DL4)HS5 subtypes.

5.2.2.1.2 Notch pathway activation in modified HS5 cells

It has been reported that the calcium-chelator EDTA may be used to activate Notch signaling [130] as it disrupts the non-covalent bond between the external ligand-binding domain of the Notch receptor and the transmembrane domain. Dissociation of these two domains is then associated with cleavage of the transmembrane domain by gamma secretase and the intracellular portion of the transmembrane domain (ICN) is then able to shuttle into the nucleus and act on its downstream targets. As trypsin 0.25%/EDTA was routinely used to dissociate all the adherent cells when harvesting, it was important to evaluate whether the five minute exposure to EDTA was sufficient to cause increased levels of ICN in the cells and potentially activate Notch signaling in the HS5 cells. Figure 5-3B shows that in all modified HS5 cells ICN1 is present when the cells are harvested using trypsin/EDTA. In contrast, when EDTA was not used, ICN1 was only seen in NL-expressing HS5 (Jag2+, DL4+ and DL1+HS5) and was not present in the NC(DL4/DL1)HS5. These observations suggested that firstly, exposure to trypsin/EDTA was associated with Notch pathway activation in all (modified) HS5 cells examined. Secondly, Notch pathway activation occurred in an EDTA-independent manner in NL-expressing HS5, supporting the fact that the NL expressed by these cells were functionally competent.

Finally Notch1 and Notch2 expression by modified HS5 cells was evaluated (Figure 5-3C). All five modified lines expressed both Notch1 and Notch2. The highest levels of both were seen in the NC(DL4/DL1)HS5 cells; it is possible that Notch1 and Notch2 is downregulated to some degree in NL-expressing cells, perhaps as part of a negative feedback loop following autocrine activation of the Notch pathway.

5.2.2.1.3 Notch activation of heterologous cells by NL-expressing HS5

U266 and MM1S cells were cultured alone or in co-culture with modified HS5 cells. Co-cultures were set up as detailed in Chapter 2 - section 2.1.11. Preliminary experiments included additional wells of HS5 cells which were treated with bortezomib (BZM) at the same doses. Minimal changes in viability or cell growth were seen in BZM-treated HS5 cells (Figure 5-4) so these control wells were not set up for subsequent assays.

The purity of the modified HS5 cells was regularly assessed by flow cytometry for GFP expression. Both DL1+HS5 and NC(DL1)HS5 were consistently >90% GFP positive (GFP+). The gating strategy used was identical to that used for HMCL co-cultured with Ap+HS5 (Chapter 4 – section 4.2.4.1).

In order to correct for any contamination of the GFP-negative (GFP−) HMCL by GFP− (untransduced) HS5, the proportion of viable GFP− HS5 cells was measured in the HS5-only wells (suspension and adherent fractions) and this value was subtracted from the number of viable MM cells. This method of correction made the assumption that HS5 cell growth was the same when cultured alone compared to cultured with HMCL, and that HS5 cell growth was not affected by treatment with anti-MM agents. In order to verify this assumption the growth of the modified HS5 cells were analysed under different conditions (Figure 5-4).

Co-culture with HMCL appeared to increase the growth of both types of modified HS5 cells (Figure 5-4A&B) although this was reduced with increasing doses of BZM. There is no evidence that BZM is directly cytotoxic to HS5 cells (Figure 5-4C). These findings suggest that HS5 cell growth is enhanced in the presence of MM cells, and that increasing BZM doses are associated with reduced numbers of HS5 cells secondary to the killing of MM cells. It is therefore likely that absolute MM cell number is slightly over-corrected for the presence of GFP− HS5 cells at higher BZM doses in the following series of experiments.

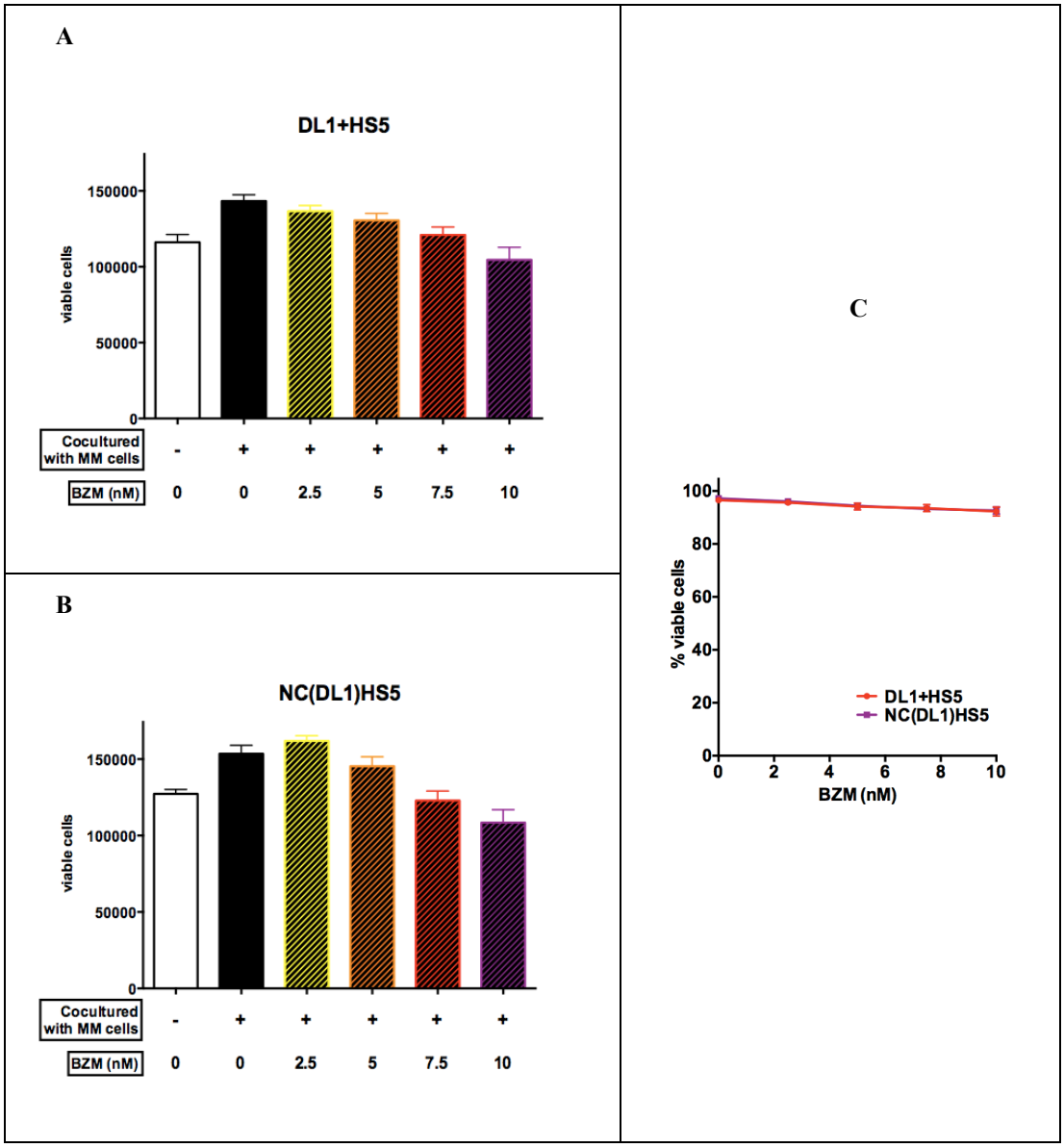

Figure 5-4 Growth of modified HS5 cultured alone or with MM cells and the effect of bortezomib.

Viable modified HS5 cells are shown - harvested cells were stained with AV-APC as per protocol section 2.4.2.2. Absolute concentrations of adherent GFP+ AV− cells are charted. ***A-C*** *DL1+HS5 or NC(DL1)HS5 cells were co-cultured with U266 or cultured alone. Modified HS5 cells were seeded on day one and U266 cells were seeded on days four to five; co-cultures were treated with BZM 24 hours later and harvested after 48 hours of treatment. Data are presented as absolute viable cell number* ***(A & B)*** *and % viable cells* ***(C)****, mean ±SEM of three experiments.*

In order to demonstrate that the NL-expressing HS5s were competent to activate Notch signaling in a paracrine manner, quantitative RT-PCR (qPCR) was undertaken on HMCL co-cultured with the modified HS5 cells (detailed methodology in Chapter

2 – section 2.8.4.1). The downstream Notch targets HES1 and Deltex-1 (DTX1) were evaluated in HMCL following co-culture with modified HS5.

DND41 T-ALL cells were also used in co-culture with the NL-expressing HS5, as these cells have constitutively active Notch signaling and therefore would be expected to have high baseline levels of Notch downstream targets, including HES1 and DTX1. DND41 cells would therefore act as positive controls for HES1 and DTX1 qPCR, and the ability of NL+ HS5s to enhance constitutive Notch activation in these cells could be evaluated.

U266, MM1S and DND41 cells were all cultured alone so that their baseline Notch activation could be compared to levels seen in co-culture. Additionally all cells cultured were also treated with a gamma-secretase inhibitor (GSI; L685) at a dose known to suppress Notch activation (1μM; [131]). This was to allow discrimination of Notch-dependent and Notch-independent target gene expression. The different experimental conditions are summarised in Table 5-1.

Table 5-1 Conditions for Notch activation assay v.1.

	HS5 cells alone		**U266**		**MM1S**		**DND41**	
GSI (L685 1μM)	-	+	-	+	-	+	-	+
Alone	✓	✓	✓	✓	✓	✓	✓	✓
Co-cultured with:								
DL1+HS5	✓	✓	✓	✓	✓	✓	✓	✓
NC(DL1)HS5	✓	✓	✓	✓	✓	✓	✓	✓
DL4+HS5	✓	✓	✓	✓	✓	✓	✓	✓
Jag2+HS5	✓	✓	✓	✓	✓	✓	✓	✓
NC(DL4)HS5	✓	✓	✓	✓	✓	✓	✓	✓

One plate was used for each modified HS5 subtype such that six TC-treated 12-well plates were set up: (1) U266, MM1S and DND41 cells cultured alone; (2) U266, MM1S and DND41 cells co-cultured with Jag2+HS5; (3) U266, MM1S and DND41

cells co-cultured with DL4+HS5; (4) U266, MM1S and DND41 cells co-cultured with NC(DL4)HS5; (5) U266, MM1S and DND41 cells co-cultured with DL1+HS5; and (6) U266, MM1S and DND41 cells co-cultured with NC(DL1)HS5.

Analysis of gene expression in modified HS5 cells grown alone revealed HES1 transcript levels were present in these cells (Figure 5-5A), with moderate suppression of HES1 expression by GSI, except in the case of NC(DL4)HS5. Interestingly, HES1 expression levels were higher in NL-expressing HS5 compared with NC(DL4)HS5. DTX1 was undetectably low in all modified HS5 subtypes (data not shown). When analysing the adherent fraction of the co-cultures it was not possible to discriminate whether the original RNA had been extracted from HS5 cells or the HMCL/DND41 cells and therefore further analysis of this fraction was not pursued.

Analysis of gene expression in DND41 cells confirmed the effectiveness of the GSI L685 (1μM) at inhibiting Notch activation and expression of both downstream targets (Figure 5-5B). Co-culture of DND41 cells with modified HS5 upregulated HES1 (Figure 5-5B, left-hand) compared to DND41 cells cultured alone, irrespective of ligand expression.

Interestingly highest expression of HES1 was seen following co-culture with NC(DL4)HS5 cells, which was greater than co-culture with either Jag2 or DL4 expressing HS5. When the DL1+HS5 and NC(DL1)HS5 were compared, there was evidence that expression of DL1 was associated with a higher HES1 transcript level. Where HES1 was upregulated in co-cultured DND41 cells, L685 was able to inhibit HES1 expression but it did not appear to be as effective as it was in DND41 cells cultured alone.

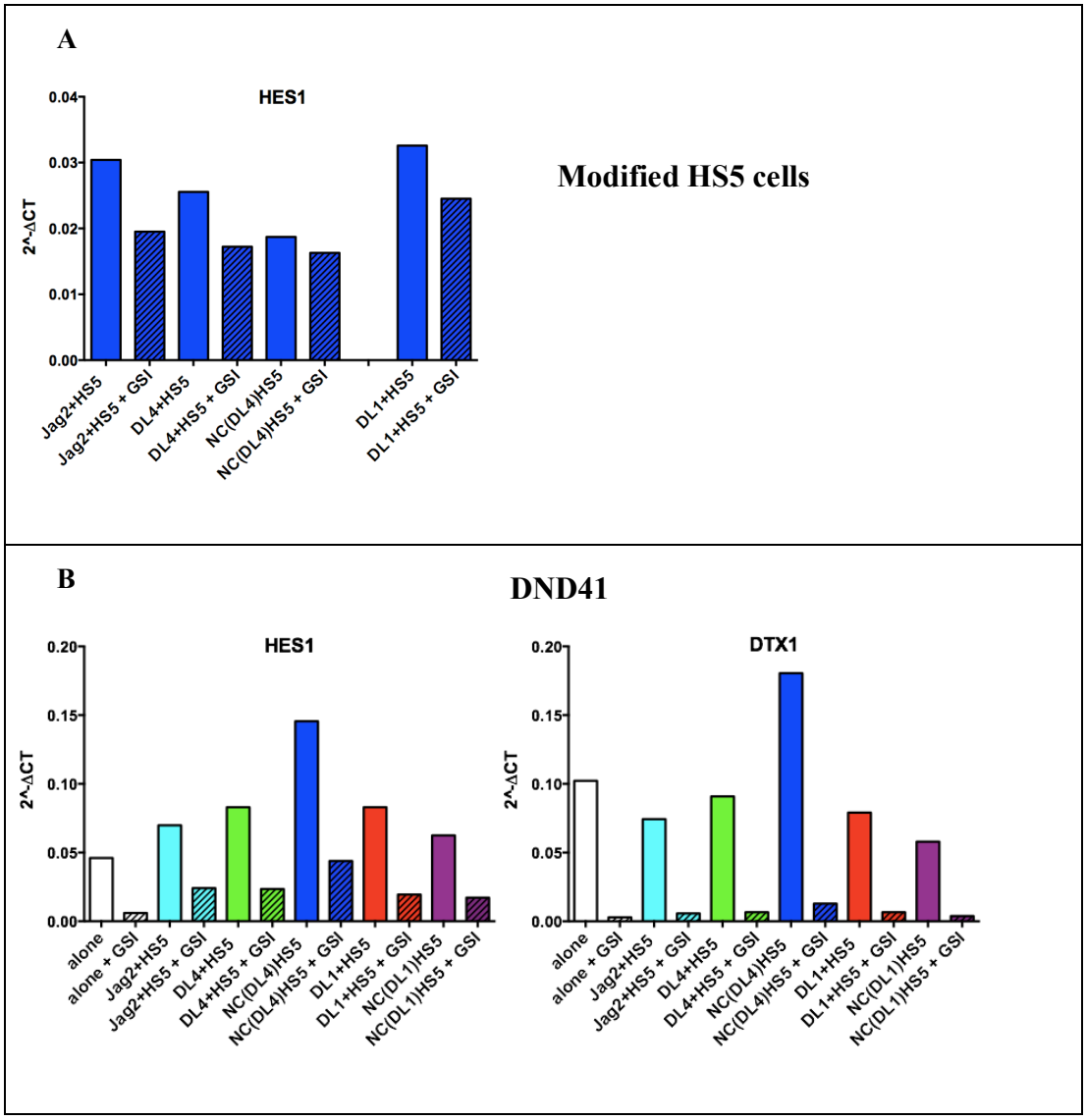

Figure 5-5 Expression of HES1 by modified HS5 cells and effect of co-culture on expression of HES1 and DTX1 by DND41 cells.

Expression of target genes HES1 and DTX1 are shown as $2^{-\Delta CT}$ *values, normalised to expression of B2M. Hashed bars represent cells treated with GSI.* ***A.*** *shows expression of HES1 by modified HS5 cells cultured alone, -/+GSI.* ***B.*** *shows expression of HES1 (left-hand) and DTX1 (right-hand) by DND41 cells, -/+ GSI, cultured alone or with modified HS5 cells. Culture conditions are as indicated.*

When DTX1 expression in DND41 cells was analysed (Figure 5-5B, right-hand), an increase in expression over that seen in cells culture alone was only seen when DND41 cells were co-cultured with NC(DL4)HS5. L685 appeared to be more effective in suppressing DTX1 transcription than in suppressing HES1.

In order to evaluate the inter-plate variation within the assay, the expression of HES1 and DTX1 by the PC and NC were measured and are displayed in Figure 5-6.

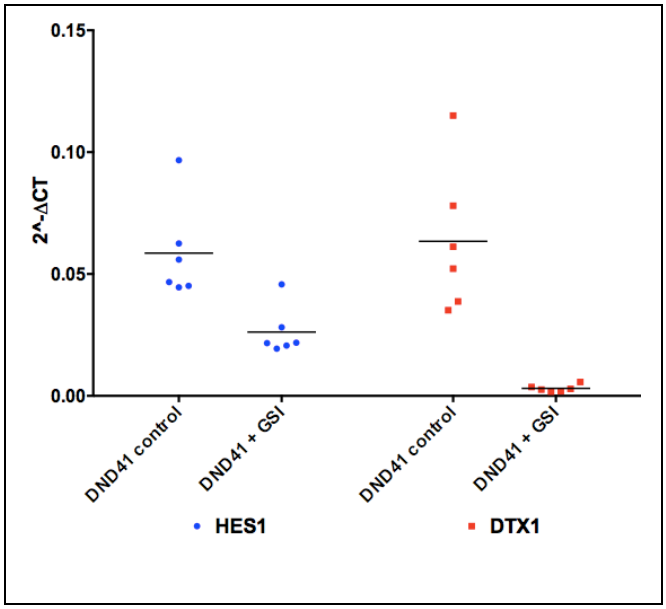

Figure 5-6 HES1 and DTX1 expression by untreated DND41 cells (PC) and GSI-treated DND41 cells (NC).

Expression of target genes HES1 and DTX1 are shown as $2^{-\Delta CT}$ *values, normalised to expression of B2M. Six replicates are shown (and the mean), with standard cDNA for each condition being used on each qPCR plate with identical primers.*

This compares transcript levels detected after qPCR using the PC and NC standard cDNA templates in each of the six suspension qPCR plates (i.e. plates 1, 2, 4, 6, 8 & 10;

The multiple conditions mandated the use of 11 PCR plates, and so to allow comparisons between PCR plates, two standard cDNA samples were amplified in triplicate for each target gene and B2M on every plate. The cDNA was derived from DND41 cells cultured alone and treated with vehicle or L685 1μM (termed positive control (PC) and negative control (NC) respectively). These were generated from a different experiment. The conditions included in each qPCR plate are detailed in Table 2-7.

Table 2-7, page 92). As the same cDNA template, primers and qPCR conditions were used, the results reflect inherent variation within the assay.

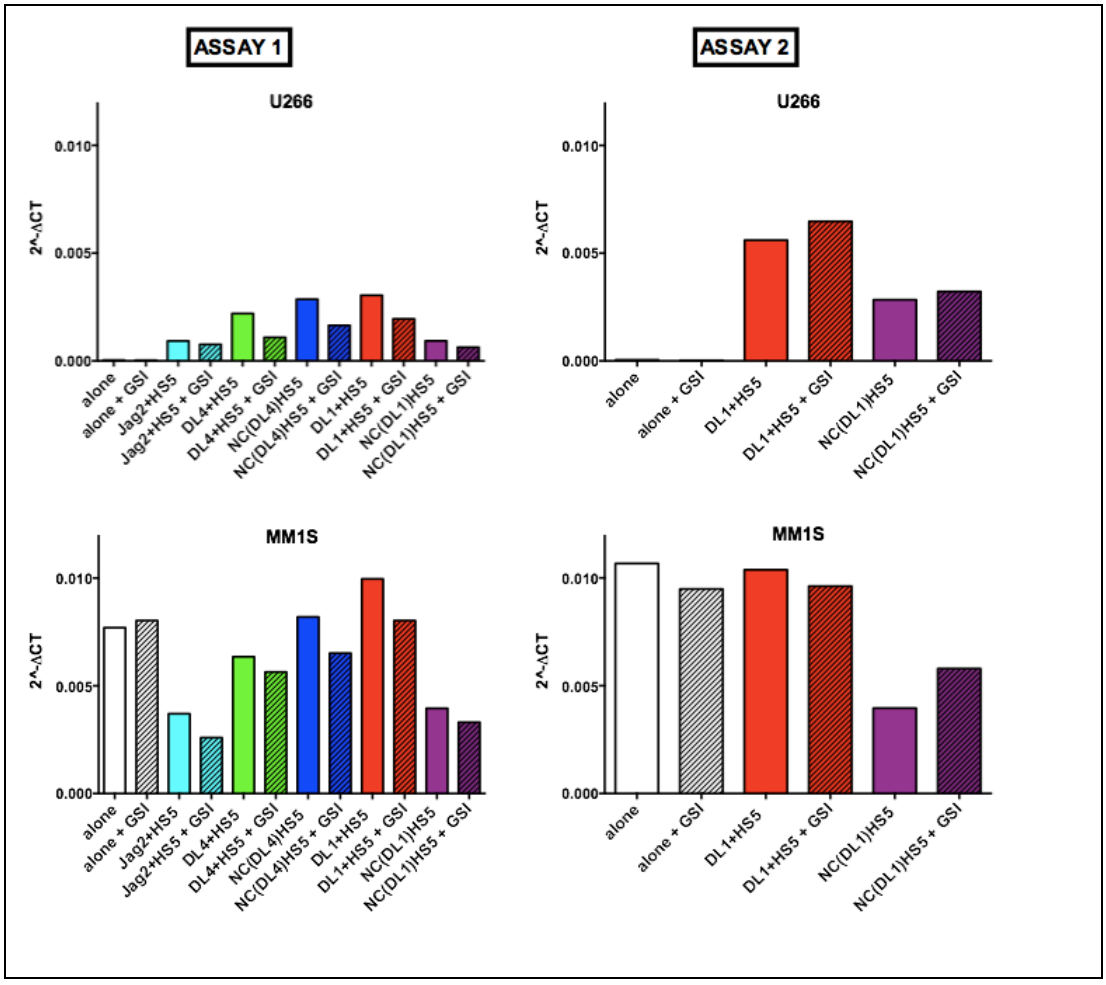

Figure 5-7 Expression of HES1 by U266 and MM1S cells co-cultured with modified HS5.

Expression of target gene HES1 by HMCL is shown as $2^{-\Delta CT}$ values normalised to expression of B2M. Experimental set up is as described in section 5.2.2.1.3 and in Methods chapter 2. Culture conditions are as indicated. Hashed bars represent HMCL treated with GSI. Results from two separate experiments (Assay 1 and 2) are shown.

Having validated the qPCR assay for HES1 and DTX1 in assessing Notch activation, the HMCL U266 and MM1S were evaluated for Notch activation under similar experimental conditions (Figure 5-7, left-hand graphs, Assay 1). Unlike the DND41 cells, DTX1 was almost undetectable in both cell lines in all conditions. For this reason, only HES1 transcript levels were compared. When cultured alone, U266 cells

expressed negligible levels of HES1 (Figure 5-7, top left-hand graph). HES1 transcript levels increased in co-culture with all subtypes of modified HS5. As seen in the DND41 cells, when the Jag2/DL4/NC group were compared, the greatest HES1 expression was seen in co-culture with NC(DL4)HS5 cells. However, within DL1/NC group, higher HES1 levels were seen after co-culture with DL1+HS5 compared to NC(DL1)HS5 cells. In all conditions HES1 levels were lower in the GSI-treated cultures, although the GSI was not able to completely ablate Notch activation.

In contrast to the U266 cells, MM1S cells cultured alone showed significant HES1 expression (Figure 5-7, bottom left-hand graph). However, general upregulation of HES1 was not seen across co-culture conditions. As with DND41 and U266 cells, when the Jag2/DL4/NC group were compared, the greatest HES1 expression was seen following co-culture with NC(DL4)HS5 cells, but this was comparable to that seen in MM1S cells grown alone. Notably, HES1 expression in MM1S cells co-cultured on DL1+HS5 was higher when compared with co-culture on NC(DL1)HS5. In the presence of GSI, HES1 expression was modestly reduced in all conditions, with the exception of MM1S cells cultured alone.

Having compared all modified HS5 in their ability to upregulate expression of HES1 in MM1S and U266 cells, it appeared that DL1+HS5 were the most effective activators of the Notch signaling pathway. The high levels of HES1 seen after co-culture with the NC(DL4)HS5 made it difficult to assess any Notch activation associated with exposure to Jag2 or DL4 in co-culture.

A second experiment was conducted, this time with U266, MM1S and DND41 cells cultured alone, and in co-culture with DL1+HS5 and NC(DL1)HS5 cells (see Table 5-2 for plan). The results of this assay are shown in Figure 5-7 (right-hand graphs; Assay 2) and show that HES1 is once again upregulated in U266 cells co-cultured with HS5 cells, and levels following co-culture with DL1+HS5 cells are higher compared to co-culture with the control NC(DL1)HS5. GSI did not suppress HES1 transcription in these cells. Similarly, HES1 levels were higher in MM1S cells co-cultured with DL1+HS5 compared to those co-cultured with NC(DL1)HS5 but not when compared to MM1S cells cultured alone.

Table 5-2 Conditions for Notch activation assay v.2.

	HS5 cells alone		U266		MM1S		DND41	
L685 1µM	-	+	-	+	-	+	-	+
Alone	✓	✓	✓	✓	✓	✓	✓	✓
Co-cultured with:								
DL1+HS5	✓	✓	✓	✓	✓	✓	✓	✓
NC(DL1)HS5	✓	✓	✓	✓	✓	✓	✓	✓

Notch activation was also assessed by Western blotting for ICN1. Whole cell lysates were prepared from the suspension fractions of all conditions from the second assay. Figure 5-8 shows cleaved intracellular Notch1 (ICN1) is completely absent from all conditions. Despite the high levels of HES1 detected in MM1S cells by qPCR, ICN1 was not seen. As U266 cells do not express Notch 1, it is perhaps not surprising that ICN1 is not seen.

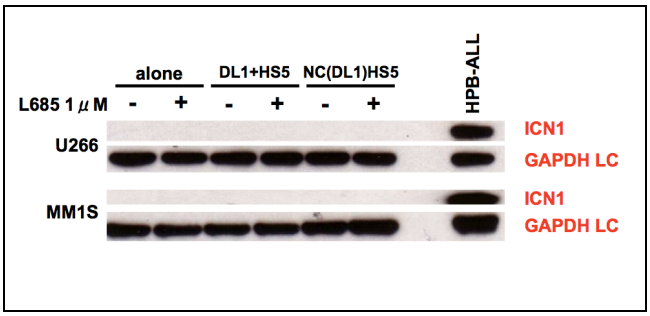

Figure 5-8 ICN1 expression in U266 and MM1S cells after co-culture with modified HS5 cells.

Whole cell lysates were prepared from U266 or MM1S cells harvested from culture alone or from co-culture with DL1+HS5 or NC(DL1)HS5 cells. 20µg protein was loaded per lane. The membrane was probed for ICN1. HPB-ALL whole cell lysate was used as a positive control for ICN1. The housekeeping gene GAPDH was used as a loading control.

Although Western blotting of suspension cells failed to detect ICN1, this does not necessarily discount Notch activation, as cells displaying highest levels of Notch-activation may be contained within the adherent fraction that was not assessed. Similarly, the qPCR results may under-estimate the degree of Notch activation in the

HMCL. Taken together, it was concluded that the DL1+HS5 displayed the greatest capability of activating Notch signaling, in comparison to the appropriate control HS5 [NC(DL1)HS5]. These cells were therefore selected for testing in cytotoxicity assays to investigate the contribution of Notch to (stromal-mediated) resistance to anti-MM treatments.

5.2.3 The effects of co-culture of HMCL with Notch ligand-expressing HS5 cells: growth and bortezomib cytotoxicity

5.2.3.1 The effect of co-culture with Notch ligand-expressing HS5 on growth of U266 and MM1S cells

Co-culture of U266 cells with modified HS5 cells resulted in lower numbers of MM cells compared to U266 cells cultured alone (Figure 5-9A), with a further statistically significant reduction in MM cell growth in the presence of DL1+HS5 (*p=0.042*, paired t-test). Absolute numbers are charted in Table 5-3.

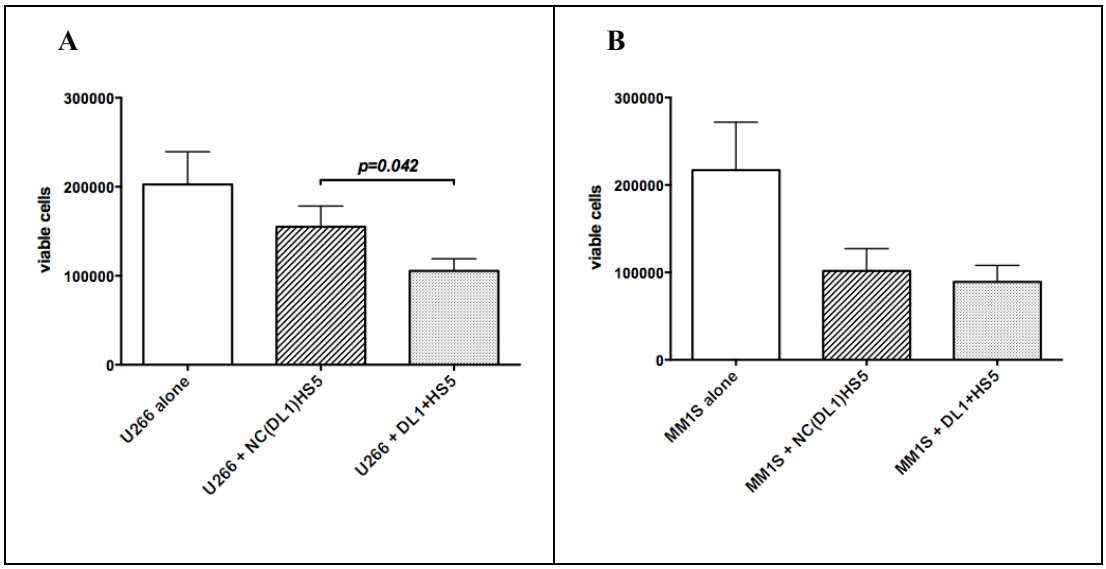

Figure 5-9 Growth of U266 and MM1S cells alone compared to co-cultured with Notch ligand-expressing HS5.

U266 ***(A)*** *or MM1S* ***(B)*** *cells (GFP−) were seeded onto confluent DL1+HS5 or NC(DL1)HS5 or cultured alone. Cells were harvested 48 hours later and stained with APC-conjugated AV and PI and analysed. Total viable (AV−PI−) GFP− cells are represented as the mean ± SEM of triplicates, corrected for viable GFP− HS5 cells (n=3).*

The same pattern was seen in MM1S cells, although there was minimal difference between MM cells cultured with NC(DL1)HS5 compared to DL1+HS5, and none of the paired t-tests showed a statistically significant difference (Figure 5-9B and Table 5-3).

Table 5-3 Growth of U266 and MM1S cells alone compared to co-cultured with modified HS5.

HMCL	**Total viable cells/ well (mean ±SEM, n =3)**		
	Cultured alone	**Co-cultured with NC(DL1)HS5**	**Co-cultured with DL1+HS5**
U266	202664 ±36669	155097 ±23286	105546 ±13571
MM1S	217091 ±54893	101761 ±25486	89200 ±18904

These findings are also demonstrated in the representative experiments shown in Figure 5-11, looking at the bars representing untreated U266 and MM1S cells cultured alone compared to those cultured with NC(DL1)HS5. As the percentage of viable cells was similar between the three groups, it is likely that the difference in the absolute number of viable cells is secondary to differences in the proliferation of HMCL. It appears that those in co-culture with HS5 cells grow more slowly, with an additional inhibition in growth for U266 cells co-cultured with a NL-expressing stromal cell (DL1+HS5).

5.2.3.2 Bortezomib cytotoxicity in HMCL cultured alone compared to those co-cultured with modified HS5 (NC(DL1)HS5)

Bortezomib (BZM) shows clear dose-dependent killing in both U266 and MM1S cells cultured alone or with NC(DL1)HS5 (Figure 5-10). It is apparent that both cell lines growing in co-culture are relatively protected against BZM killing with higher numbers of viable cells recovered from co-cultures at equivalent BZM doses in all six experiments. A 4-parameter log inhibitor dose response curve analysis confirmed that the difference between the BZM dose response curve in HMCL cultured alone and that for HMCL co-cultured with NC(DL1)HS5 was statistically significant ($p<0.0001$ for all three U266 experiments; $p<0.007$ for all three MM1S experiments).

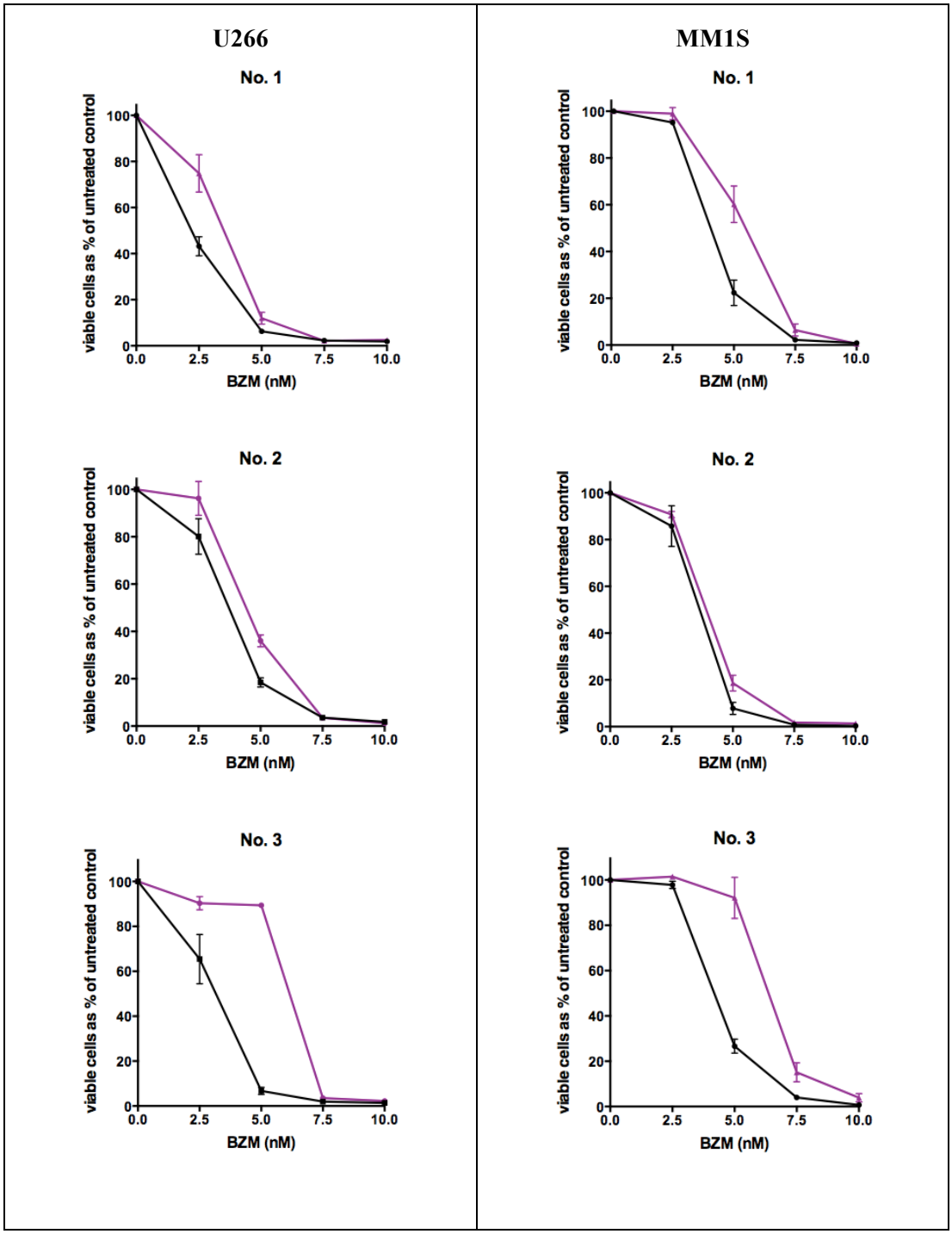

Figure 5-10 Bortezomib cytotoxicity in HMCL cultured alone compared to those co-cultured with NC(DL1)HS5.

U266 and MM1S cells were cultured alone (black) or seeded onto confluent NC(DL1)HS5 (purple). After 24 hours, cells were treated with BZM and harvested 48 hours later. Viable (AV−PI−) GFP− cells (corrected for viable GFP− HS5 cells) are shown as % of untreated control in the form of a dose-response plot for each of three assays (mean ±SD of triplicates).

This is clear evidence of protection from BZM-killing in the presence of stroma. Results from a representative experiment are displayed in absolute cell numbers in Figure 5-11 (**A** & **B** U266, **C** & **D** MM1S).

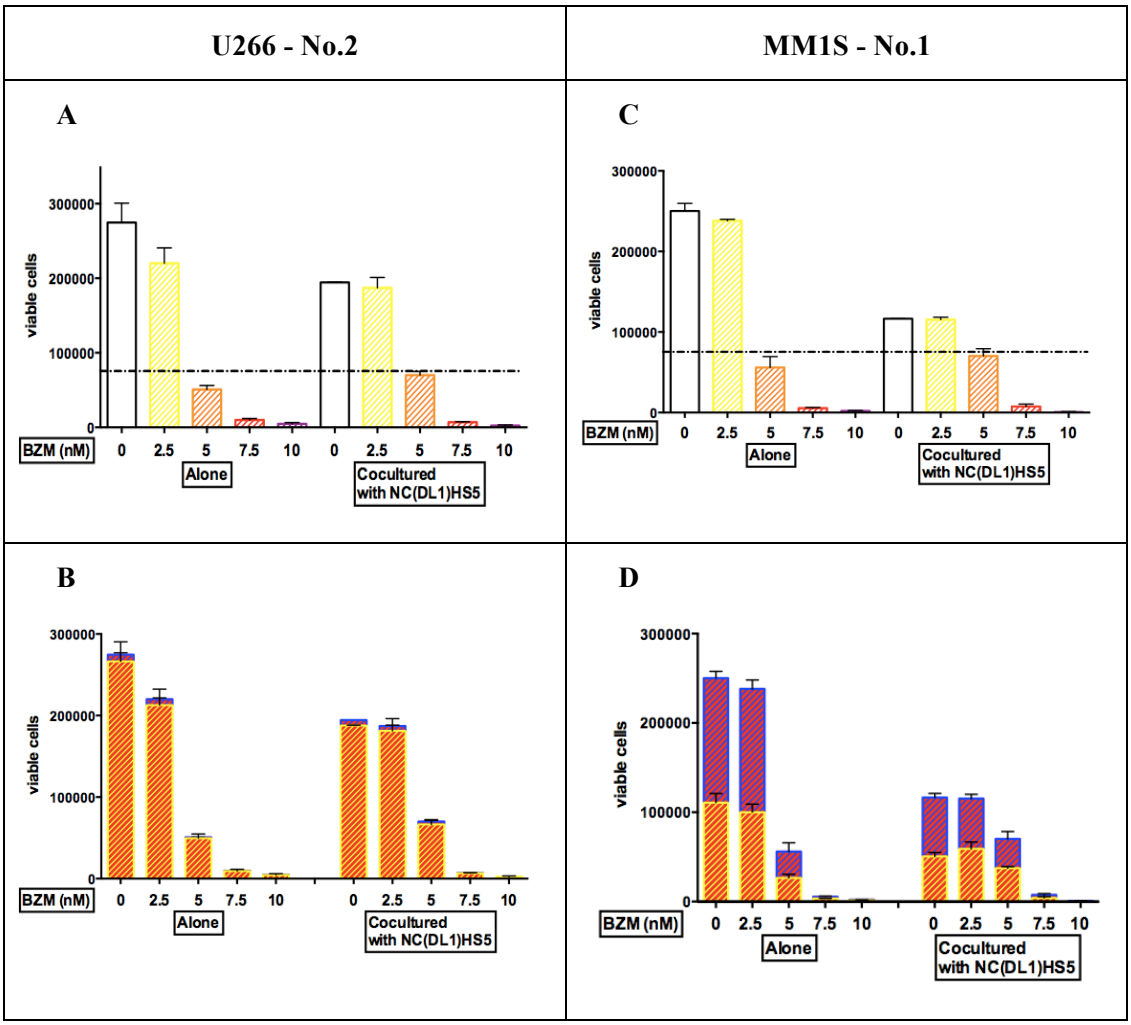

Figure 5-11 Bortezomib cytotoxicity in HMCL cultured alone compared to those co-cultured with NC(DL1)HS5 - two representative experiments.

*Experimental set-up as per Figure 5-10. The results are presented in two different ways. In graphs **A** & **B**, representative plots from the same experiment (No. 2) using U266 cells are shown, while in graphs **C** & **D**, experiment No.1 using MM1S is presented. **A** & **C** show total viable cells, treated with escalating doses of BZM. The dashed line represents the starting number of viable HMCL seeded into the culture system. **B** & **D** show absolute numbers of suspension (red bars hatched with yellow) and adherent (red bars hatched with blue) viable cells, treated with escalating doses of BZM.*

When the distribution of viable cells between suspension and adherent fractions is considered, it is apparent that U266 and MM1S cells display very different growth habits in this setting. Within U266 cells a very small proportion of the total number

of viable cells is adherent (Figure 5-11B; 3% of U266 alone and 3.5% of U266 co-cultured with NC(DL1)HS5). That proportion does not appear to change greatly after treatment with BZM.

In contrast, a large proportion of viable MM1S cells were adherent. 56% of MM1S cultured alone and 56% of MM1S co-cultured with NC(DL1)HS5 were harvested from the adherent fraction (Figure 5-11D). There is no significant difference in the size of the adherent fraction in MM1S cultured alone compared to those co-cultured with HS5 which supports the supposition that this is consistent with a known growth characteristic of the MM1S cell line. As with U266 cells, the proportion of adherent cells does not change with BZM treatment in the two culture conditions.

Comparison of the three experiments for each HMCL reveals some variation in the sensitivity of the MM cells (Figure 5-10). For example, treatment of U266 cultured alone with 2.5nM BZM results in quite different numbers of viable cells: 43.2 ±4.124, 80.13 ±7.518 and 65.43 ±10.99 (expressed as a percentage of the untreated control; mean ±SD). This likely reflects variation in the baseline growth of the HMCL at the time of each experimental set-up. It makes pooling results from the three experiments for each HMCL inappropriate.

5.2.3.3 Effect of DL1 on bortezomib cytotoxicity in HMCL

Next, the ability of DL1 expressed on stromal cells to provide further protection from BZM-mediated cytotoxicity was investigated, in each of these HMCL.

In all three experiments using U266 cells, there is a reduction in BZM cytotoxicity when U266 cells are co-cultured with DL1+HS5 compared to NC(DL1)HS5 (Figure 5-12, left-hand panel). When the dose response curves were analysed as before, a statistically significant difference between the curves was found in experiments No.1 and No. 2 ($p=0.0013$ and $p=0.0002$ respectively).

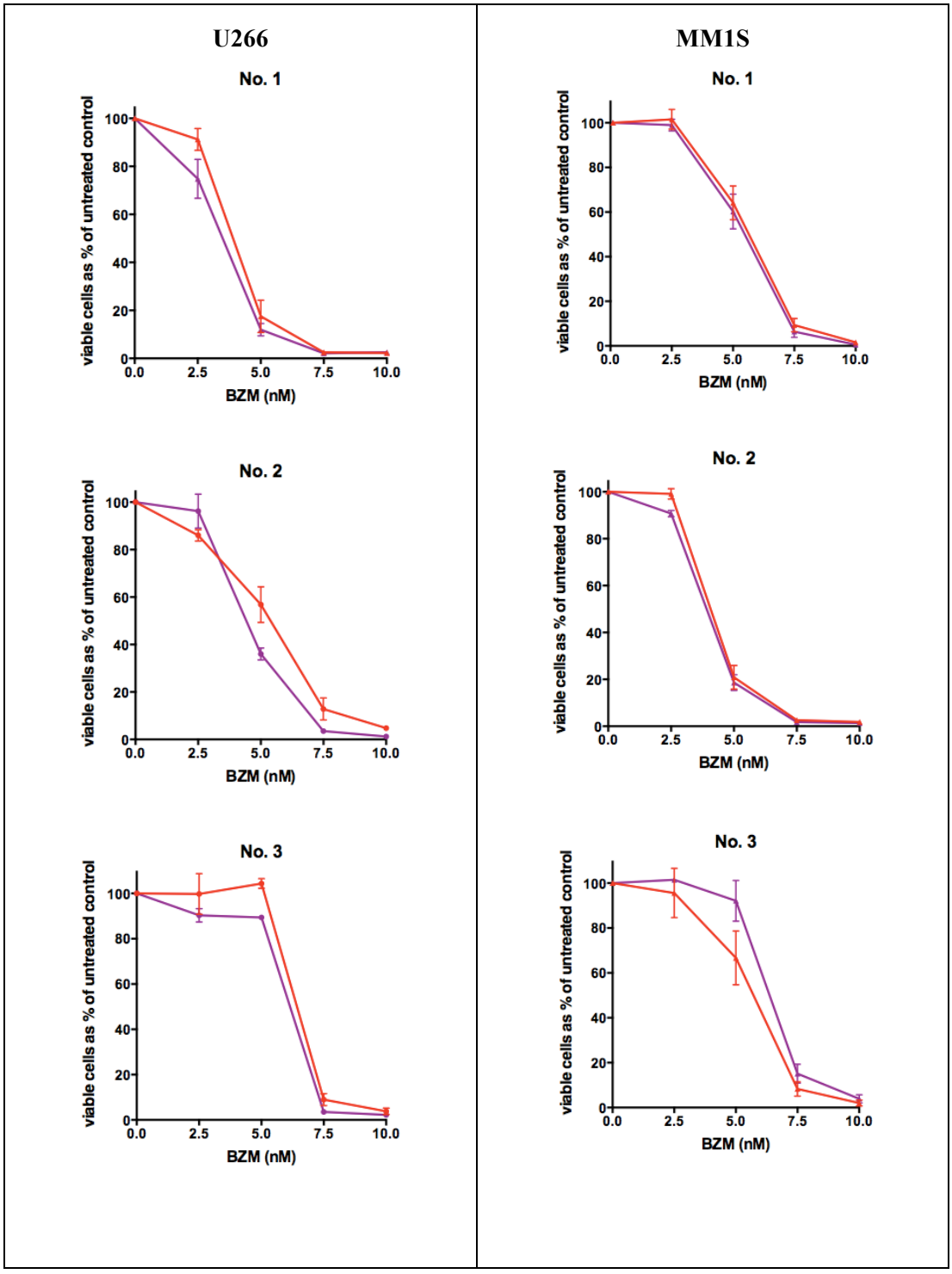

Figure 5-12 Bortezomib cytotoxicity in HMCL co-cultured with NC(DL1)HS5 compared to those co-cultured with DL1+HS5.

U266 and MM1S cells were seeded onto confluent NC(DL1)HS5 (purple) or DL1+HS5 (red). After 24 hours, cells were treated with BZM and harvested 48 hours later. Viable (AV−PI−) GFP− cells (corrected for viable GFP− HS5 cells) are shown as % of untreated control in the form of a dose-response plot for each of three assays (mean ±SD of triplicates).

The same pattern was not seen in BZM-treated MM1S cells (Figure 5-12, right-hand panel), with no difference seen in the effect of BZM in MM1S cells co-cultured with DL1+HS5 versus their negative control.

Taken together this strongly suggests that while stroma-mediated protection against BZM-killing is seen, there is an additional protective effect seen which is associated with the presence of the NL and therefore is likely to be secondary to Notch activation in MM cells.

5.3 Summary and discussion

Notch receptors and ligands were characterised in a panel of HMCL analysed, satisfying the requirements of Aim 1. Notch1 was present at high levels in MM1S and RPMI-8226 cells but absent from U266 cells. In contrast, Notch2 was expressed strongly by U266, RPMI-8226 and LP-1 cells, but much more weakly by MM1S cells. Notch3 and Notch4 were present to varying degrees on all HMCL within the panel. These findings confirm those of a number of research groups [96,98,99] and support the importance of Notch signaling within MM cells. There was no evidence of constitutive ICN1 expression in any HMCL examined. It is interesting that this is the case given that constitutive Notch activation, as evidenced by HES1 expression, has been observed by Jundt et al [98]. That said, the later findings of the Notch activation assay (section 5.2.2.1) do show that there can be a discrepancy between HES1 activity and the presence of ICN1.

The NLs Jag1, Jag2 and DL4 were also expressed by HMCL. Jag1 was strongly expressed by MM1S cells with much weaker expression by U266; in contrast, expression of Jag2 was higher on U266 cells compared to MM1S cells and DL4 was expressed exclusively by U266 cells. It was therefore possible for MM1S and U266 cells to be used to evaluate different aspects of the Notch pathway, with Notch1-dependent signaling examined using MM1S and Notch2-dependent signaling through U266 cells.

In order to evaluate the role of the Notch signaling pathway in MM cells, NL-expressing HS5 stromal cells were produced as a tool to activate Notch signaling in co-cultured MM cells (Aim 2). A number of similar approaches have been reported,

using Jag1+ 3T3 fibroblasts [96], Jag1+ HtTA-jag10 cells [98], DL1+MS5 cells [108]. The approach reported here was chosen as it would provide Notch activation in combination with some of the additional physiological signaling provided by a BM stromal line. Thus Notch activation could be examined in a system that might more accurately recapitulate the BM microenvironment. Recombinant soluble NLs were used by Nefedova et al [96] but their effects are more limited and inconsistent, and in the absence of direct cell-cell contact that is a hallmark of Notch signaling, their value as a tool is less clear.

The functional capabilities of NL-expressing HS5 stromal cells were assessed using RT-PCR to quantify expression of HES1, a key downstream target of the Notch signaling pathway used by a large number of groups in the context of MM [96,98,99,101,103,105,106,109,111]. DTX1 expression was also evaluated in MM1S, U266 and DND41 cells but while expression was substantial and modifiable in DND41 cells, it was not expressed at measurable levels in the HMCL. This suggests that the downstream effects of Notch pathway activation may differ between different haemopoietic lineages.

HMCL were cultured alone and HES1 expression was compared to those co-cultured on HS5 cells expressing Jag2, DL4 or DL1, or the appropriate empty vector negative control. MM1S cells expressed detectable HES1 at baseline, when cultured alone, but there was no evidence of upregulation of HES1 in co-culture with NL-expressing HS5 cells. In contrast, U266 cells had extremely low levels of HES1 expression at baseline, but showed upregulation in the presence of stromal cells, with additional upregulation in co-culture with NL-expressing HS5 cells. Unfortunately, striking upregulation of HES1 was seen in U266 cells co-cultured with the negative control HS5 cells for the Jag2 and DL4-expressing lines so this sub-group could not be used further. It is not known why this was the case but the concern is that the vector used for this group of lines might cause confounding Notch activation through an unknown route. Interestingly the same phenomenon was seen in DND41 cells co-cultured with the panel of modified HS5 cells - the greatest upregulation of HES1 and DTX1 was seen in DND41 co-cultured with NC(DL4)HS5 cells.

It was striking that the efficacy of GSI-L685 within the Notch activation assay varied widely between conditions. It appeared to inhibit HES1 expression most profoundly in DND41 cells cultured alone (>80% reduction; Figure 5-5B). In co-culture with all modified HS5, inhibition was reduced to ~60%. A similar, albeit less striking, effect was seen with DTX1 expression in DND41 cells. When the effect of GSI-L685 on U266 cell Notch activation was assessed, it was not possible to comment on its effects on U266 cells cultured alone as they had no detectable HES1 expression (Figure 5-7, upper plots). However, in co-cultured U266 cells, where HES1 upregulation was seen, there was modest (<50%) and highly variable inhibition of this by GSI-L685, as could be seen when the two assay versions are compared. The reasons for this are unclear. There may be pharmocokinetic changes in co-culture such that the drug is metabolised more rapidly in the presence of HS5 cells, reducing its efficacy. It is also possible that GSI-L685 has less efficacy in HMCL which may express a different gamma secretase subtype to that seen in T-ALL lines. Finally it may be that HES1 was being upregulated through a Notch-independent route, although this seems unlikely as it is a well-validated and specific Notch target in MM, and no alternative routes have been reported in the literature.

It is not clear what is responsible for the differences in Notch activation (as quantified by HES1 expression) seen in U266 and MM1S cells when co-cultured with DL1+HS5. There were a number of differences between the two HMCL used in this system. Firstly, MM1S cells cultured in TC-treated plastic-ware showed a much greater tendency to adhere to the base of the well, when compared to U266 cells. This was seen both when MM1S were cultured alone and when co-cultured with modified stroma. Up to 60% of viable MM1S cells were seen in the adherent fraction, compared to 10-20% of viable U266 cells. This may have led to a significant proportion of cells retained in the adherent fraction that were not analysed, thus leading to an under-estimation of the level of Notch pathway activation. The Transwell system was not used in this activation assay; repeating the assay with additional conditions in which co-cultured cells were separated by a Transwell insert might clarify this issue. It is also known both from this work and the literature that MM1S cells are Notch1 positive and only weakly positive for Notch2, in contrast to U266 cells which express very low levels of Notch1 and are strongly Notch2 positive.

Selective blockade of the Notch1 and Notch2 receptors using antibodies might be used to clarify this issue.

HES1 expression was consistently higher in both U266 and MM1S (and to a lesser extent, DND41) when co-cultured with DL1+HS5 cells, compared to the control NC(DL1)HS5, so this pair of modified HS5 cells was taken forward as a tool for further evaluation of the role of Notch in drug resistance of MM cells. Unfortunately the lack of success with transducing HS5 with other functionally competent Notch ligands made achieving Aim 4 impossible as it did not allow a formal comparison of the effects of different ligands.

Western blotting for ICN1 in HMCL co-cultured with modified HS5 cells did not show any ICN1 in even the cells shown to have Notch activation on the basis of HES1 upregulation (i.e. U266 cells in the presence of DL1+HS5). This may reflect sampling of protein at a time point at which ICN1 was no longer present. A time course analysis, in which lysates of U266 cells were harvested at different time points after first incubation with DL1+HS5 cells might clarify this. Alternatively, the discrepancy may reflect the known low expression of Notch1 by U266 cells. Although some cross-reactivity may be expected of the ICN1 antibody to ICN2 (given the structural homology of the two receptor subtypes), it has not been optimised for this target and therefore is likely to grossly underestimate levels of Notch2 in the cytoplasm.

Having demonstrated that U266 cells co-cultured with DL1+HS5 cells showed evidence of Notch pathway activation, the impact of this on MM cell sensitivity to anti-myeloma treatment was then assessed. U266 cells cultured alone, with DL1+HS5 or with NC(DL1+)HS5 were treated with escalating doses of the proteosome inhibitor bortezomib (BZM). Dose-dependent killing was observed, and this was reduced in U266 cells co-cultured with HS5 cells, with an additional reduction in BZM-associated killing in U266 cells co-cultured with DL1+HS5. This strongly suggested that activation of the Notch pathway in U266 cells was associated with a reduction in sensitivity to BZM treatment.

The same pattern was not seen in MM1S cells. When co-cultured with HS5 cells there was a clear stroma-associated resistance to BZM killing, with minimal additional protection conferred by DL1+HS5. This was consistent with the lack of HES1 upregulation seen in MM1S cells co-cultured with DL1+HS5 cells.

The differences in Notch activation seen between MM1S and U266 cells co-cultured with DL1+HS5 appear to predict for the level of NL-mediated protection from BZM killing. This does suggest that Notch activation contributes to BM stroma-mediated protection against BZM-killing, satisfying Aim 3. The DL1-Notch2 interaction maybe specifically implicated, but this is speculation in the absence of the additional mechanistic work outlined above. However, it is notable that Xu et al [108] used DL1+MS5 and identified Notch2 as the primary mediating receptor. They also observed that prior stimulation of murine 5T33MMvt MM cells by DL1+HS5 rendered them less sensitive to BZM.

The results presented in this chapter support the hypothesis that Notch activation attenuates BZM killing of MM cells. It was demonstrated that Notch receptors and their ligands are expressed in the majority of HMCL. Using a novel co-culture system utilising a NL-expressing BM stromal line, activation of the Notch pathway was seen in HMCL. This activation is associated with clear protective advantage against a key anti-myeloma agent. Further work is required to identify molecular mechanisms mediating this Notch-dependent protection; to explore whether protection is seen against other anti-myeloma agents; and also validate the system using alternative HMCL and primary CD138+ cells.

CHAPTER 6. DISCUSSION

6.1 The role of the stem cell progenitor compartment in MM

The MM stem cell was first proposed in the late 70s [27], but it was not until 2004 that a convincing phenotype was proposed by William Matsui's group in Baltimore [28], seemingly further validated in 2008 [40].

The work reported in Chapter 3 is not compatible with Matsui's model of the MM stem cell. When MM patient BM aspirate MNCs were phenotyped, the LC-restricted CD138− proportion was extremely small, although it appeared to increase in patients with lower BM tumour burdens. I believe this is an artefactual result of FACS analysis of very small populations of cells where the gated population (LC-restricted, LC+) is not clearly segregated from the whole. In patients with larger tumour burdens, and therefore clearer LC+ subpopulations, further analysis was more robust. It is also clear that the LC+CD138− cell fraction expressed B cell antigens very inconsistently.

The modified three-dimensional culture system optimised for the longer-term culture of clonal BM MM cells did appear to show evidence of a LC+CD138− population that increased in both relative and absolute terms over time and after drug treatment. However, cell cycle analysis (using BrdU uptake and 7AAD staining) of these primary MM cells when freshly isolated and after time in culture clearly indicated that the majority (>70%) of LC+CD138− cells were sub-G0/G1 (in comparison, <10% of LC+CD138+ cells were in sub-G0/G1). This suggested the drug treatment induced apoptosis in clonal cells, associated with a loss of CD138 expression.

These findings are entirely consistent with those of a number of groups [32,46,48,49,51,55,56,132], some of which have reported since the landmark papers of Matsui, and since the initiation of the work presented in this chapter.

The stem cell model in which the tumorigenic cell in MM is drug resistant and therefore responsible not only for disease initiation but also for relapse after apparently successful treatment is still very compelling. However, it seems unlikely that this cell has a fixed phenotype. Rather, given the bi-directional plasticity of stem

cell populations, as indicated by inducible pluripotent stem cell technology [133], it seems likely that drug resistance is a feature of a number of different clonal subpopulations over the natural history of the disease, expressing different cell surface markers. A recent report has proposed the presence of four hierarchically organised, clonally related, subpopulations in MM [134], with tumour-propagation capacity exclusively seen within a small population of so-called 'pre-PC' that are CD19−CD138−. Importantly this subpopulation appears to undergo reversible bi-directional transition to a CD19−CD138+ phenotype, through epigenetic changes. This model has yet to be confirmed by another group but offers some significant refinements on Matsui's model.

Ultimately, addressing inevitable relapse in MM needs more understanding of the mechanisms of drug resistance, as it is likely that a number of factors contribute to the protection of the tumorigenic compartment.

6.2 APRIL and drug resistance in MM

The role of APRIL as a survival factor in MM is uncontroversial [70,71], but its specific contribution to drug resistance remains unclear.

The first part of the work presented in Chapter 4 utilised primary freshly selected CD138+ MM cells cultured in culture media alone (RPMI with 20% pooled patient plasma), in the presence or absence of recombinant soluble APRIL. Dexamethasone (Dex) treatment of MM cells under these conditions revealed a consistent, albeit small calibre, protection from Dex killing in the presence of APRIL, which was not attributable to a proliferative or survival effect (APRIL alone had no effect on viable CD138+ MM cell number and all results were compared to an untreated APRIL-only control), confirming the findings of Moreaux et al. [76]. In a small series, where the protection offered by APRIL, IL-6 and IGF-I were compared, APRIL offered greater protection than IGF-I, although less than IL-6. There was some suggestion that the protection offered by APRIL was more pronounced in Cyclin D2+ (compared with Cyclin D1+) MM samples, which would be compatible with the difference in APRIL-associated cell cycle effects observed in this group [18]. In this experimental model, protection was not seen when MM cells were treated with bortezomib (BZM) or lenalidomide.

When APRIL secretion was incorporated into a novel co-culture model using modified HS-5 cells, the human myeloma cell lines - U266 and MM1S - were protected from BZM killing in the presence of stroma *per se*, but additional protection from secreted APRIL was not clearly demonstrated. This may have been related to insufficient levels of secreted APRIL, but merits further investigation.

This work indicates that APRIL is a likely component of the drug resistance provided by the BM microenvironment in MM. APRIL is produced by a number of cells within the BM, including myeloid cells and osteoclasts [70,71,76], and this production may be up-regulated in the presence of MM cells, in similar fashion to IL-6 [59,60]. However, with the modest protective effect seen in the two models employed in this work, it was not possible to undertake an additional mechanistic evaluation of this protection.

Further work in this area would usefully include extending the range of BZM doses evaluated to see if a greater protection might be evident at different doses, allowing more opportunities for evaluating the involved pathways. It would also be valuable to examine the effects of alternative anti-myeloma treatments (including Dex and lenalidomide) to see if protection varies with class of agent and mechanism of action. Finally, it would be interesting to use the co-culture system with primary MM cells, with and without drug treatments. This, however, may require further optimisation of the culture conditions for primary CD138-selected MM cells.

6.3 Notch pathway activation and drug resistance in MM

The Notch signaling pathway is an evolutionarily conserved pathway involved in cell fate, proliferation and survival in a number of tissues. It is dysregulated or abnormally activated in a number of malignancies [88], both solid tumours and haematological, e.g. T-ALL [89]. Both MM cells (primary and HMCL) and BM stromal cells express Notch receptors [96,98,99] and Notch ligands are present on BM stromal cells [95,96].

The reported effects of Notch signaling have not been consistent, with some groups demonstrating cell cycle arrest in Notch-activated MM cells [96,105], while others report that proliferation results from Notch activation [98,99,103,111], either directly or through

an intermediary such as IL-6, or the PI3K/AKT pathway. However, there appears to be a consensus that Notch activation is associated with enhanced MM cell survival and also clonogenicity [104]. Increasingly there is also a sense that Notch signaling is directly involved in drug resistance, and different ligand-receptor pairs, e.g. Jag1-Notch1 [96,106,107], DL1-Notch2 [108] have been implicated. These effects have been seen with different anti-MM agents, including mitoxantrone and bortezomib.

Chapter 5 first reports observational data regarding the expression of Notch receptors and ligands on HMCL. Constitutive Notch activation was not observed, as assessed by expression of ICN1 (Western blotting) or HES1 (RT-PCR). These results provided the rationale for selecting the two HMCL, MM1S and U266, for subsequent work: MM1S expressed Notch1 and U266 Notch2 (in keeping with the reports of other groups).

In order to evaluate the effect of Notch signaling in MM cells, a novel method of Notch activation was set up using HS5 cells modified to express different Notch ligands. The functional effect of these ligands was verified by RT-PCR to quantify the upregulation of the Notch down-stream target HES1. Based on this DL1+HS5 were used for subsequent co-culture experiments to evaluate the influence of Notch signaling on bortezomib sensitivity. There was strong evidence of Notch-associated protection in U266 cells, with the same trend seen in MM1S cells, albeit at lower levels. This difference in effect may indicate that Notch2 is the critical receptor ligating DL1, but additional work is needed to support this claim. This could be explored through the use of selective Notch1 and Notch2 blocking antibodies. Additionally other HMCL expressing Notch1 or Notch2 predominantly might be evaluated to see if a similar pattern was observed.

Within the limited time using this model it was not possible to look at the effect of co-treatment of MM cells with Notch pathway antagonists, such as GSIs or some of the newer, more specific agents e.g. SAHM1. Bortezomib treatment causes reversible inhibition of the proteasome within MM cells, and downstream effects on NF-κB signaling. It would be interesting to explore whether small molecule inhibitors of this pathway or of the PI3K/AKT pathway can attenuate DL1-associated protection. Further mechanistic work would also be relevant if testing

different myeloma agents such as dexamethasone or a novel agent such as lenalidomide, which is known to have a range of effects on the BM microenvironment.

Recombinant soluble Notch ligands have been used by some groups to activate Notch receptors and explore the effect of Notch signaling in MM cells. This would be an interesting approach to use, but a demonstration of its efficacy would be needed as these soluble agents differ so profoundly from the physiological molecule that they mimic.

6.4 Future directions

The work presented in this thesis represents an exploration of various models of drug resistance in MM cells, both primary and cell-line based. It seems that future work should reasonably focus on the Notch pathway, taking the co-culture model employed as a starting point and undertaking the work outlined above.

It might reasonably be hypothesised that crosstalk between Notch signaling and pathways activated by APRIL exists, given the shared downstream targets feeding into the NF-κB and PI3K signaling pathways. This might be evaluated through combinations of modified HS5 cells or utilising DL1+HS5 in combination with soluble recombinant APRIL.

The different genetic subtypes in MM will need to be evaluated separately, given the differences conferred by the various genetic lesions on the biology of MM cells and the diseases they generate [18,19,135]. Ultimately the hunt for novel targets within the MM cell drug resistance armoury remains critical, even in this age of novel therapies, and it seems likely that individual patients will require therapeutic interventions tailored to targets known to act more strongly in their genetic subtype.

REFERENCES

(1) Pulte, D.; Gondos, A.; Brenner, H. Improvement in survival of older adults with multiple myeloma: results of an updated period analysis of SEER data. *The oncologist* **2011**, *16*, 1600-1603.

(2) Kumar, S. K.; Rajkumar, S. V.; Dispenzieri, A.; Lacy, M. Q.; Hayman, S. R.; Buadi, F. K.; Zeldenrust, S. R.; Dingli, D.; Russell, S. J.; Lust, J. A.; Greipp, P. R.; Kyle, R. A.; Gertz, M. A. Improved survival in multiple myeloma and the impact of novel therapies. *Blood* **2008**, *111*, 2516-2520.

(3) Renshaw, C.; Ketley, N.; Moller, H.; Davies, E. A. Trends in the incidence and survival of multiple myeloma in South East England 1985-2004. *BMC cancer* **2010**, *10*, 74.

(4) Herve, A. L.; Florence, M.; Philippe, M.; Michel, A.; Thierry, F.; Kenneth, A.; Jean-Luc, H.; Nikhil, M.; Stephane, M. Molecular heterogeneity of multiple myeloma: pathogenesis, prognosis, and therapeutic implications. *Journal of clinical oncology : official journal of the American Society of Clinical Oncology* **2011**, *29*, 1893-1897.

(5) Lopez-Corral, L.; Corchete, L. A.; Sarasquete, M. E.; Mateos, M. V.; Garcia-Sanz, R.; Ferminan, E.; Lahuerta, J. J.; Blade, J.; Oriol, A.; Teruel, A. I.; Martino, M. L.; Hernandez, J.; Hernandez-Rivas, J. M.; Burguillo, F. J.; San Miguel, J. F.; Gutierrez, N. C. Transcriptome analysis reveals molecular profiles associated with evolving steps of monoclonal gammopathies. *Haematologica* **2014**, *99*, 1365-1372.

(6) van de Donk, N. W.; Palumbo, A.; Johnsen, H. E.; Engelhardt, M.; Gay, F.; Gregersen, H.; Hajek, R.; Kleber, M.; Ludwig, H.; Morgan, G.; Musto, P.; Plesner, T.; Sezer, O.; Terpos, E.; Waage, A.; Zweegman, S.; Einsele, H.; Sonneveld, P.; Lokhorst, H. M.; European Myeloma, N. The clinical relevance and management of monoclonal gammopathy of undetermined significance and related disorders:

recommendations from the European Myeloma Network. *Haematologica* **2014**, *99*, 984-996.

(7) Turesson, I.; Kovalchik, S. A.; Pfeiffer, R. M.; Kristinsson, S. Y.; Goldin, L. R.; Drayson, M. T.; Landgren, O. Monoclonal gammopathy of undetermined significance and risk of lymphoid and myeloid malignancies: 728 cases followed up to 30 years in Sweden. *Blood* **2014**, *123*, 338-345.

(8) Kyle, R. A.; Rajkumar, S. V. Monoclonal gammopathy of undetermined significance and smouldering multiple myeloma: emphasis on risk factors for progression. *Br J Haematol* **2007**, *139*, 730-743.

(9) Bird, J.; Behrens, J.; Westin, J.; Turesson, I.; Drayson, M.; Beetham, R.; D'Sa, S.; Soutar, R.; Waage, A.; Gulbrandsen, N.; Gregersen, H.; Low, E.; Haemato-oncology Task Force of the British Committee for Standards in Haematology, U. K. M. F.; Nordic Myeloma Study, G. UK Myeloma Forum (UKMF) and Nordic Myeloma Study Group (NMSG): guidelines for the investigation of newly detected M-proteins and the management of monoclonal gammopathy of undetermined significance (MGUS). *Br J Haematol* **2009**, *147*, 22-42.

(10) Kyle, R. A.; Remstein, E. D.; Therneau, T. M.; Dispenzieri, A.; Kurtin, P. J.; Hodnefield, J. M.; Larson, D. R.; Plevak, M. F.; Jelinek, D. F.; Fonseca, R.; Melton, L. J., 3rd; Rajkumar, S. V. Clinical course and prognosis of smoldering (asymptomatic) multiple myeloma. *N Engl J Med* **2007**, *356*, 2582-2590.

(11) Mateos, M. V.; Hernandez, M. T.; Giraldo, P.; de la Rubia, J.; de Arriba, F.; Lopez Corral, L.; Rosinol, L.; Paiva, B.; Palomera, L.; Bargay, J.; Oriol, A.; Prosper, F.; Lopez, J.; Olavarria, E.; Quintana, N.; Garcia, J. L.; Blade, J.; Lahuerta, J. J.; San Miguel, J. F. Lenalidomide plus dexamethasone for high-risk smoldering multiple myeloma. *N Engl J Med* **2013**, *369*, 438-447.

(12) Bird, J. M.; Owen, R. G.; D'Sa, S.; Snowden, J. A.; Pratt, G.; Ashcroft, J.; Yong, K.; Cook, G.; Feyler, S.; Davies, F.; Morgan, G.; Cavenagh, J.; Low, E.; Behrens, J.; Haemato-oncology Task Force of British Committee for Standards in, H.;

Forum, U. K. M. Guidelines for the diagnosis and management of multiple myeloma 2011. *Br J Haematol* **2011**, *154*, 32-75.

(13) Greipp, P. R.; San Miguel, J.; Durie, B. G.; Crowley, J. J.; Barlogie, B.; Blade, J.; Boccadoro, M.; Child, J. A.; Avet-Loiseau, H.; Kyle, R. A.; Lahuerta, J. J.; Ludwig, H.; Morgan, G.; Powles, R.; Shimizu, K.; Shustik, C.; Sonneveld, P.; Tosi, P.; Turesson, I.; Westin, J. International staging system for multiple myeloma. *Journal of clinical oncology : official journal of the American Society of Clinical Oncology* **2005**, *23*, 3412-3420.

(14) Chesi, M.; Nardini, E.; Lim, R. S.; Smith, K. D.; Kuehl, W. M.; Bergsagel, P. L. The t(4;14) translocation in myeloma dysregulates both FGFR3 and a novel gene, MMSET, resulting in IgH/MMSET hybrid transcripts. *Blood* **1998**, *92*, 3025-3034.

(15) Bergsagel, P. L.; Kuehl, W. M. Molecular pathogenesis and a consequent classification of multiple myeloma. *Journal of clinical oncology : official journal of the American Society of Clinical Oncology* **2005**, *23*, 6333-6338.

(16) Bergsagel, P. L.; Kuehl, W. M.; Zhan, F.; Sawyer, J.; Barlogie, B.; Shaughnessy, J., Jr. Cyclin D dysregulation: an early and unifying pathogenic event in multiple myeloma. *Blood* **2005**, *106*, 296-303.

(17) Ely, S.; Di Liberto, M.; Niesvizky, R.; Baughn, L. B.; Cho, H. J.; Hatada, E. N.; Knowles, D. M.; Lane, J.; Chen-Kiang, S. Mutually exclusive cyclin-dependent kinase 4/cyclin D1 and cyclin-dependent kinase 6/cyclin D2 pairing inactivates retinoblastoma protein and promotes cell cycle dysregulation in multiple myeloma. *Cancer Res* **2005**, *65*, 11345-11353.

(18) Quinn, J.; Glassford, J.; Percy, L.; Munson, P.; Marafioti, T.; Rodriguez-Justo, M.; Yong, K. APRIL promotes cell-cycle progression in primary multiple myeloma cells: influence of D-type cyclin group and translocation status. *Blood* **2011**, *117*, 890-901.

(19) Zhan, F.; Huang, Y.; Colla, S.; Stewart, J. P.; Hanamura, I.; Gupta, S.; Epstein, J.; Yaccoby, S.; Sawyer, J.; Burington, B.; Anaissie, E.; Hollmig, K.; Pineda-Roman, M.; Tricot, G.; van Rhee, F.; Walker, R.; Zangari, M.; Crowley, J.; Barlogie, B.; Shaughnessy, J. D., Jr. The molecular classification of multiple myeloma. *Blood* **2006**, *108*, 2020-2028.

(20) Bolli, N.; Avet-Loiseau, H.; Wedge, D. C.; Van Loo, P.; Alexandrov, L. B.; Martincorena, I.; Dawson, K. J.; Iorio, F.; Nik-Zainal, S.; Bignell, G. R.; Hinton, J. W.; Li, Y.; Tubio, J. M.; McLaren, S.; S, O. M.; Butler, A. P.; Teague, J. W.; Mudie, L.; Anderson, E.; Rashid, N.; Tai, Y. T.; Shammas, M. A.; Sperling, A. S.; Fulciniti, M.; Richardson, P. G.; Parmigiani, G.; Magrangeas, F.; Minvielle, S.; Moreau, P.; Attal, M.; Facon, T.; Futreal, P. A.; Anderson, K. C.; Campbell, P. J.; Munshi, N. C. Heterogeneity of genomic evolution and mutational profiles in multiple myeloma. *Nature communications* **2014**, *5*, 2997.

(21) Stewart, A. K.; Richardson, P. G.; San-Miguel, J. F. How I treat multiple myeloma in younger patients. *Blood* **2009**, *114*, 5436-5443.

(22) Sonneveld, P.; Goldschmidt, H.; Rosinol, L.; Blade, J.; Lahuerta, J. J.; Cavo, M.; Tacchetti, P.; Zamagni, E.; Attal, M.; Lokhorst, H. M.; Desai, A.; Cakana, A.; Liu, K.; van de Velde, H.; Esseltine, D. L.; Moreau, P. Bortezomib-based versus nonbortezomib-based induction treatment before autologous stem-cell transplantation in patients with previously untreated multiple myeloma: a meta-analysis of phase III randomized, controlled trials. *Journal of clinical oncology : official journal of the American Society of Clinical Oncology* **2013**, *31*, 3279-3287.

(23) Bonnet, D.; Dick, J. E. Human acute myeloid leukemia is organized as a hierarchy that originates from a primitive hematopoietic cell. *Nat Med* **1997**, *3*, 730-737.

(24) Al-Hajj, M.; Wicha, M. S.; Benito-Hernandez, A.; Morrison, S. J.; Clarke, M. F. Prospective identification of tumorigenic breast cancer cells. *Proc Natl Acad Sci U S A* **2003**, *100*, 3983-3988.

(25) Singh, S. K.; Hawkins, C.; Clarke, I. D.; Squire, J. A.; Bayani, J.; Hide, T.; Henkelman, R. M.; Cusimano, M. D.; Dirks, P. B. Identification of human brain tumour initiating cells. *Nature* **2004**, *432*, 396-401.

(26) Takezaki, T.; Hide, T.; Takanaga, H.; Nakamura, H.; Kuratsu, J. I.; Kondo, T. Essential role of the Hedgehog signaling pathway in human glioma-initiating cells. *Cancer Sci* **2011**.

(27) Hamburger, A.; Salmon, S. E. Primary bioassay of human myeloma stem cells. *J Clin Invest* **1977**, *60*, 846-854.

(28) Matsui, W.; Huff, C. A.; Wang, Q.; Malehorn, M. T.; Barber, J.; Tanhehco, Y.; Smith, B. D.; Civin, C. I.; Jones, R. J. Characterization of clonogenic multiple myeloma cells. *Blood* **2004**, *103*, 2332-2336.

(29) Carey, D. J. Syndecans: multifunctional cell-surface co-receptors. *The Biochemical journal* **1997**, *327 (Pt 1)*, 1-16.

(30) Beauvais, D. M.; Burbach, B. J.; Rapraeger, A. C. The syndecan-1 ectodomain regulates alphavbeta3 integrin activity in human mammary carcinoma cells. *The Journal of cell biology* **2004**, *167*, 171-181.

(31) Laguri, C.; Arenzana-Seisdedos, F.; Lortat-Jacob, H. Relationships between glycosaminoglycan and receptor binding sites in chemokines-the CXCL12 example. *Carbohydrate research* **2008**, *343*, 2018-2023.

(32) Reijmers, R. M.; Groen, R. W.; Rozemuller, H.; Kuil, A.; de Haan-Kramer, A.; Csikos, T.; Martens, A. C.; Spaargaren, M.; Pals, S. T. Targeting EXT1 reveals a crucial role for heparan sulfate in the growth of multiple myeloma. *Blood* **2010**, *115*, 601-604.

(33) Khotskaya, Y. B.; Dai, Y.; Ritchie, J. P.; MacLeod, V.; Yang, Y.; Zinn, K.; Sanderson, R. D. Syndecan-1 is required for robust growth, vascularization, and metastasis of myeloma tumors in vivo. *J Biol Chem* **2009**, *284*, 26085-26095.

(34) Derksen, P. W.; Keehnen, R. M.; Evers, L. M.; van Oers, M. H.; Spaargaren, M.; Pals, S. T. Cell surface proteoglycan syndecan-1 mediates hepatocyte growth factor binding and promotes Met signaling in multiple myeloma. *Blood* **2002**, *99*, 1405-1410.

(35) Hendriks, J.; Planelles, L.; de Jong-Odding, J.; Hardenberg, G.; Pals, S. T.; Hahne, M.; Spaargaren, M.; Medema, J. P. Heparan sulfate proteoglycan binding promotes APRIL-induced tumor cell proliferation. *Cell Death Differ* **2005**, *12*, 637-648.

(36) Ingold, K.; Zumsteg, A.; Tardivel, A.; Huard, B.; Steiner, Q. G.; Cachero, T. G.; Qiang, F.; Gorelik, L.; Kalled, S. L.; Acha-Orbea, H.; Rennert, P. D.; Tschopp, J.; Schneider, P. Identification of proteoglycans as the APRIL-specific binding partners. *J Exp Med* **2005**, *201*, 1375-1383.

(37) Pilarski, L. M.; Jensen, G. S. Monoclonal circulating B cells in multiple myeloma. A continuously differentiating, possibly invasive, population as defined by expression of CD45 isoforms and adhesion molecules. *Hematol Oncol Clin North Am* **1992**, *6*, 297-322.

(38) Szczepek, A. J.; Seeberger, K.; Wizniak, J.; Mant, M. J.; Belch, A. R.; Pilarski, L. M. A high frequency of circulating B cells share clonotypic Ig heavy-chain VDJ rearrangements with autologous bone marrow plasma cells in multiple myeloma, as measured by single-cell and in situ reverse transcriptase-polymerase chain reaction. *Blood* **1998**, *92*, 2844-2855.

(39) Bakkus, M. H.; Van Riet, I.; Van Camp, B.; Thielemans, K. Evidence that the clonogenic cell in multiple myeloma originates from a pre-switched but somatically mutated B cell. *Br J Haematol* **1994**, *87*, 68-74.

(40) Matsui, W.; Wang, Q.; Barber, J. P.; Brennan, S.; Smith, B. D.; Borrello, I.; McNiece, I.; Lin, L.; Ambinder, R. F.; Peacock, C.; Watkins, D. N.; Huff, C. A.; Jones, R. J. Clonogenic multiple myeloma progenitors, stem cell properties, and drug resistance. *Cancer Res* **2008**, *68*, 190-197.

(41) Peacock, C. D.; Wang, Q.; Gesell, G. S.; Corcoran-Schwartz, I. M.; Jones, E.; Kim, J.; Devereux, W. L.; Rhodes, J. T.; Huff, C. A.; Beachy, P. A.; Watkins, D. N.; Matsui, W. Hedgehog signaling maintains a tumor stem cell compartment in multiple myeloma. *Proc Natl Acad Sci U S A* **2007**, *104*, 4048-4053.

(42) Brennan, S. K.; Wang, Q.; Tressler, R.; Harley, C.; Go, N.; Bassett, E.; Huff, C. A.; Jones, R. J.; Matsui, W. Telomerase inhibition targets clonogenic multiple myeloma cells through telomere length-dependent and independent mechanisms. *PLoS One* **2010**, *5*.

(43) Van Valckenborgh, E.; Matsui, W.; Agarwal, P.; Lub, S.; Dehui, X.; De Bruyne, E.; Menu, E.; Empsen, C.; van Grunsven, L.; Agarwal, J.; Wang, Q.; Jernberg-Wiklund, H.; Vanderkerken, K. Tumor-initiating capacity of CD138- and CD138+ tumor cells in the 5T33 multiple myeloma model. *Leukemia* **2012**, *26*, 1436-1439.

(44) Kirshner, J.; Thulien, K. J.; Martin, L. D.; Debes Marun, C.; Reiman, T.; Belch, A. R.; Pilarski, L. M. A unique three-dimensional model for evaluating the impact of therapy on multiple myeloma. *Blood* **2008**, *112*, 2935-2945.

(45) Yaccoby, S.; Barlogie, B.; Epstein, J. Primary myeloma cells growing in SCID-hu mice: a model for studying the biology and treatment of myeloma and its manifestations. *Blood* **1998**, *92*, 2908-2913.

(46) Yaccoby, S.; Epstein, J. The proliferative potential of myeloma plasma cells manifest in the SCID-hu host. *Blood* **1999**, *94*, 3576-3582.

(47) Yang, Y.; Yaccoby, S.; Liu, W.; Langford, J. K.; Pumphrey, C. Y.; Theus, A.; Epstein, J.; Sanderson, R. D. Soluble syndecan-1 promotes growth of myeloma tumors in vivo. *Blood* **2002**, *100*, 610-617.

(48) Yang, Y.; MacLeod, V.; Dai, Y.; Khotskaya-Sample, Y.; Shriver, Z.; Venkataraman, G.; Sasisekharan, R.; Naggi, A.; Torri, G.; Casu, B.; Vlodavsky, I.; Suva, L. J.; Epstein, J.; Yaccoby, S.; Shaughnessy, J. D., Jr.; Barlogie, B.; Sanderson,

R. D. The syndecan-1 heparan sulfate proteoglycan is a viable target for myeloma therapy. *Blood* **2007**, *110*, 2041-2048.

(49) Jakubikova, J.; Adamia, S.; Kost-Alimova, M.; Klippel, S.; Cervi, D.; Daley, J. F.; Cholujova, D.; Kong, S. Y.; Leiba, M.; Blotta, S.; Ooi, M.; Delmore, J.; Laubach, J.; Richardson, P. G.; Sedlak, J.; Anderson, K. C.; Mitsiades, C. S. Lenalidomide targets clonogenic side population in multiple myeloma: pathophysiologic and clinical implications. *Blood* **2011**, *117*, 4409-4419.

(50) Nara, M.; Teshima, K.; Watanabe, A.; Ito, M.; Iwamoto, K.; Kitabayashi, A.; Kume, M.; Hatano, Y.; Takahashi, N.; Iida, S.; Sawada, K.; Tagawa, H. Bortezomib reduces the tumorigenicity of multiple myeloma via downregulation of upregulated targets in clonogenic side population cells. *PLoS One* **2013**, *8*, e56954.

(51) Chiron, D.; Surget, S.; Maiga, S.; Bataille, R.; Moreau, P.; Le Gouill, S.; Amiot, M.; Pellat-Deceunynck, C. The peripheral CD138(+) population but not the CD138(-) population contains myeloma clonogenic cells in plasma cell leukaemia patients. *British journal of haematology* **2011**.

(52) Kawano, Y.; Fujiwara, S.; Wada, N.; Izaki, M.; Yuki, H.; Okuno, Y.; Iyama, K.; Yamasaki, H.; Sakai, A.; Mitsuya, H.; Hata, H. Multiple myeloma cells expressing low levels of CD138 have an immature phenotype and reduced sensitivity to lenalidomide. *Int J Oncol* **2012**, *41*, 876-884.

(53) Hosen, N.; Matsuoka, Y.; Kishida, S.; Nakata, J.; Mizutani, Y.; Hasegawa, K.; Mugitani, A.; Ichihara, H.; Aoyama, Y.; Nishida, S.; Tsuboi, A.; Fujiki, F.; Tatsumi, N.; Nakajima, H.; Hino, M.; Kimura, T.; Yata, K.; Abe, M.; Oka, Y.; Oji, Y.; Kumanogoh, A.; Sugiyama, H. CD138-negative clonogenic cells are plasma cells but not B cells in some multiple myeloma patients. *Leukemia* **2012**, *26*, 2135-2141.

(54) Kim, D.; Park, C. Y.; Medeiros, B. C.; Weissman, I. L. CD19-CD45 low/- CD38 high/CD138+ plasma cells enrich for human tumorigenic myeloma cells. *Leukemia* **2012**, *26*, 2530-2537.

(55) Christensen, J. H.; Jensen, P. V.; Kristensen, I. B.; Abildgaard, N.; Lodahl, M.; Rasmussen, T. Characterization of potential CD138 negative myeloma "stem cells". *Haematologica* **2012**, *97*, e18-20.

(56) Jourdan, M.; Ferlin, M.; Legouffe, E.; Horvathova, M.; Liautard, J.; Rossi, J. F.; Wijdenes, J.; Brochier, J.; Klein, B. The myeloma cell antigen syndecan-1 is lost by apoptotic myeloma cells. *British journal of haematology* **1998**, *100*, 637-646.

(57) Podar, K.; Chauhan, D.; Anderson, K. C. Bone marrow microenvironment and the identification of new targets for myeloma therapy. *Leukemia* **2009**, *23*, 10-24.

(58) Kuehl, W. M.; Bergsagel, P. L. Molecular pathogenesis of multiple myeloma and its premalignant precursor. *J Clin Invest* **2012**, *122*, 3456-3463.

(59) Kim, I.; Uchiyama, H.; Chauhan, D.; Anderson, K. C. Cell surface expression and functional significance of adhesion molecules on human myeloma-derived cell lines. *Br J Haematol* **1994**, *87*, 483-493.

(60) Uchiyama, H.; Barut, B. A.; Mohrbacher, A. F.; Chauhan, D.; Anderson, K. C. Adhesion of human myeloma-derived cell lines to bone marrow stromal cells stimulates interleukin-6 secretion. *Blood* **1993**, *82*, 3712-3720.

(61) Hardin, J.; MacLeod, S.; Grigorieva, I.; Chang, R.; Barlogie, B.; Xiao, H.; Epstein, J. Interleukin-6 prevents dexamethasone-induced myeloma cell death. *Blood* **1994**, *84*, 3063-3070.

(62) Nefedova, Y.; Landowski, T. H.; Dalton, W. S. Bone marrow stromal-derived soluble factors and direct cell contact contribute to de novo drug resistance of myeloma cells by distinct mechanisms. *Leukemia* **2003**, *17*, 1175-1182.

(63) Hazlehurst, L. A.; Damiano, J. S.; Buyuksal, I.; Pledger, W. J.; Dalton, W. S. Adhesion to fibronectin via beta1 integrins regulates p27kip1 levels and

contributes to cell adhesion mediated drug resistance (CAM-DR). *Oncogene* **2000**, *19*, 4319-4327.

(64) Hahne, M.; Kataoka, T.; Schroter, M.; Hofmann, K.; Irmler, M.; Bodmer, J. L.; Schneider, P.; Bornand, T.; Holler, N.; French, L. E.; Sordat, B.; Rimoldi, D.; Tschopp, J. APRIL, a new ligand of the tumor necrosis factor family, stimulates tumor cell growth. *J Exp Med* **1998**, *188*, 1185-1190.

(65) Kimberley, F. C.; Hahne, M.; Medema, J. P. "APRIL hath put a spring of youth in everything": Relevance of APRIL for survival. *Journal of cellular physiology* **2009**, *218*, 1-8.

(66) Marsters, S. A.; Yan, M.; Pitti, R. M.; Haas, P. E.; Dixit, V. M.; Ashkenazi, A. Interaction of the TNF homologues BLyS and APRIL with the TNF receptor homologues BCMA and TACI. *Current biology : CB* **2000**, *10*, 785-788.

(67) Varfolomeev, E.; Kischkel, F.; Martin, F.; Seshasayee, D.; Wang, H.; Lawrence, D.; Olsson, C.; Tom, L.; Erickson, S.; French, D.; Schow, P.; Grewal, I. S.; Ashkenazi, A. APRIL-deficient mice have normal immune system development. *Mol Cell Biol* **2004**, *24*, 997-1006.

(68) Castigli, E.; Scott, S.; Dedeoglu, F.; Bryce, P.; Jabara, H.; Bhan, A. K.; Mizoguchi, E.; Geha, R. S. Impaired IgA class switching in APRIL-deficient mice. *Proc Natl Acad Sci U S A* **2004**, *101*, 3903-3908.

(69) Sakurai, D.; Hase, H.; Kanno, Y.; Kojima, H.; Okumura, K.; Kobata, T. TACI regulates IgA production by APRIL in collaboration with HSPG. *Blood* **2007**, *109*, 2961-2967.

(70) Belnoue, E.; Pihlgren, M.; McGaha, T. L.; Tougne, C.; Rochat, A. F.; Bossen, C.; Schneider, P.; Huard, B.; Lambert, P. H.; Siegrist, C. A. APRIL is critical for plasmablast survival in the bone marrow and poorly expressed by early-life bone marrow stromal cells. *Blood* **2008**, *111*, 2755-2764.

(71) Huard, B.; McKee, T.; Bosshard, C.; Durual, S.; Matthes, T.; Myit, S.; Donze, O.; Frossard, C.; Chizzolini, C.; Favre, C.; Zubler, R.; Guyot, J. P.; Schneider, P.; Roosnek, E. APRIL secreted by neutrophils binds to heparan sulfate proteoglycans to create plasma cell niches in human mucosa. *J Clin Invest* **2008**, *118*, 2887-2895.

(72) Matthes, T.; Dunand-Sauthier, I.; Santiago-Raber, M. L.; Krause, K. H.; Donze, O.; Passweg, J.; McKee, T.; Huard, B. Production of the plasma-cell survival factor a proliferation-inducing ligand (APRIL) peaks in myeloid precursor cells from human bone marrow. *Blood* **2011**, *118*, 1838-1844.

(73) Reijmers, R. M.; Groen, R. W.; Kuil, A.; Weijer, K.; Kimberley, F. C.; Medema, J. P.; van Kuppevelt, T. H.; Li, J. P.; Spaargaren, M.; Pals, S. T. Disruption of heparan sulfate proteoglycan conformation perturbs B-cell maturation and APRIL-mediated plasma cell survival. *Blood* **2011**, *117*, 6162-6171.

(74) Moreaux, J.; Sprynski, A. C.; Dillon, S. R.; Mahtouk, K.; Jourdan, M.; Ythier, A.; Moine, P.; Robert, N.; Jourdan, E.; Rossi, J. F.; Klein, B. APRIL and TACI interact with syndecan-1 on the surface of multiple myeloma cells to form an essential survival loop. *European journal of haematology* **2009**, *83*, 119-129.

(75) Novak, A. J.; Darce, J. R.; Arendt, B. K.; Harder, B.; Henderson, K.; Kindsvogel, W.; Gross, J. A.; Greipp, P. R.; Jelinek, D. F. Expression of BCMA, TACI, and BAFF-R in multiple myeloma: a mechanism for growth and survival. *Blood* **2004**, *103*, 689-694.

(76) Moreaux, J.; Legouffe, E.; Jourdan, E.; Quittet, P.; Reme, T.; Lugagne, C.; Moine, P.; Rossi, J. F.; Klein, B.; Tarte, K. BAFF and APRIL protect myeloma cells from apoptosis induced by interleukin 6 deprivation and dexamethasone. *Blood* **2004**, *103*, 3148-3157.

(77) Moreaux, J.; Cremer, F. W.; Reme, T.; Raab, M.; Mahtouk, K.; Kaukel, P.; Pantesco, V.; De Vos, J.; Jourdan, E.; Jauch, A.; Legouffe, E.; Moos, M.; Fiol, G.; Goldschmidt, H.; Rossi, J. F.; Hose, D.; Klein, B. The level of TACI gene

expression in myeloma cells is associated with a signature of microenvironment dependence versus a plasmablastic signature. *Blood* **2005**, *106*, 1021-1030.

(78) Yaccoby, S.; Pennisi, A.; Li, X.; Dillon, S. R.; Zhan, F.; Barlogie, B.; Shaughnessy, J. D., Jr. Atacicept (TACI-Ig) inhibits growth of TACI(high) primary myeloma cells in SCID-hu mice and in coculture with osteoclasts. *Leukemia* **2008**, *22*, 406-413.

(79) Annunziata, C. M.; Davis, R. E.; Demchenko, Y.; Bellamy, W.; Gabrea, A.; Zhan, F.; Lenz, G.; Hanamura, I.; Wright, G.; Xiao, W.; Dave, S.; Hurt, E. M.; Tan, B.; Zhao, H.; Stephens, O.; Santra, M.; Williams, D. R.; Dang, L.; Barlogie, B.; Shaughnessy, J. D., Jr.; Kuehl, W. M.; Staudt, L. M. Frequent engagement of the classical and alternative NF-kappaB pathways by diverse genetic abnormalities in multiple myeloma. *Cancer Cell* **2007**, *12*, 115-130.

(80) Endo, T.; Nishio, M.; Enzler, T.; Cottam, H. B.; Fukuda, T.; James, D. F.; Karin, M.; Kipps, T. J. BAFF and APRIL support chronic lymphocytic leukemia B-cell survival through activation of the canonical NF-kappaB pathway. *Blood* **2007**, *109*, 703-710.

(81) Dalton, W. S. The tumor microenvironment: focus on myeloma. *Cancer treatment reviews* **2003**, *29 Suppl 1*, 11-19.

(82) Markovina, S.; Callander, N. S.; O'Connor, S. L.; Kim, J.; Werndli, J. E.; Raschko, M.; Leith, C. P.; Kahl, B. S.; Kim, K.; Miyamoto, S. Bortezomib-resistant nuclear factor-kappaB activity in multiple myeloma cells. *Molecular cancer research : MCR* **2008**, *6*, 1356-1364.

(83) Hideshima, T.; Nakamura, N.; Chauhan, D.; Anderson, K. C. Biologic sequelae of interleukin-6 induced PI3-K/Akt signaling in multiple myeloma. *Oncogene* **2001**, *20*, 5991-6000.

(84) Glassford, J.; Kassen, D.; Quinn, J.; Stengel, C.; Kallinikou, K.; Khwaja, A.; Yong, K. L. Inhibition of cell cycle progression by dual

phosphatidylinositol-3-kinase and mTOR blockade in cyclin D2 positive multiple myeloma bearing IgH translocations. *Blood cancer journal* **2012**, *2*, e50.

(85) Stengel, C.; Cheung, C. W.; Quinn, J.; Yong, K.; Khwaja, A. Optimal induction of myeloma cell death requires dual blockade of phosphoinositide 3-kinase and mTOR signalling and is determined by translocation subtype. *Leukemia* **2012**, *26*, 1761-1770.

(86) Jakubowiak, A. J.; Richardson, P. G.; Zimmerman, T.; Alsina, M.; Kaufman, J. L.; Kandarpa, M.; Kraftson, S.; Ross, C. W.; Harvey, C.; Hideshima, T.; Sportelli, P.; Poradosu, E.; Gardner, L.; Giusti, K.; Anderson, K. C. Perifosine plus lenalidomide and dexamethasone in relapsed and relapsed/refractory multiple myeloma: a Phase I Multiple Myeloma Research Consortium study. *Br J Haematol* **2012**, *158*, 472-480.

(87) Steinbrunn, T.; Stuhmer, T.; Gattenlohner, S.; Rosenwald, A.; Mottok, A.; Unzicker, C.; Einsele, H.; Chatterjee, M.; Bargou, R. C. Mutated RAS and constitutively activated Akt delineate distinct oncogenic pathways, which independently contribute to multiple myeloma cell survival. *Blood* **2011**, *117*, 1998-2004.

(88) Wang, Z.; Li, Y.; Ahmad, A.; Azmi, A. S.; Banerjee, S.; Kong, D.; Sarkar, F. H. Targeting Notch signaling pathway to overcome drug resistance for cancer therapy. *Biochim Biophys Acta* **2010**, *1806*, 258-267.

(89) Grabher, C.; von Boehmer, H.; Look, A. T. Notch 1 activation in the molecular pathogenesis of T-cell acute lymphoblastic leukaemia. *Nat Rev Cancer* **2006**, *6*, 347-359.

(90) Ersvaer, E.; Hatfield, K. J.; Reikvam, H.; Bruserud, O. Future perspectives: therapeutic targeting of notch signalling may become a strategy in patients receiving stem cell transplantation for hematologic malignancies. *Bone marrow research* **2011**, *2011*, 570796.

(91) Kopan, R.; Ilagan, M. X. The canonical Notch signaling pathway: unfolding the activation mechanism. *Cell* **2009**, *137*, 216-233.

(92) Iso, T.; Kedes, L.; Hamamori, Y. HES and HERP families: multiple effectors of the Notch signaling pathway. *J Cell Physiol* **2003**, *194*, 237-255.

(93) Espinosa, L.; Cathelin, S.; D'Altri, T.; Trimarchi, T.; Statnikov, A.; Guiu, J.; Rodilla, V.; Ingles-Esteve, J.; Nomdedeu, J.; Bellosillo, B.; Besses, C.; Abdel-Wahab, O.; Kucine, N.; Sun, S. C.; Song, G.; Mullighan, C. C.; Levine, R. L.; Rajewsky, K.; Aifantis, I.; Bigas, A. The Notch/Hes1 pathway sustains NF-kappaB activation through CYLD repression in T cell leukemia. *Cancer Cell* **2010**, *18*, 268-281.

(94) Nefedova, Y.; Gabrilovich, D. Mechanisms and clinical prospects of Notch inhibitors in the therapy of hematological malignancies. *Drug resistance updates : reviews and commentaries in antimicrobial and anticancer chemotherapy* **2008**, *11*, 210-218.

(95) Weber, J. M.; Calvi, L. M. Notch signaling and the bone marrow hematopoietic stem cell niche. *Bone* **2010**, *46*, 281-285.

(96) Nefedova, Y.; Cheng, P.; Alsina, M.; Dalton, W. S.; Gabrilovich, D. I. Involvement of Notch-1 signaling in bone marrow stroma-mediated de novo drug resistance of myeloma and other malignant lymphoid cell lines. *Blood* **2004**, *103*, 3503-3510.

(97) Shin, D. M.; Shaffer, D. J.; Wang, H.; Roopenian, D. C.; Morse, H. C., 3rd. NOTCH is part of the transcriptional network regulating cell growth and survival in mouse plasmacytomas. *Cancer Res* **2008**, *68*, 9202-9211.

(98) Jundt, F.; Probsting, K. S.; Anagnostopoulos, I.; Muehlinghaus, G.; Chatterjee, M.; Mathas, S.; Bargou, R. C.; Manz, R.; Stein, H.; Dorken, B. Jagged1-induced Notch signaling drives proliferation of multiple myeloma cells. *Blood* **2004**, *103*, 3511-3515.

(99) Houde, C.; Li, Y.; Song, L.; Barton, K.; Zhang, Q.; Godwin, J.; Nand, S.; Toor, A.; Alkan, S.; Smadja, N. V.; Avet-Loiseau, H.; Lima, C. S.; Miele, L.; Coignet, L. J. Overexpression of the NOTCH ligand JAG2 in malignant plasma cells from multiple myeloma patients and cell lines. *Blood* **2004**, *104*, 3697-3704.

(100) Skrtic, A.; Korac, P.; Kristo, D. R.; Ajdukovic Stojisavljevic, R.; Ivankovic, D.; Dominis, M. Immunohistochemical analysis of NOTCH1 and JAGGED1 expression in multiple myeloma and monoclonal gammopathy of undetermined significance. *Hum Pathol* **2010**.

(101) Cheng, P.; Nefedova, Y.; Corzo, C. A.; Gabrilovich, D. I. Regulation of dendritic-cell differentiation by bone marrow stroma via different Notch ligands. *Blood* **2007**, *109*, 507-515.

(102) Choi, K.; Ahn, Y. H.; Gibbons, D. L.; Tran, H. T.; Creighton, C. J.; Girard, L.; Minna, J. D.; Qin, F. X.; Kurie, J. M. Distinct biological roles for the notch ligands Jagged-1 and Jagged-2. *J Biol Chem* **2009**, *284*, 17766-17774.

(103) Hu, J.; Zhu, X.; Lu, Q. Antiproliferative effects of gamma-secretase inhibitor, a Notch signalling inhibitor, in multiple myeloma cells and its molecular mechanism of action. *The Journal of international medical research* **2013**, *41*, 1017-1026.

(104) Chiron, D.; Maiga, S.; Descamps, G.; Moreau, P.; Le Gouill, S.; Marionneau, S.; Ouiller, T.; Moreaux, J.; Klein, B.; Bataille, R.; Amiot, M.; Pellat-Deceunynck, C. Critical role of the NOTCH ligand JAG2 in self-renewal of myeloma cells. *Blood cells, molecules & diseases* **2012**, *48*, 247-253.

(105) Zweidler-McKay, P. A.; He, Y.; Xu, L.; Rodriguez, C. G.; Karnell, F. G.; Carpenter, A. C.; Aster, J. C.; Allman, D.; Pear, W. S. Notch signaling is a potent inducer of growth arrest and apoptosis in a wide range of B-cell malignancies. *Blood* **2005**, *106*, 3898-3906.

(106) Nefedova, Y.; Sullivan, D. M.; Bolick, S. C.; Dalton, W. S.; Gabrilovich, D. I. Inhibition of Notch signaling induces apoptosis of myeloma cells and enhances sensitivity to chemotherapy. *Blood* **2008**, *111*, 2220-2229.

(107) Chen, F.; Pisklakova, A.; Li, M.; Baz, R.; Sullivan, D. M.; Nefedova, Y. Gamma-secretase inhibitor enhances the cytotoxic effect of bortezomib in multiple myeloma. *Cellular oncology* **2011**, *34*, 545-551.

(108) Xu, D.; Hu, J.; De Bruyne, E.; Menu, E.; Schots, R.; Vanderkerken, K.; Van Valckenborgh, E. Dll1/Notch activation contributes to bortezomib resistance by upregulating CYP1A1 in multiple myeloma. *Biochemical and biophysical research communications* **2012**, *428*, 518-524.

(109) Xu, D.; Hu, J.; Xu, S.; De Bruyne, E.; Menu, E.; Van Camp, B.; Vanderkerken, K.; Van Valckenborgh, E. Dll1/Notch activation accelerates multiple myeloma disease development by promoting CD138+ MM-cell proliferation. *Leukemia* **2012**, *26*, 1402-1405.

(110) Hu, J.; Huang, X.; Hong, X.; Lu, Q.; Zhu, X. Arsenic trioxide inhibits the proliferation of myeloma cell line through notch signaling pathway. *Cancer cell international* **2013**, *13*, 25.

(111) Schwarzer, R.; Kaiser, M.; Acikgoez, O.; Heider, U.; Mathas, S.; Preissner, R.; Sezer, O.; Doerken, B.; Jundt, F. Notch inhibition blocks multiple myeloma cell-induced osteoclast activation. *Leukemia* **2008**, *22*, 2273-2277.

(112) Mirandola, L.; Apicella, L.; Colombo, M.; Yu, Y.; Berta, D. G.; Platonova, N.; Lazzari, E.; Lancellotti, M.; Bulfamante, G.; Cobos, E.; Chiriva-Internati, M.; Chiaramonte, R. Anti-Notch treatment prevents multiple myeloma cells localization to the bone marrow via the chemokine system CXCR4/SDF-1. *Leukemia* **2013**, *27*, 1558-1566.

(113) Quinn, J.; Glassford, J.; Percy, L.; Munson, P.; Marafioti, T.; Rodriguez-Justo, M.; Yong, K. APRIL promotes cell cycle progression in primary

multiple myeloma cells: influence of D-type cyclin group and translocation status. *Blood* **2010**.

(114) Bossen, C.; Schneider, P. BAFF, APRIL and their receptors: structure, function and signaling. *Semin Immunol* **2006**, *18*, 263-275.

(115) Palomero, T.; Dominguez, M.; Ferrando, A. A. The role of the PTEN/AKT Pathway in NOTCH1-induced leukemia. *Cell Cycle* **2008**, *7*, 965-970.

(116) Roecklein, B. A.; Torok-Storb, B. Functionally distinct human marrow stromal cell lines immortalized by transduction with the human papilloma virus E6/E7 genes. *Blood* **1995**, *85*, 997-1005.

(117) Perez, L. E.; Parquet, N.; Shain, K.; Nimmanapalli, R.; Alsina, M.; Anasetti, C.; Dalton, W. Bone marrow stroma confers resistance to Apo2 ligand/TRAIL in multiple myeloma in part by regulating c-FLIP. *J Immunol* **2008**, *180*, 1545-1555.

(118) Perez, L. E.; Parquet, N.; Meads, M.; Anasetti, C.; Dalton, W. Bortezomib restores stroma-mediated APO2L/TRAIL apoptosis resistance in multiple myeloma. *Eur J Haematol* **2010**, *84*, 212-222.

(119) Tamura, H.; Ishibashi, M.; Yamashita, T.; Tanosaki, S.; Okuyama, N.; Kondo, A.; Hyodo, H.; Shinya, E.; Takahashi, H.; Dong, H.; Tamada, K.; Chen, L.; Dan, K.; Ogata, K. Marrow stromal cells induce B7-H1 expression on myeloma cells, generating aggressive characteristics in multiple myeloma. *Leukemia* **2013**, *27*, 464-472.

(120) Schmidmaier, R.; Baumann, P.; Meinhardt, G. Cell-cell contact mediated signalling - no fear of contact. *Experimental oncology* **2006**, *28*, 12-15.

(121) Bueler, H.; Mulligan, R. C. Induction of antigen-specific tumor immunity by genetic and cellular vaccines against MAGE: enhanced tumor protection by coexpression of granulocyte-macrophage colony-stimulating factor and B7-1. *Molecular medicine (Cambridge, Mass.)* **1996**, *2*, 545-555.

(122) Armstrong, F.; Brunet de la Grange, P.; Gerby, B.; Rouyez, M. C.; Calvo, J.; Fontenay, M.; Boissel, N.; Dombret, H.; Baruchel, A.; Landman-Parker, J.; Romeo, P. H.; Ballerini, P.; Pflumio, F. NOTCH is a key regulator of human T-cell acute leukemia initiating cell activity. *Blood* **2009**, *113*, 1730-1740.

(123) Van de Walle, I.; De Smet, G.; Gartner, M.; De Smedt, M.; Waegemans, E.; Vandekerckhove, B.; Leclercq, G.; Plum, J.; Aster, J. C.; Bernstein, I. D.; Guidos, C. J.; Kyewski, B.; Taghon, T. Jagged2 acts as a Delta-like Notch ligand during early hematopoietic cell fate decisions. *Blood* **2011**, *117*, 4449-4459.

(124) Williams, C. K.; Li, J. L.; Murga, M.; Harris, A. L.; Tosato, G. Up-regulation of the Notch ligand Delta-like 4 inhibits VEGF-induced endothelial cell function. *Blood* **2006**, *107*, 931-939.

(125) Rochlitz, C. F.; de Kant, E.; Neubauer, A.; Heide, I.; Bohmer, R.; Oertel, J.; Huhn, D.; Herrmann, R. PCR-determined expression of the MDR1 gene in chronic lymphocytic leukemia. *Annals of hematology* **1992**, *65*, 241-246.

(126) Lupberger, J.; Kreuzer, K. A.; Baskaynak, G.; Peters, U. R.; le Coutre, P.; Schmidt, C. A. Quantitative analysis of beta-actin, beta-2-microglobulin and porphobilinogen deaminase mRNA and their comparison as control transcripts for RT-PCR. *Molecular and cellular probes* **2002**, *16*, 25-30.

(127) Matthes, T.; McKee, T.; Dunand-Sauthier, I.; Manfroi, B.; Park, S.; Passweg, J.; Huard, B. Myelopoiesis dysregulation associated to sustained APRIL production in multiple myeloma-infiltrated bone marrow. *Leukemia* **2015**.

(128) Matthes, T.; Manfroi, B.; Zeller, A.; Dunand-Sauthier, I.; Bogen, B.; Huard, B. Autocrine amplification of immature myeloid cells by IL-6 in multiple myeloma-infiltrated bone marrow. *Leukemia* **2015**.

(129) Takebe, N.; Miele, L.; Harris, P. J.; Jeong, W.; Bando, H.; Kahn, M.; Yang, S. X.; Ivy, S. P. Targeting Notch, Hedgehog, and Wnt pathways in cancer stem cells: clinical update. *Nature reviews. Clinical oncology* **2015**, *12*, 445-464.

(130) Rand, M. D.; Grimm, L. M.; Artavanis-Tsakonas, S.; Patriub, V.; Blacklow, S. C.; Sklar, J.; Aster, J. C. Calcium depletion dissociates and activates heterodimeric notch receptors. *Mol Cell Biol* **2000**, *20*, 1825-1835.

(131) Trombly, D. J.; Woodruff, T. K.; Mayo, K. E. Suppression of Notch signaling in the neonatal mouse ovary decreases primordial follicle formation. *Endocrinology* **2009**, *150*, 1014-1024.

(132) Khotskaya, Y. B.; Dai, Y.; Ritchie, J. P.; MacLeod, V.; Yang, Y.; Zinn, K.; Sanderson, R. D. Syndecan-1 is required for robust growth, vascularization, and metastasis of myeloma tumors in vivo. *The Journal of biological chemistry* **2009**, *284*, 26085-26095.

(133) Greenbaum, L. E. From skin cells to hepatocytes: advances in application of iPS cell technology. *J Clin Invest* **2010**, *120*, 3102-3105.

(134) Chaidos, A.; Barnes, C. P.; Cowan, G.; May, P. C.; Melo, V.; Hatjiharissi, E.; Papaioannou, M.; Harrington, H.; Doolittle, H.; Terpos, E.; Dimopoulos, M.; Abdalla, S.; Yarranton, H.; Naresh, K.; Foroni, L.; Reid, A.; Rahemtulla, A.; Stumpf, M.; Roberts, I.; Karadimitris, A. Clinical drug resistance linked to interconvertible phenotypic and functional states of tumor-propagating cells in multiple myeloma. *Blood* **2013**, *121*, 318-328.

(135) de la Puente, P.; Muz, B.; Azab, F.; Luderer, M.; Azab, A. K. Molecularly targeted therapies in multiple myeloma. *Leukemia research and treatment* **2014**, *2014*, 976567.